UNIVERSITY OF
LIVERPOOL

The formation and function of putative IgLON *cis* heterodimeric complexes.

Thesis submitted with the requirements of the University of Liverpool for the degree of Doctor of Philosophy

By

Christine Jane McNamee

October 2008

DECLARATION

This thesis is the result of my own work. The material in the thesis has not been presented, nor is currently being presented either wholly or in part for any other qualification.

The research work was carried out in the Developmental Neurobiology Research group, led by Dr. Diana Moss, in the Human Anatomy and Cell Biology Division of the School of Biomedical Sciences, Liverpool University.

ABSTRACT

During development individual neurons have to reach specific locations in the embryo to form a connected nervous system. Molecular complexes form between receptors expressed on the surface of the developing axon and molecular guidance cues in the extracellular environment, to guide the neuron to the correct location. Synapses then connect the axons with their target location. This thesis describes the interactions between the IgLON family of cell adhesion molecules and how these interactions affect their function during neuronal development.

There are four members of the IgLON family in chick, namely LAMP, OBCAM, CEPU-1 and Neurotractin. They are highly glycosylated proteins, predominantly anchored by a GPI anchor to the extracellular surface of the cell membrane. Initially, the comparative strengths of homophilic and heterophilic *trans* interactions of CEPU-1, OBCAM and LAMP were established. Generally *trans* heterophilic interactions within the family have a higher affinity than homophilic interactions, LAMP having the highest heterophilic affinity for CEPU and OBCAM. The lowest affinity of all the *trans* interactions tested was the LAMP homophilic interaction.

Data is presented to suggest IgLONs also interact in *cis* to form heterodimeric complexes or Diglons. These putative Diglons affect the *trans* binding affinity for IgLON-FC recombinant proteins, possibly due to a conformational change altering the availability of the IgLON binding site. Biochemical and imaging studies provided additional physical evidence for the Diglon complex.

Inhibition of the initiation of neurite outgrowth from chick forebrain neurons was found to be dependent on the presence of two IgLONs in the extracellular environment to suggest formation of putative Diglon heterodimeric complexes facilitates IgLONs to function as negative axon guidance cues.

IgLONs have no cytoplasmic domain so are reliant on being part of a molecular complex on the surface of the cell membrane for signal transduction. Assays measuring neurite outgrowth from chick forebrain neurons suggested signal transduction for Diglons is linked to trimeric $G_{o/i}$ membrane proteins and/or to Rho GTPases.

This thesis is for my family John, Ami, Peter,

Paula, Ellie and Zoë.

Also for my parents Jean and Bert Shaw.

ACKNOWLEDGEMENTS

I would like to thank Diana Moss for being a fabulous supervisor and giving me the opportunity and much needed support to complete this thesis. Diana has taught me a lot, both on an academic basis and on a personal level. I am very lucky to have the opportunity to work in her research group.

Support and help from other members of the research group include present members Michael Lyons, Mohammed Akeel, and in the past James Reed. Thanks especially to Michael, who has proof read this thesis without needing too many Ibuprofen, and whose wit keeps the group smiling.

I would also like to acknowledge Human Anatomy and Cell Biology Division of Liverpool University for sponsoring me to undertake this thesis, also to thank my examiners Dr. Toni Plagge and Professor Jim Cohen.

Thanks also go to Tony Moore, who supplied us with many special offers on consumables used for experiments in this thesis.

I am also very privileged to have had great support and encouragement from my family and friends. Their support has been much needed and appreciated.

ABBREVIATIONS

ADF	actin depolymerising factor
ANOVA	analysis of variance
Arp2/3	actin related protein complex
α	alpha
β	beta
β-actin	beta actin
BMP	Bone morphogenic proteins
Bp	base pair
BSA	bovine serum albumin
Ca^{2+}	calcium
°C	degrees centigrade
CAM	cell adhesion molecule
C	cerebellum purkinje membrane protein
CEPU-1	cerebellum purkinje membrane protein
CEPU-se	secreted CEPU-1
CL	CEPU-1:LAMP Diglon
CO	CEPU-1:OBCAM Diglon
CO^{H}	CEPU-1-OBCAM Hisx6 tagged Diglon
C+O	CEPU-1+OBCAM IgLONs
CGCs	cerebellar granule cells
CHO	Chinese Hamster Ovary
CNS	central nervous system
Diglon	Dimeric IgLON
DCC	Deleted in colorectal cancer
GDNF	Gliai derived neurotrophic factor
DMEM	Dulbecco's modified Eagle's medium
DRG	dorsal root ganglion
E	embryonic day
EDTA	ethylene diamine tetra acetic acid
EGFP	enhanced green fluorescent protein
ELISA	Enzyme Linked Immuno Substrate Assay
FACS	fluorescent activated cell sorting

F-actin	Filamentous actin
FC	fragment C from the Human IgG heavy chain
FCS	foetal calf serum
FGF	Fibroblast growth factor
FGFR	fibroblast growth factor receptor
FN III	Fibronectin type III repeat
GFP	green fluorescent protein
GPI	glycosyl-phosphatidyl inositol
HBSS	Hanks balance salt solution
HBSS(-)	HBSS minus calcium and magnesium ions
HCL	Hydrochloric acid
HNT	CEPU-1 gene name
HISx6	6 histidine repeat tag
H_2SO_4	sulphuric acid
HRP	horseradish peroxidase
Ig	immunoglobulin
IgG	immunoglobulin G
IgSF	immunoglobulin super family
IgLON	Ig super family LAMP OBCAM NEUROTRACTIN/CEPU-1
Immpt	immuno-precipitation
IPTG	Isopropyl β-D-1-thiogalactopyranoside
IRES	internal ribosome entry site
pIRES	plasmid PCa*b*linkmigiresEGFPm5Cla1
kbp	kilo base pair
kD	dissociation constant
Kilon	Kindred IgLON
L	limbic associated membrane protein
LAMP	limbic associated membrane protein
LB	Luria broth
LO	LAMP:OBCAM
LO^H	LAMP-HISx6 tagged OBCAM Diglon
LIG	LAMP-IRES-GFP plasmid
LDS	Lithium dodecyl sulphate
LSAMP	LAMP gene name

M	molar
mg	milligram
ml	millilitre
mM	millimolar
NaCl	sodium chloride
N-CAMs	neuronal cell adhesion molecules
NEGRI	Kilon gene name
nm	nanamolar
ng	nanogram
Ntm	Neurotrimin
Ntr	Neurotractin
O	opiate binding cell adhesion molecule
O^H	Hisx6 tagged OBCAM
OBCAM	opiate binding cell adhesion molecule
OPCML	OBCAM gene name
%	percentage
pLIG	plasmid LAMP-IRES-GFP
pOIG	plasmid OBCAM-IRES-GFP
od	optical density
PAGE	polyacrylaminde gel electrophoresis
PBS	Dulbecco phosphate buffered saline
PCR	Polymerase chain reaction
PIC	Protease inhibitor cocktail
PiPLC	phosphatidylinositol-specific phospholipase C
PL	poly-L-Lysine
PNS	peripheral nervous system
PSA	poly-sialic acid
PTX	pertussis toxin
Robo	roundabout receptor
ROCK	Rho-associated coiled-coil-forming kinase
RT	room temperature
RTPCR	reverse transcriptase polymerase chain reaction
Sema3A	secreted semaphoring class 3
STET	sucrose triton x100 EDTA tris buffer

TA	tris acetate buffer
TAE	tris acetate EDTA buffer
TMB	3,3',5,5'-Titramethylbenzidine dihydrochloride
trans	transmembrane
Tris	Trizima base
™	Trade Mark
Unc	uncoordinated receptor
uv	ultra violet
µg	microgram
µl	microlitre
µm	micromolar
VASE	variable alternative spliced exon
WT	wild type
x-gal	x-galactosidase

TABLE OF CONTENTS

CHAPTER ONE

CHAPTER TWO

CHAPTER THREE

CHAPTER FOUR

CHAPTER FIVE

CHAPTER SIX

Chapter One

Introduction

INTRODUCTION

Beginnings of the nervous system

The development of the nervous system starts with invagination of a region of the embryonic ectoderm layer to form the neural plate (Munoz-Sanjuan and Brivanlou, 2002). This region closes to become the neural tube and goes on to differentiate into the brain regions and spinal cord of the central nervous system (CNS). A whole range of molecules are secreted by, or expressed on, the surface of embryonic cells to enable this development. There are at least four principle signalling molecules, Fibroblast growth factors (FGF), retinoic acid, Sonic hedgehog and Bone morphogenic proteins (BMP) involved during this stage of development (Wilson and Maden, 2005).

Below the neural tube is the notochord, a transient structure derived from the mesoderm, which is responsible for organising the ventral part of the embryo (Placzek et al., 1990; Stemple, 2005). One of the main secretions from the notochord is Sonic hedgehog which forms a gradient for the development of the floor plate region (Jessell and Dodd, 1990) located along the ventral midline of the neural tube (Ericson et al., 1995). The inner mesoderm layer segments into somites, regions that eventually form the dermis, skeletal muscle, and vertebrae (Wilson and Maden, 2005). The dorsal region of the neural tube, namely the roof plate, also plays a crucial role in organising the embryo, in a similar way to the floor plate (Lee et al., 2000). BMPs are secreted from the ectoderm in a gradient out from the roof plate to induce the formation of neural crest cells. These neural crest cells migrate out and away from above the roof plate to give rise to most of the peripheral nervous system, (PNS) as well as a wide variety of other cell types within the organism (LaBonne and Bronner-Fraser, 1999; Rao, 2004).

Neuroblasts form between these two regions to give rise to the different types of neurons of the nervous system. Motor neurons emanate from the ventral region, whereas sensory neurons emanate from ganglia in the dorsal region of the embryo. Interneurons form distinct trajectories and circuits to link these two regions. FGFs, produced by the mesoderm, are thought to be neuronal-inducing signals which are subsequently down regulated by retinoic acid before neuronal differentiation takes place (Chizhikov and Millen, 2005).

Axons are guided to specific locations in the developing embryo

Typically, a neuron is a complex cell comprising of a cell body, with one end extending a long axon and from the other end a branching network of short dendrites project. For a functional nervous system to develop these axons and dendrites have to extend and form a connected network throughout the length of the organism.

In 1890 Ramon Y Cajal examined sections of spinal cord stained with silver chromate and first identified a specific region at the tip of the developing axon described as the growth cone. In 1907 R.G. Harrison studied neurons in culture over extended time periods and suggested axons actually extended from a single neuronal cell body.

Electron photomicrographs demonstrated the growth cone constantly puts out lamellipodia and filopodia to probe the immediate extracellular environment. These dynamic structures rapidly respond to molecular guidance cues the growth cone meets causing the axon to either extend or retract, thus navigating the developing neuron to its appropriate target location (figure 1.1).

Guidance cues can either be contact-mediated, providing a short range cue or a gradient of secreted molecules, providing a more long distance cue The growth cone spatially and temporally expresses a variety of receptors to respond to the immediate extracellular environment (Lin and Holt, 2007). The transient interactions between these guidance cues and receptors (figure 1.2) negotiate the axons path to its correct target location (Dickson, 2002). Once at the target axons make specific contacts, or synapses to form neuronal circuits and connect the nervous system to each area of the organism (Vogt et al., 2005; Waites et al., 2005).

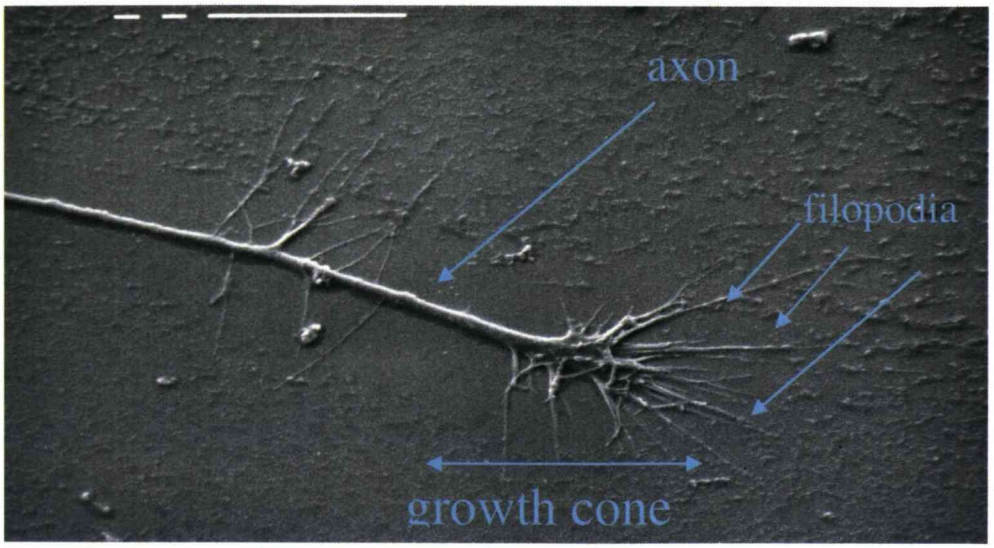

Figure 1.1 Structure of an axonal growth cone

In this scanning electron photomicrograph the growth cone tip of a developing sympathetic neuron has extended filopodia to probe the extracellular environment and direct progression of the axon. Photomicrograph courtesy of Dr. Graham Clarke, a former member of our research group at Liverpool University.

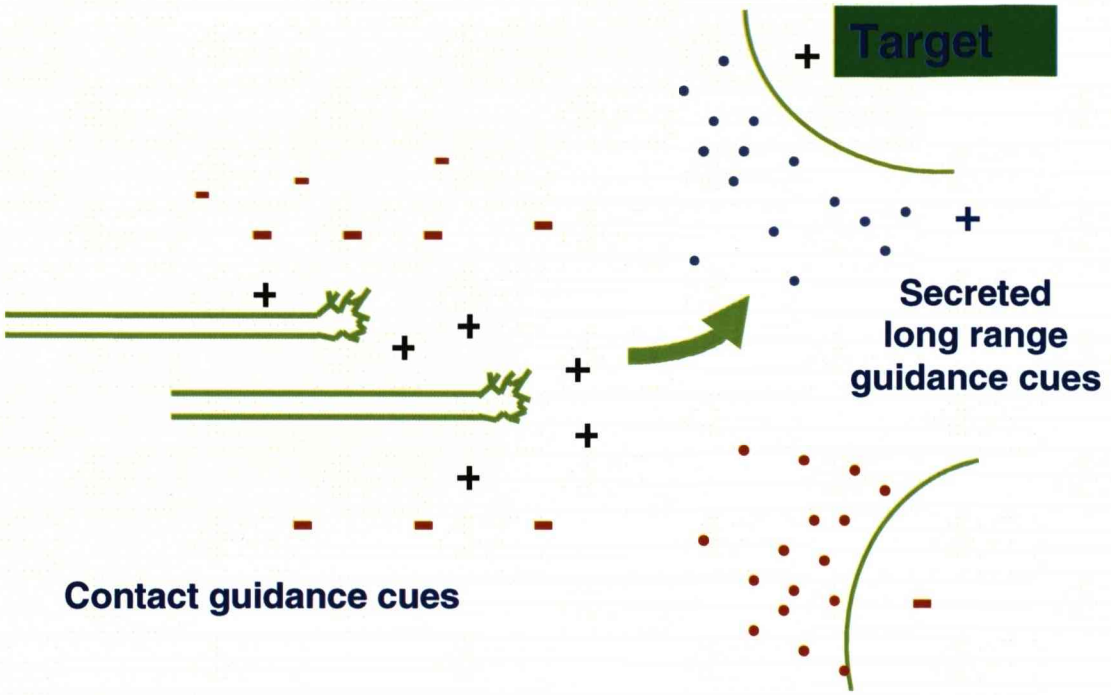

Figure 1.2 Axonal guidance cues

Illustration of how an axon (green cartoon) is guided through the developing embryo (green cartoon). At the tip of the axon is the sensitive growth cone region which is attracted in the direction of the positive contact cues (+ signs) and long range secreted guidance cues (blue spheres) and is repelled away from the negative cues (- signs and red spheres). Transient interactions between specific receptors expressed on the surface of the developing axon and these guidance cues steer the axon to reach its correct target location (figure adapted from Huber et al., 2003).

Axon guidance is dependent on specific molecular interactions

The growth cone region of the developing axon has to integrate a plethora of extracellular molecular cues to reach its target (Wen and Zheng, 2006). Guidance cues act as ligands activating specific receptors expressed on the surface of the growth cone (Chilton, 2006; Halloran and Wolman, 2006). There are several families of guidance molecules responsible for steering the developing axon to its correct target location.

Netrins

Netrin-1 is a secreted molecule first identified as a guidance cue for commissural axons in the vertebrate nervous system (Serafini et al., 1996). Netrin-1 acts either as a positive or negative guidance cue depending on the receptor complex expressed on the surface of the axon (Chisholm and Tessier-Lavigne, 1999; Mehlen, 2003). For example, Netrin-1 interacts with the deleted in colorectal cancer (DCC) receptor to promote growth cone extension and attracts commissural axons to the midline (Serafini et al., 1996). However, extension of the growth cone is converted to repulsion when uncoordinated (UNC-5) is co-expressed on trochlear motor axons (Colamarino and Tessier-Lavigne, 1995; Hong et al., 1999).

Slit

Most CNS axons are initially attracted toward the midline of the developing embryo, some actually cross the midline and then move away, whilst others are repelled and prevented from crossing. Co-ordinated expression of several guidance cues and their associated receptors is required to enable axons to cross the midline in this complicated way so as to connect the two symmetric halves of the nervous system. For example vertebrate commissural neurons are born in the dorsal spinal cord and their axons are first drawn to the midline by netrin, which emanates from the ventral floorplate (Kennedy et al., 1994). These axons cross the floor plate, turn longitudinally on the opposite (contra lateral) side, progress along the floor plate toward the brain. Commissural axons express the roundabout (Robo) receptor which responds to secret gradients of repulsive slit proteins at the floorplate (Brose et al., 1999; Hu, 1999; Kramer et al., 2001). A slit-dependent interaction then occurs between Robo 1 and the netrin receptor DCC to silence commissural axons sensitivity to netrin gradients enabling them to cross the midline (Stein and Tessier-Lavigne, 2001; Dickson and Gilestro, 2006). The Robo receptor is then re-expressed

once the axon has past the midline preventing it from crossing back again (Keleman et al., 2002; Keleman et al., 2005).

Semaphorins

Secreted Semaphorins also play a role in midline crossing. Semaphorins are a large family of molecules highly conserved in evolution from invertebrates to mammals (Rothberg et al., 1990) found in both embryonic and adult tissue (Tamagnone and Comoglio, 2004; Yazdani and Terman, 2006). During development, both secreted and membranes bound semaphorins form homodimers and then actively signal by forming complexes with members of the plexin and neuropilin (NP) receptor families expressed on the surface of axons (Raper, 2000). Plexins are essential components of the receptor complex to transduce the semaphorin extracellular signal across the axonal cell membrane to cytoplasmic signalling cascades (Tamagnone and Comoglio, 2000). Some classes of semaphorins bind directly to plexins, however, class 3 secreted semaphorins (Sema 3A) requires NP as an obligatory ligand-binding co-receptor to bind to the plexin receptor (Kolodkin et al., 1997; Takahashi et al., 1999).

Wnt

Another secreted guidance molecule to play a role at the midline is Wnt. Commissural axons initially do not respond to Wnt proteins until after they cross the midline, but once past the midline they become immediately attracted to Wnt which promotes their anterior progression. Wnt attraction is likely to be mediated by expression of Frizzled 3 receptor on the surface of commissural axons (Zou, 2004).

Ephrins

Ephrins are a different type of guidance molecule as they are membrane bound and require cell-cell contact with adjacent cells expressing their associated Ephrin (Eph) tyrosine kinase receptor in order to influence axonal growth (Cutforth and Harrison, 2002; Huot, 2004; Wilkinson, 2001) and synaptic plasticity (Knoll and Drescher, 2002) Class A Ephrins are attached to the membrane by a glycosyl phosphatidyl inositol (GPI) anchor, whereas class B Ephrins have a cytoplasmic tyrosine kinase domain. A Ephrins generally bind transmembrane Eph A receptors and B Ephrins generally bind to Eph B receptors (Kullander and Klein, 2002). The amino terminals of Eph receptors and Ephrins form *cis* dimers and then go on to interact with each other to form tetrameric *trans* complexes between apposing cell

surfaces mediating a bi-directional signal. The Eph-receptor expressing cell transduces a "forward" signal and the Ephrin-ligand expressing cell transduces a "reverse" signal, both cells being influenced by the signal (Murai and Pasquale, 2003). Specific spatial expression of gradients of Ephrins and Eph receptors are particularly important during the development of the retinal tectal system dictating the guidance of retinal ganglion cells axons into precise layer patterns to form the retinocollicular topographical map (Knoll and Drescher, 2002; Huot, 2004; Erskine and Herrera, 2007). Ephrins and Eph receptors also have a role at the midline, in hindbrain rhombomere development, migration of neural crest and during synaptogenesis (Klein, 2001).

Table 1.3 summarises the families of axon guidance molecules. Specific complexes formed by interactions between these guidance molecules and receptors expressed on the neuronal cell surface dictate whether the axon extends, turns and finally halts to form synaptic connections at the target location.

Secreted guidance molecules	**Receptor**	**Activity**
Netrin	DCC	Chemo-attractive gradient
Netrin	DCC/UNC	Chemo-repulsion gradient
Semaphorin class 3	Plexin/neuropilin(L1)	Chemo-repulsion gradient
Slit	Robo	Chemo-repulsion gradient Silences netrin chemo-attraction
Wnt	Frazzled Derailed	Chemo-attractive gradient Chemo-repulsion gradient
Contact guidance molecules		
Ephrins	Eph	Predominantly repulsion
Semaphorin class 1 & 4	Plexin A& B	Repulsion/attraction

Figure 1.3 Axonal guidance molecules involved during development

Table outlines the families of molecules recognised as neuronal guidance molecules and their associated receptors. Guidance molecules are either secreted by target location to form a gradient in the extracellular environment, or are attached to a target cell membrane to provide a contact guidance cue.

Alterations in the cytoskeleton directs axonal progression

Once activated by extracellular ligands, receptors on the surface of the developing axon signal through to the cytoskeleton and bring about changes in actin filaments and microtubules to steer the axon to its target (Zhou et al., 2002). The proximal regions of the growth cone have a region of lamellipodia and filopodia which are rich in actin filaments (Mallavarapu and Mitchison, 1999) whereas microtubules are located more to the distal region of the growth cone, but translocate to the proximal region to contribute to actin assembly and progression of the neuron (Mitchison and Kirschner, 1984; Suter and Forscher, 2000). The hypothesis is that as the growth cone meets a chemo-attractive gradient, or a contact attractive cue, actin is polymerised at the leading edge and this initially drives the growth cone forward. Microtubules explore the region, are captured, stabilise the actin filaments (Gordon-Weeks, 1991) (Gordon-Weeks and Fischer, 2000) then guide the elongation of the advancing axon (Dent and Gertler, 2003; Dent and Kalil, 2001). As one side of the growth cone selectively advances in response to a positive cue, the opposing side retracts so the growth cone moves towards the cue (Kalil and Dent, 2005). Guidance cues often activate actin and myosin-associated binding proteins to bring about these required changes in the cytoskeleton Actin binding/capping proteins prevent actin polymerisation on the retracting side; whereas assembly, anticapping and nucleating proteins promote polymerisation in response to the positive cues. As the growth cone turns and progresses, bundling/cross linking and actin binding proteins promote the extension of the actin filament, recycling proteins providing the extra actin monomers required (Dent and Gertler, 2003). Ena protein associate with the barbed end of the growth filament, preventing capping and recruits profilin (Bear et al., 2002). Profilin in turn enhances assembly by catalysing ADP-bound actin monomers to active ATP-actin for polymerisation onto the growing barbed end, elongating the actin filament (Faivre-Sarrailh et al., 1993). N-Wasp, a nucleating protein, activates the Arp2/3 complex of seven highly conserved proteins to promote branching of new filaments (Goldberg et al., 2000). Finally, actin-severing proteins ADF/cofilin and gelsolin disassembly F-actin by removing monomers from the minus pointed end of the filament, important for the recycling of actin monomers (Endo et al., 2003; Lu et al., 1997; Meberg, 2000; Meberg and Bamburg, 2000). Myosin II is the motor protein thought most likely to be associated with F-actin bundling and retrograde

flow maintaining a supply of actin monomers and so plays an important role in actin dynamics and axon guidance (Lin et al., 1996).

Microtubule associated proteins are less well understood. They initially orientate and then assist with the capture and stabilization of microtubules by the newly polymerised actin filaments (Baas, 2002). Microtubules undergo enzyme directed post-translational modification which is essential for their function. High levels of tyrosination being associated with dynamic microtubules and increased acetylation with the stabilisation of microtubules (Baas and Black, 1990; Barra et al., 1988). Acetylation and detyrosination by microtubule associated proteins occurs on the protruding side helps to stabilise the extending growth cone (Buck and Zheng, 2002; Dent and Gertler, 2003).

Guidance molecules signal to the cytoskeleton of the progressing axon

Several signalling pathways initiate changes in actin and microtubule associated proteins which then alter the cytoskeleton and so direct axonal growth. These pathways are interconnected and rely on second messengers, such as cyclic nucleotides cAMP, cGMP or calcium; levels of which can alter response of the growth cone.

The RHO signal pathway is one pathway linking guidance cues to specific cytoskeleton proteins to bring about axonal guidance during neuronal development (figure 1.4 adapted from Huber et al., 2003). There are three members of RHO GTPase proteins thought to be involved in axon guidance, namely Cdc42, Rac and Rho A. Regulation of these Rho proteins is through GTPase-activating proteins (GAPs) and GTPase nucleotide exchange factors (GEFs), GEFs exchange GDP to GTP and activate Rho GTPase signal, whereas GAPs stimulates endogenous RHO GTPase activity thus inactivating signal transduction. Axon guidance molecules activate receptors are coupled to GAPs and GEFs, which in turn modulate actin binding proteins to regulate actin assembly and myosin ATPase activity. Rho A proteins promote axon retraction by affecting the actin assembly protein cofilin, whereas Rac and Cdc42 promote actin polymerisation and axonal projection by affecting actin associated proteins like Arp2/3 complex (Higgs and Pollard, 2001) N-Wasp (Rohatgi et al., 1999) Ena and profilin (Bear et al., 2002).

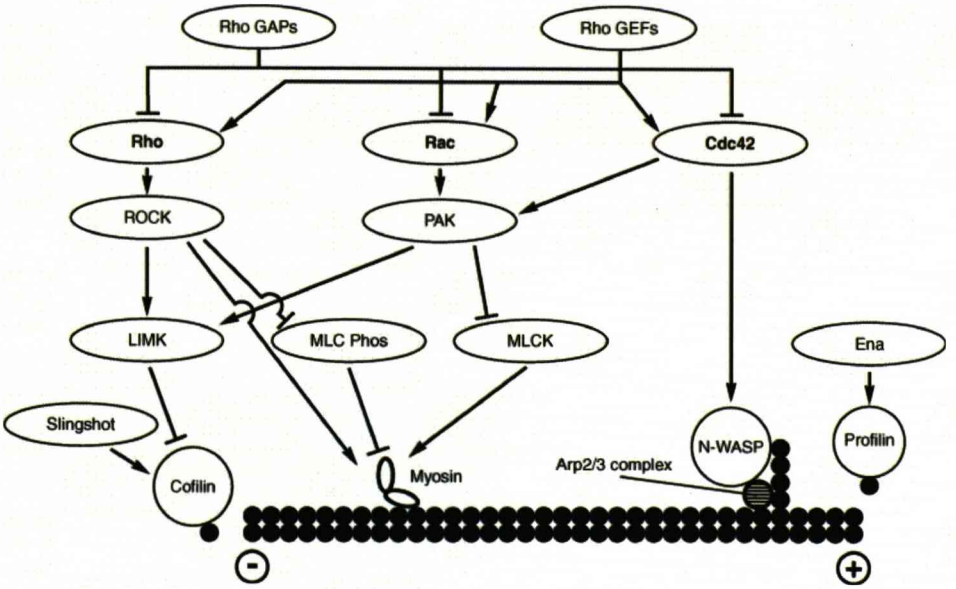

Figure 1.4 Effect of the RHO signalling pathway on actin filaments

Many axon guidance molecules signal to modulate the Rho family of GTPase proteins, Rho, RAC and Cdc 42. Actin monomers (black circles) are assembled at the extending + end of the actin filament and disassembled at the – end. GEFs activate Rho kinase (ROCK), initiating a phosphorylation cascade through Lim kinase (LIMK), and Cofilin to prevent actin assembly and growth cone progression. ROCK also maintains phosphorylation of Myosin to promote retrograde flow of F-actin by inhibiting myosin light chain kinase (MLCK) limiting the availability of actin monomers for assembly at the plus end of the filament. Slingshot, a serine/threonine phosphatase re-activates Cofilin. In contrast GEFs activating Rac and Cdc42 promote actin assembly by binding to N-WASP to activate the Arp2/3 complex and promote actin nucleation and branching. Rac also promotes actin assembly via p ^{21} activated kinase (PAK) inhibition of myosin light chain kinase (MLCK) ensuring myosin remains un-phosphorylated and actin assembly continues. Another positive regulator of actin assembly is Ena association with the barbed + end of the actin filament to prevent capping and allows actin polymerisation. Profilin in turn is localised to the cytosolic side of membrane associates with actin monomers and directs them to the positive polymerising end of the filament. Figure adapted from Huber et al., 2003).

Guidance molecules are located in lipid rafts on the axonal membrane

The physical location of receptors within the growth cone cell membrane is important during axonal development. Several receptors, along with their associated axon guidance molecules, are often required to locate to precise areas within the membrane described as lipid rafts. Location to this region facilitates the formation of complexes that initiate signalling mechanisms and so direct axonal growth. For example, the localisation of DCC to rafts was found to be a pre-requisite for intracellular transmission of the netrin-1 signal and extension of outgrowth from commissural neurons (Herincs et al., 2005). Lipid rafts also play a role in Ephrin signalling (Gauthier and Robbins, 2003) and in signalling by secreted molecules such as Semaphorin 3A, brain-derived growth factor and glial-derived neurotrophic factor neurotrophins. These ligands require association with their specific receptors and location to lipid rafts to transducer a signal across the axonal membrane (Guirland et al., 2004; Kamiguchi, 2006b).

Lipid rafts are regions in the cell membrane rich in cholesterol and sphingolipids to give them a more ordered lipid environment, which may be important for signal transduction figure 1.5, (Nakai and Kamiguchi, 2002). These regions are detergent insoluble and have a low density, allowing them to be isolated by detergent extraction and centrifugation through a sucrose gradient (Simons and Ikonen, 1997; Brown and London, 2000).

Fluorescent resonance energy transfer assays suggested between 20-40% of cell surface GPI anchored cell adhesion molecules are located to rafts less than 5 nm in size, composed of around four diverse molecules (Sharma et al., 2004). Antibody patching and cross-linking experiments further suggested individual rafts cluster together, possibly to facilitate signal transduction (Friedrichson and Kurzchalia, 1998; Harder et al., 1998). Proteins within a raft are modified by specific local kinases or phosphatases to initiate downstream signalling pathways and are protected from non-raft phosphatases (Simons and Toomre, 2000).

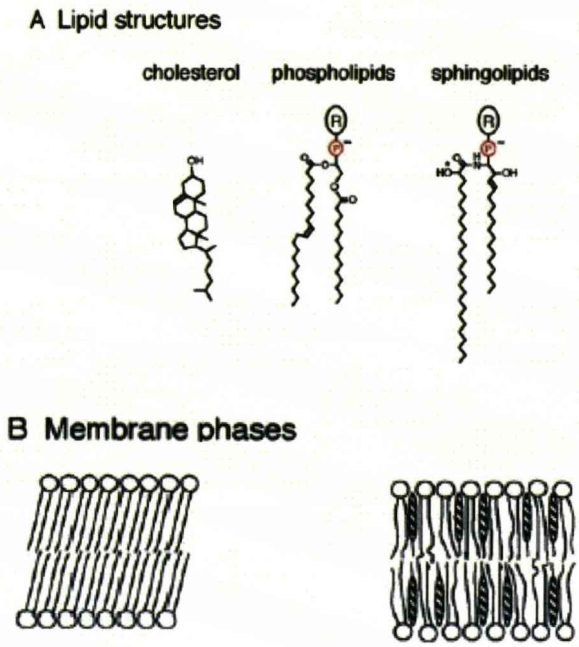

Figure 1.5 Lipid raft structure

Diagram to illustrate how the addition of cholesterol alters the plasma membrane structure (based on a figure taken from (Munro, 2003). Part A represents the three classes of lipids found in eukaryotic cell membranes. Phospholipids and sphingolipids have a head group R and acyl chains. Part B illustrates the effect of lipid components on the type of membranes. When only phospholipids are present the membrane has a more gel like structure whereas the addition of cholesterol (hatched ovals) orders the acyl chains of the phospholipids and provides a more fluid membrane.

The role of cell adhesion molecules in axonal development

In addition to specific guidance molecules cell adhesion molecules (CAMs) of the Integrin, Immunoglobulin super family (IgSF) (Rougon and Hobert, 2003) Cadherin families (Juliano, 2002; Ranscht, 2000) and secreted molecules, such as neurotrophins (Huang and Reichardt, 2001; Sofroniew et al., 2001) also influence axonal progression. Integrins interact with extracellular matrix (ECM) molecules, such as laminin and fibronectin (Clegg et al., 2003) whereas cadherins and IgSF molecules interact with other CAMs expressed on the surface of opposing cells to mediate cell-cell adhesion (Takeichi, 2007). CAMs and cadherins being dependent on location to lipid rafts to promote axonal extension (Nakai and Kamiguchi, 2002).

The role of cell adhesion molecules during synaptogenesis

Upon reaching the correct location the axon or dendrite has the potential to form a whole host of interactions to innervate target cells, but tight regulation of interactions between intercellular adhesion molecules ensures specific adhesive contacts or synapse junctions form to facilitate communication (Chen et al., 2007a; Muller et al., 2008).

Synapse formation is complicated due to the enormous heterogeneity of the cells involved, but basically follows three stages of contact initiation, recruitment of pre/post-synaptic proteins, and finally stabilization. Cadherins are involved with target recognition; protocadherins for target selection (Frank and Kemler, 2002; Serafini, 1997; Shapiro and Colman, 1999; Takeichi, 2007) SynCAM and neuroligins promote presynaptic differentiation and drive recruitment of synaptic proteins (Biederer et al., 2002; Levinson et al., 2005; Sara et al., 2005). Finally several adhesion complexes including neuroligins (Chih et al., 2005) neurexin (Dean et al., 2003) nectin (Mizoguchi et al., 2002), cadherins, Integrins and members of the IgSF stabilise the synapse (Friedman et al., 2000; Gerrow and El-Husseini, 2006; Hopf et al., 2002). The two sides of the synapse are linked by puncta adherent junctions (van Driel et al., 1990).

Several members of the IgSF have been found to play a role in synaptogenesis. For example, Sidekick 1,2 concentrate at pre and post synaptic sites in largely non-overlapping subsets of retinal axons associated with promoting lamina-specific connectivity in the inner plexiform layer of the retina (Yamagata et

al., 2002). In the cerebellum neurofascin, and L1 has been located to basket neurons forming synapses with Purkinje cells (Ango et al., 2004).

At chemical synapses the membrane on the presynaptic side of the axon contains vesicles loaded with neurotransmitters, whereas the postsynaptic dendritic membrane expresses a wide range of transmembrane, cytoskeleton, and signalling proteins ready to respond to the release of neurotransmitters to facilitate communication (Lardi-Studler and Fritschy, 2007).

An outline of some of the CAM's involved in linking the axon to the dendritic site of a connecting neuron at synaptic junctions is given in figure 1.6 (Yamada and Nelson, 2007).

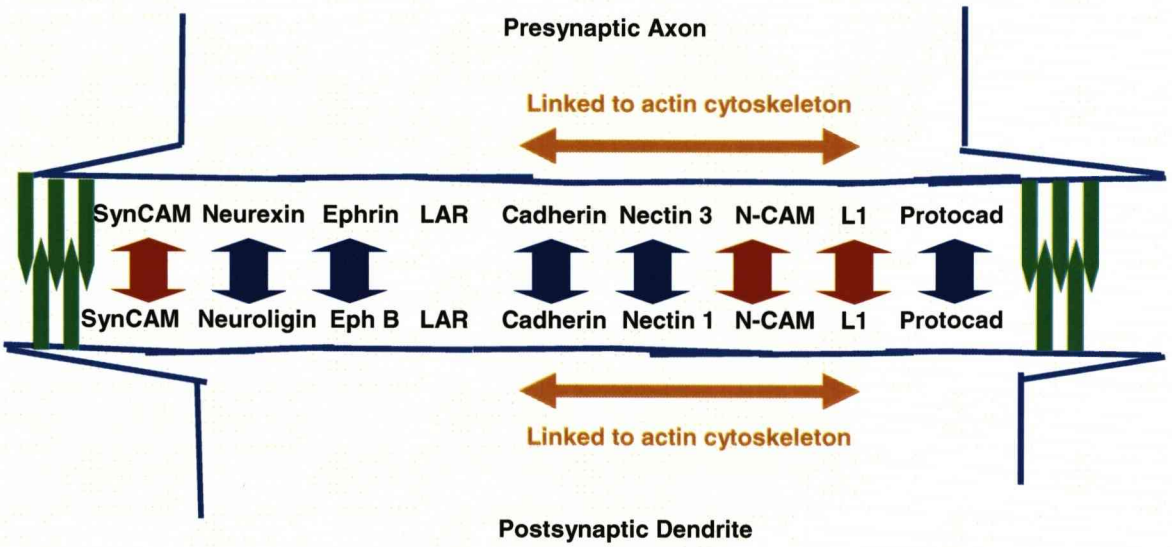

Figure 1.6 Molecular interactions involved during synaptogenesis

Figure adapted from Yamada and Nelson, 2007 outlines some of the proteins involved during synaptogenesis. Red double arrows represent homophilic interactions, whereas blue arrows heterophilic interactions. The green lines represent the Puncta adherents which link the presynaptic and postsynaptic membranes. Some of the membrane proteins are proposed to link to the cytoskeleton and may direct the growth cone into forming the synapse.

IgSF of cell adhesion molecules

The IgSF family are important during all stages of development and go on to play an important role in the adult. Members of the IgSF are characterised by the presence of a specific Ig motif, first identified in immunoglobulin proteins. There are several subfamilies with varying numbers of Ig and fibronectin type III (FN III) repeat extracellular domains. They are predominantly cell surface proteins, either with a transmembrane domain, or are attached by a GPI anchor to the cell surface, associating them with lipid rafts. Some transmembrane members of the family possess additional tyrosine kinase or phosphatase intracellular cytoplasmic domains (Crossin and Krushel, 2000). DCC, UNC, L1 and Robo members of the IgSF act as receptors for axon guidance molecules.

Neuronal cell adhesion molecules (N-CAMs) are a specific group of IgSF molecules expressed on the surface of most neuronal cells that play a major role in development of the nervous system. The homophilic cell-cell interactions between N-CAMs are capable of promoting axonal extension over a variety of cells such as astrocytes, Schwann and muscle cells (Brackenbury et al., 1987; Chiba and Keshishian, 1996) and also play a role in regulating the effect of growth factor signalling molecules (Ditlevsen et al., 2008). At the target location N-CAMs have an important and diverse role in synaptogenesis, and continue to regulate synaptic plasticity associated with learning and memory in the adult (Doherty et al., 1995).

N-CAMs

There are three major isoforms of N-CAMs in humans, classified by their apparent molecular weight, N-CAM 180 is expressed mainly on neuronal cells, whereas N-CAM-120 is associated with glial cells and the third isoform N-CAM 140 is expressed by both neuronal and glial cells (Noble et al., 1985). The extracellular domain of all three isoforms consists of five Ig domains and two FN-III domains, whereas the intracellular domains vary, isoform 140 is GPI anchored, whereas 120 and 180 isoforms have a cytoplasmic domain. The optional insertion of a variable alternative spliced exon (VASE) in the fourth Ig domain and posttranslational addition of poly-sialic acid (PSA) to the fifth Ig domain further modifies the N-CAM family. Expression of PSA decreases during development and is only found in areas with a high degree of plasticity in the adult. In contrast the VASE exon increases

during development, leading to the hypothesis that an increase in VASE expression and a decrease in PSA act in concert to switch N-CAM from a plasticity-promoting molecule to a stability-promoting molecule. The decrease in PSA allowing the formation of a more compact "zipper like" interaction between Ig domains 1&3 and both Ig 2 domains as the N-CAM molecules form homophilic transmembrane (*trans*) interactions, whereas PSA-N-CAMs are less tightly packed in a "one-dimensional zipper" that favours association with the fibroblast growth factor receptor FGFR (Ronn et al., 2000).

The cytoplasmic domains of N-CAM 140 and 180 have no known catalytic activity *per se* to initiate an intercellular signalling pathway so are reliant on extracellular and intracellular binding partners to activate downstream signal complexes. The FGFR plays an essential role in N-CAM mediated axonal extension ((Kiselyov et al., 2003; Neiiendam et al., 2004; Saffell et al., 1997). Whilst the exact mechanism of N-CAM activation of FGFR is not fully understood, it is hypothesised that 85% of N-CAM is present on the cell surface as a dimer, once activated by a *trans* N-CAM homophilic interaction clusters of FGFR bound N-CAM molecules increase the local concentration of FGFR enabling dimerization and activation of the FGFR (Kiselyov et al., 2005). N-CAM 140 and 180 are found both within and outside lipid raft areas of the membrane. Raft-associated N-CAM 140 can signal independently of the FGFR, probably via the FYN/FAK complex, raft-excluded N-CAM 140 signals mainly via the FGFR (Niethammer et al., 2002). N-CAM 180 and 140 are targeted to lipid rafts due to palmitoylation of four residues in the intracellular juxtamembrane region whereas N-CAM 120 is assumed to locate to lipid rafts via its GPI anchor (Neiiendam et al., 2004).

L1

L1 is another IgSF transmembrane glycoprotein comprising of 6 Ig domains and 5 FN III repeats (Brummendorf and Rathjen, 1996) and is crucial for axon elongation. L1 is regulated by being internalised into the central domain of the growth cone and then recycled back to the leading edge, where it is phosphorylated by a raft associated Src kinase allowing it to remain on the cell surface (Kamiguchi, 2006a). L1 is required for the correct formation of the pyramidal tract, connecting cerebral cortical motor neurons and interneurons to the spinal cord. Neurons from L1

deficient mice were found not respond to the repulsive signal Sema 3A secreted from the ventral spinal cord, suggesting cross-talk occurs between L1 and Sema3A signalling pathways during axon guidance in the corticospinal tract. L1 was found to associate in *cis* with NP-1 through their extracellular domains to become an essential part of the NP-Plexin-Sema3A receptor complex (Castellani et al., 2000). An additional *trans* interaction of L1 with the L1-NP-1 *cis* complex switches secreted Sema3A activity from repulsion to attraction. Co-immuno-precipitation and binding assays revealed that extracellular domains of L1 and Npn-1 interact via a specific *trans* binding site; mutational studies located the site to Ig domain 1 of L1. Thus *cis* and *trans* interactions with L1 influence the response of progressing axons to Sema 3A signalling (Castellani, 2002).

IgLON IgSF

This thesis studies how specific interactions between different members of the IgLON family of IgSF CAMs have an influence on developing axons. The name IgLON refers to three members of the family LAMP, OBCAM and Neurotrimin (Pimenta et al., 1995). Mammalian members of the IgLON family are opiate-binding cell adhesion molecule (OBCAM) (Schofield et al., 1989) limbic system-associated membrane protein (LAMP) (Brummendorf et al., 1997; Hancox et al., 1997; Wilson et al., 1996; Zhukareva and Levitt, 1995) Neurotrimin (Ntm) (Struyk et al., 1995) and the fourth member of the family, kindred-IgLON (Kilon) (Funatsu et al., 1999). In the chick there are two homologue proteins, cerebellum-Purkinje-1 (CEPU-1) for Neurotrimin (Spaltmann and Brummendorf, 1996) and Neurotractin for Kilon (Marg et al., 1999). GP55 protein is a related chick adult glycoprotein that contains a mixture of IgLONs (Wilson et al., 1996). Table, figure 1.7, gives an outline of the IgLON family.

Mammalian protein	LAMP	OBCAM	Neurotrimin	Kilon
Chick homologue	LAMP	OBCAM	CEPU-1	Neurotractin
Abbreviation	LAMP	OBCAM	Ntm/CEPU-1	KILON/Ntr
Gene name	LSAMP	OPCML	HNT	NEGRI

Figure 1.7 IgLON family members

Table illustrates members of the IgLON family of cell adhesion molecules, giving their name in mammals, the chick homologues, and abbreviations used in this thesis along with their gene name.

Structure of IgLONs

The structure of IgLONs consists of three extracellular Ig domains with a GPI anchor which locates them to lipid rafts regions on the surface of the cell membrane (figure 1.8). IgLONs are conserved, sharing a high sequence homology within the family, for example CEPU-1 has a 78% sequence homology to Ntm, 68% identity with OBCAM and 54% with LAMP (Spaltmann and Brummendorf, 1996). As a monomer IgLONs migrate to approximately 55 kDa in size on immuno-blots (Struyk et al., 1995; Spaltmann and Brummendorf, 1996; Brummendorf et al., 1997). Chick Neurotractin has an additional two Ig domain shorter isoform of 37 kDa in size (Marg et al., 1999). IgLONs are all highly glycosylated, which increases their molecular mass by > 20%. In chick there are several different isoforms of IgLON proteins; OBCAM, CEPU-1 and LAMP have α1 & α2 isoforms, which differ in that the α1 has a longer N-terminal signal peptide sequence (Lodge et al., 2000) CEPU-1 and LAMP have β isoforms, with an additional exon region adding 11 or 12 amino acid sequences downstream of the third Ig domain (Lodge et al., 2000; Spaltmann and Brummendorf, 1996). The function of this additional sequence is as yet unknown. CEPU-1 has a secreted isoform CEPU-1-Se, lacking the GPI anchor (Lodge et al., 2001). This research group has isolated a similar secreted isoform of OBCAM (unpublished data).

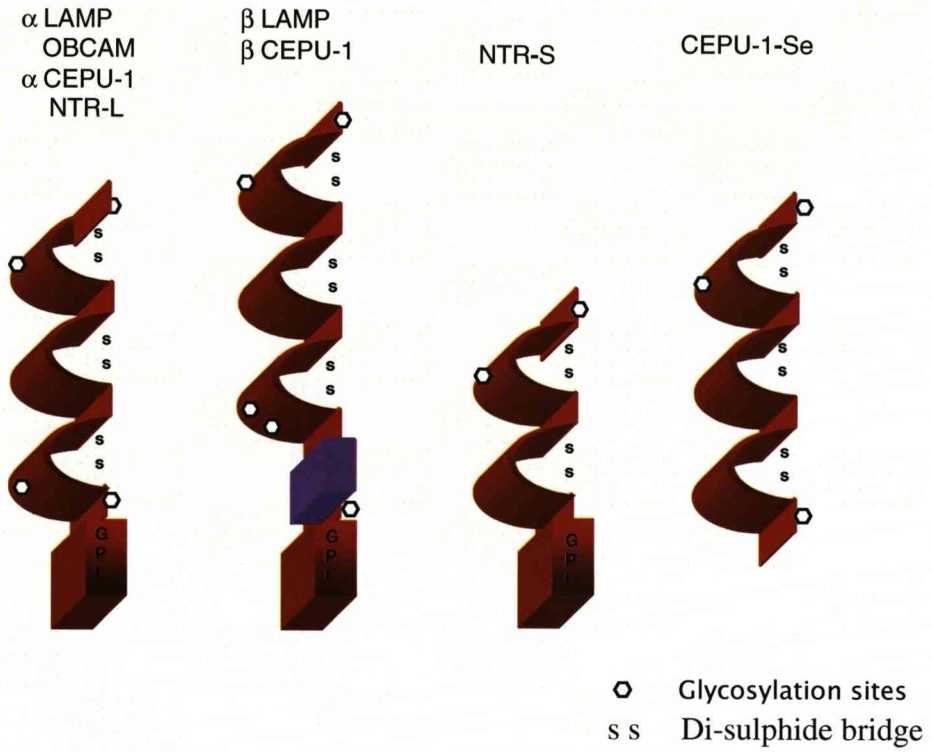

Figure 1.8 Structure of IgLON cell adhesion molecules

IgLONs predominantly have 3 Ig domains, except for a short isoform of Ntr which has only has 2 Ig domains. There are β isoforms of LAMP and CEPU-1 with an additional exon region, but no such isoform has been isolated for OBCAM. IgLONs are generally GPI anchored onto the cell membrane, but there is a secreted isoform CEPU-1 se identified lacking this GPI anchor. Figure courtesy of Mark Howard

Expression of IgLONs

Expression of the IgLON family is found throughout the nervous system both during development and in the adult. In early development IgLONs are thought to play a role in the migration and differentiation of neuronal precursors in the brain and retina, expressions increases going on to modify axonal outgrowth, finally IgLONs are proposed to be involved in synaptogenesis. Expression is relatively higher in the adult and may have a role in synapse plasticity, associated with memory and learning and in regeneration of neurons post injury. Outside of the nervous system IgLONs are thought to have an additional role acting as tumour suppressor genes.

IgLON expression during early neuronal development

In the early stages of development IgLONs are thought to be involved in differentiation of brain regions. Using double in situ hybridization, alongside specific mid-hindbrain markers, faint CEPU-1 expression was found in the anterior ectoderm region of the chick embryo, migrating mesenchyme and becomes more intense in the neural plate region. As the embryo develops CEPU-1 mRNA expression becomes located to a broad band relating to the forebrain, midbrain and anterior hindbrain areas, but by embryonic day (E) 2 narrows to a distinct band at the isthmus, or midbrain-hindbrain boundary (Jungbluth et al., 2001).

LAMP mRNA expression was detected in the anterior region of the neural tube and on most of the migrating neural crest cells, whereas CEPU-1 was not found in these areas. At the level of the trunk, LAMP was detected in the notochord, moving on to the floor plate. These results suggest IgLONs may be involved in the interaction and segregation of neuro-epithialium and neural crest cells (Kimura et al., 2001). At this early stage of development the expression of IgLONs is similar to that of several important receptor molecules including Wnt1, FGF8, EphB3, so the authors suggest IgLONs could potentially be functioning as part of a receptor complex (Kimura et al., 2001).

Our research group has in situ hybridization data showing expression of CEPU-1, OBCAM and LAMP IgLONs in the notochord of E3 chick embryos with CEPU-1/CEPUse and OBCAM being expressed by the floor plate, suggesting IgLONs may be associated with inducing the differentiation of neural plate midline

cells into the floor plate. Expression of the fourth IgLON, Neurotractin, was not found at this early stage of development in this study (Sahar Youssef PhD thesis Liverpool University 2006).

IgLON expression during axonal development

As the embryo develops, expression patterns of IgLONs suggest they may play a role in modifying axonal development. In the brain, LAMP is expressed primarily by cortical and subcortical neurons of the limbic system and medial nucleus of the thalamus, parts of the brain ultimately associated with cognitive behaviour, learning, memory and autonomic function (Levitt, 1984; Horton and Levitt, 1988; Pimenta et al., 1996; Reinoso et al., 1996). The early restricted expression pattern of LAMP in the thalamo-cortical regions was proposed to be responsible for selectively guiding axons to specific regions of the cerebral cortex. LAMP was suggested to attract limbic thalamic axons expressing LAMP and repel nonlimbic thalamic axons, which do not express LAMP (Mann et al., 1998). However, no obvious differences were observed in axonal projections in the knock out mouse to support a role for LAMP in axonal path finding (Catania et al., 2008) Ntm (CEPU-1) is highest in primary sensory and motor regions of the rat brain. Expression appears to be restricted to post mitotic neurons with increased expression around E15 in the rat forebrain (Struyk et al., 1995; Gil et al., 2002). OBCAM expression is predominantly in the cerebral cortical plate and hippocampus regions of the brain (Struyk et al., 1995; Miyata et al., 2003b). Kilon (Ntr) is detected at embryonic stage E16 in rat brain and gradually increases during development. Kilon is found in the cortex and throughout the hippocampus in early postnatal rats. Expression alters in the adult as levels of Kilon decrease in the cortex, but remain high in the cerebellum and dentate gyrus region of the hippocampus. The dentate gyrus region of the hippocampus being an area where neurogenesis can take place and also where new memories form (Funatsu et al., 1999; Brauer et al., 2000). Ntr expression is found in chick on subsets of developing commissural and longitudinal axon tracts in the central nervous system, expression increasing during development and persists in the adult (Marg et al., 1999).

IgLONs also play a role in the development of the nervous system outside of the brain region. At E7 LAMP is expressed in the optic fibre layer of the chick retina

and the tectum suggesting LAMP may play a role in the development of the visual system (Brummendorf et al., 1997). At E3 CEPU-1 expression has been associated with guiding motor axons innervations of limb muscles (Kim et al., 1999).

Co-expression of IgLONs

Two members of the IgLON family are often co-expression in particular areas and at specific stages of development. Kilon and OBCAM are co-expressed to a high degree in the cerebral cortex and hippocampus, both increasing post-natally (Miyata et al., 2003b) Expression of Ntm (CEPU-1) often overlaps with OBCAM especially in the hippocampus (Struyk et al., 1995). There is also a strong correlation of Ntm expression with LAMP. Ntm antibody studies suggested Ntm was present on a subset of CNS neurons taken from rat E16 dorsal root ganglion (DRG) E18 thalmus, olfactory bulb and hippocampus. When dual stained with specific antiserum LAMP co-localised with Ntm on the surface of the majority hippocampal neurons (an occasional neuron expressing Ntm alone) and 80-90% of olfactory neurons expressed both LAMP and Ntm with only 10% expressing LAMP alone (Gil et al., 2002).

IgLON expression during synaptogenesis

There is evidence that expression of IgLONs on dendrites maybe linked to synaptogenesis and the formation of functional circuits in both brain and retina. Expression pattern studies suggest a role for Ntm (CEPU-1) in the formation of excitory synapses during cerebellum development and their stabilization on into adulthood (Chen et al., 2001). LAMP is initially expressed on axons and dendrites in limbic brain tissue, but remains predominantly on dendrites at post-synaptic sites postnatally (Horton and Levitt, 1988; Zacco et al., 1990). Kilon has been observed on dendrites in the cerebral cortex and hippocampus and on soma of pyramidal neurons (Funatsu et al., 1999). Co-staining with post-synaptic vesicle protein synaptophysin located Ntr (Kilon) to dendrites (Schafer et al., 2005). Confocal imaging studies confirmed both Kilon and OBCAM co-localised on dendrites with the vesicle-associated membrane protein 2 (another synaptic marker protein) mainly at post-synaptic sites and on somatic synapses in both immature and adult brains (Miyata et al., 2003b). Co-expression of Kilon and OBCAM has been described in

hypothalamic magnocellular neurons, associated with neuronal secretary cells, particularly on dendrites (Miyata et al., 2000). Altering the level of expression of OBCAM on dendrites of hippocampal neurons suggested an active role for OBCAM during synaptogenesis. In these experiments specific antibody and antisense oligonucleotides inhibition of OBCAM expression significantly reduced the number of synapses, whereas over-expression of OBCAM mRNA increased the formation of synapses (Miyata et al., 2003c; Yamada et al., 2007).

Previous immuno-localisation studies on E18 retina frozen sections suggested there to be distinctive patterns of IgLON expression in the plexi-form layers of the retina, areas high in synapses. Comparison of the relative intensity of staining patterns revealed co-expression of LAMP and CEPU-1, but no OBCAM in the outer plexi-form layer where bipolar cells form synapses with photoreceptors. All three IgLONs were expressed in the inner nuclear layer on cell bodies of amacrine, horizontal and bipolar cells. Co-expression of LAMP and OBCAM was demonstrated in the inner plexiform layer where retinal ganglion cells form synapses with bipolar cells (Lodge et al., 2000). Expression of Neurotractin is also found in the plexiform layers.

OBCAM is thought to be required for post-natal development of the visual cortex, since OBCAM was one of several genes unregulated at the time of eye opening in kittens. Kittens require visual experience and accompanying synapse activity to complete this last stage in development of the visual cortex (Prasad et al., 2002).

Adult IgLON expression

IgLONs are highly expressed in various adult tissues, both within and outside of the nervous system so are not just related to development. Altered IgLON expression in the adult is beginning to emerge as having a role in cancer biology and mental health.

IgLONs have been suggested to act as tumour suppressor genes, loss of expression increasing cell division and leading to particular carcinomas. The loss of OPCML (OBCAM) gene expression is associated with epithelial ovarian cancer (Sellar 2003) and also with gliomas (Reed et al., 2007). A study comparing expression of IgLONs in epithelial ovarian tumours to normal ovarian tissue revealed

reduced gene expression of OPCML (OBCAM), LSAMP (LAMP) and NEGR1 (Kilon) but increased levels of HNT (Ntm). The loss of LSAMP and NEGR1 was correlated to the histology found in a particular type of tumour, with the reduction of LSAMP expression leaving patients with a poor prognosis (Ntougkos et al., 2005). A loss of OPCML expression and down-regulation of LSAMP has been related to familial clear cell renal cell carcinoma (Chen et al., 2007b).

IgLON expression is high in the adult limbic system and cerebral cortex linking IgLONs to synaptic plasticity during learning and the development of new memories (Levitt, 1984; Pimenta et al., 1996; Struyk et al., 1995; Funatsu et al., 1999). When LSAMP was over-expressed in rats they become anxious and less inclined to explore an elevated plus-maze, (Nelovkov et al., 2003) whereas LSAMP deficient mice were less cautious and increased their activity in exploration of a novel maize (Catania et al., 2008) suggesting IgLONs may have a role in mental health.

CEPUse secreted IgLON

There are secreted isoforms of IgLONs; however their function is as yet not well understood. Our group identified CEPUse, the secreted isoform of CEPU-1 and have unpublished data of a secreted isoform of OBCAM isolated from chick heart fibroblast culture medium. RT-PCR also detected co-expression of an alternately spliced OBCAM isoform in E3 chick embryos and E15 chick sciatic nerve which may be the secreted isoform of OBCAM (Sahar Youssef, PhD thesis Liverpool University 2006).

CEPUse mRNA is co-expressed with CEPU-1 mRNA in retina, cerebellum and DRG neurons during development and continues to be expressed in the adult cerebellum. CEPUse, in the monomeric form, demonstrated no homophilic or heterophilic interaction with IgLON-transfected CHO cell lines. However, when presented as a dimer CEPUse was able to bind to CEPU-1, OBCAM and LAMP-CHO cell lines, suggesting IgLONs must be divalent before they form a *trans* interaction. Experiments using dissociated DRG neurons were unaffected by a CEPUse/laminin substrate, but DRG explants cultured on laminin would not extend neurites to a region coated with CEPUse, suggesting CEPUse may modulate IgLON interactions. CEPUse may possibly alter dimerization, clustering of membrane bound

IgLONs to prevent *trans* IgLON interactions, or alter the recruitment of a yet unknown transmembrane receptor (Lodge et al., 2001)

In Drosophila there is a secreted IgLON isoform amalgam. Immuno-staining of whole mount embryos suggests amalgam is expressed throughout development and associates with the cell surface due to a weak hydrophobic region at the C-terminus (Seeger et al., 1988). Amalgam has three Ig domains, interacts both homophilically and heterophilically as part of a receptor complex to modulate cell adhesion and axonal outgrowth. Aggregation assays suggested the first Ig domain is responsible for amalgam homophilic interaction. Co-immuno-precipitation suggested amalgam interacts with neurotactin and this was confirmed by pull down assays in which Schneider 2 cells, transfected with neurotactin, eluted amalgam from Drosophila embryo extracts (Fremion et al., 2000). Neurotactin is a type II single transmembrane protein belonging to the cholinesterase-homologous protein family. Upon activation by amalgam the cytoplasmic region of neurotactin is thought to signal via Abl tyrosine kinase through to the cytoskeleton to modulate axonal growth (Liebl et al., 2003).

GP55 mixture of IgLONs

A glycoprotein of 55 kDa in size was isolated from adult chick brain and found to contain a mixture of IgLONs (Wilson et al., 1996). In a series of neurite outgrowth assays, forebrain and DRG neurons were unable to initiate the extension of neurites when cultured on a substrate of GP55. Furthermore, an island of GP55 provided a distinct boundary and restricted neurite outgrowth from DRG and forebrain neuronal cell bodies (Clarke and Moss, 1994; Clarke and Moss, 1997). These assays suggested IgLONs could potentially play a role as negative guidance molecules restricting axonal extension during development. Studies using the $G_{i/o}$ protein inhibitor pertussis toxin (PTX) suggested the involvement of $G_{i/o}$ proteins as part of the receptor complex involved in IgLON signalling (Clarke and Moss, 1994).

Interactions between individual IgLONs

IgLON-transfected cell lines and IgLON-FC recombinant proteins have been used to investigate the interactions between individual members of the IgLON family. Binding studies using LAMP-FC recombinant protein bound to fluorescent covaspheres confirmed a homophilic interaction for LAMP (Zhukareva and Levitt, 1995). Immuno-affinity studies of recombinant IgLON–FC proteins binding to

IgLON transfected cell lines confirmed homophilic and heterophilic *trans* interactions for CEPU-1, OBCAM and LAMP (Brummendorf et al., 1997) (Lodge et al., 2000). Ntm-FC (CEPU-1) and OBCAM-FC bound to LAMP-CHO cells, whereas no binding was observed with other IgSF molecules, NCAM, contactin, or L1 recombinant FC proteins. This suggested IgLONs bind heterophilically only within the IgLON family and not within other members of the IgSF (Gil et al., 2002). Binding studies using the fourth family member Ntr-FC (Kilon) recombinant protein with transfected CHO cell lines demonstrated the long (3 Ig) isoform of Ntr has a strong heterophilic interaction with CEPU-1-CHO, but only a weak interaction with LAMP-CHO and no homophilic interaction. The shorter isoform of Ntr also had a strong interaction with CEPU-1-CHO, but a much weaker interaction with LAMP-CHO (Marg et al., 1999). A homophilic interaction for Kilon was confirmed using immuno-affinity covaspheres, and a heterophilic *trans* interactions was demonstrated with OBCAM (Miyata et al., 2003b). The binding of recombinant proteins to transfected CHO cells showed that the homophilic interactions of CEPU-1 had a higher dissociation constant (kd) than of LAMP (Marg et al., 1999). The relative homo and heterophilic *trans* binding affinities between other IgLON family members has as yet not been tested.

There is biochemical evidence for both homo and heterophilic *cis* interactions between IgLONs. A CHO cell line expressing myc epitope tagged Ntm (CEPU-1) was cross-linked, the IgLONs released from the cell membrane into solution, captured and analysed on a western blot for a change in molecular weight. Immuno-staining with Ntm antiserum detected a molecular weight shift on the western blot suggesting non-covalent Ntm complexes had been released from the cell surface, to provide evidence for a *cis* Ntm homophilic interaction (Gil et al., 1998). Our research group has similar unpublished data of *cis/trans* IgLON interactions from cross-linking experiments. Western blots were used to compare the size of IgLON complexes released from sub-confluent CHO cells, with those released from confluent CHO cells, which have increased cell-cell contact and the potential for *trans* interactions. The sub-confluent cells provided evidence of dimeric IgLONs, particularly for CEPU-1 and OBCAM, whereas the confluent CHO cells had strong evidence for the formation of larger dimeric and tetrameric complexes for CEPU-1 OBCAM, but weaker evidence for LAMP complexes. On the surface of sub-confluent cells (with reduced cell-cell contact) IgLON were most likely to be

forming *cis* homodimeric complexes, whereas on the confluent cells the increased cell-cell contact produced larger complexes most likely due to the formation of *trans* homotetrameric complexes. Immuno-staining of western blots of IgLONs released from cross-linked rat brain cortical tissue gave a significant shift in molecular size, consistent with the size of two IgLONs, to provided *in vivo* evidence for IgLON *cis* complexes (Miyata et al., 2003b).

Using domain deletion, antibody perturbation and covasphere binding analysis the function of each individual Ig domain interaction was investigated. IgI domain was suggested to enhanced LAMP-induced outgrowth, whilst IgII domain was thought to be the heterophilic binding site involved in neurite inhibition, but required IgI&III domains for biological activity, with no specific role described for IgIII domain (Eagleson et al., 2003)

Function of IgLONs

From the evidence that individual members of the IgLON family bind homo and heterophilically in *trans*, possibly also in *cis,* axons expressing IgLONs would be expected to bind to an IgLON substrate. However, in a series of adhesion and outgrowth experiments the ability of chick axons to bind to, and be affected by, single IgLON substrates gave results that were confusing and rather inconsistent. DRG neurons displayed some preference for adherence to CEPU-1-FC over OBCAM-FC, but there was very little adhesion to LAMP-FC. Adherence of sympathetic neurons was slightly increased on CEPU-1-FC substrate, but there was no significant adhesion to OBCAM-FC or CEPU-1-FC. DRG and sympathetic neurons express LAMP, CEPU-1 and low levels of OBCAM (Wilson et al., 1996; Lodge et al., 2000) so they would be expected to adhere to all IgLON substrates including LAMP through heterophilic *trans* interactions with their surface IgLONs.

Furthermore, initiation of neurite outgrowth from DRG neurons was unaffected when single IgLON-CHO cells and individual IgLON-FC proteins were used as a substrate. Even a mixture of IgLON-FC recombinant proteins had no effect on neurite outgrowth (McNamee et al., 2002). This was unexpected since adult GP55 protein (containing a mixture of IgLONs) was able to inhibit initiation of neurite outgrowth from DRG and forebrain neurons (Clarke and Moss, 1994; Clarke and Moss, 1997).

Other groups have tried to elucidate the function of individual members of the IgLON family with varying results. Telencephalon neurons, with high expression of Ntr, were cultured on Ntr-FC. The long 3 Ig isoform of Ntr-FC promoted adhesion, but had no significant effect on promoting neurite extension, whereas the 2 Ig short isoform mediated only weak adhesion interaction with CEPU-1-CHO and an even weaker interaction with LAMP-CHO (Marg et al., 1999). In a stripe assay, hippocampal neurons appeared to prefer the long Ntr isoform substrate (Schafer et al., 2005)

In vitro outgrowth assays comparing LAMP expressing limbic neurons to non-limbic neurons (not expressing LAMP) showed LAMP promoted adhesion and branching of limbic axons, but reduced branching from non-limbic axons, however LAMP was not essential for outgrowth of limbic fibres *per se* (Zhukareva and Levitt, 1995). Stripe assays comparing outgrowth from limbic thalamic with that from cortical neurons on recombinant LAMP-FC protein suggested LAMP displayed a bi-function activity, attracting limbic thalamic axons by homophilic interaction; whilst repelling nonlimbic thalamic axons. LAMP was proposed to be preventing those axons not expressing LAMP from innervating inappropriate regions in the limbic cortex (Mann et al., 1998).

Ntm-FC protein bound homophilically in *trans* to rat DRG and hippocampal axons expressing Ntm (Zhukareva and Levitt, 1995; Gil et al., 1998). Ntm was also suggested to have a bifunctional effect on neurites, supporting DRG and to a lesser extent hippocampal axonal outgrowth, but inhibiting neurite outgrowth from sympathetic neurons (not expressing Ntm). Cultures of DRG neurons (expressing Ntm, but lower levels of LAMP or OBCAM) on a substrate of LAMP-CHO cells had reduced length of neurite outgrowth which suggested a heterophilic *trans* interaction between Ntm and LAMP had inhibited neurite extension (Gil et al., 2002).

In all these experiments enhancement of neurite length was minimal (~10-12%) possibly not significant enough to direct axonal outgrowth *in vivo*. The experiments used recombinant proteins which may have an altered conformation to IgLONs found *in vivo*, since the FC portion may prevent IgLON heads forming complexes. So far, individual IgLONs have not been able to replicate GP55 inhibition of adhesion or outgrowth of neurites and no definite function in axon guidance has been established for single IgLONs.

Aim of thesis

This thesis focuses on the homo and heterophilic interactions between CEPU-1, OBCAM and LAMP. The proposal is two different members of the IgLON family form *cis* heterodimers on the surface of axons. *Trans* interactions between heterodimeric IgLONs then go on to inhibit the initiation of neurite outgrowth from forebrain neurons.

Since IgLONs are widely expressed both within and outside of the nervous system, play a role during development and have a function in adulthood, understanding how they interact may help provide advances in various fields; including neurodegenerative conditions, mental health and cancer biology.

In this thesis *cis* interactions describe those within the plane of the membrane, as opposed to *trans* interactions which form between the axon and the extracellular environment. *Cis* and *trans* interactions can be homophilic, between the same molecule, and heterophilic, between different molecules (figure 1.9).

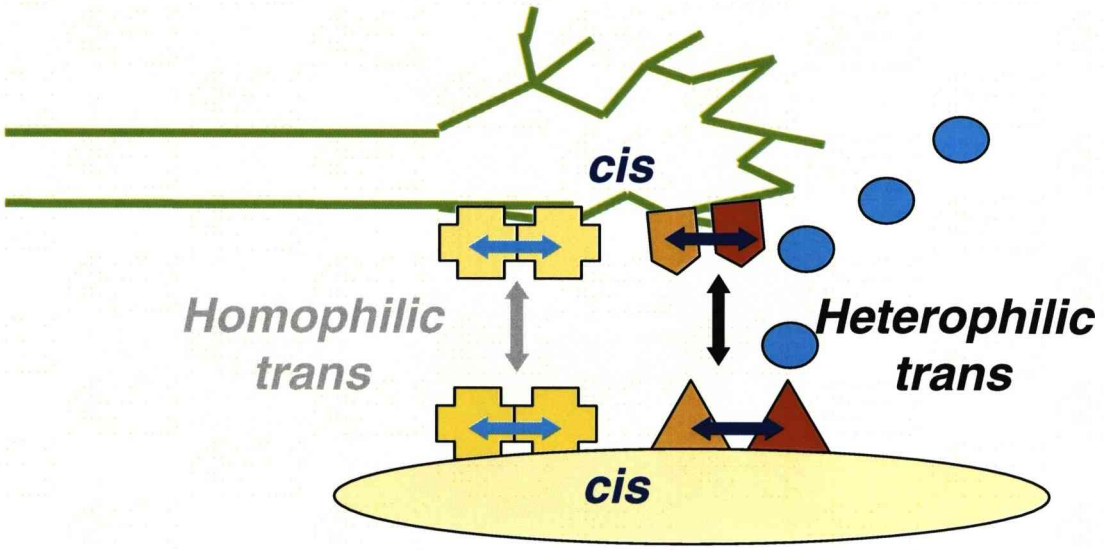

Figure 1.9 Cis and trans molecular interactions

Interactions that occur within the plane of the membrane are described as cis interactions, whereas transmembrane (trans) interactions occur between molecules on opposing membranes. The yellow crosses represent homophilic interactions i.e. between the same members of the IgLON family occurring in cis (light blue arrows). The orange block arrows and triangles represent heterophilic interactions between two different members of the family, as a receptor (block arrows) or as a ligand (triangle in cis (dark blue arrows). The cis complexes form additional homophilic and heterophilic trans interactions between adjacent membranes (grey and black arrows). Blue circles are secreted molecules in the extracellular environment that interact with cis and trans complexes to further modify axonal development. Specific temporal and spatial expression of molecules in the extracellular environment (blue circles, darker yellow crosses and orange triangles) and expression of their associated receptors on the surface of growth cone (light yellow crosses and orange block arrows) are all involved during development of the nervous system.

Chapter Two

Material and Methods

MATERIALS AND METHODS

2.1. IgLON-FC recombinant protein production

Recombinant IgLON- FC recombinant proteins were prepared from transfected cell lines (Howard et al., 2002). To prepare these cell lines individual IgLON sequences, for α2βCEPU-1(Z72497) α2OBCAM (Y08170) and α1LAMP (Y08171) (GenBank accession numbers) minus their GPI anchor and stop codon were cloned into the pIG plasmid vector which contained the FC sequence, plus a signal sequence (kind gift from Frank Walsh). Once translated, omission of the GPI anchor sequence prevented the IgLON locating to the cell membrane; omission of the stop codon added an FC sequence directly onto the IgLON, the additional signal sequence then direct expression of the recombinant IgLON-FC protein for secretion. The recombinant protein sequence was sub-cloned into pcDNA3 (Wilson et al., 1996; Lodge et al., 2000). Linearized pcDNA3 plasmids containing the CEPU-1-FC and OBCAM-FC IgLON sequences was electroporated into J588L mouse myeloma cells; and the transfected myeloma cells were selected by G418 antibiotic resistance.

CEPU-1 and OBCAM-FC expressing myeloma cells were cultured in a Vivascience miniPERM bioreactor to produce approximately 1-10mg protein/100ml culture medium (Howard et al., 2002). Briefly, the myeloma cells were cultured in the bioreactor for 7 days and the culture medium was harvested, cell debris was removed by centrifugation and filtration through a 0.45 um pore filter, and COMPLETE^{TM} protein inhibitor cocktail (PIC Promega) was added to prevent endogenous protease activity. The pH of the medium was adjusted to 8.0 with 2 M trizima base pH 8.0 and passed through a Protein A agarose (Sigma) bead column to purify the recombinant protein from the culture medium. The column was washed with 10 mM trizima base pH 8.0 buffer and recombinant protein was eluted from the column in fractions by adding 0.2 M glycine at pH 2.5. The pH of the protein fractions was adjusted back to pH 8 with 2 M trizma base pH 8.0 and the fractions were analysed for IgLON-FC recombinant proteins.

Preparation of LAMP-FC protein

LAMP-FC was produced from transfected CHO cell lines cultured for 4 days in 150cm dishes in medium containing 5% low IgG serum (Hyclone) by the same method. 2µl of each fraction was dot blotted onto nitrocellulose and stained with 1:10,000 LAMP specific antiserum followed by 1:10,000 horseradish peroxidise conjugated rabbit anti rat antibody (Dako) diluted in western blocking buffer containing 1% Bovine serum Albumin (BSA) figure 2.1.A. The fractions containing LAMP-FC were pooled and the protein concentration measured using Invitrogen Quantit™ system and the purity of LAMP-FC assessed by non-reduced LDS-PAGE using the Invitrogen NUPAGE™ 3-8% Tris-acetate gel system. Gels were stained with 1% Coomassie blue dye in 20% methanol plus 10% glacial acetic acid; excess stain removed with 20% methanol plus 10% glacial acetic acid. Coomassie protein staining of LDS-PAGE separation of purified proteins from culture medium revealed a single major protein band of 120 kDa, suggesting LAMP-FC, CEPU-1-FC and OBCAM-FC recombinant proteins were the main proteins eluted by protein A agarose beads figure 2.1.B. Analysis by western blot (section 2.13) stained with LAMP specific antiserum, confirmed that the major band was LAMP-FC protein figure 2.1.C. Similar western blots confirmed the production of CEPU-1-FC and OBCAM-FC recombinant proteins (data not shown).

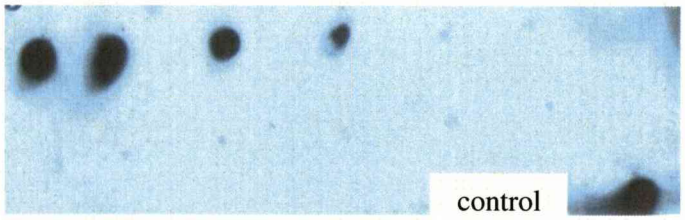

Figure 2.1.A Dot Blot identification of fractions containing LAMP-FC

After 4 days incubation culture medium was collected from LAMP-FC-CHO cells and recombinant LAMP-FC protein was purified from the culture medium on a Protein A column in fractions of 0.5ml. 2 ul amounts of each fraction was Dot blotted onto nitrocellulose, along with 2 ul of a LAMP-FC positive control and stained with LAMP rat antiserum (details section 2.2) followed by HRP conjugated rabbit anti rat antibody, at dilutions of 1:10,000, visualised with chemiluminescence and exposure to Kodak film. LAMP-FC was detected in the first four fractions so these were pooled and further analysed.

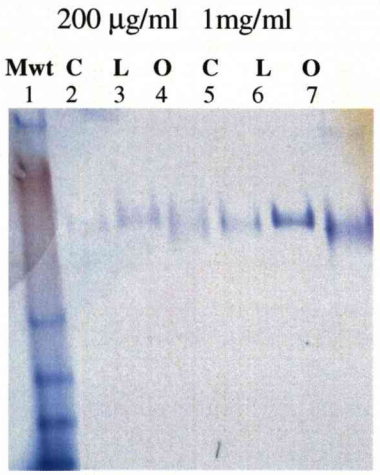

Figure 2.1.B Coomassie staining of LDS-PAGE separated proteins

Proteins eluted from CEPU-1-FC, LAMP-FC and OBCAM-FC (C, L, O) expressing cells at concentrations of 200 µg/ml in lanes 2-4 and 20 µl samples of 1mg/ml in lanes 5-7, were evaluated on a LDS-PAGE stained with Coomassie blue protein dye. When compared to Invitrogen molecular weight marker See Blue™ lane 1, the single protein bands were ~120 kDa in size, the size expected IgLON-FC recombinant proteins. Since there was only one predominant band of at each concentration the protein prepared from culture medium appeared to be predominantly IgLON-FC and not to be significantly contaminated with other non-specific proteins.

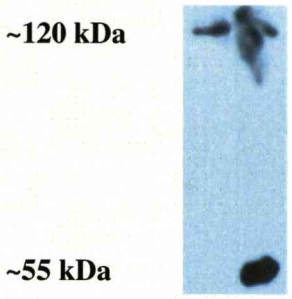

Figure 2.1.C Western blot identification of LAMP-FC protein.

Lane 1 contains 10 µl of the pooled protein fractions isolated from the LAMP-FC-CHO cell medium by the Protein A column. Lane 2 contains a 5 µl sample of monomeric LAMP as a positive control for the LAMP rat antiserum (monomeric LAMP being prepared by PiPLC enzyme digestion of LAMP from the surface of LAMP-CHO cells, details section 2.12). LAMP specific rat antiserum detected monomeric LAMP ~55 kDa in size in the PiPLC supernatant and LAMP~120 kDa in size in the pooled isolated protein fractions lane 1 (sizes compare to molecular weight marker not shown). This western blot confirmed the major protein ~120 kDa in size highlighted on the previous Coomassie gel as being LAMP-FC.

2.2. Polyclonal IgLON antisera production

Briefly 50 μg of recombinant proteins CEPU-FC, LAMP-FC and OBCAM-FC were used for initial sub- cutaneous inoculation, and as subsequent boost injections, into individual Wistar strain male rats. Specificity of each antisera obtained was determined by PAGE and western blotting against CEPU-1, LAMP and OBCAM individual IgLONs (Wilson et al., 1996; Lodge et al., 2000). Covlab laboratories commercially produced polyclonal rabbit CEPU-1 and OBCAM antisera from respective IgLON -FC proteins.

2.3. Tissue culture of CHO-cell lines

CHO cell lines were routinely cultured in Dulbecco's modified Eagle's medium DMEM/F12 medium plus Glutamax (Sigma) containing 5-10% foetal calf serum, (Hyclone/GIBCO) 2 mM glutamine (GIBCO) 100 U/ml penicillin and 100 μg/ml streptomycin (GIBCO) in 5% CO_2 atmosphere, at 37°C. Once confluent, cells were washed in Hanks balance salt solution minus calcium and magnesium ions (HBSS (-), GIBCO) and routinely passaged by trypsinization in 1% trypsin/EDTA (GIBCO) in HBSS (-) and reseeded at a ratio of 1:5 to 1:10 every 3-7 days. For some experiments cells were counted using a Haemocytometer and plated at a specific density.

2.4. Preparation of IgLON-CHO cell lines

Briefly α2βCEPU-1, α2 OBCAM and α1 LAMP cDNAs were cloned into pcDNA3 plasmid vectors (Lodge et al., 2000). Wild type Chinese hamster ovary-K1 cells (WT-CHO) were transfected using Effectene (Qiagen) reagent with the individual IgLON plasmid vectors. CHO cells expressing the IgLON-pcDNA3 plasmids were selected due to accompanying antibiotic resistance by culturing in DMEM/HAMs F12 growth medium containing 400 μg/ml G418 antibiotic (McNamee et al., 2002). Confirmation of 100% stable transfection of the cell lines was by immuno-cytochemistry (figure 2.6.1). One hour after plating the CHO cells were live stained with specific IgLON antiserum to confirm IgLONs were trypsin insensitive and were still expressed on the surface of the CHO cells.

2.5. Live staining of cells with IgLON-FC recombinant protein

CHO cells were cultured overnight at 37°C, 5% CO_2 atmosphere at a density of $1.5x10^4$ cells on glass coverslips in a 24 well tissue culture plate in DMEM/F12 growth medium (Sigma) containing 10% FCS (Hyclone). The coverslips were carefully removed and the CHO cells live stained, in triplicate by adding 30 µl aliquots of recombinant protein, diluted to 2.5 µg /ml in 0 Millonig's 0.12 M phosphate pH 7.4 buffer containing 1% BSA onto the coverslips. Following incubation for 20 minutes at room temperature (RT) coverslips were drained and dip washed three times in HBSS. IgLON-FC protein binding to the CHO cells was detected by incubation for a further 20 minutes at RT with 30µl of Texas-Red™-conjugated goat anti-human IgG antibody (Jackson laboratories) titred out to a dilution of 1:100 in Millonig's/BSA buffer. Coverslips were dip washed, drained and fixed by incubation for two minutes in PBS containing 2% paraformaldehyde in PBS. Following washing in HBSS and water, coverslips were dried and mounted in Dako™ mounting medium.

2.6. Live staining of cells with IgLON antisera

CHO cells were lived stained with specific antisera to confirm the presence of IgLONs on the CHO cell surface by the same method (figure 2.6.1). Triplicate coverslips were incubated with 30 µl aliquots of IgLON specific rat antisera titred out to a dilution of 1:100 in Millonig's buffer pH 7.4 containing 1% BSA. Following incubation for 20 minutes at RT antiserum binding to the CHO cells was detected by incubation for a further 20 minutes with 30µl of goat anti-rat IgG secondary antibody conjugated with Texas-Red ™ (Jackson laboratories) or in the case of rabbit CEPU-1 and OBCAM rabbit antiserum Alexa 488™ conjugated anti rabbit secondary antibody (Invitrogen) titred out to a concentration of 1:100 in Millonig's/BSA buffer. Secondary antibodies were tested with pre-immune serum and shown to be specific.

Adsorption of rat antiserum

Specificity of antiserum was tested by staining CHO cell lines with each IgLON anti-serum. Some cross-reactivity was found between CEPU-1 and OBCAM so these antibodies were adsorbed against each other. 100 µl of CEPU-1 antiserum was diluted to 1ml with 0.12 M phosphate Millonig's buffer containing 1% BSA and placed on a 9 cm tissue culture dish of confluent OBCAM–CHO cells and rocked for 1 hour at room temperature to remove antibodies recognising OBCAM from the CEPU-1 antiserum. Remaining CEPU-1 antiserum was collected from the CHO cells and further diluted 1:10, giving a final concentration of antiserum equivalent to 1:100 for subsequent staining. Similarly CEPU-1-CHO cells were used to adsorb OBCAM antiserum. LAMP did not cross-react with either CEPU-1 or OBCAM so was not adsorbed.

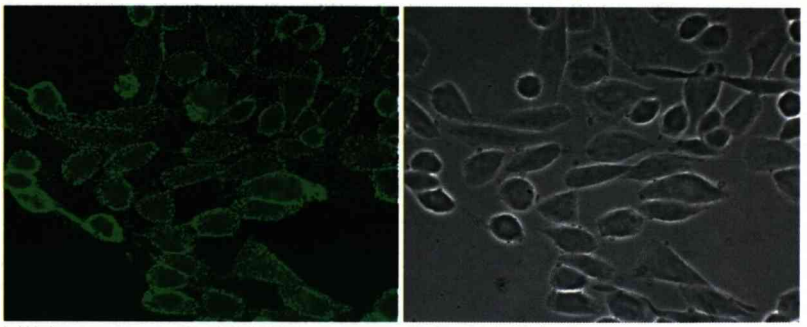

CEPU-1-CHO

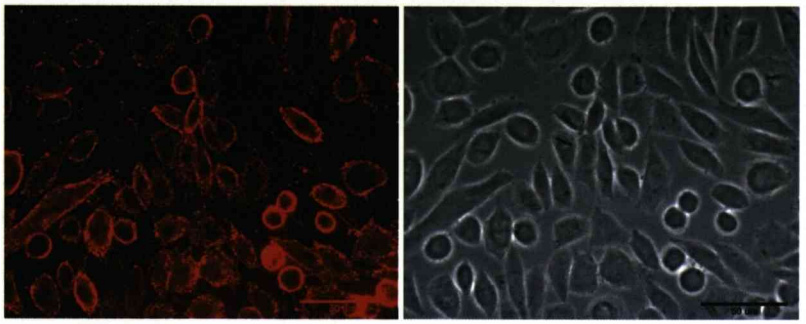

OBCAM-CHO

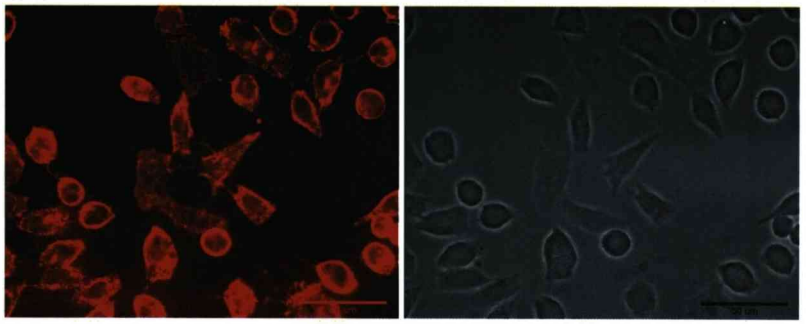

LAMP-CHO

Figure 2.6.1 Characterisation of transfected CHO cell lines.

CHO cells were stained with 1:100 dilutions of specific antisera, CEPU-1 with rabbit antiserum visualised with 1:100 dilution of Alexa 488™ conjugated goat anti rabbit secondary antibody, whereas OBCAM and LAMP were stained with rat antisera, and visualised by 1:100 goat anti rat Texas Red™ conjugated secondary antibody. The first photomicrograph of each pair was taken using Metamorph™ software on a LEICA LEITZ DM microscope at x40 magnification under oil. The second, phase contrast image, taken in parallel, highlights all the CHO cells on the coverslips. Comparison of the two photomicrographs reveals all the CHO cells to be positively stained and so indicates the CHO cell lines are 100% transfected to express their respective IgLON.

2.7. Fluorescent microspheres aggregation assay

IgLON homophilic interactions were measured by fluorescent microspheres aggregation. Carboxylated, polystyrene microspheres (Polysciences Inc) 1 μm in diameter, labeled with fluorescein (excitation max. 445 nm, emission max 500 nm) or brilliant blue (excitation max. 365 nm, emission max 435 nm) were covalently coupled with 400 μg/ml recombinant protein G (Calbiochem) using the carbodiimide method. Briefly the protocol (Polyscience data sheet 238C) to covalently couple proteins to the microspheres involved washing 0.5 ml of 2.5% microspheres suspension in 0.1 M sodium carbonate buffer (pH 9.6) followed by re-suspension in 625 μl of 0.2 M sodium phosphate buffer (pH 4.5). The microspheres binding sites were activated by adding 625 μl freshly prepared 2% carbodiimide (1-3 dimethylaminopropyl-3-ethyl carbodiimide hydrochloride dissolved in phosphate buffer) to the microspheres drop wise, followed by incubation for 4 hours at RT with end-to-end mixing. The microspheres were washed in 0.2 M sodium phosphate buffer (pH 4.5) three times to remove any un-reacted carbodiimide, and finally re-suspended in 1 ml sodium borate buffer pH (8.5). Un-reacted sites on the microspheres were blocked by adding 50 μl ethanolamine 2-aminoethanol and mixing gently for 30 minutes at RT. The active protein binding sites on the microspheres were bound with protein G by overnight incubation in 400 μg/ml protein G (Sigma) at RT with end-to-end mixing. The microspheres were washed in borate buffer to remove excess protein G and any non-specific protein binding sites on the microspheres were blocked by adding 1 ml borate buffer containing 5% ovalbumin for 30 minutes at RT with end-to-end mixing. Microspheres were sonicated and a 20% suspension of single microspheres was prepared in 100 μl borate buffer. Individual aliquots of beads were incubated with 2.5 μg of each of the IgLON-FC recombinant proteins at RT with gentle agitation for 15 minutes. Individual 20 μl aliquots of microspheres bound with IgLON-FC protein were diluted with 1 ml FACS Flow™ running buffer (Becton Dickenson) and analyzed using the Becton Dickenson fluorescent activation cell sorting, (FACS) Vantage™ SE equipped with a laser configured to 488 nm ultraviolet light (Coherent Enterprise) and a model 127 He/Ne laser to 633 nm (Spectra-Physics). The number of microspheres remaining single as opposed to the number aggregated into clumps was determined by analyzing 10,000 events per sample using Cell Quest™ Pro 4.0

(Becton Dickenson) software. Data was analyzed with SPSS using one-way analysis of variance (ANOVA) and PRISM software to present data. Negative controls of microspheres coupled with only protein G, and coupled with protein G plus Ox40 human immunoglobulin were tested alongside those bound with IgLON proteins. Ox40 protein was kindly donated by Dr. Stuart Marshall-Clarke, Department of Human Anatomy and Cell Biology, Liverpool University.

2.8. ELISA assay

ELISA assay measured IgLON homo and heterophilic *trans* interactions. WT-CHO control cells, and CHO cell lines expressing single CEPU, LAMP and OBCAM IgLONs on the cell surface were plated out in triplicate at a density of $3x10^4$ cells/well into a 96 well tissue culture plate and cultured overnight in CHO cell culture medium at 37°C, 5% CO_2. The culture medium was removed and replaced with 40 µl of individual IgLON-FC recombinant proteins, diluted to 0 µg, 0.1 µg, 1 µg and 10 µg/ml in CHO cell culture medium. Following incubation for one hour at RT excess recombinant IgLON-FC protein was removed and the individual wells washed carefully three times with Dulbeccco phosphate buffered saline (PBS GIBCO pH 7.4). The cells were fixed with PBS containing 4% paraformaldehyde, plus 120 mM sucrose for 15 minutes and then washed with PBS. IgLON-FC protein binding was detected by incubation for one hour at RT with 40 µl of goat anti-human FC horseradish peroxidise (HRP) conjugated antiserum, diluted to 1:5000 with growth medium. Duplicate washes with PBS followed by 0.05 M phosphate-citrate buffer pH 5 containing 0.03% sodium perborate (Sigma, 1 capsule dissolved in 100 ml deionised water) removed any excess secondary antiserum. Freshly prepare 0.1 mg/ml 3,3',5,5'-titramethylbenzidine dihydrochloride (TMB) substrate (Sigma, 1 mg/ml TMB substrate tablet dissolved in 10 ml phosphate-citrate buffer) was added at 75 µl/well and incubate at RT for 30 minutes. The reaction was terminated using 25 µl of 1 M H_2SO_4 (Merck). ELISA plates were then analysed using a jBIO LP 400 ELISA plate reader at an absorbance wavelength of 450 nm. Visualisation was by HRP enzymatic activity producing a colour change in the TMB substrate; thus the amount of bound recombinant protein was directly related to the absorbance wavelength of 450 nm (Liem et al., 1979). The experiment was repeated three times and data was analysed using the Prism programme.

2.9 Construction of pOIG plasmid vector

Plasmids OBCAM-IRES-GFP (pOIG) and LAMP-IRES-GFP (pLIG) were constructed by introducing chicken α 1OBCAM sequence (GenBank accession number AF292934) and chicken α 1LAMP sequence (GenBank accession number Y08171) into the PCaβlinkmigiresEGFPm5Cla1, (pIRES-GFP) plasmid vector (figure 2.9.1). The pIRES GFP plasmid vector was a gift from Jon Gilthorpe, Department of Developmental Neurobiology, King's College London. In this vector the β-actin promoter is located upstream of an internal ribosome entry site (IRES) and controls expression of the IgLON sequence and enhanced green fluorescent protein (EGFP). All molecular biology products were from Invitrogen unless otherwise stated.

Cloning strategy

Restriction sites *Not1 and Cla1* were required at the 5' and 3' ends of the OBCAM sequence to enable cloning of the sequence into the pIRES-GFP vector (figure 2.9.2). To prepare the OBCAM sequence for the first cloning step into pSlax an *Nco 1* site had to be introduced at the 5' end of the OBCAM sequence prior to the start site. Polymerase chain reaction (PCR) primer sequences were designed to contain a mismatch to the original α1OBCAM sequence to generate the required *Nco*-1 restriction enzyme site in an open reading frame upstream of the α1OBCAM start sequence. PCR on pCDNA3 plasmid containing the α1OBCAM sequence DNA with these primers generated the OBCAM 1046 base pair (bp) sequence modified with an *Nco 1* site.

PCR to construct pOIG plasmid vector

forward primer:- 5'-TGGCTGTCGACCATGGGGGTC-3' and

reverse primer:- 5'-ATCAAAAGTCGAGGAGGAGGCG-3'

Red bases at the start of the sequence denoting the mismatched sequence that generated the *Nco1* restriction site.

PCR reaction:-

0.1 µg – 0.001 µg Plasmid DNA	1 µl
10mM dNTP mix	1 µl
10µM of both forward and reverse primers	1 µl
50 $MgCl_2$	1.5 µl
10 Taq polymerase buffer	5 µl
HotStar Taq polymerase	0.25 µl
PCR grade water	make total to volume 50µl

A negative control minus DNA was also prepared. PCR reaction of 30 cycles at 58°C followed by 72°C in a Hybaid Sprint ™ thermal cycler amplified the α1OBCAM DNA sequence.

PCR reaction times were:-

Temperature	Time	Cycles	Function
94°C	10 minutes	1	activation of Taq
94°C	1 minute		denaturing DNA
58°C	1 minute	30	annealing primer
72°C	2 minutes		strand extension
72°C	10 minutes	1	strand completion

Taq polymerase has a terminal transferase activity which adds a single deoxyadenosine base to the 3' ends of the PCR product. The linearized pCR 2.1 TOPO™ vector has a single 3' deoxythymidine base overhang which allows PCR products to be ligated efficiently into the vector.

Analysis of DNA by agarose gel electrophoresis

PCR products with were mixed with 2 µl of x5 Blue juice™ Invitrogen loading buffer plus 1 µl/sample SYBR™green DNA dye (Sigma) and loaded onto a 1% agarose gel prepared and separated in electrophoresis TAE buffer containing 40 mM Tris-acetate 1mM EDTA (50x stock 242g Tris base 57.1 ml glacial acetic acid, 100 ml 0.5 M EDTA pH 8.0 per liter). PCR product DNA was visualized by UV excitation of SYBR™green at a wavelength of 586 nm and emission of 605 nm. Comparison with molecular weight markers identified the PCR product as being the expected size of ~1.1 kbp, (results figure 2.9.3)

Recovery of DNA from agarose gel

PCR bands were excised from the agarose gel under UV light with a razor blade and gel slices microfuged at top speed through a glass wool column to shatter the gel and release the DNA. DNA was precipitated from the fractionated gel with 1:10 volume of 3M sodium acetate and 2 volumes ethanol, incubated at -80°C for a minimum of 1 hour and pelleted from solution by centrifugation at 15,000 x g for 30 minutes. DNA pellet was air dried and resuspended in 50 µl sterile de-ionised water.

Ligation of PCR product into pCR 2.1 TOPO™ vector

PCR product was TA cloned into pCR 2.1 TOPO™ vector using the Invitrogen TOPO TA™ cloning kit. 2 µl PCR DNA, was incubated with 1 µl TOPO™ vector, 1 µl TOPO™ salt buffer; and 2 µl sterile water at RT for 5 minutes, placed on ice for 20 minutes and used to transform Top 10 F' competent bacteria.

Plasmid transformation of competent bacteria

Top 10 F' competent bacteria were thawed on ice and 2 µl of the ligation reaction was gently mixed into the bacteria cells. After a further incubation for 15 minutes on ice the cells were heat shocked for 30 seconds in a water bath at 42°C. 250 µl of SOC medium was added to the competent bacteria and incubated on a shaker at 200 rpm for 1 hour at 37°C.

Plasmid selection

Post incubation 10 and 100 µl of transformed bacteria were selected on Luria broth (LB) agar plates containing 50 µg/ml ampicillin. The plates were pre-treated by spreading with 40 mg/ml X-gal and 100mM IPTG to permit blue/ white screening of colonies. Top 10 F' bacteria contain the *lac* repressor gene so those bacteria containing the ligated plasmid (i.e. plasmid plus PCR insert) will express *lac* gene and produce a white coloured colony. Those colonies containing an un-ligated plasmid will remain blue. Selected colonies were cultured in 5ml LB nutrient broth containing 50 µg/ml ampicillin antibiotic and plasmid DNA was prepared using a Qiagen mini plasmid preparation kit.

Restriction enzyme digestion of DNA

Bam Hl- Ncol restriction enzyme on DNA from mini plasmid preparations mapped the orientation of the insert cloned in the pCR2.1 plasmid vector (outlined in figure 2.9.4). Restriction digests were set up containing 8 µl plasmid DNA, 1 µl restriction enzyme buffer, 0.5 µl *Bam*-Hland 0.5 µl *Nco*-1 restriction enzymes and incubated for 1 hour at 37 °C and analysed on a 0.7% agarose gel (results figure 2.9.5).

The mini plasmid preparation containing the OBCAM sequence in the correct orientation in pCR2.1 was selected and digested with restriction enzymes *Ncol* and *Notl* to release the OBCAM sequence from pCR2.1 mini plasmid for subcloning into pSlax shuttle vector. This sub-cloning would add the additional restriction enzyme site required for the final cloning into the IRES-GFP plasmid vector. Commercial DNA sequencing confirmed that colony 6 contained the OBCAM PCR product cloned into pCR2.1 in the required orientation.

Sub-cloning of DNA insert into a plasmid vector

Nco-1 and *Not*-1 restriction enzymes digested the pSlax vector and the OBCAM PCR product DNA from pCR2.1 plasmid in 20 µl reactions. Following incubation at 37 °C for 1 hour the digested DNAs were separated by electrophoresis on a 0.7% agarose gel, the bands excised and DNA collected using a glass wool column and concentrated by ethanol precipitation (results figure 2.9.6).

Ligation of DNA insert into a plasmid vector

The DNA concentration of plasmid and DNA insert was calculated using Invitrogen Quantit™ and the amount of DNA required for the ligation reaction was calculated :-

$$\frac{\text{ng of vector} \times \text{kb size of insert}}{\text{kb size of vector}} \times \text{molar ratio or } \frac{\text{insert}}{\text{vector}} = \text{ng of insert}$$

Incubation of a ratio of 6:1 OBCAM insert: pSlax vector overnight at 14°C with T4 ligase enzyme ligated the OBCAM insert into the pSlax vector. Top 10 F' competent bacteria were transformed with 1 µl of this ligation and transformed bacteria selected on agar plates containing 50 µg/ml ampicillin antibiotic.

STET preparation of plasmid DNA

Selected colonies were cultured overnight in 5 ml LB broth containing 50 μg/ml ampicillin. 1 ml culture was pelleted and plasmid DNA released by incubation for 5 minutes in 350 μl STET buffer containing 8% sucrose, 5% Triton X-100, 50 mM EDTA pH 8.0, 0.1 M Tris HCL pH 8.0 and 25 μl of 1 mg/ml lysozyme enzyme, followed by heating at 95°C for 3 minutes. Plasmid DNA was precipitated with 350 μl isopropanol and microfuged for 7 minutes at top speed into a pellet and resuspended in 50 μl deionised water and heated for 10 minutes at 60°C. Screening by *Nco*-1 and *Not*-1 restriction enzyme double digestion mapping confirmed plasmid DNA contained the OBCAM insert. Qiagen mini plasmid kit was used to prepare plasmid DNA from the remaining culture. OBCAM insert was then cloned into IRES-GFP plasmid vector using *Not*-1 *Cla*-1 restriction enzymes. Confirmation of successful cloning of α1OBCAM into IRES-GFP plasmid was by restriction enzyme mapping with *Cla1-Not1* enzymes (results figure 2.9.7).

The LAMP sequence was cloned into the IRES-GFP plasmid by a similar method to produce the pLIG plasmid (Reed *et al,* 2004).

DNA sequencing and plasmid preparation

Both pOIG and pLIG were sequenced (Lark) to confirm the successful cloning of the IgLON insert into the pIRES vector plasmid. Bacterial colonies containing the pOIG and pLIG plasmid vectors were cultured and endotoxin-free plasmid preparations of pOIG and pLIG were made using a Sigma maxi plasmid preparation kit to produce DNA suitable for transfection into CHO cells.

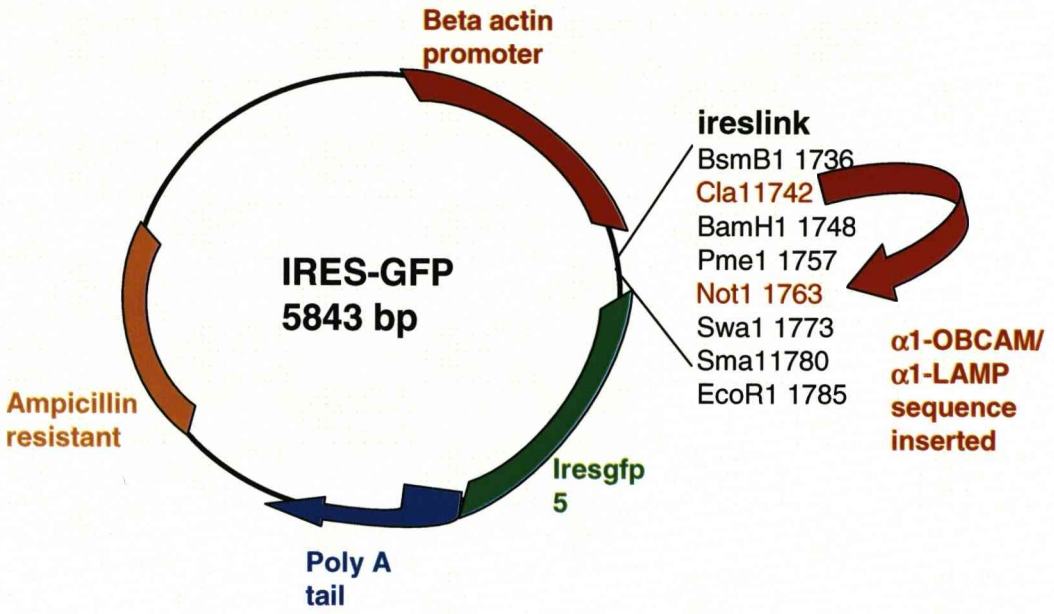

Figure 2.9.1 Diagram of pOIG and pLIG plasmid vectors

Plasmids OBCAM-IRES-GFP (pOIG) and LAMP-IRES-GFP (pLIG) were constructed by introducing α1–LAMP sequence or α1–OBCAM sequence into the pCaβlinkmigires plaEGFPCla1 plasmid vector (IRES-GFP) between Cla 1 and Not 1 restriction enzyme sites. In this vector the β-actin promoter is located upstream of an internal ribosome entry site (IRES) and controls expression of both the IgLON sequence and accompanying enhanced green fluorescent protein (GFP). Plasmid selection was via ampicillin resistance.

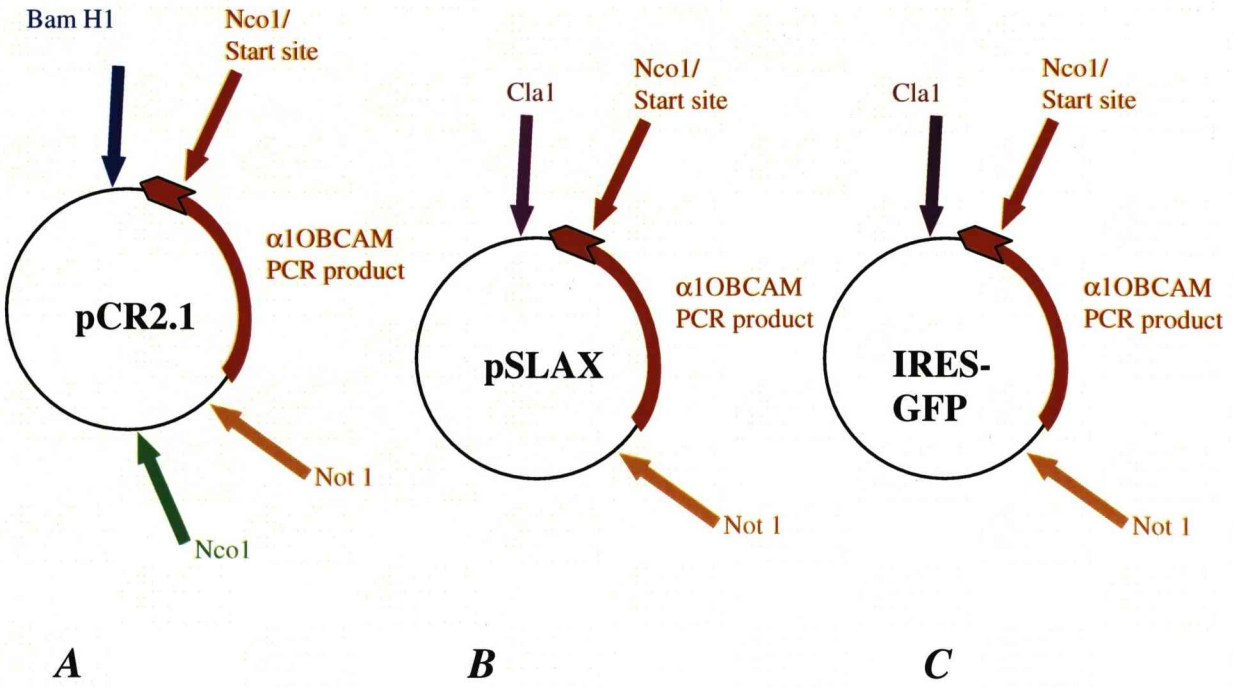

Figure 2.9.2 Cloning strategy used to introduce α1OBCAM DNA sequence into the IRES-GFP plasmid vector.

To enable cloning of the α1-OBCAM sequence into IRES-GFP plasmid vector additional restriction enzymes sites Nco1 and Cla1 had to be introduced onto the OBCAM sequence in two steps. First, primers were designed with sequence miss-matches to create the Nco1 restriction enzyme site at the 5' end of the α1-OBCAM sequence. These OBCAM primers generated Nco1-α1-OBCAM, in a PCR reaction and this sequence was cloned into the pCR2.1 plasmid using Invitrogen TA™ cloning kit (A). Restriction enzymes Nco1 and Not1 digested α1-OBCAM insert from pCR 2.1 and sub-cloned it into pSLAX shuttle vector between restriction sites Nco1 and Not1 (B). This shuttle vector provided the Cla1 site for the final cloning step into the IRES-GFP plasmid vector. The OBCAM sequence was excised form pSLAX shuttle vector and cloned into the IRES-GFP plasmid vector between restriction sites Not1 and Cla1 (C).

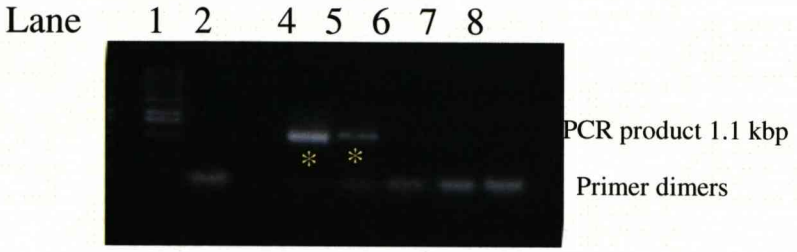

Figure 2.9.3 Agarose gel analysis of PCR amplification of α 1 OBCAM sequence.

Lane 1 Invitrogen 100bp DNA marker

Lane 2 negative control, minus template DNA.

Lanes 4-8 contain PCR products of 10 fold dilutions (1:100 to 1:100,000) of pCDNA3 plasmid DNA containing the αl-OBCAM sequence.

*Top bands in lanes 4 & 5 marked * correspond to ~1.1 kbp, when compared to DNA molecular weight marker. Lower, smaller bands in lanes 2, 4-8 were likely to be due to primer dimerization. This PCR reaction had generated the OBCAM sequence from the pCDNA3 plasmid since each dilution produced a single band of the size expected. Control lane 2 (minus DNA template) contained no DNA, small band was most likely a result of primer dimerization.*

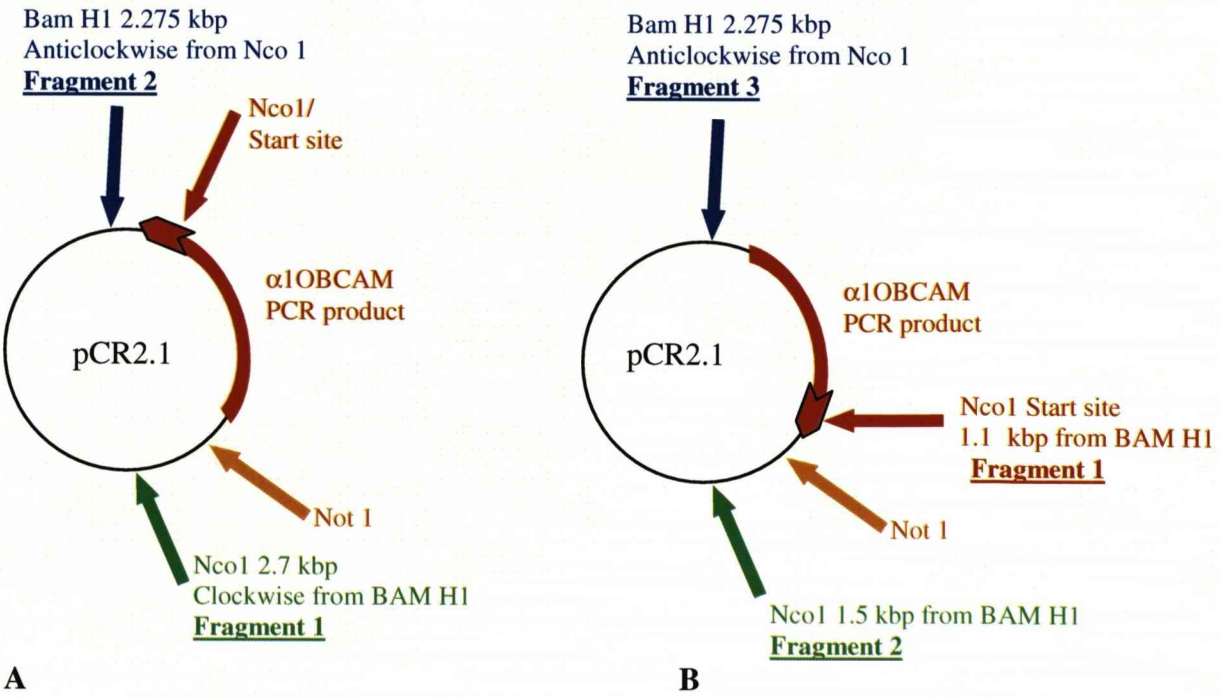

Figure 2.9.4 Orientation of α1OBCAM PCR product TA cloned into pCR2.1 plasmid.

During cloning, the α1-OBCAM PCR product can ligate into pCR2.1 in either orientation A or B shown in the diagram. Restriction enzyme mapping using Bam H1 and Nco1 double digestion confirmed the orientation of OBCAM in pCR2.1 plasmid. After digestion, two bands will separate on an agarose gel if OBCAM is in orientation A, a band of 2.7 kbp corresponding to digested plasmid plus insert DNA (running clockwise BamH1:Nco1) and a second band of 2.275 kbp plasmid DNA (running anticlockwise Nco1:BamH1) and a small undetected fragment of insert DNA. Whereas in orientation B three bands will separate after digestion, 1.1 kbp and 1.5 kbp bands containing the insert DNA (running clockwise BamH1:Nco1) and a 2.275 kbp band of plasmid DNA (running anticlockwise Nco1:BamH1). Plasmid DNA was isolated from selected colonies containing the pCR2.1 plasmid with the α1-OBCAM insert in both orientations and sequenced. The OBCAM sequence is in the correct reading frame in orientation A, whereas in orientation B the OBCAM sequence is in reverse.

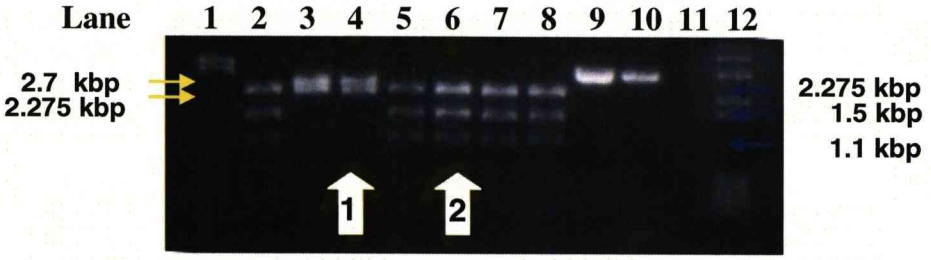

Figure 2.9.5 Agarose gel analysis of cloning of α1-OBCAM PCR product into pCR2.1 plasmid.

Lanes 1-10 contain Bam H1 and Nco1 restriction enzyme digested pCR2.1 plasmid DNA from selected colonies. Lane 12 contains Invitrogen 1kb DNA molecular marker. Double digestion with Bam H1 and Nco1 determined the orientation of the α1OBCAM sequence. The OBCAM sequence produced 2 bands in the correct reading fame orientation, lanes 3 & 4 white arrow 1, whereas in the reverse orientation 3 bands were produced, lanes 5-8 white arrow 2. When compared to the DNA molecular marker in lane 12 the bands in lane 4 correlated to 2.7 and 2.275 kbp (yellow arrows) the sizes expected when OBCAM is in the required reading frame and the bands in lane 6 to 2.275, 1..5 and 1.1 kbp when the OBCAM sequence is in reverse (blue arrows).

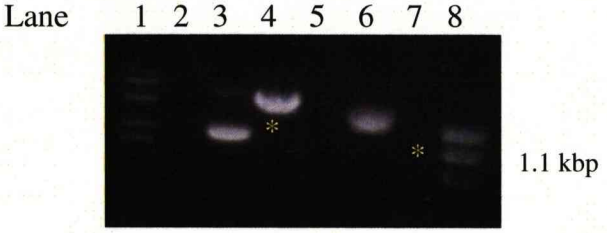

Figure 2.9.6 Preparation of pCR2.1-OBCAM for ligation into pSlax digestion

Lane 1 Invitrogen 1kb DNA molecular markers.

Lane 3 undigested pSlax shuttle vector plasmid DNA.

Lane 4 Nco1 and Not1 restriction enzyme digested pSlax plasmid DNA.

Lane 6 undigested pCR2.1 plasmid DNA containing αlOBCAM sequence.

Lane 8 Nco1 and Not1 restriction enzyme digested αlOBCAM- pCR2.1 plasmid DNA.

*To subclone the αlOBCAM sequence from the pCR2.1 plasmid vector into pSLAX vector, both plasmids were digested with Nco1 and Not1 restriction enzyme and the products separated by agarose gel electrophoresis. The molecular weight shift between lanes 3 & 4 indicated the pSlax shuttle vector was enzyme digested since linear DNA in lane 4 did not migrate as fast as super coiled undigested pSlax in lane 3. When compared to lane 1 molecular marker the lower band in lane 8 was the size expected for the αlOBCAM insert digested by Nco1 and Not1 from pCR2.1 plasmid. Bands marked with * were carefully excised from the gel, DNA was isolated and the αlOBCAM insert form lane 8 was ligated into the digested pSlax vector lane 4.*

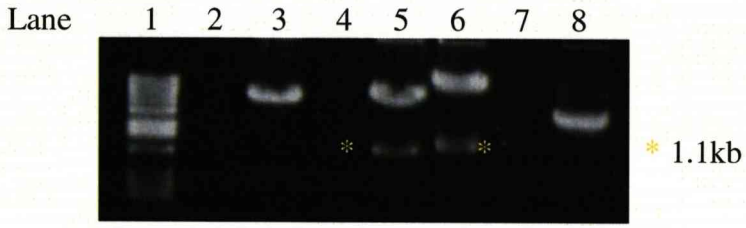

Figure 2.9.7 Agarose gel analysis of α1-OBCAM sequence cloned into the IRES-GFP plasmid.

Lane 1 Invitrogen 1kb DNA molecular marker.

Lane 3 selected IRES-GFP plasmid DNA containing α1OBCAM insert

Lanes 5 & 6 Cla1-Not1 restriction enzyme digested IRES-GFP plasmid DNA.

Lane 8 IRES-GFP plasmid prior to cloning.

*Once OBCAM sequence was ligated into the IRES-GFP plasmid the difference in migration between bands in lanes 3 and 8 suggested the IRES-GFP plasmid in lane 3 contained additional DNA to the original IRES-GFP plasmid in lane 8. Mapping with Cla1-Not1 restriction enzymes released a band of ~1.1 kbp in lanes 5 & 6 marked * (compared to the DNA molecular marker in lane 1) confirmed the plasmid contained the OBCAM insert.*

2.10.1. Transient transfection of pOIG and pLIG into CHO cell lines

Stably transfected IgLON CHO cells were cultured at a density of $1.5x10^4$ cells on glass coverslips in a 24 well tissue culture plate in DMEM/F12 containing 10% FCS growth medium overnight at 37°C, 5% CO_2 atmosphere. A complex of pOIG and pLIG plasmid DNA was formed in a 1:3 weight/volume ratio with FuGENE 6 transfection reagent (Roche) according to manufacturer's protocol. Briefly, 0.6 µl FuGENE reagent was added to 25 µl DMEM/F12 salt solution followed by 0.2 µg pOIG or pLIG plasmid DNA, incubated for 45 minutes at RT to form a DNA complex which was then added directly to the CHO cells. The cells were cultured for 48 hours at 37°C, 5% CO_2 atmosphere, to allow plasmid DNA expression.

2.10.2 Recombinant protein binding assay to transiently transfected CHO cells

The CHO cells were stained with IgLON-FC recombinant proteins and examined using a LEICA LEITZ LB fluorescence microscope. Expression of the intracellular GFP-tag with filters (excitation 495nm, and emission 525nm) identified the transiently transfected cell population expressing both IgLONs. Recombinant protein binding to the two populations of cells was identified by 1:100 dilution of Texas Red™ conjugated goat anti-human IgG antibody (Jackson laboratories) secondary antibody binding to the FC portion of the recombinant protein (filters select for excitation at 596nm, 620nm emission). Photomicrographs were prepared using Metamorph™ imaging software.

2.11. Preparation of doubly transfected CHO-cell lines

The pBUD plasmid was used to prepare CHO cells expressing two members of the IgLON family on the cell surface.

2.11.1 Construction of pBUD plasmid vector containing two IgLON DNA sequences

The pBUD CE 4.1 plasmid vector (Invitrogen) contains two separate cloning sites into which individual IgLON-GPI sequences were inserted. The α2 CEPU-1 sequence was cloned downstream of the EF1-α promoter region between restriction sites *Kpn* I and *Xho* I. The α2-OBCAM sequence was cloned downstream of the CMV promoter region between restriction sites *Hind* III and *Xba* I figure 2.11.1 (James Reed).

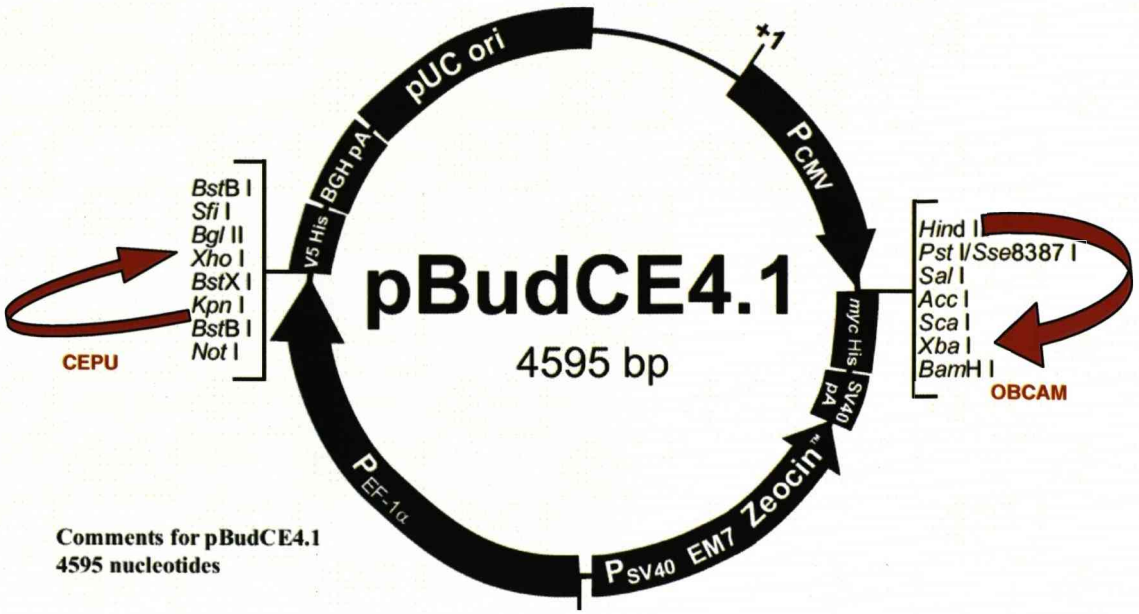

Figure 2.11.1 pBUD plasmid

α2 CEPU-1 sequence was cloned between restriction sites Kpn I and Xho I downstream of the EF1-α promoter region, and α2 OBCAM sequence was cloned between restriction sites Hind III and Xba 1 downstream of the CMV promoter region in pBUD CE 4.1 vector. A second vector containing the αl LAMP sequence in place of the OBCAM sequence was also constructed (Reed et al., 2004).

2.11.2. Transfection of two IgLON sequences into CHO-cells

WT-CHO cells were cultured at a density of $12x10^4$ cells/well in a 6 well tissue culture plate in DMEM/F12 medium containing 5% FCS overnight. Fugene-6 transfection reagent (Roche) in a 3:1 volume: weight ratio introduced 1 μg pBUD plasmid vector containing the CEPU-1 and OBCAM sequences into these WT-CHO cells. Briefly, 3 μl of Fugene-6 reagent in 100 μl DMEM/F12 with incubated with 1 μg pBUD plasmid vector construct DNA for 45 minutes at RT and then added to the CHO cells. After 48 hours in culture, medium was exchanged to DMEM/F12 containing 2% FCS plus 400 μg /ml Zeocin antibiotic, to select for transfected cells. The cell density was maintained below 50% confluence for 7 days, with medium changes to remove detached non-transfected cells. 0.25% trypsin EDTA removed the cells from the dish and they were resuspended in culture medium. Using a haemocytometer, cells were counted and 100 cells were resuspended in 10 mls of DMEM/F12 containing 10% FCS plus 400 μg /ml Zeocin culture medium and distributed over a 96 well tissue culture plate, at a density of ~ 1 cell/well to establish single CHO cell colonies. The plate was cultured until single cells had undergone several rounds of division to establish a colony.

Established colonies were expanded in 24 well tissue culture plates containing 10 mm glass coverslips. Coverslips were removed and live stained with specific IgLON antiserum to confirm 100% expression of both CEPU-1 and OBCAM on the surface of the CHO cells. Colonies expressing both IgLONs were expanded and further characterised by removing the IgLONs off the surface of the CHO cells using phospholipase C enzyme and western blotting the supernatant. A cell line expressing CEPU-1 and LAMP was also prepared by the same method.

A second cell line expressing the α2 CEPU-1 α2-LAMP IgLONs was prepared in the same way using the pBUD plasmid containing the α2CEPU-1 sequence cloned downstream of the EF1-α promoter region (between restriction sites *Kpn*I and *Xho*I) and α2-LAMP sequence cloned downstream of the CMV promoter region (between restriction sites *Hind*III and *Xba*I).

2.12. PiPLC digestion of IgLONs into solution

Transfected CHO cell lines were cultured on 15 cm tissue culture dishes to confluence and the IgLONs were digested from the cell surface into solution by phosphatidylinositol-specific phospholipase C PiPLC (Invitrogen) enzyme cleavage from their GPI anchor. Culture dishes were washed with Ca^{2+} Mg^{2+}-free PBS, and then incubated with 1 unit PiPLC in 1ml Ca^{2+} Mg^{2+}-free PBS for 2 hours at RT with gentle rocking. COMPLETE™ PIC (ROCHE) was added to prevent unwanted protease activity. The supernatant was harvested and microfuged at top speed for 5 minutes to pellet any cell debris. The resulting supernatant was concentrated 10 fold through a VIVASPIN™ (Sartorious) protein concentrator column and analysed by western blotting.

2.13. PAGE western blot analysis

The Invitrogen NuPAGE™ (PAGE polyacrylaminde gel electrophoresis) Novex gel system was used for western blotting analysis. Lithium dodecyl sulfate (LDS) sample buffer x4 (Invitrogen) was added to PiPLC supernatant samples and loaded onto Novex™ 3-8% Tris Acetate polyacrylamide gels and run in NuPAGE™ Tris Acetate buffer at 20-30 volts. Sample proteins were transferred on to BioTrace™ (Pall Gelman laboratory) nitrocellulose transfer membrane sandwiched between 3M chromatography paper soaked in O.3 M tris pH 10.4 bottom buffer and 25 mM tris pH 9.4 top buffer containing 20% methanol using a Biorad Trans-Blot™ semi-dry transfer cell. Nitrocellulose membrane was blocked overnight in 150mM NaCl, 10mM tris pH 8.4, 0.2% Tween 20 blocking buffer and stained with individual IgLON rat antisera titred out to a dilution of 1:5,000-1:10,000 in blocking buffer plus 1% BSA, followed by Horseradish peroxidase (HRP) conjugated rabbit anti rat antibody (DAKO) also titred out to a dilution of 1:5,000-1:10,000. Visualisation of protein bands was by addition of Pico™ and Femto™ chemiluminescent substrates (Pierce–Perbio) and exposure of nitrocellulose onto HyperFilm™ ECL (Amersham) chemiluminescent film, developed using Kodak photo chemicals (Sigma).

2.13 Construction of OBCAM HISx6 tagged plasmid vector

A plasmid was constructed to contain the OBCAM-HISx6 sequence for transfection into CHO cells to prepare HIS tagged OBCAM-CHO cell line. pcDNA3 plasmid vector containing the HISx6 sequence was a kind gift from David Fernig Biological Sciences, Liverpool University (figure 2.13.1). Cloning the OBCAM sequence minus its signal peptide and start codon into this plasmid added a HISx6 tag and a signal peptide to the N-terminus of OBCAM.

To clone the OBCAM sequence into the HISx6 pcDNA3 plasmid primer sequences were designed with mismatches to the original α2 OBCAM sequence, shown in red, generate a ggatcc *Bam-H1* site at the start of the OBCAM sequence and tctaga *Xba-1* restriction enzyme sites at the end of the sequence (figure 2.13.2).
5'-3' forward primer GCAGGAGGATCCGTGCGCAG,
5'-3' reverse primer CCCTCCACTTCTAGATCAAAAGTC

OBCAM HISx6 PCR reaction

Using these primers, on 0.1 μg – 0.001 μg dilutions of -pcDNA3 plasmid containing the full α2 OBCAM sequence, one step PCR conditions of 30 extension cycles at 52°C generated the 1058 bp modified OBCAM sequence, which was TA cloned into pCR2.1 TOPO™ vector and used to transform TOP 10 F' competent bacteria. These bacteria were screened on 50 μg/ml ampicillin antibiotic agar plates, selected colonies containing the plasmid were cultured and plasmid DNA was prepared using mini plasmid preparation kit (Qiagen). OBCAM insert was identified by restriction enzyme mapping with *Bam-H1* and *Xba-1* restriction enzymes. These restriction enzymes then digested the OBCAM sequence from pCR2.1 and ligated it into the pcDNA3-HISx6 plasmid vector as previously described (results figure 2.13.3). Colonies containing the plasmid were identified from STET preparations (results figure 2.13.4) Commercial DNA sequencing of the plasmid construct DNA by LARK confirmed the successful tagging of the α1OBCAM sequence.

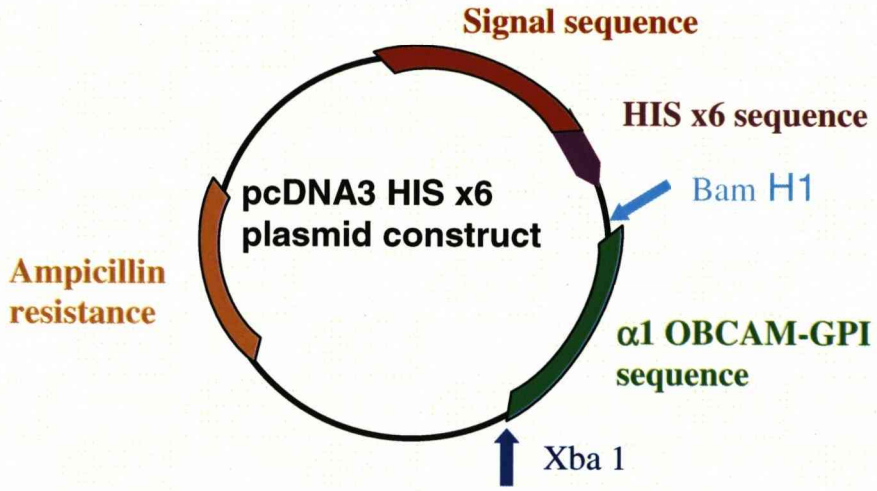

Figure 2.13.1. HISx6 tagged OBCAM plasmid vector.

The αl OBCAM-GPI sequence (highlighted in green) was cloned into pcDNA3 plasmid using restriction enzyme sites BamH1 and Xba1. This plasmid added a new signal sequence and the HISx6 epitope tag to the N-terminus of OBCAM sequence.

ggatcc Bam H1

cgtcctctgtctcaggctgctcttccttgtgcc **cgcaggaggatccgtgcgca**
gcggagatgccaccttccccaaagctatggacaacgtgactgtgcggcaaggggagagtgccacgctcaggtgtaccg
tggatgacagggtgaggcgggtagcgtggttgaaccgcagcaccatcctttatgctggcaatgacaagtggtctatagac
aaccgcgtggtcatcctctccaacaccaaaacccagtacagcatcaagatccacaacgtggatgtgtacgatgaggggc
cctacacctgctctgtgcagacagacaatcaccccaaaacatcgcgcgtccacctcatcgtgcaagtccccctcagattg
tcaacatctcatcagacatcaccgtgaacgaaggcagcagtgtgaccctcatgtgcttggcctttgggaggccggagccc
actgtcacgtggcggcatctctctgggaaagggcaaggctttgtgagtgaggatgagtacctggagatcacgggcatca
cacgggagcagtcgggcgagtatgagtgcagtgctgtcaatgatgtggccgtcccagatgtccggaaagtcaaagtcac
tgtcaactacccgccgtacatctccaatgccaagaacacaggcgcctcagtgggccagaagggcatcctgcagtgcgag
gcctcggctgtccccgtggcagagtttcagtggttcaaggaggacaccaggttagcaaatgggctggagggcgtgcgg
atcgagagcaagggccgcctctcgacgctgaccttcttcaatgtgtcggagaaggactatggcaactacacgtgtgtggc
cacaaacaagttgggcaacaccaatgccagcatcatcctgtacgggcccggagcggtgcacgacagtggcaatgcagc
ctcccgggcagccgctggcctctgcctctgggccaccctcctcgctcgcctcctcctc
gacttttgatctagaagtggaggg tcccgggacggccg

tctaga

Xba 1

Figure 2.13.2 HISx6 tagged OBCAM sequence

Primer sequences are in bold print and underlined, red bases are those altered to form restriction sites, and the green bases indicate the stop codon. The pale blue bases are the signal sequence and HISx6 tag added on to the α2OBCAM sequence by the plasmid.

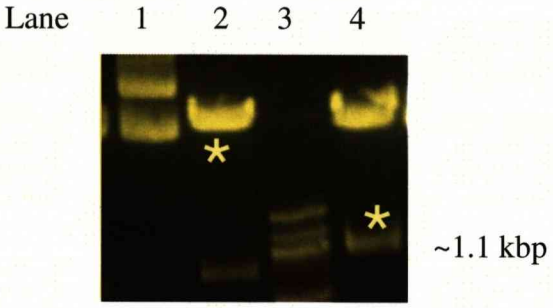

Figure 2.13.3 Ligation of OBCAM sequence into pcDNA3 HISx6 plasmid

Lane 1 undigested pcDNA3 HIS x6 plasmid.

Lane 2 Bam-H1 and Xba-1 restriction digested pcDNA3 HIS x6 plasmid

Lane 3 Invitrogen 1 kb DNA molecular marker.

Lane 4 Bam-H1 and Xba-1 restriction digested pCR2.1 plasmid containing OBCAM modified sequence.

*Bam-H1 and Xba-1 restriction enzymes digested the OBCAM sequence from pCR2.1 plasmid (band marked * lane 4). pcDNA3 HIS x6 plasmid was also digested with restriction enzymes Bam-H1 and Xba-1 (band marked * lane 2) to prepare the cloning sites to accept the OBCAM insert. The marked bands were excised, DNA recovered, and the OBCAM insert was ligated into pcDNA3 HIS x6 plasmid between restriction sites Bam-H1 and Xba-1.*

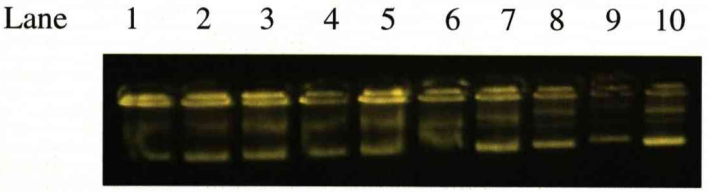

Figure 2.13.4 DNA STET preparations identified OBCAM HIS x6 pcDNA3 plasmid construct.

The OBCAM sequence ligated into the pcDNA3-HISx6 plasmid was used to transform Top 10 competent bacteria and positive colonies were selected on ampicillin agar. 10 colonies were selected, cultured, plasmid DNA isolated using STET buffer and separated on an agarose gel (lanes 1-10). Colonies corresponding to lanes 7, 8 and 10 were selected as containing the plasmid construct, expanded and plasmid DNA isolated.

2.14 1 Production of HISx6 tagged OBCAM CHO cell line

Fugene-6 ^{TM} reagent transfected the OBCAM-HISx6 pcDNA3 plasmid construct into WT-CHO cells and G418 antibiotic selected for those CHO cells expressing the plasmid. These cells were sub-cloned and colonies from a single cell were amplified to prepare the HISx6 tagged OBCAM (O^H)-CHO cell line (cell line prepared by Mohammed Akeel). Confirmation of 100% transfection of the CHO cell line was by live staining with both HISx6 and OBCAM antiserum (data not shown).

2.14.2 Production of doubly transfected OBCAM HISx6 tag CHO cell lines

pBUD CE 4.1 plasmid was previously constructed to contain the LAMP-GPI sequence under the CMV promoter, alongside a GFP-cytoplasmic marker sequence under the EF-1α promoter sequence (James Reed). Fugene 6^{TM} reagent transfected this plasmid into the O^H-CHO cell line and Zeocin antibiotic resistance selected the cells expressing LAMP-GFP. These cells were sub-cloned and colonies expanded from a single cell were initially analysed by visualisation of intracellular GFP fluorescence. Expression of LAMP on the surface of all the CHO cells was confirmed by immuno-cytochemical detection of LAMP. Similarly, the CEPU-1 sequence under the EF-1α promoter, was introduced into O^H-CHO via a CEPU-1-pBUD CE 4.1 plasmid to prepare the CEPU-1-O^H-CHO cell line, 100% expression of CEPU-1 was identified by immuno-cytochemistry.

Cell lines expressing LAMP-O^H (LO^H) and CEPU-1-O^H (CO^H) were expanded and PiPLC enzyme digested CO^H and LO^H off the CHO cell surface into solution. Western blotting of this supernatant confirmed expression of the HISx6 tag on the CO^H-CHO cells (results figure 2.14.2.).

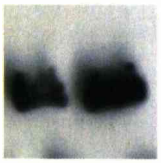

Figure 2.14.2 Characterisation of HISx6 tag on CO^H CHO cell line.

PiPLC digested CO^H from CHO-cells and the supernatant was concentrated 10 fold. 10 µl aliquots were separated on a LDS-PAGE gel and western blotted onto nitrocellulose. The HISx6 tag was detected by staining the nitrocellulose with 1:500 dilution of mouse anti HISx6 antiserum (Sigma), followed by 1:1000-1:2000 dilutions of anti-mouse HRP secondary antibody (Dako) lanes 1&2, visualised with Pico™ chemiluminescent substrate, exposure for 2 minutes on Amersham film.

2.15. Immuno-precipitation of putative IgLON complexes

Protein A agarose beads (Sigma) concentrated the IgLON antibody molecules from 0.5 ml CEPU-1 and OBCAM rabbit antiserum commercially produced by Covlab. A 25 µl aliquot of protein A beads was added to 0.5 ml IgLON rabbit antiserum and rotated overnight at 4°C. The beads were collected by microfuging at top speed for 2 minutes, washed twice with 1ml aliquots of 10 mM Tris buffer pH 8.0 and the attached IgLON antibody molecules were eluted from the beads by washing twice with 50 µl 0.2 M glycine pH 2.5. The pH of the antibody solution was then adjusted to pH 8.0 with 2 M Tris buffer pH 8.0. Four 13 mm circles of nitrocellulose membrane were each coated with 25 µl of concentrated antibody solution, and blocked overnight in 150 mM NaCl, 10 mM Tris (pH 8.4) 0.2% Tween 20 buffer. The PiPLC supernatant from 4x150 mm dishes of confluent CHO cells was concentrated to 50 µl and added to the nitrocellulose circles then incubated for 1-2 hours at RT. Any unbound PiPLC supernatant was carefully washed off the nitrocellulose with 10 mM Tris (pH 8.4) buffer. The IgLONs captured by the antibody bound to the nitrocellulose were eluted with two washes of 20 µl 0.2 M glycine pH 2.5 and the pH adjusted to pH 8.0. Eluted protein samples were separated across two 3-8% TA NuPAGE gels, and IgLON protein bands were identified by western blot analysis.

2.16. Affinity-isolation of putative IgLON complexes

A similar experiment was carried out using OBCAM-HISx6-CHO cell line transfected with a second IgLON CEPU-1 or LAMP. To capture the HISx6 epitope tagged OBCAM, 25 µl nickel Probond beads (Invitrogen) were added to 100 µl of the concentrated PiPLC supernatant and rotated for two hours at RT. The nickel beads were collected washed in 20 mM sodium phosphate buffer containing 0.5 M NaCl (pH 8.0) and potential IgLON complexes was remove from the nickel beads by adding 40 µl NuPAGE sample buffer.

2.17. Primary cell culture of forebrain neurons

Aclar coverslips were coated for 1 hour with 10 mg/ml Poly-L-Lysine in 100 mM sodium borate buffer pH 8.4. The forebrain from E6-8 chicks was dissected and incubated in 1ml x 0.05% trypsin in HBSS (-) Sigma) containing 100 µg/ml DNAse (Sigma) for 30 minutes at 37°C. The tissue was washed in HBSS and HBSS containing 1 mg/ml soybean trypsin inhibitor (Sigma) for 2 minutes. Following these washings, DMEM/F12 plus Glutamax (Sigma) growth medium containing 1.5% glucose, 100 µg/ml transferrin (Sigma), 100 µg/ml insulin (Invitrogen) and 50 units penicillin/streptomycin (Invitrogen) was added and the forebrain tissue and a polished glass Pasteur pipette dissociated the tissue into to a single cell suspension (Aizenman et al., 1986). Poly-L-Lysine coated Aclar coverslips were washed in HBSS and placed in a 24 well plate. Forebrain neurons were seeded at a density of $2x10^5$ cells per well in 0.5 ml culture medium onto the coverslips.

2.18. Antibody co-clustering of IgLONs on forebrain neurons

Dissociated E8 forebrain neurons were cultured for 4-5 days at a density of $2x10^5$cells/well on 13 mm^2 Aclar coverslips coated with poly-L-Lysine. The cells were live stained with combinations of IgLON rat and rabbit antiserum, visualised with Texas Red™-conjugated goat anti-rat IgG antibody (Jackson Laboratories) and Alexa 488 green-conjugated goat anti-rabbit antibody (Invitrogen). Staining was as previously described at RT for 20 minutes with antisera and secondary antibody dilutions of 1:100 in 1% BSA/Millonig's buffer and fixation was in 2% paraformaldehyde. Specificity of IgLON antiserum was tested by staining IgLON CHO cells with combinations of each antiserum visualised with fluorescently labelled secondary antibodies. Species cross-reactivity between the secondary antibodies was tested by staining the forebrain neurons with rat and rabbit pre-immune serum plus secondary antibody, alongside IgLON rat and rabbit antiserum plus secondary antibody e.g. pre-immune rat serum plus rat Texas Red™ labelled secondary antibody was tested and rabbit CEPU-1 and OBCAM antiserum plus Alexa 488 green labelled secondary rabbit antibody. The coverslips were examined using a LEICA AOBS SP2 confocal microscope with lasers at excitation 488 nm, 594 nm and photomicrographs produced. Staining patterns were then examined using LEICA overlay image software. As a negative control for non-specific co-

localisation the forebrain neurons were stained with IgSF molecules outside of the IgLON family. T-cadherin rabbit antiserum or F11 rabbit antiserum visualised with Alexa 488 green-conjugated goat anti-rabbit antibody (Invitrogen) alongside each rat IgLON antiserum plus Texas Red™ secondary antibody. The staining patterns of at least 3 different areas from 2 coverslips were analysed with Image J software and presented as a histogram using PRISM software.

2.19. Neurite outgrowth assay on CHO-cell lines

CHO cell lines were plated at a density of $2x10^5$ cells/well into a 24 well plate containing a glass cover slip and cultured overnight to confluence. Dissociated forebrain neurons from E6-8 chick brains were prepared at a density of $2x10^5$ cells/well in 0.5 ml forebrain culture medium and added to the CHO cell coverslips. IgLON insensitivity to trypsin had previously been demonstrated by immunofluorescent staining of IgLON-CHO cells after trypsinization so preparing the forebrain neurons with trypsin was not considered to affect IgLON expression. After 24 hours incubation the culture medium was removed and the cells fixed and permeabilized by incubation in ice-cold methanol at -20°C for 15 minutes. To visualise neurite extension from the forebrain neurons coverslips were incubated for 1 hour with neuronal specific GAP43, rabbit antisera, titred out to a dilution of 1:500 in 1% BSA Millonig's buffer, detected by 1:200 Texas Red™-conjugated donkey anti-rabbit antibody (DAKO) and mounted in DAKO fluorescent mounting medium. Counts of forebrain neurons extending neurites were made without knowing the conditions to avoid prejudice, at x 40 magnification under oil on a LEICA LEITZ RB DM fluorescent microscope, using filters 596 nm excitation 620 nm emissions. In each experiment 100-200 individual neurons/cover slip from triplicate cover slips were counted and the percentage of neurons showing extension of neurites twice that of the diameter of the cell body calculated. The neurons counted were carefully selected as single neuronal cell bodies, avoiding clumps, which may have had an influence on each other and affected overall neurite outgrowth. Photomicrographs were produced using Metamorph software. Experiments were repeated three times and analysis of data was carried out using the PRISM software programme; significant values were calculated using the Newman-Keuls analysis of variance multiple comparison test in the PRISM programme.

2.20. Neurite outgrowth assay on IgLON substrates

Glass coverslips was coated with 20 µl of nitrocellulose membrane solution prepared by dissolving 2 cm x 3 cm square of Protran BA 85 nitrocellulose membrane (Schleicher & Schuell) in 2 ml tissue grade methanol (Merck). Once dried, the coverslips were coated with IgLON PiPLC supernatant prepared from approximately half a 15 cm culture dish, plus 10 µg/ml Poly-L-Lysine, diluted to 100 µl with PBS and spread over three coverslips, then incubated for 1 hour at RT. The coverslips were blocked by incubation with 1% tissue culture grade BSA (Sigma) in PBS for 1 hour. Dissociated E7/8 forebrain neurons were added to the coverslips at a density of $2x10^5$ cells/well and following 24 hours in culture were fixed using Luduena fixative containing 12 M sucrose 0.5 M $CaCl_2$, , 2% gluteraldehyde in 0.12 M phosphate buffer pH 7.4. Coverslips were stained to visualise neurites with 1% weight: volume Cresyl violet crystals (Sigma) dissolved in PBS, containing 1% acetic acid at RT for 5 minutes. Finally the coverslips were washed, mounted and the percentage of forebrain neurons extending neurite outgrowth was calculated as before.

Chapter Three

Homophilic and Heterophilic *Trans* Affinity of IgLONs

HOMO AND HETEROPHILIC *TRANS* AFFINITY OF IgLONs

INTRODUCTION

Individual IgLON family members have demonstrated both homophilic and heterophilic *trans* interactions. In binding studies LAMP homophilic interaction aggregated microspheres and LAMP expressing limbic axons bound preferentially to purified LAMP substrate when compared to non-limbic axons (LAMP negative) (Zhukareva and Levitt, 1995). LAMP expression on a subset of thalamocortical projections showed a preference for LAMP in a stripe assay (Mann et al., 1998). Similarly, cross-linking studies, aggregation, binding and cell adhesion assays using Ntm (CEPU-1) transfected CHO cells and Ntm-FC recombinant protein demonstrated a homophilic interaction for Ntm (Gil et al., 1998). Several other studies using IgLON-FC recombinant proteins binding to various IgLON expressing cell lines have revealed homo and heterophilic interactions between CEPU-1, LAMP, OBCAM and Ntr (Kilon) (Brummendorf et al., 1997; Gil et al., 1998; Marg et al., 1999; Lodge et al., 2000; Gil et al., 2002; Miyata et al., 2003b).

As a result of these homophilic and heterophilic *trans* interactions neuronal cells expressing IgLONs would be expected to adhere to an IgLON substrate. Chick DRG (dorsal root ganglion) and sympathetic neurons express LAMP, OBCAM and CEPU-1 but only adhered to CEPU-1-FC and not to LAMP-FC recombinant protein (McNamee et al., 2002). Similarly, cerebellum granule cells (CGC) demonstrated an adhesion preference to CEPU-1-FC and did not adhere to LAMP-FC substrate (Reed et al., 2004). Furthermore, neurons expressing IgLONs generally have a reduced affinity for IgLON-FC recombinant proteins in general and appear not to bind any LAMP-FC.

To try to explain this anomaly of the inability of neurons to interact with LAMP the relative homo and heterophilic affinities between three members of the IgLON family, CEPU-1, OBCAM and LAMP were examined. Ntr (Kilon), the fourth member of the family was not available so could not be included in these experiments. Initially, homophilic interactions were measured using IgLON-FC recombinant proteins attached to fluorescent microspheres. The hypothesis was IgLON homophilic interactions would aggregate the microspheres into clumps and

measurement of the number of microspheres remaining single by fluorescent activation cell sorting (FACS) would give an indication of the strength of the homophilic affinity. The greater the number of single microspheres remaining indicting a lower strength of homophilic interaction. Heterophilic *trans* interactions between IgLONs were then investigated using an ELISA type assay. In this assay the amount of IgLON-FC recombinant protein binding to IgLON-CHO cells was measured to give a comparative measure of the relative affinities between the three members of the family.

IgLON-FC recombinant proteins and transfected CHO cell lines were already available at the start of this thesis for these assays (details of preparation Chapter 2 Materials and Methods section 2.1). Addition of an FC-portion to an existing protein is a commonly used technique to produce a recombinant protein. The FC portion provides an epitope tag for purification of the protein (with Protein A or G) and commercial FC antibodies are available for easy identification of the recombinant protein. Furthermore, recombinant FC proteins are dimeric so are ideal for measuring low affinity interactions (figure 3.1).

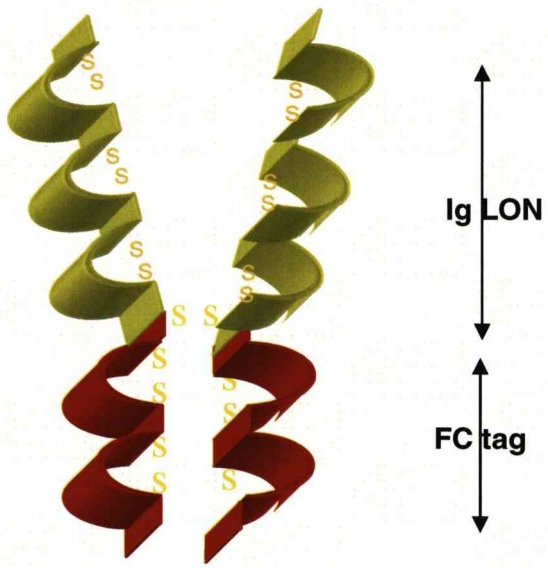

Figure 3, 1 Structure of IgLON-FC protein

Illustration of IgLON-FC recombinant proteins used in this thesis. The FC portion is represented as two red Ig domains and IgLON heads are represented as three green Ig domains. During post translational processing stable disulphide bridges are formed (yellow S:S) linking the Ig domains and the protein is glycosylated to produce the functional homodimeric IgLON-FC recombinant protein.

AIM

This chapter will aim to compare the affinity of homophilic and heterophilic *trans* interactions between CEPU-1, OBCAM and LAMP and produce a hierarchy of the strength of their interactions.

RESULTS

Microspheres aggregation assay to measure *trans* homophilic interactions of IgLONs

Protein G was coupled to fluorescent microspheres to capture the FC portion of IgLON-FC recombinant proteins and orientate the IgLON head portions for maximal binding interaction. Aliquots of these microspheres were incubated with 2.5 μg of recombinant protein and aggregation of the microspheres into clumps was analyzed by FACS flow cytometry. Since higher homophilic affinity results in fewer single microspheres, the percentage of microspheres remaining single was calculated and presented as a histogram (figure 3.2.A). Based on the measurement of 10,000 detection events, 80% of microspheres covalently coupled with Protein G remained single and 68% microspheres remained single when Protein G microspheres were incubated with Ox40 control protein to measure non-specific protein-protein interactions. Ox40 is a lymphocyte protein of the IgSF, engineered in the same way as IgLON-FC recombinant proteins. Since Ox40 has no significant homophilic binding interaction it was not expected to aggregate the microspheres and so acted as a negative control. Ox40 only slightly increased aggregation of the microspheres when compared to Protein G alone, suggesting non-specific protein-protein interactions were not significantly influencing aggregation of the microspheres. On incubation with IgLON recombinant proteins aggregation increased leaving only 22% of microspheres single when incubated with CEPU-1-FC, 30% single with OBCAM-FC and 45% with LAMP-FC. Incubation with each of the IgLON-FC proteins had significantly increased aggregation of the microspheres, suggesting all three IgLONs were capable of homophilic interactions. Since the aliquots of microspheres and concentrations of recombinant proteins were equivalent homophilic affinities between the three recombinant proteins could be directly

compared. CEPU-1-FC had the least number of single microspheres remaining, so was considered to have the strongest homophilic binding affinity; LAMP-FC had the most single microspheres remaining, so was the weakest. OBCAM-FC homophilic affinity was not significantly weaker than that of CEPU-1-FC, but was significantly higher than LAMP-FC (figure 3.2.A).

Comparison of microspheres clump sizes

Comparison of FACS traces of the number of microspheres in each clump indicated CEPU-1 had a greater number of larger clumps than LAMP (figure 3.2 B). The ability of CEPU-1 to form these larger clumps of microspheres supports CEPU-1 having a higher homophilic binding affinity than LAMP.

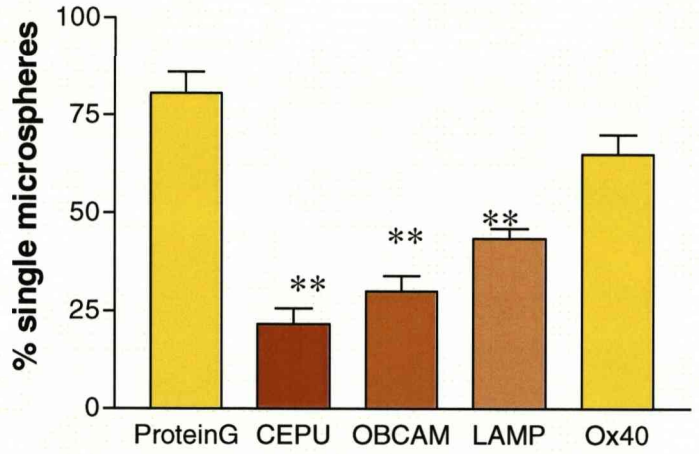

Figure 3.2.A Fluorescent microspheres aggregation assay measured IgLON homophilic affinity.

*Histograms represent the number of single microspheres remaining following incubation of 100 µl aliquots of a 20% suspension of fluorescent microspheres with 25 µg of IgLON–FC recombinant proteins for 15 min at room temperature (orange bars). Protein G and Protein G coupled with OX40 protein negative controls remained predominantly as single microspheres (yellow bars). Ox40 protein had a weak effect on microspheres aggregation compared to protein G alone based on 2 experiments ($p < 0.05$). CEPU-1, OBCAM and LAMP-FC recombinant proteins aggregated the Protein G microspheres, leaving significantly fewer single microspheres compared to Protein G alone ($p < 0.001$ for all IgLON-FC proteins marked as **) and compared to Protein G plus Ox40 microspheres ($p < 0.01$ for LAMP-FC; $p < 0.001$ for CEPU-1-FC and OBCAM-FC, based on 4 experimental repeats for LAMP and OBCAM, 3 for CEPU-1-FC. CEPU-1 had the least single microspheres remaining so was considered to have the highest homophilic affinity. A similar number of microspheres remained single after the homophilic interactions of CEPU-1 and OBCAM ($p > 0.05$) but LAMP had significantly more single microspheres, so was considered to have a much weaker homophilic affinity than OBCAM and CEPU-1 ($p < 0.05$).*

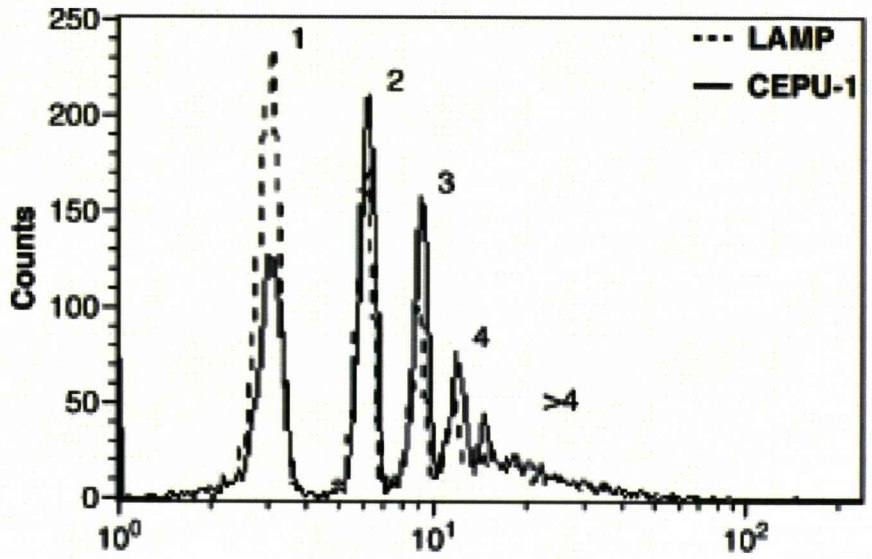

Figure 3.2.B Comparison between CEPU-1-FC and LAMP-FC ability to aggregate microspheres

Each peak represents an aggregate containing a different number of microspheres. Peak 1 corresponds to single microspheres, peaks 2-4 are aggregates of increasing size, corresponding to groups of 2, 3 and 4 microspheres respectively. LAMP-FC coupled microspheres (dotted line peak) have a greater number of single microspheres in peak 1 over CEPU-1-FC coupled microspheres (solid peak line) which suggested LAMP has a lower homophilic binding affinity. The ability of CEPU-1 to produce a larger number of clumps of 2 and an even higher number of 3 and 4 microspheres in the following peaks supported the suggestion that CEPU-1 has a higher homophilic binding affinity than LAMP. Only the CEPU-1 homophilic interaction was able to produced clumps of more than 4 microspheres end peaks.

HETRELOPHILIC AFFINITY OF IgLONs

CEPU-1 was established as having the highest *trans* homophilic interaction of the three IgLONs tested, but microspheres aggregation assays provided no information on heterophilic interactions between IgLONs. Heterophilic interactions were compared by measuring the affinity of IgLON-CHO cell lines for recombinant proteins in an ELISA type assay. CHO cell lines were available for the start of this thesis (details of their preparation and characterisation are described in Chapter 2 Materials and Methods section 2.4 and figure 2.6.1).

The affinity of confluent mono-layers of IgLON-CHO cell lines for IgLON-FC protein was measured in this ELISA assay (diagram figure 3.3). CHO-cell lines were incubated with combinations of recombinant proteins, followed by HRP-conjugated specific FC-antibody and 3,3',5,5'-Titramethylbenzidine dihydrochloride (TMB) substrate. The enzyme activity of the HRP tag on the antibody produced a colour change in the TMB substrate which directly related to the amount of recombinant IgLON-FC bound and was detected at wavelength 450 nm in an ELISA plate reader. The strength of the TMB bound to the CHO-cells gave a comparative measure of both homo and heterophilic IgLON interactions.

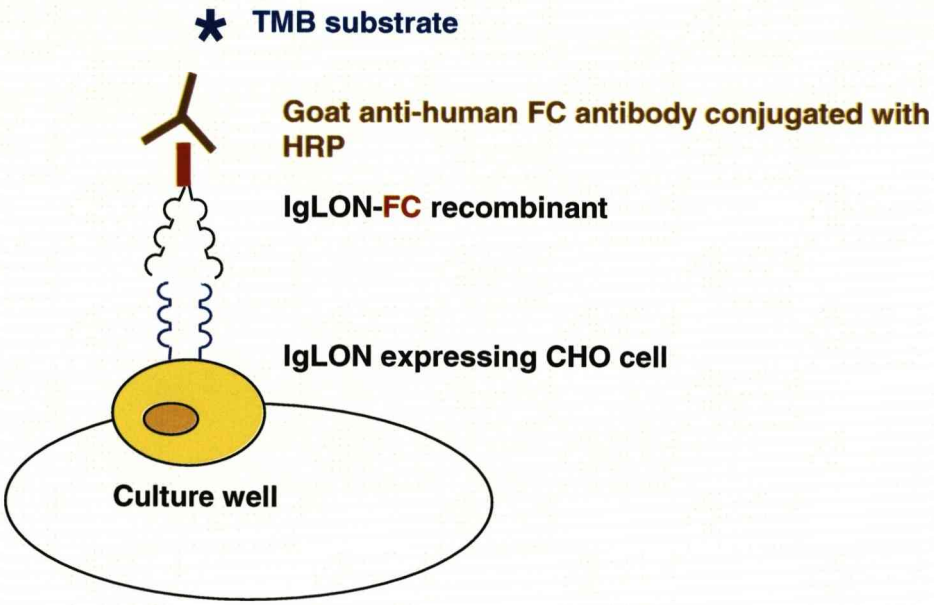

Figure 3.3 ELISA assay

IgLON expressing CHO cell lines were cultured on a 96 well plate to confluence and incubated with individual IgLON-FC recombinant proteins. Incubation with 1:500 dilution of goat anti human-IgG-HRP-conjugated antibody bound to the FC portion of the recombinant protein and TMB substrate was added. The HRP attached to the goat antibody produced a colour change in the TMB substrate, detected at a wavelength of 450 nm in an ELISA plate reader equal to the amount of bound protein.*

IgLON-FC proteins binding to WT-CHO

In the first experiment WT and transfected IgLON-CHO cell lines were incubated with individual IgLON-FC recombinant proteins to establish the background level of non-specific FC-protein binding to CHO cells. The binding of CEPU-1-FC recombinant protein to WT-CHO was substantially less at all concentrations tested than the binding to the CEPU-1-CHO cells (figure 3.4) OBCAM-FC and LAMP-FC binding to WT-CHO was also considerably less than to OBCAM-CHO and LAMP-CHO respectively (data not shown). This suggested there were minimal non-specific recombinant protein interaction with CHO cells *per se,* so all interactions between IgLON-FC proteins and the IgLON-CHO cell lines were considered to be specific.

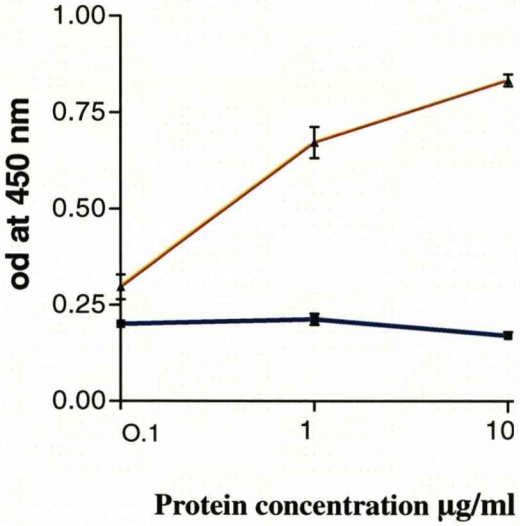

Figure 3.4 WT CHO affinity for IgLON-FC proteins

In an ELISA assay TMB substrate colour change was measured at an optical density (OD) of 450 nm to give the amount of CEPU-1 recombinant protein bound to WT and CEPU-1-CHO cells. Very little CEPU-1-FC bound to WT-CHO cells at each concentration, 0.1-10 µg/ml (flat blue line). Whereas there was a linear increase with each concentration of CEPU-1-FC binding to CEPU-1-CHO cells (red line). From this graph it was concluded that CEPU-1-FC binding was specific to CEPU-1-CHO and not to CHO cells per se. Similarly OBCAM-FC and LAMP-FC did not bind to WT-CHO cells (data not shown).

IgLON-FC proteins binding to IgLON-CHO cell lines

Once non-specific recombinant protein binding to CHO cells was established not to be significant, each of the three IgLON-CHO cells lines was incubated for 1 hour at room temperature with CEPU-1-FC, OBCAM-FC and LAMP-FC recombinant proteins at a concentration range of 0.1-10 μg/ml, followed by goat α human-IgG-HRP-conjugated antibody, diluted 1:5000 in culture medium, for 1 hour, finally TMB substrate was added. All data sets are based on three separate experiments and are calculated minus the value obtained for incubation of the CHO cells without recombinant protein, to eliminate background of secondary antibody binding. Graphs illustrating the amounts of recombinant proteins bound to each IgLON CHO cell line were prepared using the Prism program (figures 3.5 A-C).

CEPU-1-CHO affinity for IgLON-FC proteins

In the first of these graphs (figure 3.5 A) CEPU-1-CHO cells show a higher affinity for LAMP-FC, than for CEPU-1-FC and least affinity for OBCAM-FC. From this data it was concluded that CEPU-1:LAMP had the highest heterophilic interaction, followed by CEPU-1:CEPU-1 homophilic interaction and CEPU-1:OBCAM was the weakest of the interactions.

OBCAM-CHO affinity for IgLON-FC proteins

In the second graph (figure 3.5 B) OBCAM-CHO cells had a higher affinity for LAMP-FC above CEPU-1-FC and OBCAM-FC. This suggested the two heterophilic interactions of OBCAM: LAMP and OBCAM: CEPU-1 were stronger than the OBCAM homophilic binding interaction.

LAMP-CHO affinity for IgLON-FC proteins

Finally, LAMP CHO cells had similar affinities for CEPU-1-FC and OBCAM-FC, but the affinity for LAMP-FC was markedly reduced and was not much above background level, even at highest concentration of 10 μg/ml (figure 3.5 C). These graphs suggested LAMP has a strong heterophilic interaction with both CEPU-1 and OBCAM, but a very weak homophilic interaction.

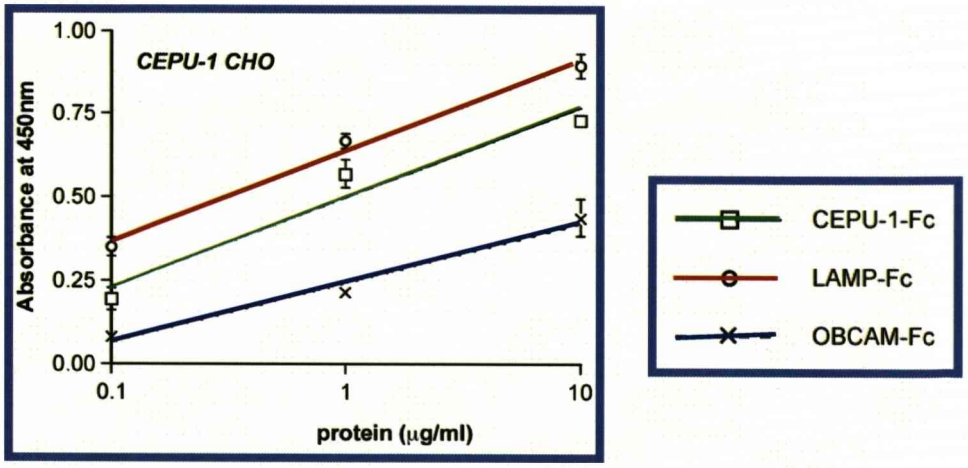

Figure 3.5 A CEPU-1-CHO binding of IgLON-FC proteins

The affinity of triplicate wells of CHO cell lines for IgLON-FC recombinant proteins, diluted 0.1-10 µg/ml was measured in three separate experiments. The amount of protein bound was calculated from TMB substrate colour change, measured at an optical density of 450nm (OD 450 nm) minus a control OD value containing no recombinant protein. In this first figure CEPU-1 CHO cells had a higher affinity for LAMP-FC (red line) than CEPU-FC (green line) with OBCAM-FC (blue line) having the least amount of protein bound. This suggested the strongest interaction is the CEPU-1:LAMP trans heterophilic interaction, followed by the CEPU-1 homophilic interaction and finally the heterophilic CEPU-1:OBCAM interaction is the weakest of these interactions.

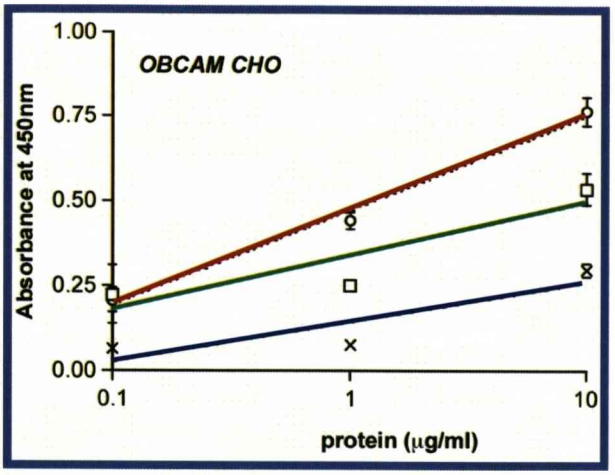

Figure 3.5.B OBCAM-CHO binding of IgLON-FC proteins

OBCAM-CHO cells had a higher affinity for LAMP-FC (red line) than CEPU-FC (green line) with OBCAM-FC (blue line) having the least amount of protein bound. This suggested OBCAM has high trans heterophilic interactions with LAMP, and CEPU-1, but a low homophilic interaction.

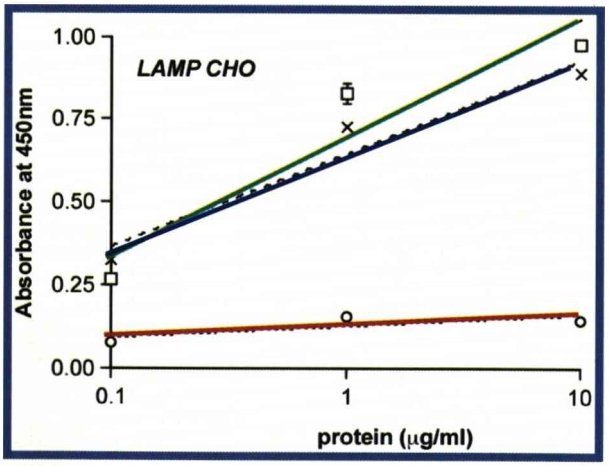

Figure 3.5.C LAMP-CHO binding of IgLON-FC proteins

LAMP-CHO cells had a more distinct difference in their affinity for IgLON-FC proteins. LAMP-CHO had a similar affinity for CEPU-1-FC (green line) and OBCAM-FC (blue line) but a very low affinity for LAMP-FC (red line). The affinity for LAMP-FC was not much higher than the background level, minus recombinant protein, even at highest concentration of 10 µg/ml. This suggests LAMP has a high trans heterophilic interaction with CEPU-1 and OBCAM, but a very weak homophilic trans interaction.

Homo and heterophilic interactions of IgLONs

The optical density value for the highest concentration of recombinant protein was used to correlate the data for each IgLON binding interaction into a histogram. Two sets of data were combined for each heterophilic interaction i.e. LAMP-FC on CEPU-1-CHO is combined with CEPU-1-FC on LAMP-CHO, since these are the same *trans* IgLON interaction, whereas there is only one set of data for the homophilic interaction (figure 3.6.A).

Overall, the highest affinities were those between LAMP with both CEPU-1 and OBCAM, suggesting that *trans* heterophilic interactions with LAMP are generally stronger than *trans* homophilic interactions. This was followed by the affinity between CEPU-1 with both CEPU-1 and OBCAM; finally the weakest interactions were the homophilic OBCAM:OBCAM and LAMP:LAMP interactions.

The results of IgLON interactions in this ELISA assay are used to propose a hierarchy of the binding interactions between IgLONs (figure 3 6.B). This figure represents the relative affinities of both hetero-and homophilic *trans* interactions between the three members of the IgLON family.

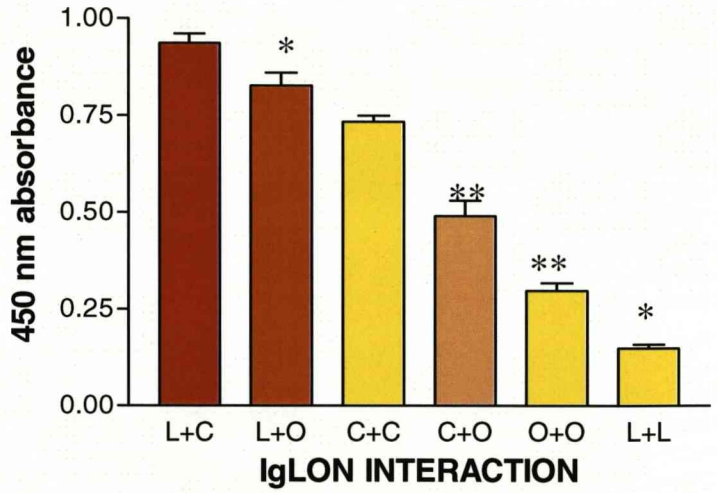

Figure 3.6.A IgLON trans binding interactions

Strengths of trans binding interactions between IgLON CHO cells and recombinant proteins are illustrated in this histogram. The orange bars represent the heterophilic interactions and are based on 6 sets of experimental data; yellow bars represent homophilic interactions, based on 3 repeats. Asterisks denote the level of significant difference between neighbouring bars i.e. LAMP:CEPU-1 (L+C) interaction is significantly stronger than LAMP:OBCAM (L+O $p<0.05$). CEPU-1:CEPU-1 (C+C) interaction is the strongest of the homophilic interactions and is similar in strength to the L+O interaction. The lighter orange bar of CEPU-1:OBCAM (C+O) interaction is mid range, but is significantly lower than the CEPU-1 homophilic interaction ($p<.001$**). Finally the homophilic interactions of OBCAM and LAMP are the weakest of the IgLON interactions. OBCAM (O+O) homophilic interaction is significantly weaker than C+O ($p<0.001$ **) heterophilic interaction and LAMP (L+L) homophilic interaction is weaker than that of OBCAM ($p<0.05$*).*

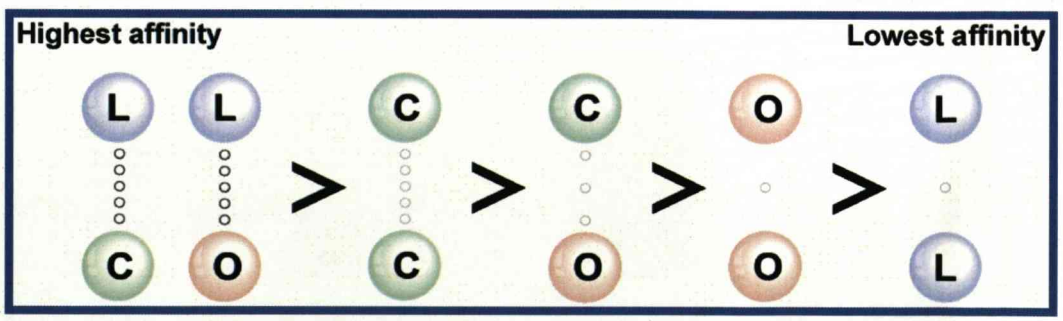

Figure 3.6.B Hierarchy of the IgLON trans binding interactions

The relative affinities for trans hetero and homophilic interactions between the three members of the IgLON family LAMP (L) CEPU-1 (C) and OBCAM (O) based on ELISA assay measurements are presented in this diagram.

DISCUSSION

The aggregation assay of microspheres bound with IgLON-FC proteins suggested there to be *trans* homophilic binding interactions between IgLONs, CEPU-1 having the highest homophilic affinity, followed by OBCAM and LAMP. ELISA assays confirmed aggregation of microspheres data, in that CEPU-1 once again had the highest homophilic affinity and LAMP the weakest. However, the higher resolution of the ELISA assay detected CEPU-1 homophilic interaction to be significantly stronger than that for OBCAM. This comparison is made with the caveat that the levels of IgLON expression on the surface of the CHO cells was assumed to be similar in the ELISA assays and does not take into account any differences in the levels of expression that may have existed between the cell lines.

The higher homophilic *trans* affinity of CEPU-1 in part explains previous data where DRG and sympathetic neurons adhered to CEPU-1-FC in preference to OBCAM-FC and LAMP-FC (McNamee et al., 2002). CGCs neurons confirmed this adhesion preference to CEPU-1-FC but showed no adhesion to a LAMP-FC substrate confirming the preference for a heterophilic interaction (Reed et al., 2004). Ntr-FC (rat homology of CEPU-1) has been shown to bind to DRG and hippocampal IgLON expressing neurons (Gil et al., 1998). In all these experiments the IgLON heads are attached to a FC tail which limits their ability to rotate freely but does not prevent a *trans* interaction. However, in contrast to these experiments LAMP expressing limbic neurons have been demonstrated to adhere to a LAMP substrate prepared from immuno-purified IgLON PiPLC-digested from adult hippocampal neurons suggesting a homophilic interaction for LAMP (Zhukareva and Levitt, 1995).When LAMP is purified by this method it does not have the constraints of the FC-tail and may be interacting with other IgLONs present on the surface of the hippocampal neurons. LAMP purified by this method also differs to these experiments in that it aggregated microspheres to suggest some homophilic interaction (Zhukareva and Levitt, 1995). These binding and ELISA assays propose there is a homophilic interaction for LAMP but it is relatively weak compared to other interactions within the family.

Homophilic interactions may not be the most important of the IgLON interactions, since heterophilic IgLON *trans* interactions are generally stronger than homophilic interactions; with the exception of the CEPU-1 which is comparable to the CEPU-1:OBCAM heterophilic interaction. Ntr (the fourth member of the IgLON

family) was not available to be included in this study, however the apparent dissociation constant for the binding of recombinant Ntr protein to CEPU-1-CHO cells has previously been calculated as 3 x 10^{-8} M; which is physiological relevant in terms of receptor/ligand binding interactions. The binding of Ntr to LAMP-CHO was approximately five times weaker; and no homophilic binding interaction has been detected for Ntr (Marg et al., 1999; Gil et al., 2002). This data would suggest Ntr is similar to LAMP in that it has a high affinity for CEPU-1, a much lower affinity for LAMP and no significant homophilic binding affinity. These ELISA and microspheres aggregation assays suggest that OBCAM and CEPU-1 are most similar in terms of their binding affinities.

Based on these *in vitro* binding assays LAMP-FC would be predicted to bind well to neurons expressing CEPU-1 and OBCAM due to this strong heterophilic *trans* interactions. So far there is no explanation for the weak interactions between LAMP-FC and DRG, sympathetic or CGC neurons

Chapter Four

IgLONs Form Putative cis Heterodimeric Complexes

IgLONs FORM PUTATIVE *CIS* COMPLEXES

INTRODUCTION

This thesis has presented data for *trans* interactions between IgLONs, but there is also evidence to suggest that IgLONs may form *cis* interactions in the plane of the membrane. Cross-linking studies using Ntm (rat CEPU-1) transfected cell lines revealed non-covalent *cis* homodimers and *trans* multimers form on the cell surface (Gil et al., 1998). Western blots analysis of cross-linked sub-confluent and confluent IgLON-CHO cell lines revealed the presence of *cis* homodimers on sub-confluent CHO cells, particularly on CEPU-1-CHO, with no *cis* homodimers on LAMP-CHO cells (unpublished data James Reed). Also the formation of tetramer and multimer complexes on confluent CEPU-1 and OBCAM and to a lesser extent on LAMP-CHO, suggests there to be both *cis* and *trans* interactions between IgLONs. The higher homophilic affinity of CEPU-1 and OBCAM may explain why the larger *trans* complexes observed more readily formed on the confluent cells.

There is some evidence that IgLONs prefer to interact as dimeric molecules as opposed to monomers. Monomeric CEPUse (the secreted isoform of CEPU-1) did not detectably bind to transfected CEPU-1-CHO cell line until it was presented as a homodimeric molecule suggesting both heads of IgLON molecules must bind for the *trans* interaction to be stabilised (Lodge et al., 2000) so IgLON may well form dimers in *cis* rather than remaining as monomers.

The suggestion that IgLONs may interact in *cis*, prefer to act as dimers and have a strong heterophilic interaction in *trans*, raised the possibility that IgLONs may also come together to form *cis* heterodimeric complexes. In principle, this may occur *in vivo* since expression of more than one IgLON has been demonstrated on individual neurons in several areas of the developing and adult nervous system (Struyk et al., 1995; Gil et al., 2002; Miyata et al., 2000).

A series of experiments examines the hypothesis that co-expression of two members of the IgLON family on the surface of CHO-cells results in the formation of putative *cis* heterodimeric complexes. The formation of these complexes may result in an altered *trans* affinity for other IgLONs and begins to explain the inability of LAMP-FC to bind to the surface of some neurons.

Identification of IgLON putative *cis* complexes

AIM

The aim was to introduce a second IgLON onto the surface of transfected CHO cell lines and detect the formation of any putative heterodimeric complexes by measuring alterations in *trans* binding affinity for IgLON-FC recombinant proteins.

RESULTS

pOIG and pLIG plasmid vectors to introduce a second IgLON onto the surface of CHO cells.

In order to introduce the additional IgLON onto transfected CHO cell lines two plasmid vectors were constructed with α1-OBCAM-GPI or α1-LAMP-GPI sequence under the control of the Beta actin (β-actin) promoter in the IRES-GFP plasmid. For convenience OBCAM sequence cloned into the IRES-GFP plasmid vector is identified as pOIG and LAMP sequence as pLIG (Reed et al., 2004). Details of plasmid construction are in Materials and Methods section 2.9.

Confirmation of pOIG and pLIG expression on CHO cells

Endotoxin free pOIG and pLIG plasmid DNA was prepared from bacterial cultures using a Sigma maxi kit and used to transiently transfect WT-CHO cells using Fugene^{TM} transfection reagent. Cells transfected with the plasmids were identified by intracellular GFP expression, on a LEICA LEITZ microscope using filters, with excitation 495nm, and emission 525nm. Expression of either OBCAM or LAMP was identified by staining with specific rat antisera, labeled by a second Texas Red^{TM} conjugated anti-rat antibody, visualized using filters to select for excitation at 596nm, 620nm emission. Some WT-CHO cells stained positively for expression of OBCAM or LAMP but without distinct detection of the GFP fluorescent tag, indicating there may be an underestimation of the sub-population of CHO cells expressing OBCAM or LAMP in future experiments (data not shown).

An alternative plasmid vector, pBUD CE 4.1 (Invitrogen) was tested in similar experiments to evaluate IgLON expression with accompanying GFP expression. LAMP or OBCAM IgLON sequences along with GFP-tag sequences were cloned into separate polylinkers within the pBUD CE4.1 plasmid (James Reed). In this case some

cells expressed GFP but failed to express detectable levels of accompanying OBCAM or LAMP. In addition a small percentage of cells expressed LAMP or OBCAM but GFP-tag expression was not detectable (data not shown). This plasmid was not consistent enough with either IgLON or GFP tagged expression, so it was decided to use the pOIG and pLIG vectors for all future experiments, with the caveat that there may be an underestimation of doubly transfected CHO cells in the population due to a low percentage of cells expressing OBCAM or LAMP but not the GFP tag.

Transient expression of two IgLONs

Transient transfection of pOIG and pLIG plasmids introduced OBCAM or LAMP respectively on to the surface of a sub-population of IgLON expressing CHO cell lines, resulting in a culture with two distinct populations of cells. Identification of the individual CHO cells transiently transfected with pOIG or pLIG was by GFP expression in the cytoplasm. IgLON *trans* affinity to the two populations of cells was measured by live staining with 30 µl of 25 µg/ml IgLON-FC recombinant proteins, visualized by binding of a 1:100 dilution of Texas Red™ conjugated specific FC secondary antibody, examined on a LEICA LEITZ microscope. An altered *trans* binding affinity for the recombinant protein by the transiently transfected CHO cells would suggest the formation of putative *cis* heterodimers (figure 4.1).

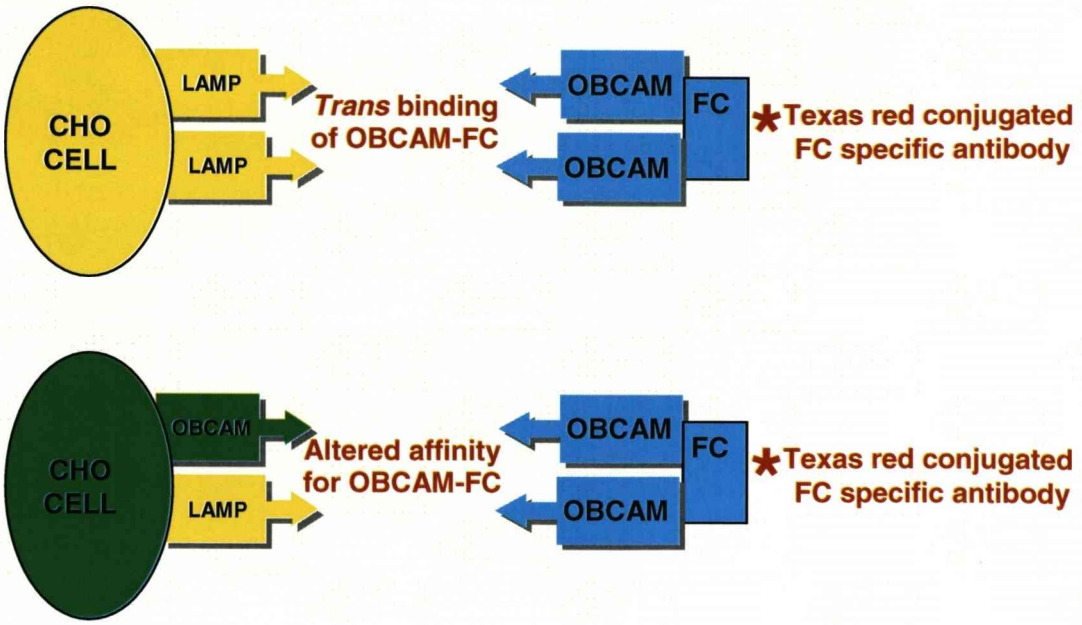

Ffigure 4.1 Altered trans affinity for IgLON-FC proteins suggests a putative cis heterodimeric IgLON complex

*The first part of the diagram illustrates the heterophilic trans interaction between LAMP on the CHO cell surface with OBCAM-FC recombinant protein (opposing yellow and blue shapes). The second part of the diagram illustrates additional OBCAM (green shape) transiently transfected by the pOIG plasmid onto the CHO cell surface. Accompanying cytoplasmic GFP expression (green oval) identifies the CHO cells expressing the additional IgLON. Texas Red™-labelled antibody bound to the FC portion of the OBCAM-FC recombinant protein, visualised as red fluorescence *gave a measure of the affinity for OBCAM-FC by the two populations of CHO cells. An alteration in the trans binding affinity for OBCAM-FC protein by the green subpopulation of CHO cells expressing both LAMP and OBCAM would suggest a putative heterodimeric complex had formed on the CHO cell membrane.*

Affinity for IgLON-FC protein by two populations of CHO cells

The binding of recombinant protein to the IgLON-CHO cells are presented as a series of photomicrographs (figures 4.2 A-D). The first photomicrograph in the series is a phase contrast image of the CHO cells in the field (i). The second photomicrograph highlights green fluorescent CHO cells transiently transfected to express the additional OBCAM or LAMP and cytoplasmic GFP (ii). The third photomicrograph identifies IgLON-FC recombinant protein bound to the CHO cells as Texas Red™ fluorescence (iii). The final photomicrograph is a composite of images two and three (iv). This composite image allows comparison of the binding affinity for IgLON-FC recombinant protein on the two populations of CHO cells. Any alteration in Texas Red ™ fluorescence intensity on the green cells suggests the additional OBCAM or LAMP expressed by these cells have altered IgLON *trans* binding affinity.

Introduction of OBCAM expression onto LAMP-CHO cell line

In the first experiment, pOIG introduced OBCAM expression onto LAMP-CHO cells and the binding affinity for OBCAM-FC recombinant protein was tested. The CHO cells expressing LAMP and OBCAM are marked with arrows in figure 4.2.A i, ii, iii. In photomicrograph iv, a definite variation in Texas Red™ fluorescence was detected between the two populations of CHO cells. There is a significant reduction in Texas Red™ fluorescence on the sub-population of green fluorescent CHO cells expressing both LAMP and additional OBCAM. This reduction in Texas Red™ fluorescence (in some cases to below the level of detection) suggested that introduction of OBCAM onto LAMP-CHO cells had altered the *trans* binding affinity for OBCAM-FC. When tested with CEPU-1-FC recombinant protein there was a similar reduction in Texas Red™ fluorescence intensity on the green cells (figure 4.2.B). In contrast, LAMP-FC recombinant protein Texas Red™ fluorescent intensity increased on the green cells suggesting the affinity for LAMP-FC had increased (figure 4.2.C).

This first set of results demonstrated that introducing expression of OBCAM onto LAMP-CHO cells significantly altered the *trans* binding interaction of IgLON-FC proteins. The CHO cells expressing LAMP had a high affinity for OBCAM-FC and CEPU-1-FC, consistent with ELISA assay data, but this affinity declined with the introduction of OBCAM onto the CHO cell surface.

Introduction of LAMP expression onto OBCAM CHO

The second vector pLIG introduced LAMP on to a sub-population of OBCAM-CHO cells. In this experiment LAMP-FC Texas Red™ fluorescence was visible on the surface of OBCAM-CHO cells, but substantially decreased on the sub-population of CHO cells expressing additional LAMP (figure 4.2.D). There was also a difference in affinity for OBCAM-FC recombinant protein by these two populations of cells. The CHO cells expressing LAMP and OBCAM had slightly increased Texas Red™ fluorescence intensity, suggesting these cells had a higher affinity for OBCAM-FC than the surrounding OBCAM-CHO cells (figure 4.2.E). The OBCAM-CHO cells high affinity for LAMP-FC was consistent with the previous ELISA assay data, and once again introducing a second IgLON onto the surface of the CHO cells altered *trans* binding interaction of recombinant protein.

Introduction of LAMP expression onto CEPU-1-CHO

When pLIG introduced LAMP onto the surface of CEPU-1-CHO cells, there were once again changes in the affinity for recombinant proteins. Texas Red™ fluorescence intensity indicated CEPU-1-CHO had a high affinity for LAMP-FC but this substantially reduced on the sub-population of CHO cells expressing both LAMP and CEPU-1 (figure 4.2.F). In contrast a slight increase in Texas Red™ intensity on the CHO cells expressing both LAMP and CEPU-1 compared to the CEPU-1 only indicated the affinity for OBCAM-FC had increased (figure 4.2.G).

Introduction of OBCAM-GFP into CEPU-1-CHO

In the final series of experiments, pOIG introduced OBCAM-GFP expression into CEPU-1-CHO cells (figure 4.2.H-J). A high Texas Red™ fluorescent intensity on both populations of cells suggested a higher overall affinity for LAMP-FC (figure 4.2.H). The overall Texas Red™ fluorescent intensity for bound OBCAM-FC and CEPU-1-FC was lower than in previous experiments and there was no significant change in fluorescent intensity was detected between the two populations of cells (figure 4.2.I, J). The *trans* binding affinities between CEPU-1 and OBCAM was found to be similar in the ELISA assays and so may explain why introducing OBCAM into these CEPU-1-CHO cells produced no change in the affinity for IgLON-FC recombinant protein. This final set of experiments acted as a control to demonstrate that merely increasing the level of IgLON expression on the CHO cell surface (by introducing additional OBCAM on to the CEPU-1-CHO surface) was not increasing the overall *trans* affinity for IgLON-FC recombinant proteins.

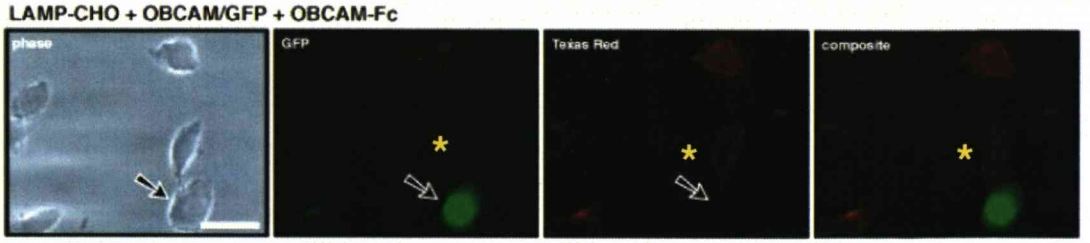

i **ii** **iii** **iv**

Figure 4.2.A Photomicrographs of OBCAM-FC binding to LAMP-CHO cells transiently transfected with pOIG

pOIG plasmid introduced expression of OBCAM onto a subpopulation of LAMP-CHO cells and the affinity for OBCAM-FC was compared on the two populations of cells. Photomicrograph i, is a phase image of the CHO cells in the field of view. In photomicrograph ii, green fluorescence identifies a LAMP-CHO cell-expressing OBCAM is highlighted with an arrow. In photomicrograph iii, OBCAM-FC protein binding to the CHO cells is visualised as Texas Red™ fluorescence. Image ii is merged with image iii to give composite photomicrograph iv. There is a substantial reduction in Texas Red™ fluorescence intensity on the green fluorescent cell expressing both LAMP and OBCAM on the cell surface. A cell highlighted by yellow asterisk (*) has reduced red fluorescence in image iii and iv but does not appear to be expressing the pOIG plasmid as green fluorescence is not detected in image i. On initial testing of the pOIG plasmid in WT-CHO some cells were found to express the IgLON without detectable levels of GFP. This cell is most likely to be expressing additional OBCAM but possibly at a lower level of expression so producing a lighter red fluorescent stain (discussed page 93). Scale bar is 25 μm.

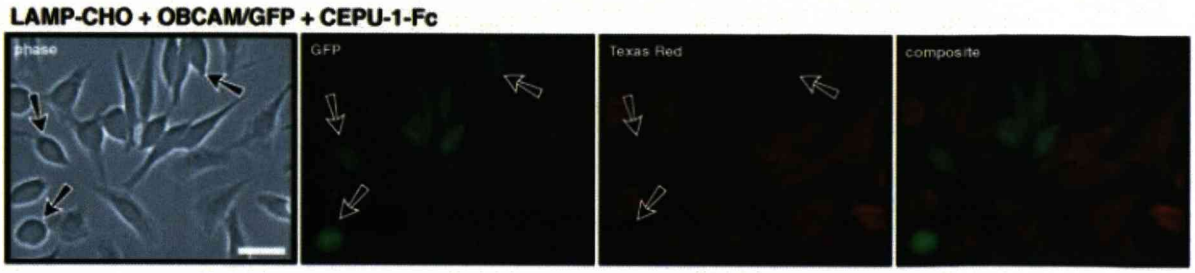

Figure 4.2.B Photomicrographs of CEPU-FC-binding to LAMP-CHO cells transiently transfected with pOIG

These photomicrographs have the same format, but illustrate the affinity of the two populations of CHO cells for CEPU-1-FC. The sub-population of CHO cells expressing both OBCAM and LAMP are visualised by green fluorescence in image ii, arrowed cells. Note the reduction in Texas Red™ fluorescence on these arrowed cells in iii. Composite image iv clearly identifies the CHO cells co-expressing OBCAM and LAMP have reduced Texas Red™ fluorescence compared to the remaining cells expressing LAMP.

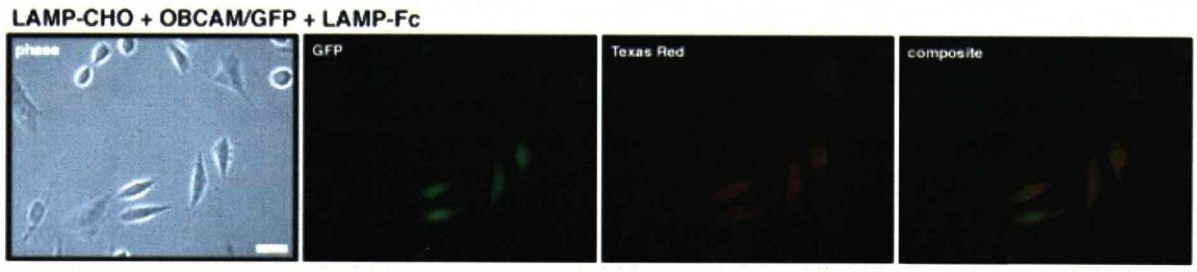

Figure 4.2.C Photomicrographs of LAMP-FC-binding to LAMP-CHO cells transiently transfected with pOIG

Comparison of the affinity for LAMP-FC by the two populations of cells showed an increase in Texas Red™ fluorescent intensity on some cells image iii. Composite image iv identifies the increase in intensity is on the green fluorescent cells, expressing both LAMP and OBCAM, whereas the remaining LAMP-CHO cells have an extremely weak affinity for LAMP-FC.

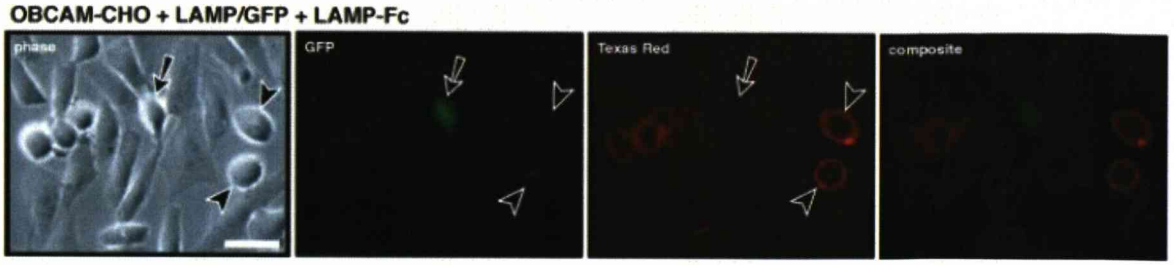

Figure 4.2.D. Photomicrographs of LAMP-FC-binding to OBCAM-CHO cells transiently transfected with pLIG

pLIG plasmid introduced expression of LAMP onto a subpopulation of OBCAM-CHO cells and the affinity for LAMP-FC was compared on the two populations of cells. In phase contrast image i some cells have a more rounded morphology and thicker, phase bright, plasma membrane. In photomicrograph iii note how these phase bright OBCAM-CHO cells have increased Texas Red™ fluorescent intensity resulting from their thicker cell membrane (highlighted by arrowheads in images i, iii) An OBCAM-CHO cell, expressing LAMP is identified by green fluorescence and highlighted with an arrow in photomicrographs i,ii and iii. In composite image iv, there was a substantial reduction in Texas Red™ fluorescent intensity on the green cell expressing both OBCAM and LAMP which suggested these cells have a lower affinity for LAMP-FC.

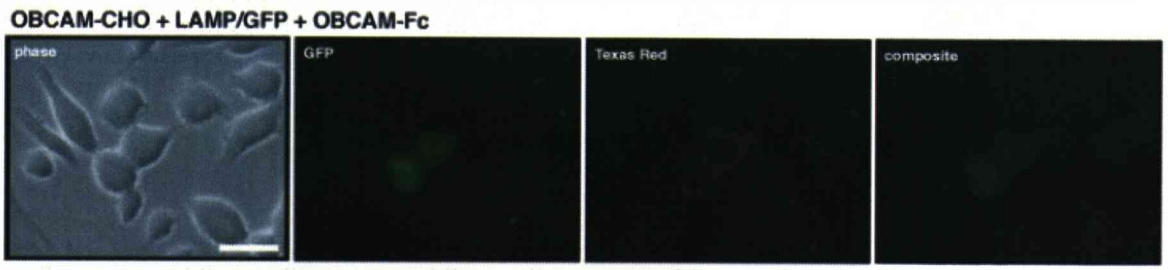

Figure 4.2.E. Photomicrographs of OBCAM-FC-binding to OBCAM-CHO cells transiently transfected with pLIG

When the affinity for OBCAM-FC recombinant protein was tested on the pLIG transfected OBCAM-CHO cells there was a slight increase in Texas Red™ fluorescent intensity on the green cells expressing both OBCAM and LAMP compared to the surrounding OBCAM-CHO cells, composite photomicrograph image iv.

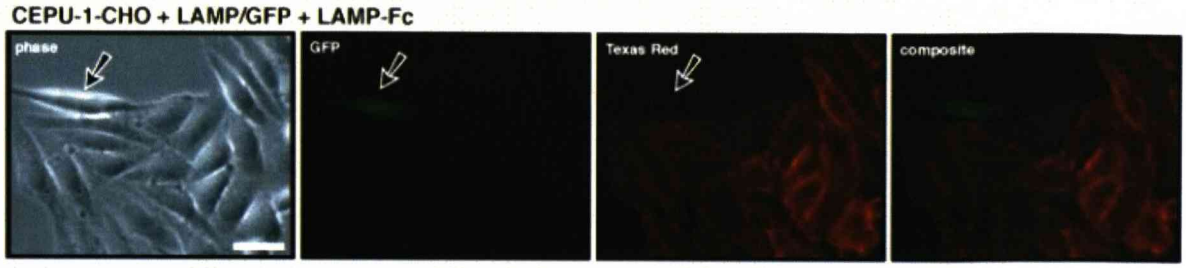

i ii iii iv

Figure 4.2.F. Photomicrographs of LAMP-FC-binding to CEPU-1 CHO cells transiently transfected with pLIG

pLIG plasmid introduced expression of LAMP onto a subpopulation of CEPU-1 -CHO cells and the affinity for LAMP-FC was compared on the two populations of cells. A CEPU-1-CHO cell expressing LAMP, identified by green fluorescence, is highlighted with an arrow in photomicrographs i ii and iii. In composite image iv there was a substantial reduction in Texas Red™ fluorescent intensity on this green cell which suggested a lower affinity for LAMP-FC.

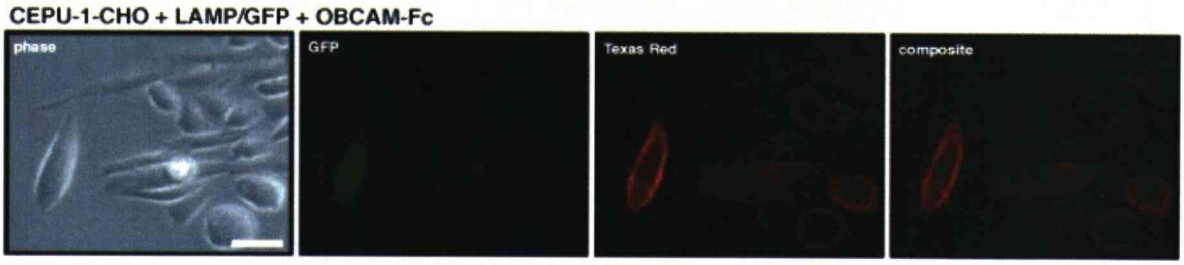

i ii iii iv

Figure 4.2.G. Photomicrographs of OBCAM-FC-binding to CEPU-1 CHO cells transiently transfected with pLIG

Affinity for OBCAM-FC recombinant protein was tested on the same culture of CHO cells. In composite photomicrograph image iv there was a slight increase in Texas Red™ fluorescent intensity on the green cell (expressing both CEPU and LAMP) compared to the surrounding OBCAM-CHO cells suggesting a higher affinity for OBCAM-FC recombinant protein.

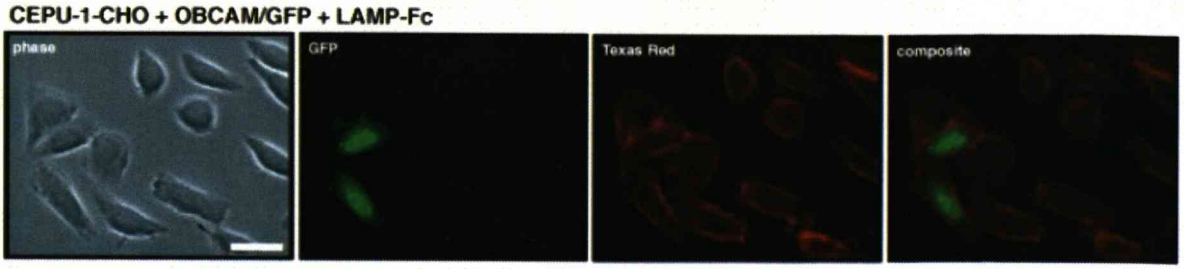

i ii iii iv

Figure 4.2.H. Photomicrographs of LAMP-FC-binding to CEPU-1 CHO cells transiently transfected with pOIG

pOIG plasmid introduced expression of OBCAM onto a subpopulation of CEPU-1 - CHO cells and the affinity for LAMP-FC was compared on the two populations of cells. In composite image iv Texas Red™ fluorescent intensity was similar on both the green fluorescent CHO cells expressing CEPU-1 and OBCAM and on the cells expressing only CEPU-1 suggesting there to be no change in binding affinity for LAMP-FC.

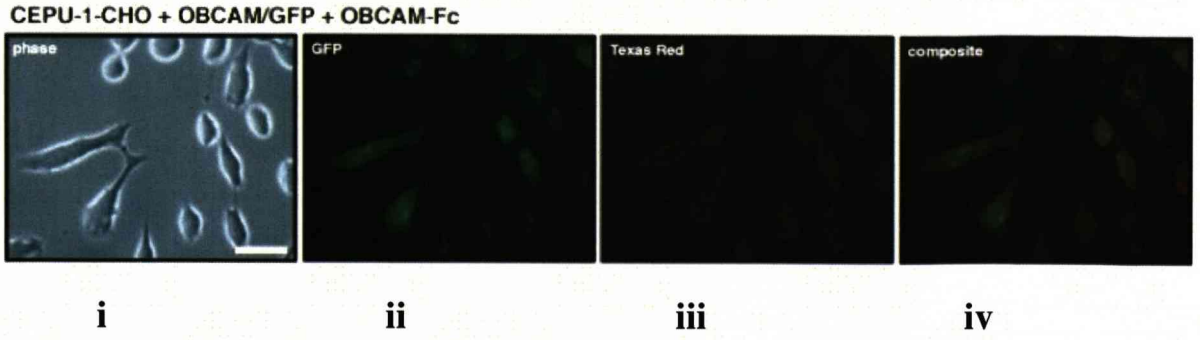

Figure 4.2.I. Photomicrographs of OBCAM-FC-binding to CEPU-1 - CHO cells transiently transfected with pOIG

Affinity for OBCAM-FC recombinant protein was tested on the same two populations of CHO cells Texas Red™ fluorescent intensity of bound OBCAM-FC was generally weaker than in the previous experiments on all the CHO cells reflecting an overall lower affinity for OBCAM-FC.

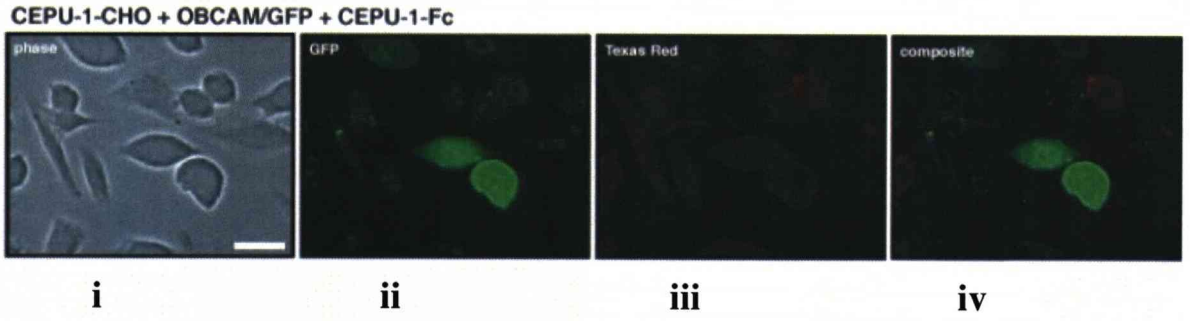

Figure 4.2.J. Photomicrographs of CEPU-1-FC-binding to CEPU-1 - CHO cells transiently transfected with pOIG

Overall Texas Red™ fluorescent intensity of bound CEPU-1-FC was again weaker and remained unchanged on both CEPU-1-CHO and CEPU-1- transfected with OBCAM.

Summary of altered *trans* affinity for IgLON-FC recombinant protein identification of *cis* heterodimers

In summary, introducing a second IgLON onto the surface of CHO cells altered the *trans* affinity for recombinant proteins. There was a reduced affinity for OBCAM-FC and CEPU-1-FC, but enhanced LAMP-FC binding affinity when pOIG-introduced OBCAM onto the surface of LAMP-CHO to suggest a putative *cis* LAMP–OBCAM (LO) complex had formed. pLIG introducing LAMP onto both OBCAM and CEPU-1-CHO reduced LAMP-FC affinity, but increased the binding affinity for OBCAM-FC. This supported the formation of a putative *cis* LO and suggested the formation of a LAMP-CEPU-1 (CL) complex. Due to their similar *trans* binding affinities pOIG introducing OBCAM onto the surface of CEPU-1-CHO did not provide any evidence for a putative CEPU-1-OBCAM (CO) complex, but demonstrated that merely increasing IgLON expression on the CHO cell surface was not responsible for altering IgLON-FC recombinant binding.

Proposed *trans* binding interactions of IgLON-FC with double IgLON-CHO cells

Since IgLONs prefer to act as dimers each IgLON head of the recombinant protein should interact in *trans* with an IgLON monomer on the CHO cell surface for the binding of the recombinant protein to be stabilised. The *trans* interactions between each portion of the IgLON-FC and IgLONs on the CHO cell surface are illustrated in diagrams figure 4.3.A-J. Data of the comparative strengths of IgLON binding affinities from the previous chapter then propose an explanation as to how introducing LAMP or OBCAM onto the CHO-cell surface may have the altered the *trans* affinity for recombinant proteins and caused their binding to be destabilised.

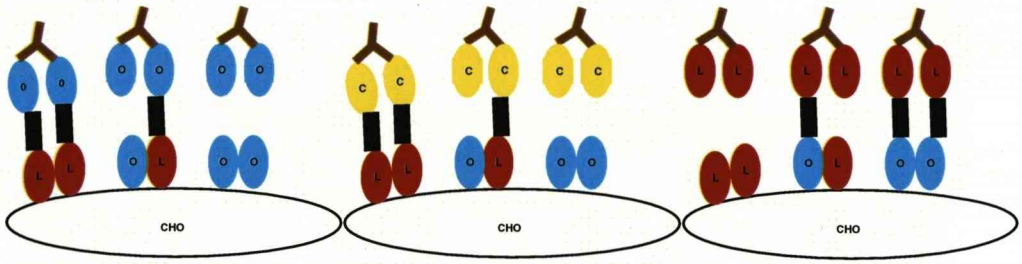

A i ii iii B i ii iii C i ii iii

Figure 4.3.A-C IgLON-FC trans interactions with LO putative heterodimer

The hierarchy of trans binding affinities between IgLONs may explain the altered affinity for recombinant proteins. The strength of the trans affinity between each IgLON head of the recombinant protein and each monomer on the CHO cell surface is considered in the following diagrams. The black lines highlight a high affinity trans interactions, single letters represent IgLON molecules on the CHO cell surface C-CEPU-1, O-OBCAM, L-LAMP; C monomers are represented as yellow ovals, O as blue ovals and L as red ovals. In the first example evidence for LO heterodimer complex was based on the reduction in both CEPU-1-FC and OBCAM-FC recombinant protein binding when additional O was expressed on L-CHO cells. L alone expressed on the surface of CHO cells allows both heads of OBCAM-FC to interact with L monomers (Ai). Following introduction of O it is proposed that a putative LO cis complex forms and destabilises OBCAM-FC binding since only the L portions of the complex is strong enough to interact with the OBCAM-FC protein, the OBCAM trans homophilic interaction being too weak to support an interaction(Aii). Additional O monomers or homodimers may possibly be present on the cell surface further weakening OBCAM-FC interaction (Aiii). A similar situation occurs with CEPU-1-FC (B), CEPU-1-FC initialy binds with high affinity when only L is on the cell surface (Bi) but introduction of O forms an LO complex destabilises the CEPU-1-FC interaction due to the weaker CEPU-1:OBCAM trans interaction (Bii). The reverse situation may explain the increased binding of LAMP-FC when OBCAM is on the CHO cell surface (C). The stronger OBCAM: LAMP trans affinity may have enabled some weak interaction between the O portions of LO complex allowing some binding of LAMP-FC (Cii). Over-expression of pOIG may have resulted in additional O on the cell surface, further increasing the affinity for LAMP-FC (Ciii).

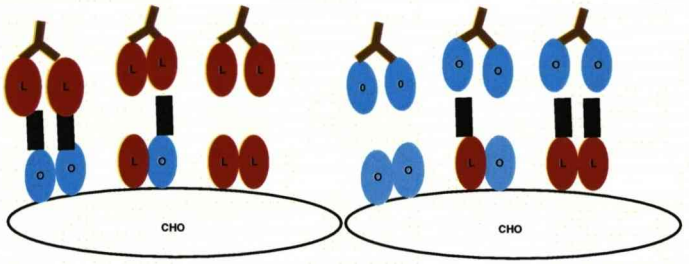

D i ii iii E i ii iii

Figure 4.3.D-E IgLON-FC trans interactions with LO putative heterodimer

Initially O on the CHO cell surface had a high trans affinity for LAMP-FC (Di) but pLIG introduced expression of L onto the surface of O-CHO cells and the formation of a putative LO complex destabilised the binding of LAMP-FC because of the weak homophilic trans affinity of the L portion of the complex for LAMP-FC (Dii). Furthermore, any additional L on the cell surface would not interact with LAMP-FC (D iii). By contrast the homophilic affinity between O on the CHO cell and OBCAM-FC has a weak affinity, but when L was introduced the affinity for OBCAM-FC began to increase since there is a high trans affinity between OBCAM-FC and the L portion of the LO complex (E ii) additional O on the CHO cell surface may have further increased the affinity for OBCAM-FC (E iii).

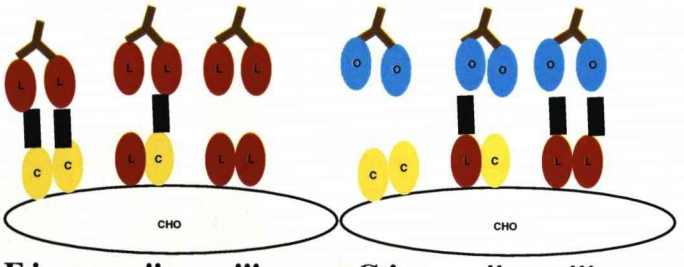

F i ii iii G i ii iii

Figure 4.3.F-G IgLON-FC trans interactions with CL putative heterodimer

Similarly pLIG introduction of L onto CEPU-1-CHO resulted in a reduced affinity for LAMP-FC to support the formation of a putative CL cis complex. The putative CL complex had the same effect as LO complex on recombinant protein binding. The weak affinity between the L portions of the complex no longer stabilised the binding of LAMP-FC (F ii). By contrast, additional expression of L increased OBCAM-FC recombinant protein affinity (G ii, iii).

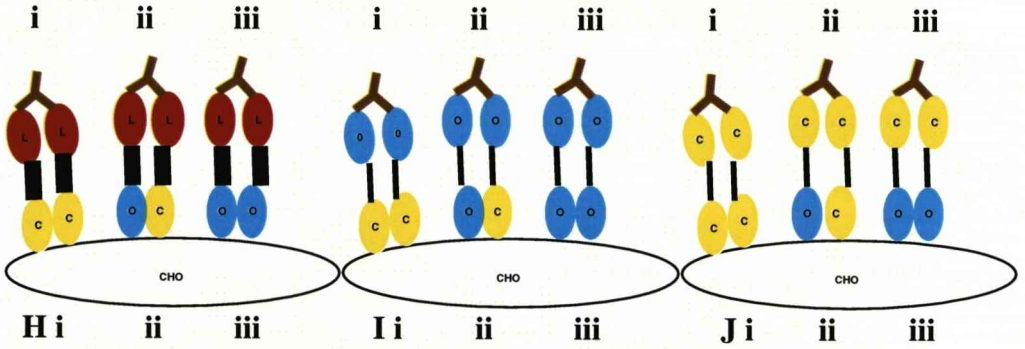

Figure 4.3.H-J IgLON-FC trans interactions with CO putative heterodimer

When OIG introduced O onto the cell surface (Hii) there was no change in recombinant protein binding because both C and O portions of the complex have similar trans binding affinities. LAMP has a similar trans affinity with both portions of the putative CO complex so the strong affinity for LAMP-FC was maintained when additional O was on the surface of the CHO cells (H ii). Even though OBCAM-FC and CEPU-1-FC binding was generally weaker compared to LAMP-FC (indicated by the thinner black lines I-J) it remained constant (I ii, iii; J ii, iii). Additional expression of O on the surface of the CHO cells had no affect on the overall affinity for the recombinant proteins so this experiment could not provide any evidence for a putative CO heterodimer, but it did show mearly incresing the level of expression of IgLONs was not responsible for increasing IgLON-FC binding .

Quantization of putative *cis* complex affinity for IgLON-FC proteins

In these experiments the amount of bound IgLON-FC recombinant proteins to the two populations of CHO-cells was made by visually comparing Texas Red™ fluorescence intensity and did not provide any quantitative measure. Metamorph™ software quantified the fluorescent intensity of bound OBCAM-FC and CEPU-1-FC to LAMP-CHO and LAMP plus OBCAM-CHO cells to give an actual measurement for the *trans* interaction between the CHO cells and the recombinant protein, figure 4.4, courtesy of James Reed, (Reed et al., 2004).

The fluorescent intensity of bound OBCAM-FC and CEPU-1-FC recombinant proteins was measurably reduced on LAMP-OBCAM–CHO cells compared to LAMP-CHO cells to confirm the visual observations in the previous experiment.

Introduction of a second IgLON onto CHO cells does not alter overall IgLON expression

One possible explanation for the change in the binding affinity for IgLON-FC recombinant proteins was the additional IgLON introduced onto the CHO cells had altered the overall level of IgLON expression. To confirm that OBCAM expression was unchanged with the co-expression of LAMP, the CHO cells were immuno-stained with OBCAM rat antiserum and visualised with a Texas-Red™ conjugated goat anti-rat secondary antibody. Measurement of the fluorescent intensity demonstrated there was no significant difference in OBCAM expression on the two populations of cells. This suggested OBCAM expression was unaffected and not compromised by the incorporation of LAMP onto the cell membrane, histograms figure 4.5 courtesy of James Reed, (Reed et al., 2004))

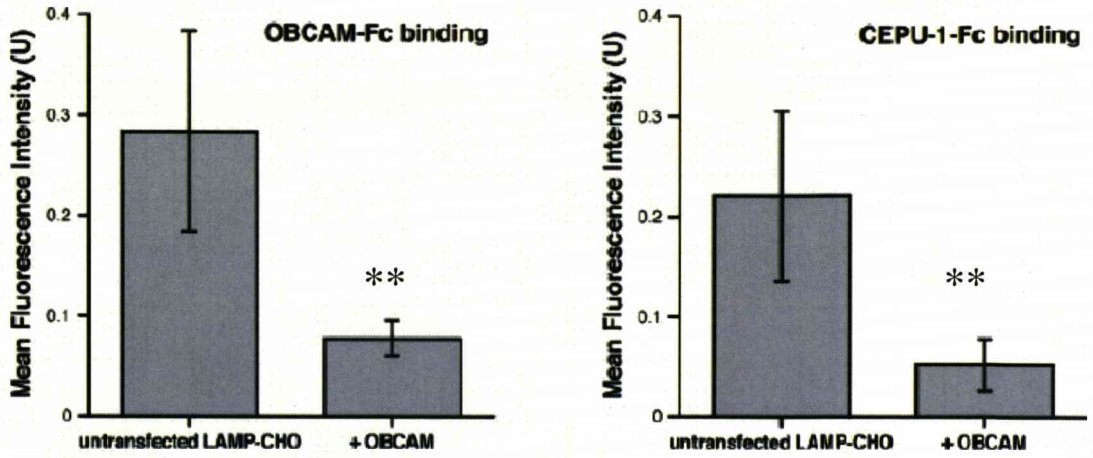

A B

Figure 4.4 Quantification of fluorescent intensity of bound IgLON-FC proteins to LAMP CHO and LAMP+OBCAM-CHO

The first histogram in each pair corresponds to binding of recombinant protein to LAMP-CHO cells; the second histogram has additional OBCAM transfected on to the LAMP-CHO cell surface. The affinity for OBCAM-FC significantly reduced on the CHO cells expressing both LAMP and OBCAM compared to the LAMP-CHO (A). CEPU-1-FC affinity similarly reduced on LAMP-OBCAM CHO (B). Data based on measurements of 100 cells, normalised to remove background and statistics compiled using Microsoft Excel (figures courtesy of Reed et al., 2004)).

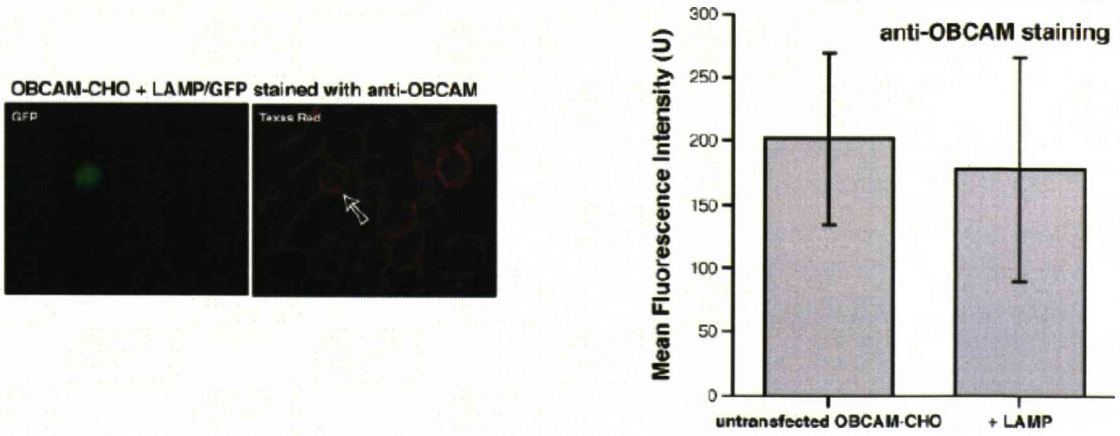

A B

Figure 4.5. Additional co-expression of LAMP did not alter expression of OBCAM

In part A the arrow identifies a CHO cell expressing both OBCAM and LAMP. Once stained with OBCAM specific antiserum there was no visual difference in staining intensity between those CHO-cells expressing OBCAM and those expressing additional LAMP. Histogram part B compares measurement of fluorescence intensity on 100 cells from both populations. There was no significant difference between the fluorescence intensity of OBCAM on both populations of cells so the addition of LAMP on the CHO cells had not compromised OBCAM expression.

Preparation of double IgLON CHO cell lines

The previous experiments provided evidence of putative heterodimeric *cis* LAMP-OBCAM (LO) and CEPU-1-LAMP (CL) complex formation, but did not provide any evidence for *cis* complex formation between CEPU-1 and OBCAM (CO). A CO-CHO stably transfected cell line was prepared to investigate the formation of putative CO complexes, alongside a CL-CHO cell line. In these cell lines the balance of expression of the two IgLONs was more consistent and so enabled further experiments to investigation the function of putative heterodimeric IgLON complexes. The pBud CE 4.1 (Invitrogen) plasmid vector was choosen to prepare these cell lines since it contains two separate cloning sites and could introduce both IgLON sequences simultainiously into the CHO-cells (details Materials and Methods section 2.11). CO and CL CHO-cell lines were selected in a similar way to original single CHO cell lines and characterised by immuno-cytochemistry (figure 4.6.A).

ELISA-assay confirms CO-CHO express CEPU-1 and OBCAM

An ELISA assay on the CO-CHO cell line using specific CEPU-1 and OBCAM rabbit antiserum further confirmed expression of both CEPU-1 and OBCAM on the surface of the CHO cells (figure 4.6.B).

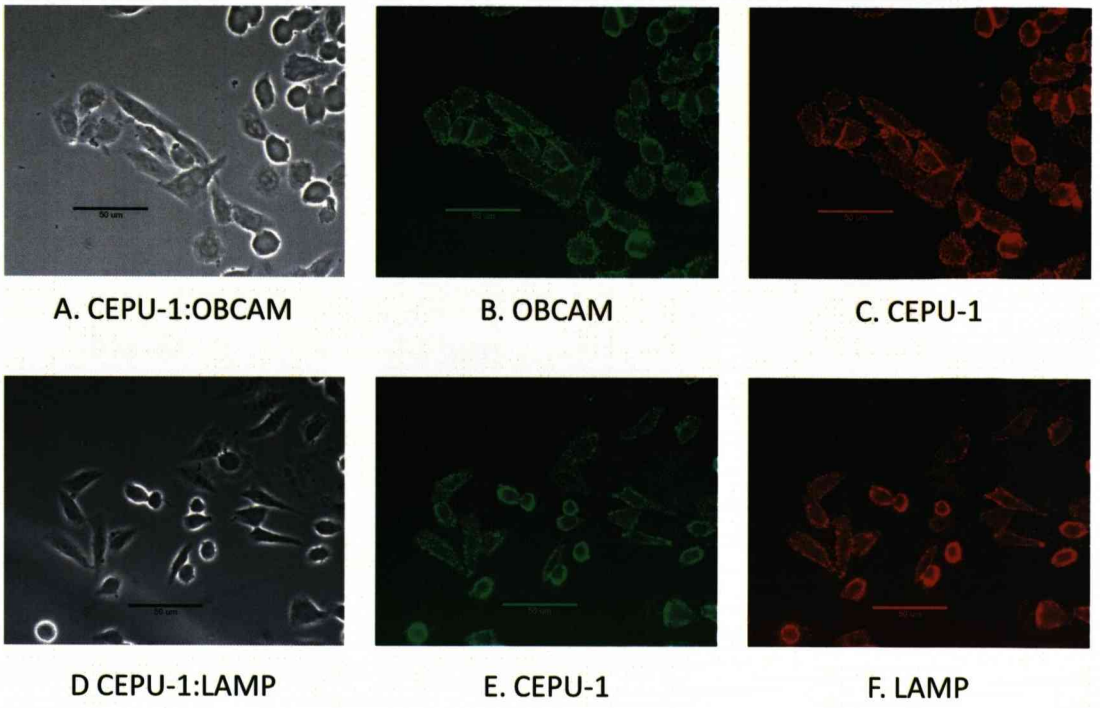

Figure 4.6.A. Characterisation of CO and CL--CHO cell lines

The CHO cells in the field are visible in phase contrast image photomicrograph A. Staining with OBCAM rabbit antiserum, detected with Alexa green 488™ labelled goat anti rabbit secondary antibody (Invitrogen) confirmed all the cells expressed OBCAM, photomicrograph B. Similarly staining with CEPU-1 specific rat antiserum, detected with Texas-Red™ labelled donkey anti rat (Jackson laboratories) confirmed all the cells co-expressed CEPU-1, photomicrograph C. CEPU-1 rabbit (E) and LAMP rat antisera (F) confirmed the cells in phase contrast photomicrograph (D) expressed both CEPU-1 and LAMP. Primary and secondary antibodies were previously tested and shown to be specific.

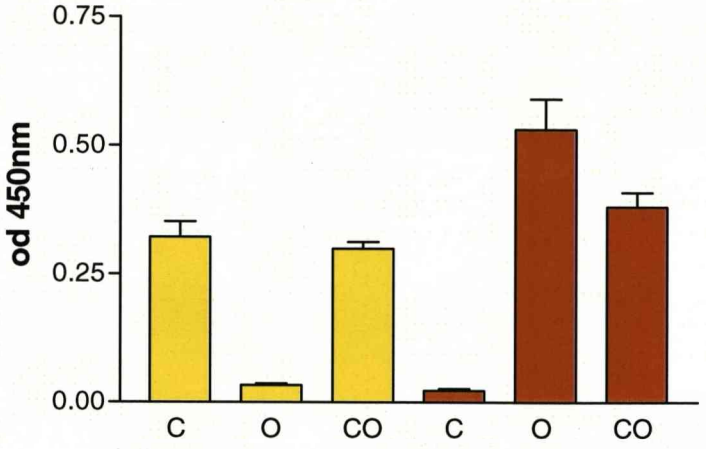

Figure 4.6.B. ELISA-assay confirms CO-CHO cell line expresses both CEPU-1 and OBCAM

ELISA-assay in which CEPU-1 and OBCAM expression on CEPU-1- CHO (C) OBCAM-CHO (O) and CO-CHO cell lines is detected with 1:2000 dilutions of CEPU-1 (yellow bars) and OBCAM specific rabbit antiserum (orange bars) followed by 1:2000 dilution of HRP conjugated goat anti rabbit antibody (Dako) and visualised using TMB substrate colour change measured at wavelength 450nm. CEPU-1 expression was detected on C-CHO (first yellow bar) and OBCAM expression on O-CHO (fifth orange bar). There was minimal cross reactivity between the two antisera since CEPU-I did not significantly detect OBCAM on OBCAM-CHO (second yellow bar) and vice-versa OBCAM antiserum did not detect CEPU-1 on CEPU-1-CHO (fourth orange bar). Both CEPU-1 and OBCAM were detected on the CO-CHO cell line (third yellow bar and last orange bar respectively).

ELISA-type assay supports putative CO complex formation

To detect the formation of a CO complex an ELISA assay measured the CO-CHO cell line affinity for LAMP-FC recombinant protein and compare it to that of individual CEPU-1 OBCAM and LAMP single CHO cell lines. LAMP-FC *trans* binding affinity was reduced significantly on the LAMP-CHO cell line compared to that on CEPU-1 and OBCAM-CHO cell lines. This was expected since a weak homophilic *trans* interaction for LAMP has already been established. The binding of LAMP-FC to CO-CHO cell line was also reduced to a similar level as that found on LAMP-CHO (figure 4.7). This was unexpected since the strong heterophilic *trans* interaction between LAMP with both CEPU-1 and OBCAM expressed on the CO-CHO cell line should have had a high affinity for LAMP-FC protein. This alteration in *trans* binding of LAMP-FC provides the first evidence to suggest that CEPU-1 and OBCAM also form a complex in *cis*.

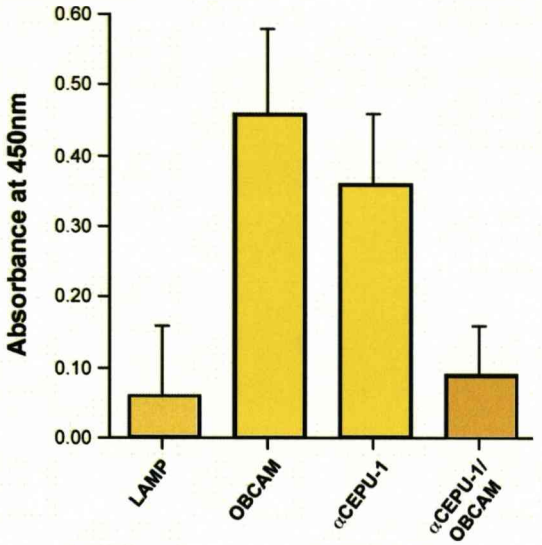

Figure 4.7. CO CHO cells affect the trans binding of LAMP-FC.

*In this ELISA assay binding of 1 μg/ml LAMP-FC protein to CHO cells expressing LAMP, OBCAM, CEPU-1 and CO CHO was again quantified by measurement of change in TMB substrate measured absorbance at 450 nm wavelength. In three experiments, LAMP-FC binding in trans to LAMP-CHO cells was significantly reduced compared to binding onto OBCAM and CEPU-1-CHO cell lines (p> 0.01 **). LAMP-FC binding to CO-CHO cell line was similarly reduced to the low level found on LAMP-only CHO cells (p>0.01 **).*

DISCUSSION

The results described in this chapter provide the first evidence that IgLONs may interact in the plane of the membrane. The evidence is indirect and depends on interpreting differential binding affinities of IgLON-FC recombinant proteins by a mixed culture of CHO cells expressing either one or two IgLONs. A marked reduction in the affinity for recombinant proteins was detected when a second IgLON was present on the surface of the CHO-cell. The altered trans affinities are summerised in figure 4.8. A *cis* interaction between the two IgLONs on the cell membrane is proposed to bring about this alteration in *trans* affinity to provide initial evidence for putative IgLON *cis* heterodimeric complexes.

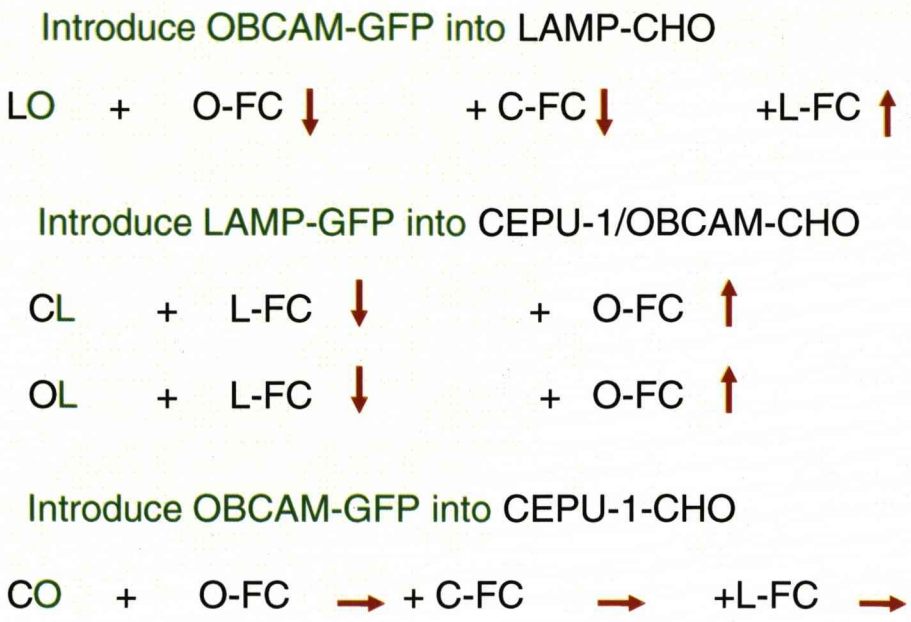

Figure 4.8 CIS heterodimers alter the trans affinity for IgLON-FC recombinant proteins.

*Green letters indicate the introduction of the second IgLON onto CHO cell lines + sign the trans binding interaction, the direction of the red arrows indicates how the additional IgLON altered the affinity for recombinant proteins (**-FC**). When **O** was introduced onto **L**-CHO the binding affinity for **O-FC** and **C-FC** was reduced, whereas affinity for **L-FC** increased. **L** introduction onto **C** and **O**-CHO reduced **L-FC** binding but increased that of **O-FC**. Introduction of **O** onto **C**-CHO did not alter recombinant protein binding.*

The key result obtained was that LAMP-FC bound effectively to OBCAM-CHO but when LAMP was introduced on to the CHO cells this binding was markedly reduced. It was proposed LAMP and OBCAM had formed a putative LO *cis* complex on the surface of the CHO cell and the weak *trans* interaction between the LAMP portion of the complex and the LAMP head of LAMP-FC had de-stabilised the recombinant protein binding. This result was supported by similar altered binding affinity for LAMP-FC when LAMP was introduced onto CEPU-1-CHO cells.

The *trans* binding affinities of CEPU-1 and OBCAM are so similar this affinity for recombinant protein assay was not sensitive enough to detect formation of a *cis* CO heterodimeric complex. However, this assay did suggest that merely increasing IgLON expression *per se* on the CHO cell surface, by adding additional OBCAM onto the surface of CEPU-1-CHO cells, had not increased the affinity for IgLON-FC recombinant proteins. Addition of OBCAM onto the CEPU-1-CHO cell surface would have been more likely to increase LAMP-FC affinity than to decrease it since LAMP-FC has a high *trans* affinity for both CEPU-1 and OBCAM.

To demonstrate that transfection of a second IgLON was not simply compromising the IgLON present on the CHO cell surface LO-CHO were stained with specific OBCAM antiserum and the fluorescent intensity of OBCAM expression was measured and compared to that on OBCAM-CHO cells. There was no significant difference in OBCAM expression on the cells suggesting the addition of LAMP had not compromised OBCAM expression. Combined this data suggests that altered affinity for recombinant protein was not simply due to altering the levels of IgLON expression on the CHO cell surface.

The more sensitive ELISA assay on CO-CHO cell line detected a very low affinity for LAMP-FC recombinant protein, which was similar to the weak homophilic *trans* affinity between LAMP-FC and LAMP-CHO cell line. This was a slightly different result to LAMP-FC *trans* binding assay to CEPU-1 CHO cells transiently transfected to express additional OBCAM, which detected some affinity for LAMP-FC. When pOIG was introduced into CEPU-1-CHO LAMP-FC was most likely binding to CEPU-1 and OBCAM homodimers present on the CHO-cell surface. By comparison the CO-CHO cell line was selected to have a more balanced expression of CEPU-1 and OBCAM and so the ELISA assay provided more sensitive accurate evidence for a putative CO *cis* complex. The inability of LAMP-FC to bind to these CO-CHO cells may have theoretically arisen due to the FC portion of the

recombinant protein holding the IgLON heads in a conformation that prevented access to their binding site. However, LAMP-FC was capable of binding to both single OBCAM and CEPU-1-CHO cell lines, so this was not likely.

The failure of LAMP-FC recombinant protein to bind to the CO-CHO cells was suprising considering the heterophilic affinity of LAMP with both portions of the proposed CO complex, so the *trans* affinity of each IgLON head stabilising the binding of the recombinant protein as initially proposed is over-simplfied. The results from this ELISA assay suggest it is more likely some sort of conformational change alters individual CEPU-1 and OBCAM binding sites to prevent LAMP-FC *trans* binding. Whilst it cannot be predicted which surfaces of the IgLON molecule are used for *cis* and *trans* interactions, the *trans* binding site being occupied by a *cis* interaction would provide an explaination why LAMP-FC did not bind to CO and suggest *cis* and *trans* interactions may form at the same binding site. If this is the case the strong heterophilic *trans* affinity between LAMP with both CEPU-1 and OBCAM and between CEPU-1 with OBCAM would predict CL, LO, and CO *cis* heterodimers readily form on the cell surface.

There are examples in the literature of Ig superfamily members undergoing conformational changes following interactions in both *cis* and *trans*. For example Axonin 1 forms homodimeric *cis* complexes. Axonin 1 has 6 Ig domains, as the complexes form the end 3 Ig domains undergo a conformational change, hook around to interact in zipper-like homophilic interactions between the heads (Kunz et al., 2002). Furthermore, IgSF members do form functional *cis* complexes, for example, DCC and UNC from part of a receptor complex to inhibit neurite outgrowth (Stein and Tessier-Lavigne, 2001).

The original reason for investigating homo and heterophilic interations of the IgLON family was to understand why neurons do not bind to LAMP-FC, despite a strong heterophilic affinity for LAMP by the IgLONs expressed on the surface of neurons. In particular LAMP-FC failed to bind to CGC, DRG and sympathetic neurons even though LAMP, OBCAM and CEPU-1 are expressed on their surface. IgLONs existing as heterodimeric complexes, with a change in conformation altering the availablility of binding sites, provides a possible explaination of why LAMP-FC fails to bind to neurons.

Chapter Five

FUNCTIONAL EFFECTS OF PUTATIVE IgLON *CIS* COMPLEXES

FUNCTIONAL EFFECTS OF PUTATIVE IgLON *CIS* COMPLEXES

INTRODUCTION

Results in the previous chapter suggested IgLONs form *cis* heterodimeric complexes which affect their *trans* binding affinity. This chapter investigates a function for putative *cis* heterodimeric complexes. Several papers have proposed single IgLONs have modified neurite outgrowth (Zhukareva and Levitt, 1995; Gil et al., 2002) but the measured effects have been minimal, so the exact role of single IgLONs on neurite outgrowth has remained unclear and confused. Only CHO cells expressing the putative *cis* CO complex were able to inhibited the initiation of neurite outgrowth from a sub-population of cerebellar granule cells (CGC) whereas single IgLON-CHO cells had no effect (McNamee et al., 2002). This suggests IgLONs may only be functional when they form *cis* heterodimeric complexes (Reed et al., 2004). Furthermore, the distinct ability of GP55 substrate to inhibit neurite outgrowth (Clarke and Moss, 1994; Clarke and Moss, 1997; Wilson et al., 1996) may arise because the mixture of IgLONs in GP55 contain putative heterodimeric complexes. The next part of this thesis uses forebrain neurons in neurite outgrowth assays to further investigate the function of putative *cis* IgLON complexes and goes on to investigate the potential signalling pathways involved in inhibiting initiation of neurite outgrowth.

Previous studies adding the $G_{i/o}$ protein inhibitor Pertussis toxin (PTX) to the culture medium in neurite outgrowth assays on GP55 protein substrate reversed inhibition of neurite outgrowth, to suggest the involvement of a G protein coupled receptor in IgLON inhibition (Clarke and Moss, 1994; Clarke and Moss, 1997). PTX will investigate whether there is a similar link to G protein signalling by putative *cis* IgLON complexes.

Many axon guidance molecules signal through the Rho signalling pathways to direct axonal growth (Huber et al., 2003). Y27632 is a specific inhibitor to Rho-associated coiled-coil-forming kinase (ROCK I &II) having no effect on other Rho-associated kinases (such as PAK) in the Rho signal transduction pathway (Ishizaki et al., 2000; Narumiya et al., 2000). Adding Y27632 to the medium in neurite outgrowth assays will give an indication if ROCK is involved in IgLON signalling.

AIM

This chapter will use neurite outgrowth assays to help determine if putative IgLON complexes have a functional effect on forebrain neurons. Specific inhibitors will further investigate the signalling pathway initiated by these complexes.

RESULTS

Neurite outgrowth assay

Neurite outgrowth assays measured the ability of forebrain neurons to initiate the extension of neurites on substrates containing CO and CL heterodimeric complexes. In the first experiment the number of forebrain neurons able to initiate outgrowth of neurites from the cell body were counted after 24 hours in culture on mono-layers of CHO cell lines expressing different compliments of IgLONs. To facilitate counting, forebrain neurons were methanol-fixed, the neurites stained with GAP43 (neuronal specific antiserum) and visualised by Texas Red^{TM}-conjugated secondary antibody labelling of the GAP43 antiserum (figure 5.1). To avoid any bias of the counting single forebrain cell bodies were selected (as opposed to clumps of forebrain neurons) and without knowing the details of the culture substrate. Approximately 300 counts were made per experiment, with three experimental repeats, to calculate the percentage of forebrain able to initiate neurite outgrowth, with a length twice that of the diameter of the cell body. Data is presented as a series of histograms using PRISM software.

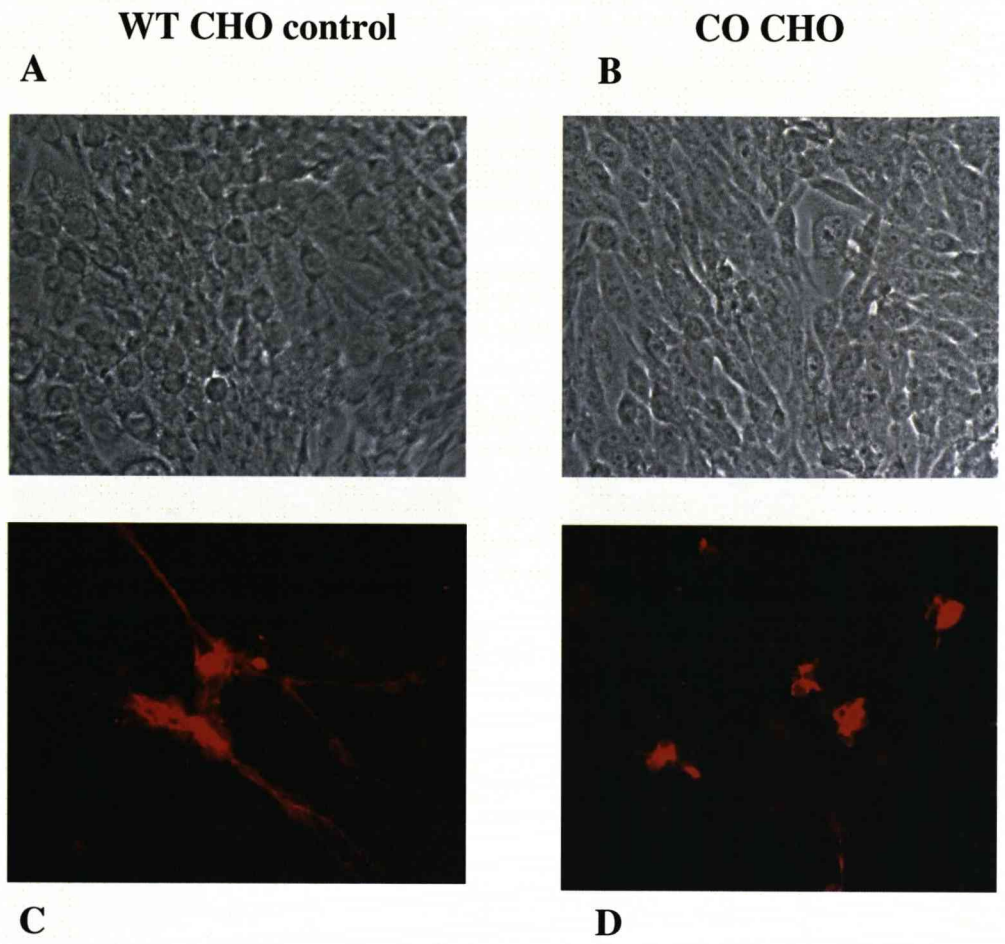

Figure 5.1 Neurite outgrowth from dissociated E8 forebrain neurons cultured on CHO cell mono-layers.

A and B are phase contrast photomicrographs images of E8 forebrain neurons cultured for 24 hours on mono-layers of confluent WT and CO-CHO cells in a neurite outgrowth assay. The expression of IgLONs cannot be visualised in these phase contrast images; nor are the forebrain neurons easily detected. The cells were methanol fixed and the neurons were visualised by immuno-labelling with 1:500 dilution of GAP43 rabbit antiserum, followed by 1:100 dilution of Donkey anti rabbit Texas Red™-conjugated second antibody. Figure C highlights dissociated forebrain neurons cultured on WT-CHO cells with extended neurites. An area was selected to show the reduction in the number of forebrain neurons extending neurites cultured on CO-CHO in figure D.

E7/8 forebrain neurons cultured on IgLON-CHO cell mono-layers

The number of forebrain neurons initiating the extension of neurite outgrowth on mono-layers of WT and single CEPU-1 (C)or OBCAM (O)-CHO cell lines was compared to that on CEPU-1 and OBCAM expressing CHO cells (CO-CHO). Over 70% of E7/8 forebrain neurons were able to initiate the extension of neurites on WT, C or O-CHO cell mono-layers, but this significantly decreased to 40% on CO-CHO cells (figure 5.2.A). In a second series of experiments WT-CHO cells were compared to CO-CHO cells and CHO expressing both CEPU-1 and LAMP (CL). Once again 70% of forebrain neurons initiated extension of neurites on WT-CHO, but this was reduced to 34% on CO-CHO cells and 36% on CL-CHO (figure 5.2.B). CO expression on the CHO cells significantly reduced initiation of outgrowth from a proportion of E7/8 forebrain neurons in both these sets of experiments to demonstrate the assay was reproducible. The presence of two IgLONs on the CHO cell surface had prevented approximately half of the E7/8 forebrain neurons from extending neurites.

E6 forebrain neurons cultured on IgLON-CHO cell mono-layers

However, when the experiment was repeated with E6 forebrain neurons there was no reduction in the number of neurons initiating the extension of neurite outgrowth on CO or CL-CHO lines. The number of E6 forebrain neurons extending neurites remained at 63% on CO-CHO, 60% on CL-CHO cell lines compared to 69% on WT-CHO (figure 5 3). IgLONs in the extracellular environment appeared to have no effect on these earlier stage neurons.

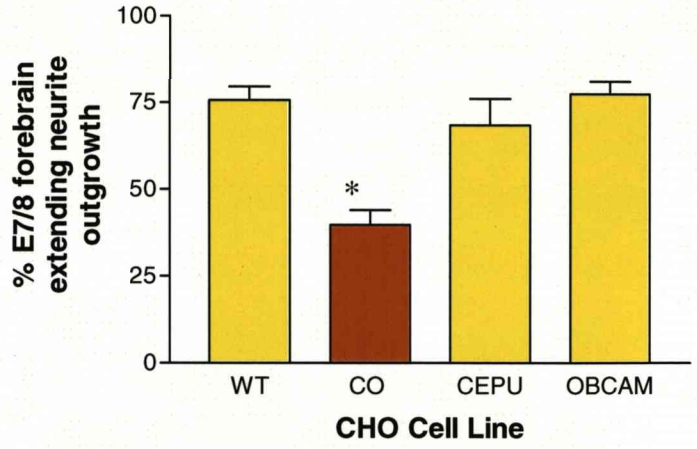

Figure 5.2.A CO-CHO cell line reduced the initiation of neurite outgrowth from E7/E8 forebrain neurons

E7/8 forebrain neurons were cultured on confluent mono-layers of CHO cells and the percentage of neurons able to extend neurites of a length at least twice the diameter of the cell body was calculated. When cultured on WT, C and O-CHO 74%, 68% and 77% of dissociated forebrain neurons extended neurites (yellow bars p>0.5). Only 40% forebrain neurons extended outgrowth on CO-CHO cell mono-layers (orange bars, p<0.01). All data based on counts from three experimental repeats.*

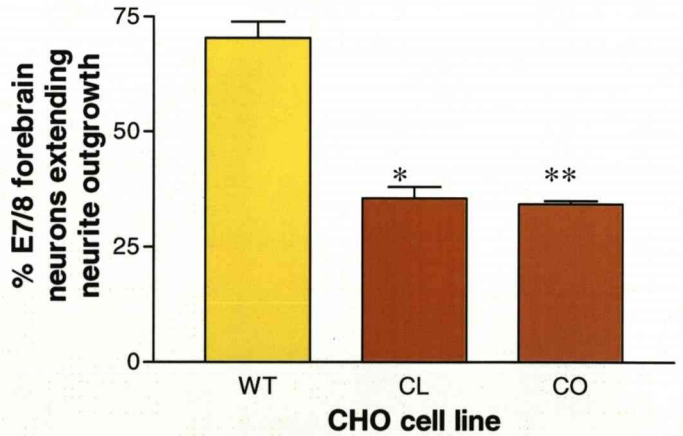

Figure 5.2.B CO and CL -CHO cell line reduced initiation of neurite outgrowth from E7/E8 forebrain neurons

In a repeat experiment 70% forebrain neurons were able to extend neurites on WT-CHO cell mono-layers but this was reduced to only 36% and 34% on CL and CO-CHO cell mono-layers (orange bars, p <0.01, <0.001**) Data based on counts from four experimental repeats.*

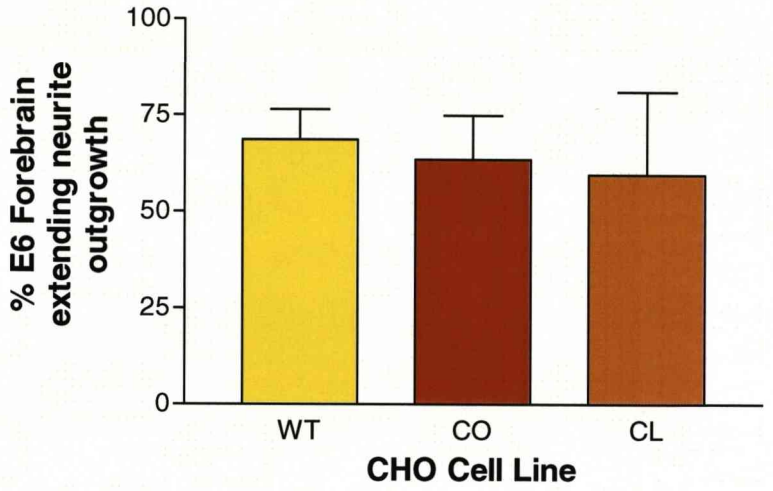

Figure 5.3 E6 forebrain neurons extended neurite outgrowth on CO and CL-CHO cell lines

At the younger age of E6, 69% of forebrain neurons extended neurites when cultured on WT CHO cell substrate (yellow bar) 63% on CO-CHO cells (dark orange bar) and 60% on CL-CHO cells (lighter orange bar). The expression of CO or CL on the CHO cell lines had not significantly reduced the number of E6 forebrain neurons extending neurite outgrowth. WT, CO data based on counts from four experimental repeats, CL data based on two experimental repeats.

Overall length of neurites from E7/8 forebrain neurons is unaffected by CO IgLONs

In previous experiments, GP55 substrate inhibited neurite outgrowth from the majority of forebrain neurons (Clarke and Moss, 1994; Clarke and Moss, 1997; Wilson et al., 1996) whereas in these experiments only a sub-population of forebrain neurons were inhibited from initiating neurite outgrowth in response to CO and CL. Individual lengths of neurites were measured using Metamorph™ Imaging software to test if the overall length of neurites was being affected by the presence of two IgLONs. The length of 100 neurons was counted on CO-cell line and compared to that on WT, C and O-CHO cell lines. Lengths were found to vary between 20-140 μm and results are presented as a graph showing the percentage of neurites at each length (figure 5.4). There was no difference in the number of neurons at each length on CO compared to C, O or WT-CHO to suggest CO had no effect on the overall length of neurite outgrowth, but had prevented a sub-population of forebrain neurons from initiating neurite outgrowth.

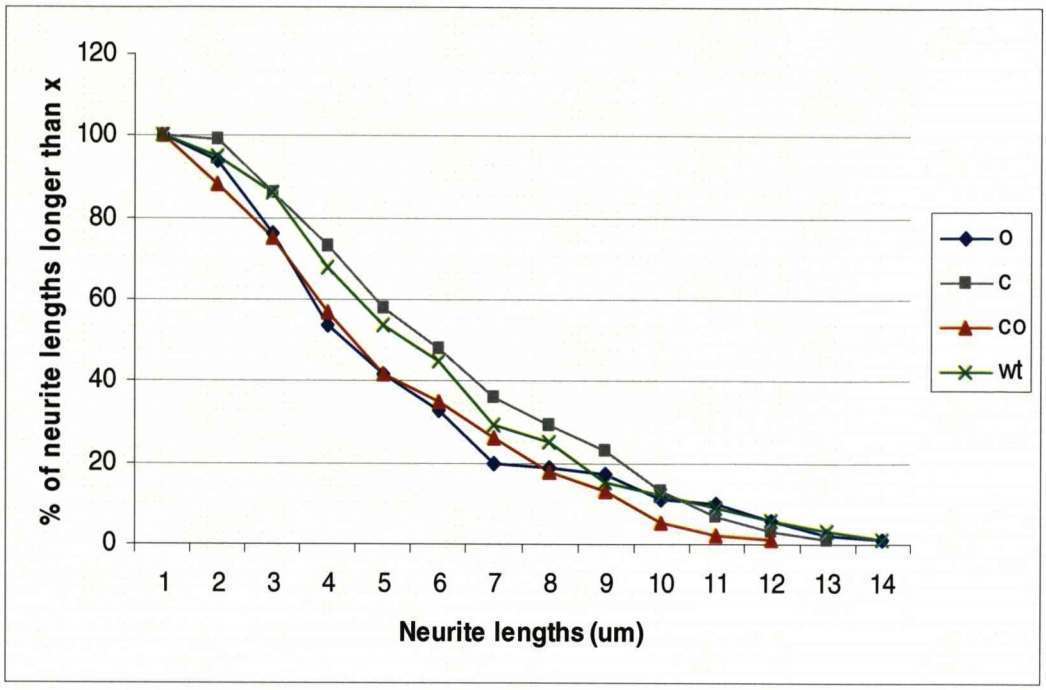

Figure 5.4. Length of neurite outgrowth from E7/8 forebrain neurons is unaffected by CO

The length of individual neurites was measured using Metamorph™ Imaging software and presented as a graph showing the % of neurites at each length between 20-140 μm. There was no significance difference in the number of E7/8 forebrain neurons able to extend neurites at each length when cultured on OBCAM (blue line) CEPU-1 (grey line) wild type (green line) and CEPU-1-OBCAM (red line) CHO cell lines to suggest overall length of neurites was unaffected by CO.

Initiation of neurite outgrowth from E7/8 forebrain is inhibited by CO and C plus O substrates

To provide more evidence that IgLONs are forming a complex and were not merely acting in synergy on the CHO cell surface, the IgLONs were enzyme digested by PiPLC and presented as a substrate in a series of similar forebrain neurite outgrowth assays. The ability of E 7/8 forebrain neurons to extend neurites on a permissive poly-L-lysine (PL) substrate, plus PiPLC digested supernatants from WT, C, and O-CHO cells, were compared to that from CO-CHO cells and a mixture of C+O single IgLON-CHO cell supernatants. CO substrate continuing to inhibit initiation of neurite extension would suggest the putative CO complex had remained stable even when not attached to the CHO cell membrane. Mixing of C and O substrates from single CHO cells would give an indication whether two IgLONs could act in synergy to affect neurite extension from forebrain neurons.

When cultured on coverslips coated with PL, 66% of forebrain neuron extended neurites. The addition of PiPLC supernatants from WT; C or O CHO cells to the PL did not have any effect on the initiation of neurite outgrowth from E7/8 forebrain neurons, 67% 55% and 52% still extended neurite outgrowth respectively. By comparison only 34% of the forebrain neurons extended neurites on PL plus CO-CHO cell supernatant and 33% when cultured on a mixture of C+O-CHO cell supernatants (figure 5. 5).

CO remaining functional even when released from the cell surface into solution suggested that once formed the putative CO complex remains stable even when released from the CHO cell membrane. There was also a similar reduction in initiation of neurite outgrowth from a sub-population of E7/8 forebrain neurons on the substrate of PL plus a mixture of C+O single CHO supernatants. There are two possible explanations for this, either the single IgLONs had formed a complex in solution, or they were acting in synergy.

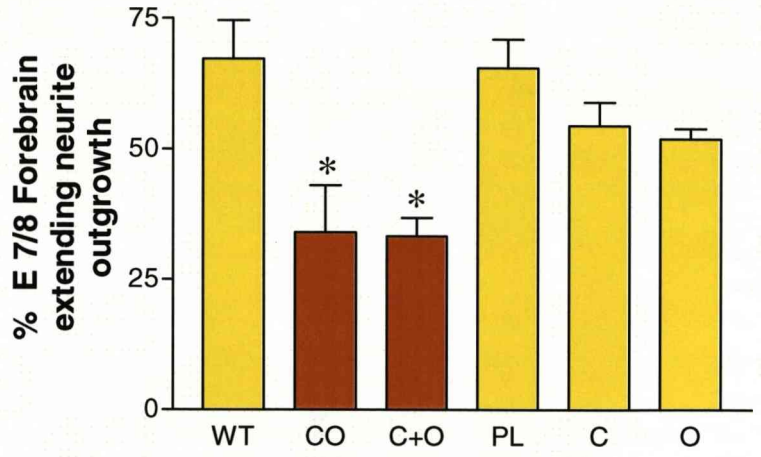

Figure 5.5 CO and a mixture of C+O substrates reduced the initiation of neurite outgrowth from forebrain neurons

*E7/8 forebrain neurons were cultured on coverslips coated with PL plus supernatants of IgLONs released by PiPLC digestion from the surface of CHO cell lines. There was no significant difference between the number of forebrain neurons able to extend neurite outgrowth on PL or PL plus from WT and single C or O-CHO cells supernatant 66%, 67% 55% and 52% respectively (yellow bars). Neurite outgrowth was significantly reduced to only 34% of the forebrain population on PL plus CO and to 33% from a mixture of C+O-CHO cell supernatants (orange bars p <0.05 *). All data based on counts from four experimental repeats, except for C-CHO where data was from two repeats.*

Investigation of signalling pathways involved in IgLON inhibition of neurite outgrowth

Putative heterodimeric IgLONs must signal through to the neuronal cytoskeleton to bring about changes required to inhibit the extension of neurites. Specific inhibitors were incorporated into a series of forebrain neurite outgrowth assays to investigate how putative IgLON complexes might initiate signal transduction pathways. PTX had previously reversed GP55 inhibition of neurite outgrowth from forebrain neurons, so was the first inhibitor tested. Y27632 inhibitor was also tested to provide evidence for involvement of the RHO signalling pathway.

In the first experiment, 10 ng/ml of PTX inhibitor was added to the medium of forebrain neurons cultured on single CHO cell lines to demonstrate PTX had no overall effect on the initiation of neurite outgrowth. After 24 hours in culture 70%, 72% and 75% forebrain neurons extended neurites on WT, and C or O-CHO lines respectively. Outgrowth remained at levels of 73%, 67% and 69% on WT, C and O-CHO cells in the presence of PTX inhibitor to confirm PTX had no overall effect on neurite outgrowth (figure 5.6.A). In the second experiment the number of forebrain neurons extending neurites reduced to 34% on CHO cell lines expressing CO and 36% on CL-CHO cells. The addition of PTX inhibitor to the culture medium increased the number of forebrain neurons extending neurites to 61% on CO and 64% on CL-CHO cells, a similar level to that found on the WT, and WT+PTX controls (figure 5.6.B).

Forebrain neurite outgrowth assays were repeated adding 10nm Y27632 inhibitor to the culture medium. On WT-CHO cells 63% of E7/8 forebrain neurons extended neurite outgrowth, compared to 76% whenY27632 inhibitor was added to the culture medium. This suggested Y27632 had no overall effect on the initiation of neurite outgrowth from forebrain neurons. However, the addition of Y27362 to the medium of forebrain neurons cultured on CO-CHO significantly increased initiation of neurites from 34% to 59%, a similar level to that on the WT controls (figure 5.7). Y27632 had reversed the CO inhibition of neurite outgrowth suggesting the potential involvement of the RHO signalling pathway in transmitting of the IgLON signal to the cytoskeleton.

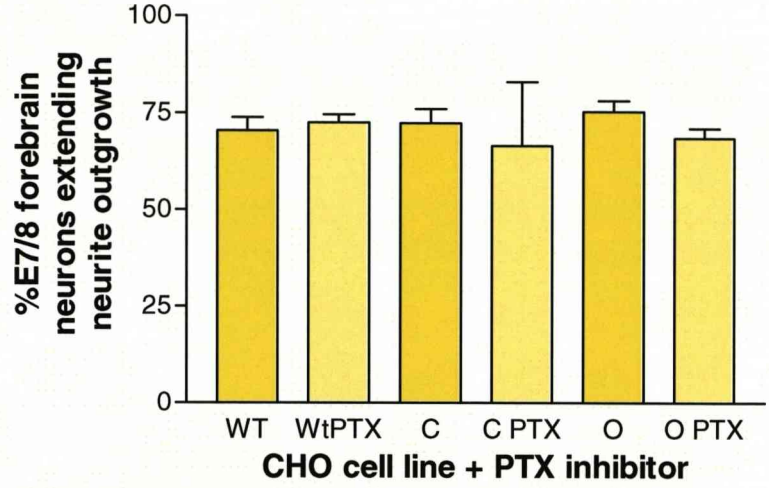

Figure 5.6.A PTX inhibitor had no effect on neurite outgrowth from E7/8 forebrain neurons

When cultured on a monolayer of WT, C and O-CHO cells 70%, 72% and 75% respectively of dissociated forebrain neurons were able to initiate the extension of neurites (yellow bars). The presence of PTX in the culture medium had no effect on outgrowth; 73%, 67% and 69% of forebrain neurons extended neurites on WT, C and O- CHO cell lines (pale yellow bars).

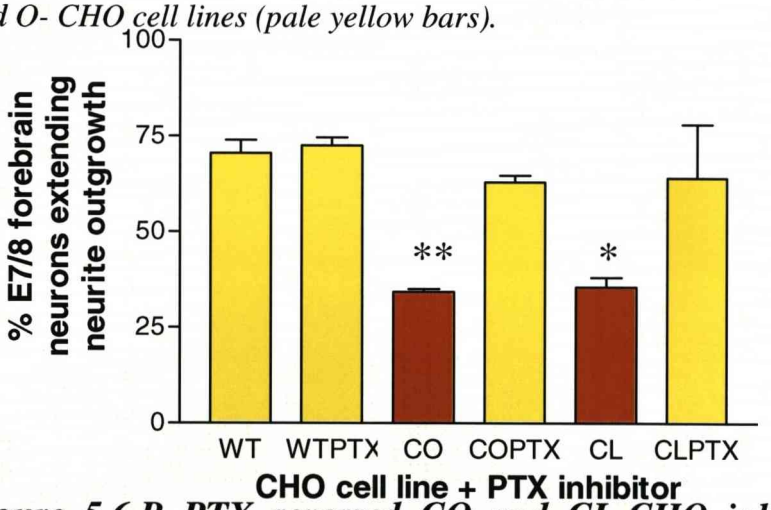

Figure 5.6.B PTX reversed CO and CL-CHO inhibition of neurite initiation from E7/8 forebrain neurons

*Over 70% of forebrain neurons were able to extend neurites on WT plus and minus PTX in the culture medium (first two yellow bars), whereas only 34% and 36% extended neurites when cultured on CO and CL-CHO cell substrate (orange bars, p <0.001** <0.01*). Incorporating PTX into the culture medium increased the number of forebrain extending neurites on both CO and CL-CHO to a similar level to the control (61% and 68% yellow bars p<0.05). PXT had reversed CO and CL inhibition of neurites. Data based on counts from four experimental repeats.*

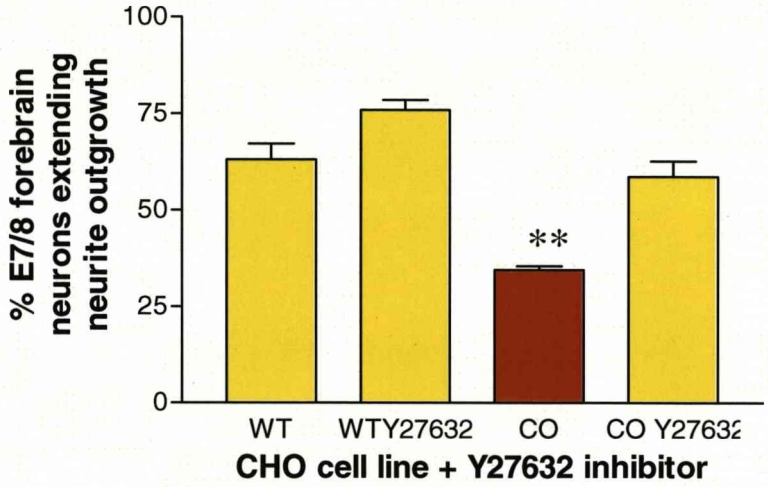

Figure 5.7 Y27632 reversed CO inhibition of neurite initiation from E7/8 forebrain neurons

*Dissociated E7/8 forebrain neurons were able to extend neurites on WT plus and minus Y27632 in the culture medium (63% and 76% first two yellow bars), whereas the number of forebrain neurons extending neurites was reduced to 34% on CO-CHO cell substrate (orange bar, p <0.001**). Incorporating Y27632 into the culture medium increased the number of forebrain extending neurites to 59%, a similar level to the control (third yellow bar p<0.05). Y27632 had reversed the inhibition of CO. Data based on counts from three experimental repeats.*

DISCUSSION

A reduction in the number of forebrain neurons able to initiate neurite outgrowth was only brought about when two IgLONs were present in the extracellular culture substrate. These experiments began to replicate the data obtained with GP55 mixed IgLON substrate, whereas single IgLONs have never been able to replicate this data. Neurite outgrowth was only inhibited from a sub-population of E7/8 forebrain neurons in these experiments, whereas GP55 was more efficient and inhibited neurite outgrowth from all forebrain and DRG neurons (Clarke and Moss, 1994; Clarke and Moss, 1997). However, these experiments suggest a *trans* interaction with more than one member of the family is required to inhibit initiation of neurite outgrowth and single IgLONs may not be functional. Taking into account the evidence in the previous chapter of two IgLONs forming a *cis* complex, it is proposed that only when IgLONs form these putative heterodimeric complexes are they able to inhibit neurite outgrowth. IgLONs functioning as heterodimers is a novel concept for GPI anchored glycoproteins (Reed et al., 2004).

When released from the surface of CHO cells and used as a substrate CO continued to inhibit neurite outgrowth from a sub-population of forebrain neurons. This added support to there being some *cis* interaction between C and O on the CHO cell surface, which was relatively stable as it remained functional even when detached from the CHO cell membrane.

Single IgLONs released from the surface of C and O-CHO cells mixed together also inhibited neurite outgrowth from a similar sub-population of E7/8 forebrain neurons. Whilst this could indicate that IgLONs are functioning in synergy previous observations in our laboratory using a mixture of IgLON-FC recombinant proteins have not detected any reduction in neurite outgrowth from E7/8 forebrain neurons (data not shown). In these assay the IgLON heads were in close proximity but were attached by the FC tag making an interaction between the individual heads unlikely; whereas in solution C and O monomers had the opportunity to form putative complexes and so inhibited neurite outgrowth.

The actual length of forebrain neurite outgrowth was measured and found to be uncompromised on CO-CHO cells; to suggest it was a sub-population of forebrain neurons that responded to the putative CO complex, rather than CO inhibiting the overall length of neurite outgrowth of the neurons *per se.*

At the younger age of E6 neurite outgrowth from forebrain neurons was unaffected by both CO and CL putative complexes. Together these experiments suggest response to IgLON complexes is only by forebrain neurons during a later stage of development. Throughout development axonal guidance is dependent on specific spatial and temporal expression of a whole range of molecules and interactions with their associated receptors. Possibly, forebrain neurons express an additional receptor on their surface as they mature allowing them to respond to extracellular IgLONs. Alternately since IgLON expression increases with development E6 forebrain neurons may have a lower level of expression on their cell surface and so cannot respond to IgLONs in the extracellular environment.

The next set of experiments incorporated specific inhibitors into the culture medium to investigate potential pathways IgLONs use for signal transduction. When PTX was added to the culture medium the sub-population of E7/8 forebrain neurons extending neurites on CO and CL-CHO cell lines returned to the control level. This data is consistent with PTX reversal of GP55 inhibition of neurite outgrowth from forebrain neurons (Clarke and Moss, 1994; Clarke and Moss, 1997) and suggests CO and CL are possibly bringing about neurite inhibition in the same way as GP55 through a $G_{o/i}$ protein coupled receptor (Igarashi et al., 1993). The mechanism of how $G_{o/i}$ proteins inhibit neurite outgrowth is as yet not fully understood.

A second inhibitor Y27632 investigated the signal transduction pathway used by CO to inhibit neurite initiation. Y27632 is a specific inhibitor of ROCK; part of the RHO kinase signalling pathway, used by several guidance molecules to regulate axon guidance (Huber et al., 2003). Incorporation of Y27632 had no overall effect on neurite extension from forebrain neurons cultured on WT-CHO; however Y27632 reversed the inhibitory effect of CO-CHO suggesting involvement of the RHO signalling pathway in IgLON signal transduction. Ephrin-A5 signals by activating ephexin, a guanine exchange factor, stimulating ROCK to inhibit retinal ganglion axonal progression (Wahl et al., 2000). The Ephrin-A family are similar to IgLONs in that they are located to lipid raft regions of the cell membrane by a GPI anchor. Sema 3A is an example of a secreted guidance molecule that uses RHO to signal through LIMK to inhibit neurite outgrowth (Aizawa et al., 2001).

Chapter Six

Direct Physical Evidence For Putative Heterodimeric IgLON *Cis* Complexes.

DIRECT PHYSICAL EVIDENCE FOR PUTATIVE HETERODIMERIC IgLON *CIS* COMPLEXES.

INTRODUCTION

Binding and functional studies have presented indirect evidence for the formation of putative *cis* IgLON complexes. Previously, immuno-cytochemistry has detected expression of different members of the IgLON family on various types of neuronal cells, for example LAMP, OBCAM and CEPU-1 are expressed on chick DRG; sympathetic neurons and CGCs (Lodge et al., 2000; Reed et al., 2004) Kilon and OBCAM are co-expressed on hypothalamic neurons (Miyata et al., 2000). Furthermore, staining of tissue sections has demonstrated different members of the IgLON family have distinctive overlapping patterns of expression. For example CEPU-1 and OBCAM have overlapping expression in the hippocampus (Struyk et al., 1995). In the E18 chick retina; LAMP and OBCAM overlap in the inner plexiform layer; whereas LAMP and CEPU-1 are co-expressed in the outer plexiform layer (Lodge et al., 2000). These definite patterns of expression would suggest there are opportunities for IgLONs to form putative complexes *in vivo*.

Some direct evidence is required for a physical interaction between IgLONs to substantiate heterodimeric *cis* complexes form. This evidence came from the hypothesis that if IgLONs were removed from the surface of doubly transfected CHO cell lines into solution a heterodimeric complex could be identified by purifying one portion of the complex and then analysing for an associated IgLON by western blotting. In these experiments PiPLC enzyme digested IgLONs from the surface of CO-CHO cells into solution, OBCAM immuno-precipitated the OBCAM portion, and co-detection of associated CEPU-1 will identify the CO complex.

A second approach of antibody co-clustering of two different members of the IgLON family to the same location on the cell membrane of neurons will indicate a putative complex is likely to form *in vivo*. CEPU-1 polyclonal antibody stimulated CEPU-1 to cluster on the cell membrane of forebrain neurons; drawing of either OBCAM or LAMP into that cluster will provide evidence for the presence of IgLONs as heterodimeric complexes on the surface of neurons.

AIM

This final chapter aims to provide some direct physical evidence for the formation of putative IgLON complexes by immuno-precipitation experiments and by measuring the ability of IgLONs to co-cluster to the same location on the surface of forebrain neurons.

RESULTS

Immuno-precipitation of putative CO *cis* complex

C, O and CO-CHO cell lines were cultured on 150mm tissue culture dishes to confluence and PiPLC enzyme digested the IgLONs from the surface of the cells into solution. Immuno-precipitation with OBCAM antiserum followed by capture on Sepharose G beads precipitated O from the PiPLC supernatant. However, in this initial experiment the antiserum was not cross-linked to the beads and so was co-eluted and obscured the IgLON bands on western blot analysis (data not shown). To overcome this problem, antibodies from OBCAM rabbit antiserum were immobilised on nitrocellulose and then used to immuno-purify O from CHO-cell supernatants.

OBCAM rabbit antibodies were purified from rabbit antiserum with protein A agarose beads, eluted and immobilised onto nitrocellulose membrane. The membrane was incubated with a concentrated solution of IgLONs digested from C, O and CO-CHO cell lines. Proteins immuno-purified by OBCAM antibodies were separated by LDS-PAGE across two gels, western blotted onto nitrocellulose and stained with both CEPU-1 and OBCAM specific rat antiserum, followed by HRP conjugated rabbit anti rat antibody and visualised with Femto™-chemiluminescent substrate, exposed on Amersham hyperfilm (figure 6.1 A and B).

The first three lanes on the western blots are control bands of WT, C and O-CHO cell PiPLC supernatant starting material, concentrated approximately 10 fold (figure 6.1 A& B, lanes 1-3). Comparison of the staining patterns suggested CEPU-1 and OBCAM rat antisera were specific to their respective C and O-CHO cell supernatants, and there was no cross reactivity, or non-specific staining of the WT supernatant on western blots. Both OBCAM and CEPU-1 antisera positively stained the starting CO-CHO supernatant (figure 6.1 A& B lane 4, higher molecular weight band marked *).

OBCAM immuno-purification of O appeared to be efficient, since a band of similar intensity to the initial supernatant was visible in the purification supernatant and this band was no longer visible post immuno-purification (figure 6.1 B lanes 3, 9, 11). A band was detected with CEPU-1 antiserum from OBCAM immuno-purification of C from the C-CHO supernatant (figure 6.1 A lane 7 marked **X**). Whilst there was no cross-reactivity between OBCAM and CEPU-1 antiserum detected on western blots there has been some previous evidence of OBCAM antiserum recognising CEPU-1 in immuno-histochemical staining of CEPU-1-CHO cells (data not shown). OBCAM antibodies had purified some CEPU-1 from the C supernatant due to this cross-reactivity with the native protein. In these experiments the total amount of protein immuno-purified from the C supernatant was loaded onto the gels; therefore a small fraction of non specific binding was concentrated into this sample. Femto™-chemiluminescent detected this small amount of protein since it detects as low as femto-gram amounts of protein. A significant amount of C remained in the post purification sample confirming the purification of CEPU-1 by OBCAM was minimal.

OBCAM antibodies co-precipitated CEPU-1 alongside OBCAM from the CO-CHO cell supernatant (figure 6.1 A lane 9, higher molecular weight band marked **). This purification appeared to be efficient since there was no evidence of any CEPU-1 remaining in the CO supernatant post purification (figure 6.1 A lane 12). OBCAM antiserum should also have detected OBCAM purification from the CO supernatant, but this was below the level of detection (figure 6.1 B lane 8 marked **X**).

One surprising feature was the size of the band detected by CEPU-1 antiserum being between 110-120 kDa. Since this is a non-reducing gel it is possible that the non-covalent interactions between CEPU-1 and OBCAM had retained the CO complex as a heterodimer (figure 6.1 A lanes 4, 9). In principle it is also possible that the higher molecular weight band is a CEPU-1 homodimer. However, as the protein band was precipitated by OBCAM antibodies it would be expected to contain a portion of OBCAM rather than CEPU-1 alone, so is more likely to be the heterodimer. OBCAM antiserum should also have detected this band but staining of the initial CO supernatant was weaker with OBCAM than with CEPU-1 antiserum suggesting OBCAM antiserum may have been less sensitive; or possibly some of the OBCAM binding sites were obscured by their interaction with CEPU-1 resulting in the OBCAM antiserum not being able to detect the OBCAM portion efficiently.

OBCAM immuno-purification of CEPU-1 from the CO supernatant provided some evidence for the formation of the putative CO complex, as the CEPU-1 portion should only have been eluted alongside OBCAM. However, in theory as OBCAM antibodies had immuno-precipitated some CEPU-1 from the C supernatant they may have also immuno-purified the C portion of the complex, making the results inconclusive.

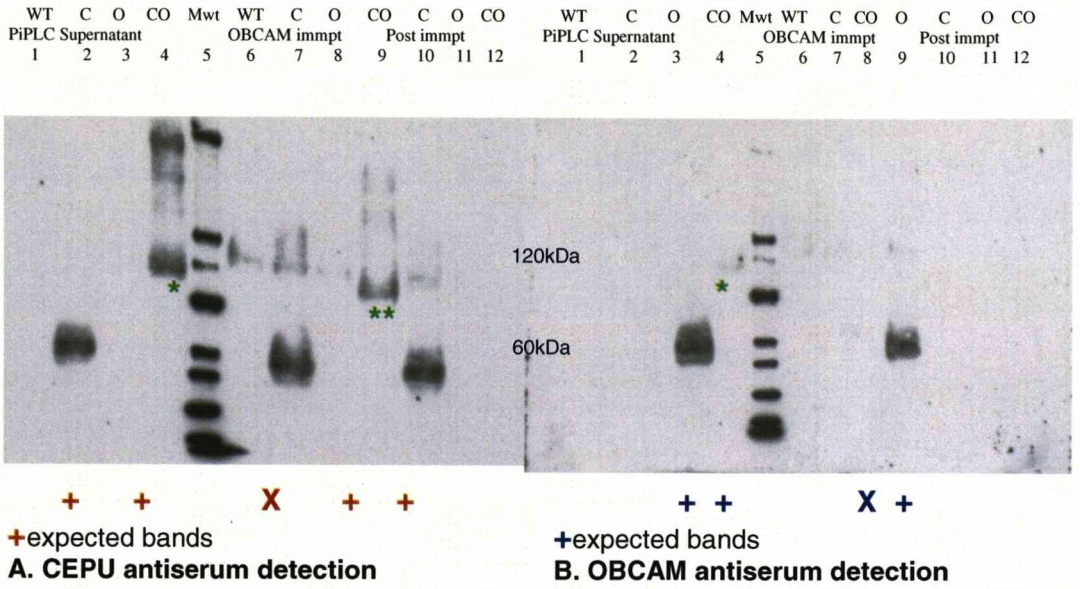

Figure 6.1 Immuno-precipitation of CO complex

IgLONs were PiPLC digested from the CHO cell surface and supernatants from 2 x 150 mm confluent dishes were concentrated to 200 µl. Western blot A is stained with CEPU-1 antiserum and B with OBCAM. The first 4 lanes correspond to 10 µl/well of WT, C, O and CO-CHO starting material. CEPU-1 antiserum staining was specific to C (+ lane 2 A, B) and OBCAM specific to O supernatants (+ lane 3 A, B). CO supernatant stained with both antiserum (lane 4) note this band had a molecular weight of ~110 kDa when compared to Magic Mark™ Invitrogen molecular weight marker (lane 5). A band of ~110 kDa was affinity-purified by OBCAM from the CO supernatant, and visualised with CEPU-1 antiserum (lane 9 A**) but this band was not detected by OBCAM antiserum (X lane 8 B). This suggested C had been co-immuno-purified alongside O from the CO supernatant, but this band needs to be confirmed with OBCAM antiserum. CEPU-1 was also immuno-purified from the C supernatant by OBCAM (X lane 7 A) and remained post immuno-purification, suggesting the OBCAM purification of C was inefficient (+ lane 10 A). The purification of O from the O-supernatant (+ lane 9 B) was more efficient since no O band was detected in the post purification supernatant (lane 11 B). Blots were stained with 1:5000 dilution of rat antiserum (A CEPU-1, B OBCAM) followed by 1:5000 dilution of goat anti rat HRP conjugated antiserum; visualisation was with Femto™ chemiluminescent substrate, exposed to Amersham film for 30 seconds, developed with Sigma photo chemicals.*

Affinity –isolation of heterodimeric IgLON complexes

A similar technique of affinity-isolation was used to overcome the difficulty of the cross-reactivity of OBCAM antibodies recognising and purifying CEPU-1 from the PiPLC supernatant. In these experiments CHO cell lines expressing OBCAM with a HISx6 tag alongside CEPU-1 and LAMP were prepared, so as the HISx6-epitope tag could be used for affinity-isolation of the putative IgLON complex rather than immuno-purification with OBCAM antibodies. The preparation of the doubly transfected CHO cell lines was in two stages. Initially CHO cells were transfected with OBCAM-HISx6 (O^H) then CEPU-1 (CO^H) and LAMP ($LO^{H)}$ were transfected into this cell line (details section 2.13 materials and methods).

HISx6 tag affinity-isolation of the putative CO^H complex

C, O^H, and CO^H-CHO cells were cultured to confluence on 2 x 150 mm dishes, the IgLONs were PiPLC digested off the cell surface into solution and concentrated 10 fold, to a final volume of 200 µl. The HISx6 tags on O^H proteins were affinity-isolated by incubating these supernatants with aliquots of Proban^{TM} nickel beads. Proteins isolated by the beads were eluted into gel sample buffer; loaded across two LDS-PAGE gels; western blotted onto nitrocellulose and stained with CEPU-1 and OBCAM specific rat antiserum, followed by HRP conjugated rabbit anti rat secondary antibody, visualised by Femto^{TM} chemiluminescent substrate, exposed on Amersham film.

The first four lanes on the western blot in figure 6.2 correspond to 10 µl of starting PiPLC supernatant from WT, C, O^H, and CO^H-CHO cell lines, blot A was stained with CEPU-1 and blot B with OBCAM antiserum. CEPU-1 antiserum specifically stained the C-PiPLC substrate (figure 6.2 A&B lane 2). WT negative controls did not stain with either antiserum, indicating there was no non-specific binding of the antiserum to CHO-cells (figure 6.2 A & B, lane1). There with some slight background staining of C-PiPLC supernatant with OBCAM antiserum (figure 6.2 B, lane 2) whereas OBCAM antiserum specifically stained the O-supernatant (figure 6.2 A&B, lane 3).

Proteins affinity-isolated by the nickel beads from the O^H supernatant stained positively with OBCAM antiserum confirmed the HISx6 epitope tag was being captured by the beads (figure 6.2 B, lane 7). Some non-specific binding of CEPU-1

to the nickel beads was detected since CEPU-1 was affinity-isolated from the C supernatant (figure 6.2 A, lane 6). The total amount of protein isolated by the beads from the C-CHO cell supernatant was loaded across the two gels, which resulted in concentrating the eluted proteins into a small sample. Femto chemiluminescent substrate is highly sensitive and detected this small amount of protein. However, CEPU-1 remained in the supernatant post incubation with the beads, suggesting the beads were very inefficient in purifying CEPU-1 (figure 6.2 A, lane 12). Taking this into account the amount of CEPU-1 isolated probably represented only about 5% of the total amount in the supernatant, but the high sensitivity of Femto chemiluminescence produced a significant band.

Both CEPU-1 and OBCAM were present in the initial supernatant PiPLC digested from the CO^H cell line (figure 6.2 A, B, lane 4) and in the affinity-isolated proteins from the CO^H cell line (figure 6.2 A, B, lane 8). This suggested that the beads had isolated OBCAM via the HISx6 epitope tag and CEPU-1 was co-eluted from the CO^H supernatant. In principle CEPU-1 could only be eluted from the CO^H supernatant if it was complexed with the O^H on the CO^H-CHO cell surface. Both O^H and CO^H remained in the supernatant after incubation with the beads suggesting the nickel beads were probably overloaded in this experiment (figure 6.2 B, lanes 11&12).

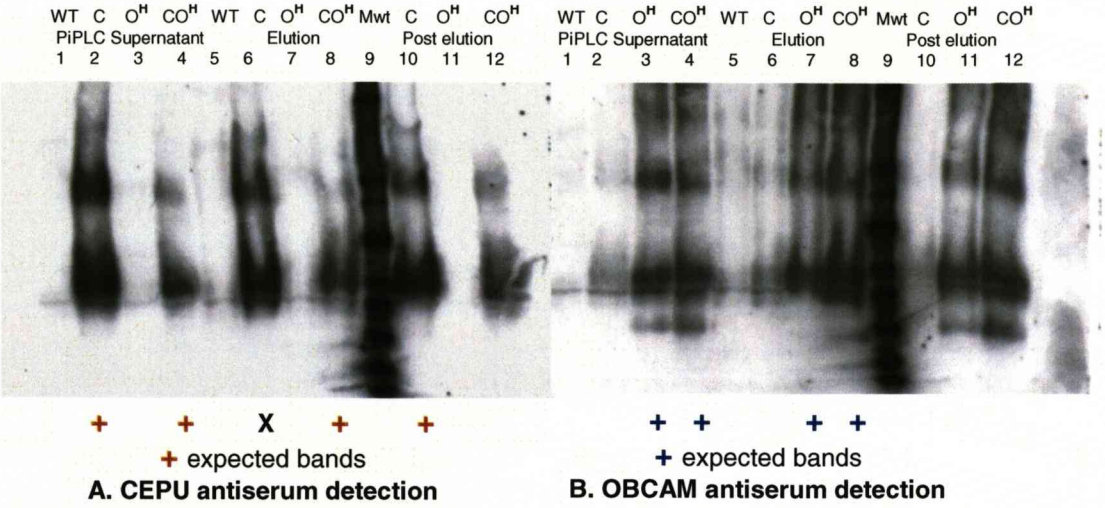

Figure 6.2 HISx6 *affinity-isolation of* CO^H *complex*

Western blots were stained with CEPU-1 blot A and OBCAM blot B antisera. Lanes 1-4 contain 10 µl samples of concentrated PiPLC digest supernatants from WT, C, O^H *and* CO^H*-CHO cell lines. Lanes 5-8 contain the HISx6 tagged proteins affinity-isolated by Proban™ nickel beads from 200 µl of WT, C,* O^H *and* CO^H*-CHO supernatants, eluted with sample buffer and loaded across the two blots. Lanes 10-12 contain 10 µl samples of remaining supernatant, post incubation with the nickel beads. Comparison of the staining patterns suggested CEPU-1 had some slight background staining with OBCAM antiserum, lanes 2 A, B but OBCAM antiserum was more specific, as* O^H *supernatant stained only with OBCAM antiserum lanes 3 A, B.* CO^H *initial supernatant stained with both CEPU-1 and OBCAM antisera lanes 4 A, B. Band in lane 7B, stained with OBCAM antiserum, confirmed affinity-isolation of* O^H *from the* O^H*-CHO PiPLC supernatant. The proteins affinity-isolated from* CO^H *PiPLC supernatant stained with both CEPU-1 and OBCAM antiserum, lanes 8 A, B, suggesting C had been co-eluted with* O^H*. However, staining with CEPU-1 antiserum suggested CEPU-1 had also been affinity-isolated from the C PiPLC supernatant by the beads (lane 6 A marked* ***X****) but this was probably due to non-specific binding.* O^H *and* CO^H *remained in the supernatant suggesting the nickel beads were not very efficient, or overloaded, lanes 11, 12, B. Lane 9 is Magic Mark™ Invitrogen molecular weight (Mwt) marker. Both gels were stained with 1:5000 dilution of rat antiserum, gel A CEPU-1, gel B OBCAM, followed by a 1:5000 dilution of goat anti-rat HRP conjugated secondary antibody; visualisation was with Femto™ chemiluminescent substrate, exposed on Amersham film for 30 seconds.*

HISx6 tag affinity-isolation of the putative LO^H complex

The experiment was repeated using LO^H-CHO cell line in place of CO^H cells, and was stained with LAMP and OBCAM rat antiserum to detect the putative LO^H complex. To overcome problems of non-specific IgLON binding to the nickel beads, 20mM imidizole was added to the post incubation wash buffers, and to ensure all the IgLONs were eluted from the beads 250mM imidizole was added to the sample buffer. Also the less sensitive Pico™ chemiluminescent substrate was used to visualise specific protein binding. Pico™ chemiluminescence detects pictogram levels of protein and so will not detect very low levels of non-specific protein binding.

CHO cell lines were cultured on 150 mm dishes and PiPLC digested L, O^H and LO^H from the surface of the cells into solution. These PiPLC supernatants were concentrated and Invitrogen Quantit™ measured actual protein concentrations. Proban™ nickel beads were added to supernatants containing 100µg total protein to capture the HIS tagged proteins. Proteins eluted from the beads were separated by LDS-PAGE and analysed on western blots, stained with LAMP and OBCAM antisera. The protein concentration was either too low in the initial PiPLC supernatant from LO^H to be detected by Pico™ chemiluminescence with both LAMP and OBCAM antiserum, or the antiserum may be less sensitive as some recognition sites may be lost as IgLONs form putative *cis* complexes (figure 6.3 C, D lane i). The nickel beads captured the epitope tagged O^H and enhanced the protein concentration in the eluted sample to a level where O^H was detected with OBCAM antiserum (figure 6.3 D, lane ii). LAMP was also detected (figure 6.3 C, lane ii) suggesting LAMP had been co-eluted with OBCAM from the LO^H supernatant. Note the two bands, one of molecular weight ~55 kDa and one ~110 kDa; the lower band being the size expected for a single IgLON and the higher band the size for a dimeric IgLON on this type of non-reduced gel.

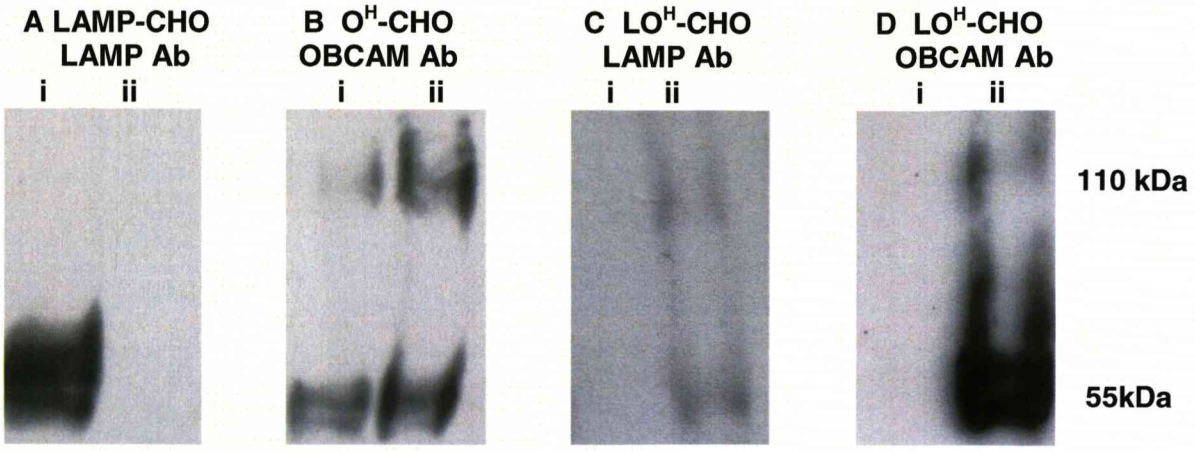

Figure 6.3 HISx6 affinity isolation of LO^H complex

Lanes i in each figure contain the PiPLC supernatant starting material, whereas lanes ii contain proteins eluted by Proban^{TM} nickel beads. LAMP antiserum detected LAMP in the initial PiPLC supernatant off LAMP-CHO cells, but no LAMP was eluted by the nickel beads Ai, ii. OBCAM antiserum detected OBCAM in the PiPLC supernatant off the O^H-CHO cell line and the nickel beads increased the concentration of OBCAM Bi, ii. LAMP antiserum did not detect LAMP in the PiPLC supernatant from the LO^H -CHO cell line Ci but LAMP was present in the nickel bead elution from LO^H –CHO PiPLC supernatant Cii. This suggested L was complexed with O^H in the LO^H supernatant and the beads had concentrated the amount of protein in the elution enough to detect LAMP. Similarly OBCAM antiserum did not detect OBCAM in the initial PiPLC supernatant from the LO^H -CHO cell line Di but the nickel beads concentrated the amount of OBCAM sufficiently to be detected in the elution Dii. Note how LAMP appears as a monomer in the PiPLC supernatant from the LAMP-CHO cells Ai, but appears at the higher molecular weight in the LO^H –CHO PiPLC supernatant Cii, suggesting it may now be a dimer. OBCAM appears as both a monomer and homodimer Bi, ii. As the PiPLC supernatant was taken from confluent O^H-CHO cells the stronger homophilic interaction of OBCAM may have produced homodimers from both cis and trans interactions. In contrast LAMP has a weak homophilic interaction in trans so no homodimers were detected in the initial PiPLC supernatant Ai, therefore the dimer eluted from LO^H –CHO, Cii, is more likely the result of a cis interaction. Some OBCAM eluted from the LO^H -CHO Dii appeared as a dimer, but predominantly as a monomer possibly due to some LAMP having been lost during the elution washes.

Co-localisation of IgLONs on the surface of forebrain neurons

The experiments so far have provided evidence compatible with the formation of putative heterodimeric IgLON complexes on the surface of CHO cells. The next set of experiments used antibody patching to investigate their formation on the surface of neuronal cells to demonstrate IgLON *cis* heterodimers may form *in vivo* (figure 6.4). This approach involved staining forebrain neurons with two specific IgLON antisera, followed by confocal microscopy to establish if IgLONs actually co-localise on the surface of forebrain neurons. The hypothesis is that live staining with individual IgLON polyclonal antiserum would cluster IgLONs to specific patches on the surface of forebrain neurons, subsequent identification of pairs of IgLONs co-clustered to the same location on the membrane would help to confirm the formation of putative heterodimeric complexes on neurons.

E8 forebrain neurons were cultured on coverslips for 72 hours and live stained with LAMP or CEPU-1 rat antiserum, detected by Texas-Red™ labelled second antibody, alongside an opposing CEPU-1 or OBCAM rabbit antisera detected by Alexa green 488 ™ labelled second antibody. Photomicrographs were produced using LEICA confocal microscope and LEICA Lite™ software to show the location of each IgLON on the surface of the neurons. Forebrain neurons were also stained with two other cell adhesion molecules, T-cadherin and F11 rabbit antiserum followed by with Alexa green 488 ™ labelled second antibody, alongside IgLON rat antisera followed by Texas-Red™ labelled second antibody as negative controls There is no evidence to suggest IgLONs interact with other molecules outside the IgLON family so even though T-cadherin, F11 and IgLONs are all GPI-anchored glycoproteins that locate to lipid raft regions of the membrane T-cadherin and F11 would not be expected to actually co-cluster alongside IgLONs.

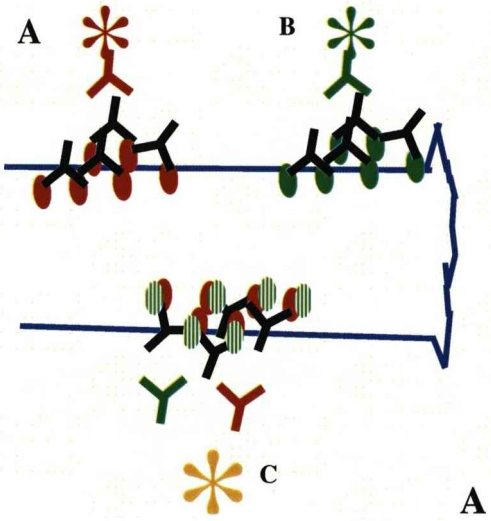

Figure 6.4 Antibody patching of IgLONs on forebrain neurons

*Antibody molecules within LAMP polyclonal antiserum recognise a variety of different LAMP epitopes so when forebrain neurons are live stained each LAMP molecules (red ovals) expressed on the surface of the forebrain neuron is captured by more than one LAMP rat antibody molecule (**Y**) resulting in antibody patching as in A. LAMP rat antiserum is recognised by Texas Red™ labelled secondary antibody (Y) increases patching and is visualised as punctuate staining along the forebrain plasma membrane marked as an asterisk*. A similar situation is in B where T-cadherin rabbit antiserum clusters several T-cadherin molecules together, (green oval) followed by Alexa 488™ green labelled second antibody, and visualised as green punctuate staining along the length of the neuron represented *. Overlay of confocal images of the staining patterns should locate LAMP and T-cadherin to separate patches A and B on the neuron, thus, T-cadherin acts as a negative control. By comparison if IgLONs form heterodimeric cis complexes they will co-cluster to the same region on the surface of the forebrain neuron. In part C, CEPU-1 molecules lined green ovals, are complexed with LAMP red ovals, detected with CEPU-1 rabbit antiserum and Alexa 488™ green labelled second antibody as green punctuate staining. Overlay of the two staining patterns using Image J co-localisation Plugin™ software will locate the CEPU-1 and LAMP clusters to the same region and be visualised *. This co-clustering of IgLON staining patterns provides more evidence for the formation of the putative heterodimeric complexes.*

Specificity of secondary antibodies and antiserum

To test for secondary antibody specificity the rat and rabbit primary antisera were tested against the opposing species of rat and rabbit pre-immune antisera i.e. LAMP, OBCAM and CEPU-1 rat antiserum was tested against rabbit pre-immune serum; T-cadherin, and OBCAM rabbit antiserum were tested against rat pre-immune serum. The photomicrograph images of each pair of staining patterns are overlaid in figure 6.5 A. Only single red or green fluorescence staining was visible in these photomicrographs, confirmed there was no cross reactivity by either of the secondary antibodies.

The specificity of the IgLON antiserum was demonstrated by staining IgLON CHO cell lines with each IgLON specific antiserum. Some cross reactivity was initially found between CEPU-1 and OBCAM antiserum so these antiserum were adsorbed against each other (details materials and methods section 2.6) and re-tested figure 6.5 B. LAMP antiserum stained only LAMP-CHO and did not cross react with either CEPU-1 so it was not necessary to adsorb the LAMP antiserum figure 6.5 C. Similarly, LAMP antiserum did not cross-react with OBCAM-CHO (data not shown). The fluorescently labelled second antibodies used had previously been tested for non-specific binding to the CHO cells (data not shown).

Since both the IgLON antisera and secondary antibodies were specific they could be confidently used to co-cluster individual IgLONs.

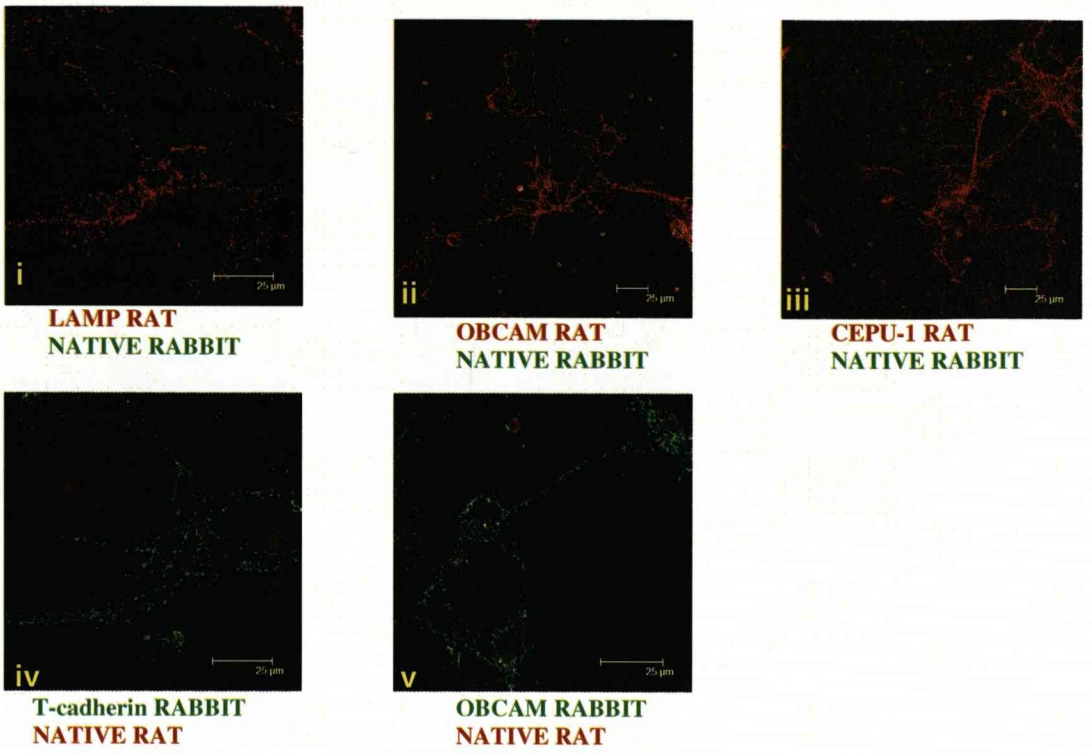

Figure 6.5.A Specificity of secondary antibodies

Photomicrographs are overlay of staining patterns of E8 forebrain neurons, cultured for 72 hours and stained with a specific rat antiserum and a pre-immune rabbit antiserum, and vice versa to test the specificity of the secondary antibodies. Forebrain neurons were co-stained with LAMP, OBCAM and CEPU-1 rat antiserum, detected by Texas-Red™ conjugated goat anti rat secondary antibody and pre-immune rabbit antiserum, followed by Alexa 488™ green goat anti-rabbit second antibody ***i-iii****. Only red fluorescence is visible in these overlays indicating there was no non-specific binding of the rabbit pre-immune serum and no cross reactivity of anti rabbit secondary antibody detecting the rat primary. Similarly, forebrain neurons stained with T-cadherin, and OBCAM rabbit antiserum, detected by Alexa 488™ secondary antibody, is co-stained with rat pre-immune antiserum, detected by Texas-Red™ secondary antibody,* ***iv, v****. Only green fluorescence is visible in these overlays indicating staining with the rabbit antiserum were specific and there was no cross reactivity with the rat secondary antibody. All staining was carried out on live cells with antiserum dilutions of 1:100. Confocal photomicrographs were prepared using LEICA Lite™ software, scale bar is 25 μm*

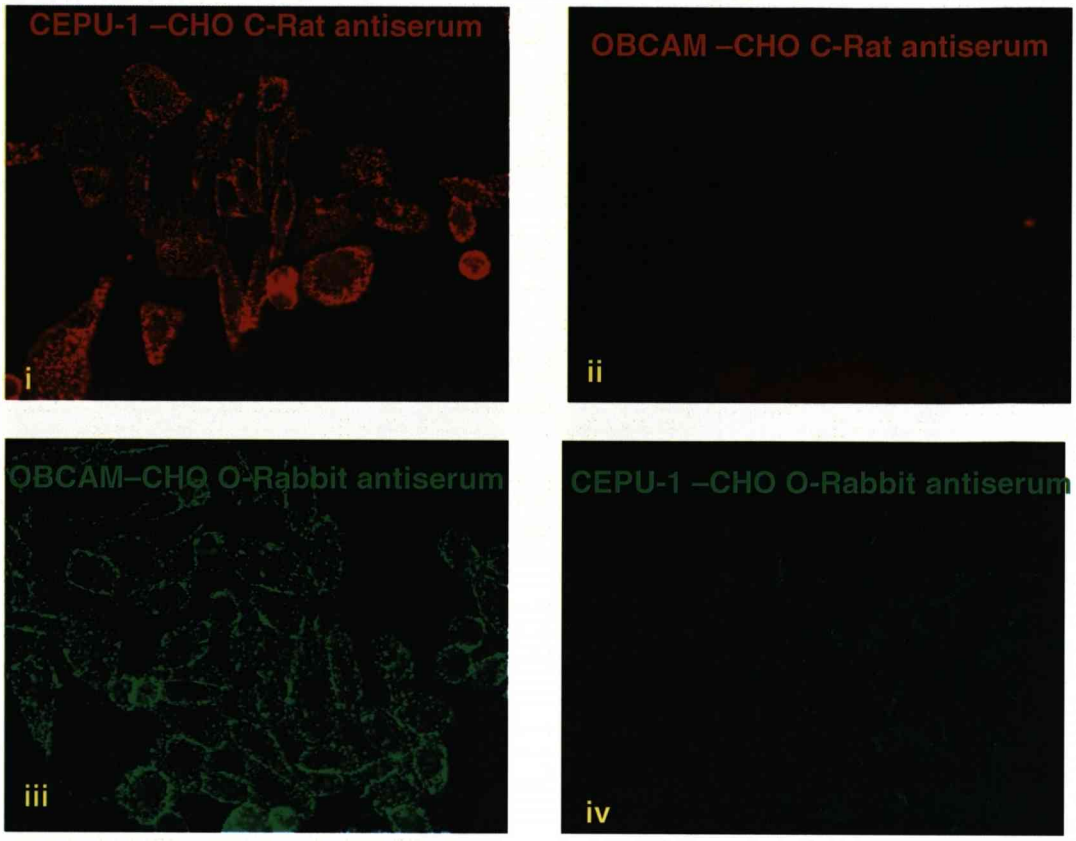

Figure 6.5. B Specificity of CEPU-1 and OBCAM antiserum

CEPU-1 antiserum was adsorbed against OBCAM-CHO cells and OBCAM antiserum against CEPU-1-CHO cells to remove cross reactivity. Adsorbed CEPU-1 rat antiserum stained CEPU-1-CHO cells ***i*** *but not OBCAM-CHO* ***ii.*** *Adsorbed OBCAM rabbit antiserum stained OBCAM-CHO cells* ***iii*** *but not CEPU-1-CHO* ***iv****; suggesting CEPU-1 and OBCAM antiserum were specific and no longer cross-reacted.*

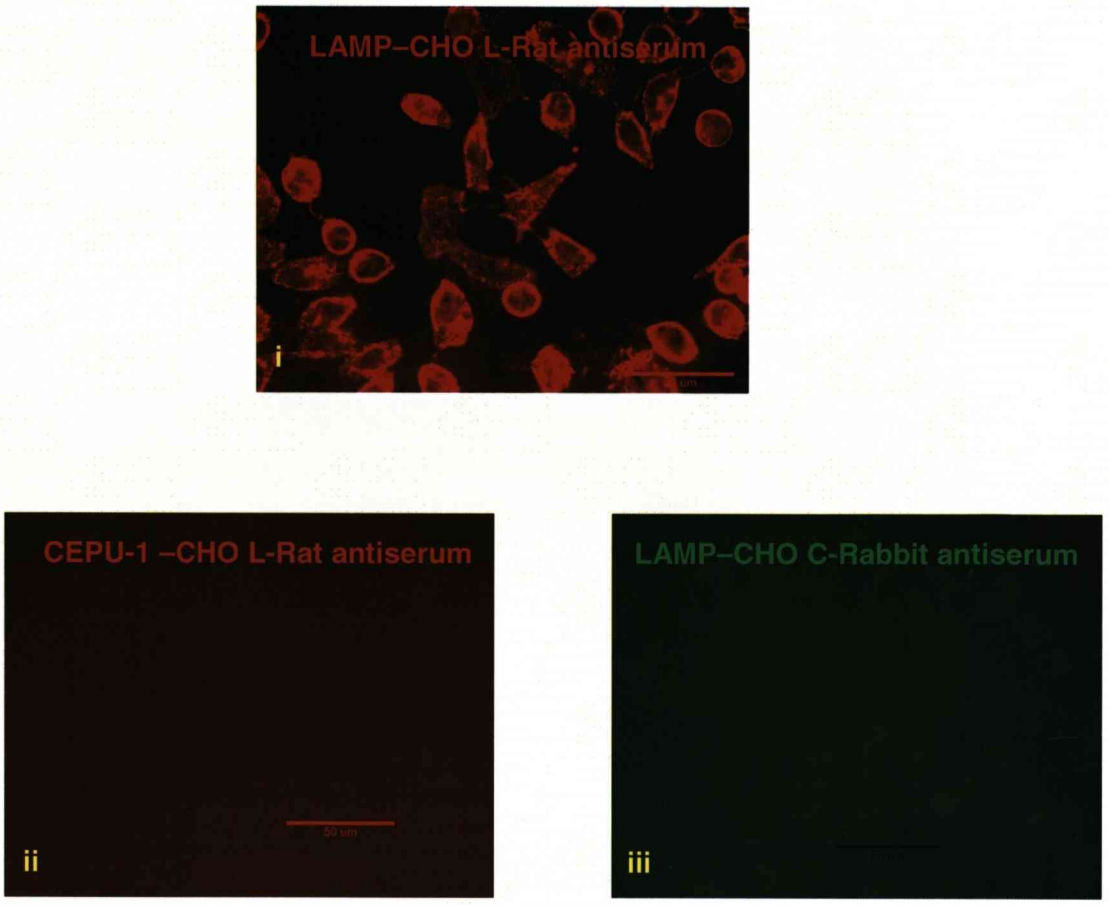

Figure 6.5. C Specificity of LAMP antiserum

LAMP rat antiserum specifically stained LAMP-CHO cells ***i*** *and did not stain CEPU-1 –CHO cells* ***ii****. CEPU-1 rabbit antiserum did not stain LAMP-CHO cells* ***iii*** *suggesting no cross reactivity between LAMP and CEPU-1.*

IgLONs co-cluster on the surface of forebrain neurons

The staining patterns of LAMP or CEPU-1 rat antisera alongside OBCAM or CEPU-1 rabbit antiserum are compared in photomicrographs figure 6.6 A-C. The first two photomicrographs in each column **i** and **ii** show the individual IgLONs stain as either green or red fluorescence. The two fluorescent staining patterns are overlaid in the third photomicrograph **iii** using Image Plugin ™ co-localisation software, where white fluorescence indicates the staining patterns are co-localised on the cell membrane. The staining patterns of T-cadherin rabbit antiserum (labelled with goat anti rabbit Alexa green 488 ™ secondary antibody) alongside LAMP and CEPU-1 rat antisera (labelled with goat anti rat Texas Red ™ secondary antibody) are viewed as either red or green fluorescence in figure 6.6 D-E **i ii**, with overlay of the staining patterns as the third photomicrograph **iii**. There is visibly more co-localisation of the two IgLONs staining patterns in the third photomicrographs of A-C **iii** series, than in the D-E **iii** series where T-cadherin is overlaid alongside LAMP and CEPU-1.

Analysis of LO, CL and CO co-localisation on forebrain neurons

Analysis with Image J plugin™ co-localisation software produced scatter plots in which the white pixels correspond to areas where the red and green staining image pixels co-localise. The scatter plots relating to the comparison of staining between the IgLONs (figure 6.7 A-C) have a higher correlation than that between T-cadherin with either LAMP or CEPU-1 (figure 6.7 D-E) and F11 with either CEPU-1 or OBCAM (figure 6.7 F-G). This suggests IgLONs co-cluster to the same position on the forebrain cell surface, whereas T-cadherin and F11 do not have the same strong correlation of staining with any of the three IgLONs.

Calculation of Pearson's correlation coefficient

To provide more quantitative evidence for putative IgLON heterodimeric complexes individual axons with equal CEPU-1 and LAMP antisera staining patterns were selected using LEICA Lite™ software for further analysis. Areas selected were de-speckled to remove any non-specific background and Image J plugin™ software calculated Pearson's correlation coefficient on three different areas of staining of the forebrain axonal membrane, chosen from two sets of photomicrographs. Pearson's coefficient calculates the degree of linear relationship between the red and green

staining pixels, ranging in value from +1 to -1. A correlation of +1 represents a perfect positive linear relationship between the two staining patterns, no linear relationship gives a 0 value and negative linear relationship between the staining patterns gives a correlation value of -1. The values calculated for Pearson's coefficient for each set of antiserum staining are represented as histograms figure 6.8 A-B. The first histogram indicates LAMP and CEPU-1 have a significantly higher correlation (value ~ 0.48) than does T-cadherin with either LAMP or CEPU-1 (values 0.19-0.1). This confirms LAMP or CEPU-1 are recruited into the some clusters by the antibody patching and supports the formation of putative *cis* CL complex. The co-clustering appears to be specific to the IgLON family members since T-cadherin did not co-localise to the same cluster with LAMP or CEPU-1 on the surface of the forebrain neurons.

CEPU-1 and OBCAM co-localised to the same cluster with a Pearson's value of 0.666 whereas the Pearson's value of F11 co localisation with CEPU-1 and OBCAM was only 0.1002 and 0.09 (figure 6.8 B) once again suggesting CEPU-1 and OBCAM specifically co-localise.

The Pearson's value for LAMP and OBCAM co-clustering was 0.5058, confirmed all three IgLON combinations co-localise to specific areas of the forebrain neuronal membrane.

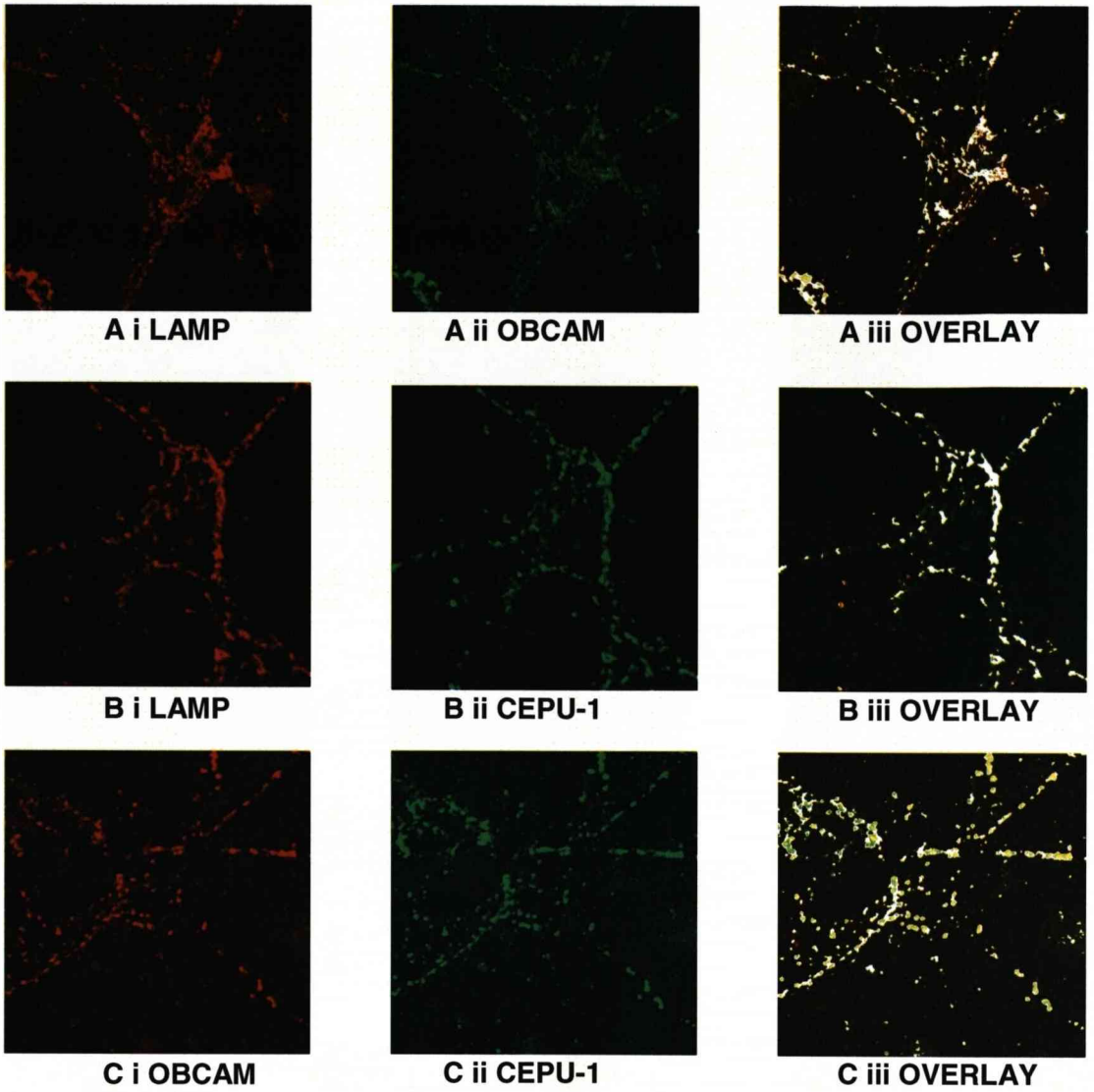

Figure 6.6 A-C Co-clustering of IgLONs on E8 forebrain neurons.

Dissociated E8 forebrain neurons were cultured for 72 hours and live stained with two different IgLON antisera to show co-clustering of IgLONs to the same location on the surface of the neurons. The first photomicrograph ***i*** *in each row corresponds to a specific IgLON rat antisera detected by Texas-Red™ conjugated goat anti rat antibody, the second photomicrograph* ***ii*** *to specific IgLON rabbit antisera detected by Alexa 488™ green conjugated goat anti rabbit antibody. Light fluorescence in the final photomicrograph* ***iii*** *shows the areas of co-localisation of the two IgLON fluorescent staining patterns. Row A is LAMP rat antiserum co-stained with rabbit OBCAM antiserum. Row B is LAMP rat antisera co-stained with rabbit CEPU-1 antisera and row C is CEPU-1 rat antisera with OBCAM rabbit antisera. The overlays all show a strong correlation between the two IgLON staining patterns.*

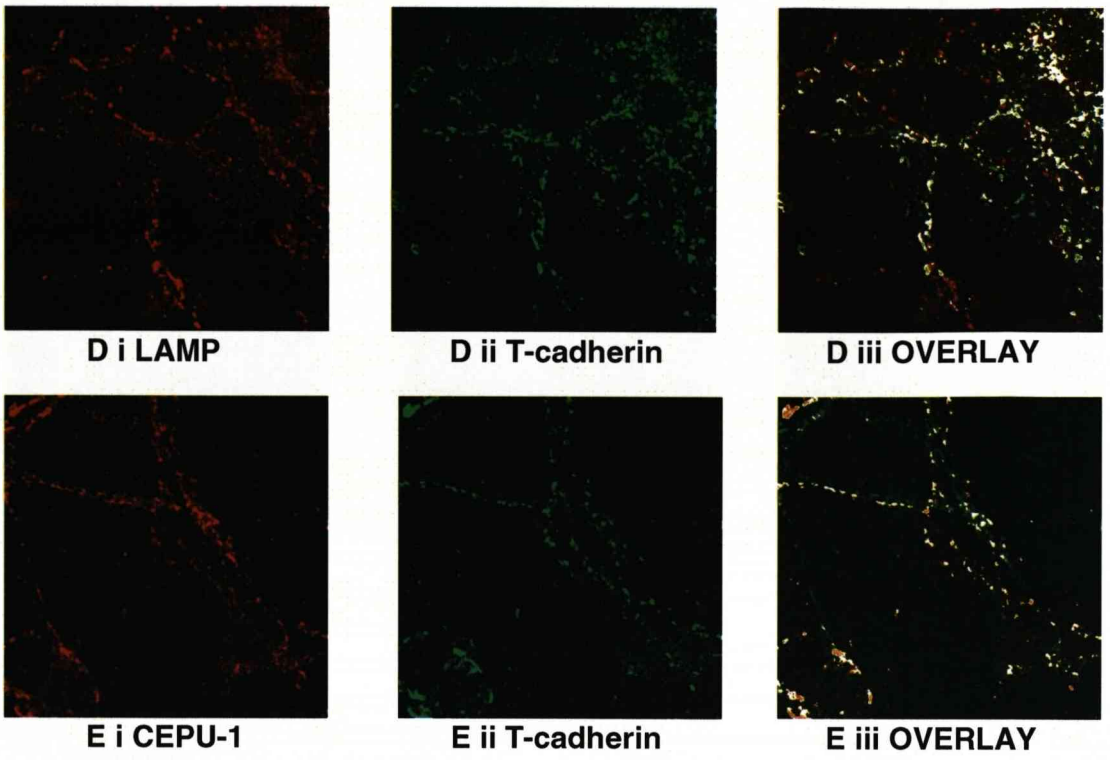

Figure 6.6 D-E IgLONs do not co-cluster with T-cadherin on E8 forebrain neurons.

E8 forebrain were cultured and live stained with IgLON antisera and T-cadherin. The first photomicrograph ***i*** *in each row corresponds to IgLON rat antisera visualised as Texas-Red™ fluorescence and the second photomicrograph* ***ii*** *to T cadherin rabbit antisera visualised as Alexa 488™ green fluorescence. In the third photomicrograph* ***iii*** *in each row the overlap between and LAMP, and CEPU-1 with T-cadherin is visualised as white pixels. Whilst there are some areas of co-expression of the IgLONs with T-cadherin on the surface of forebrain neurons there is no strong overlap of staining patterns localised to a particular area of the membrane as was detected in the previous photomicrographs of the two IgLON staining patterns.*

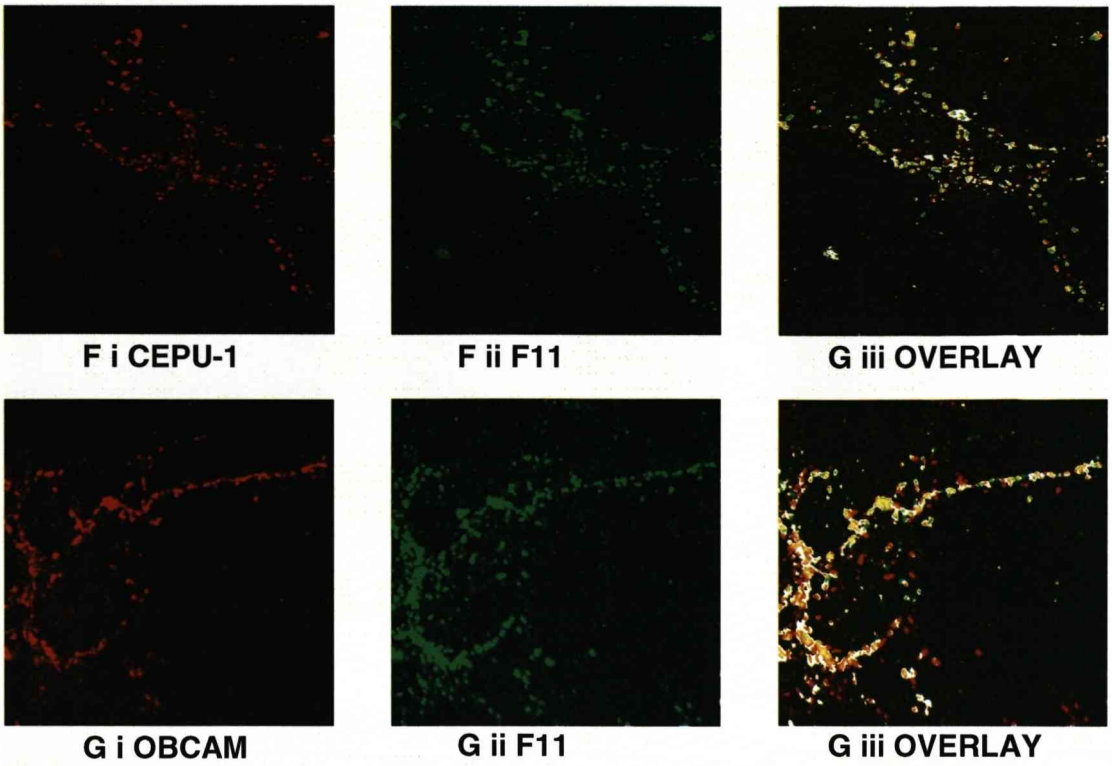

Figure 6.6 F-G IgLONs do not co-cluster with F11 on E8 forebrain neurons.

E8 forebrain neurons were live stained with rat IgLON and rabbit F11 antiserum visualised as Texas-Red™ fluorescence ***i*** *and Alexa 48™ green fluorescence* ***ii.*** *In the third photomicrograph* ***iii*** *in each row the overlap between and CEPU-1 and OBCAM with F11 is visualised as white pixels. Once again there are some areas of co-expression of the IgLONs with F11 on the surface of forebrain neurons but there is no strong overlap of staining patterns localised to a particular area of the membrane as was detected in the two IgLONs.*

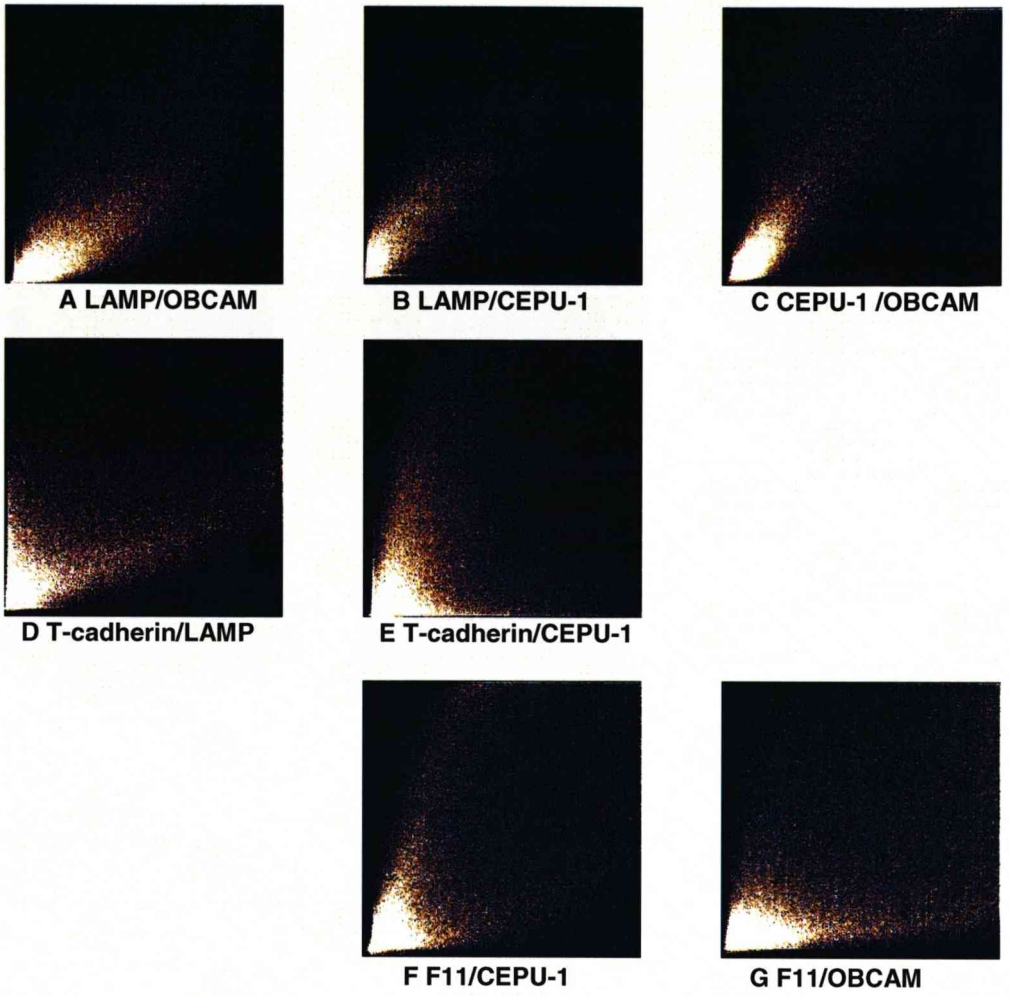

Figure 6.7 Scatter plot analysis of forebrain staining patterns

Red and green fluorescent pixels of LAMP-OBCAM, LAMP-CEPU-1, and CEPU-1-OBCAM staining clusters compact to a small area of white pixels on the scatter plots (A-C). T-cadherin plus LAMP and CEPU-1 (D-E) or F 11 plus CEPU-1 and OBCAM (E-G) have a much more cone shaped scatter plot, indicating there is not such a high correlation between the staining pixels of either T-cadherin or F 11 with the IgLONs. These scatter plots suggest IgLON clusters have significantly higher overlap on the surface of forebrain neurons compared to clusters of either T-cadherin or F11 with IgLONs.

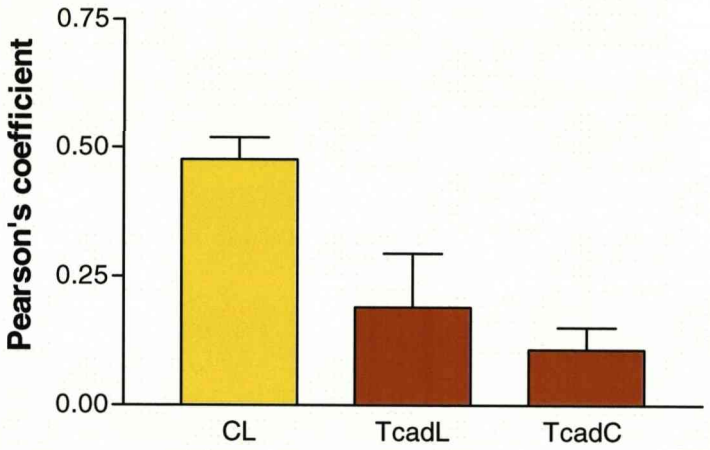

Figure 6.8 A Pearson's correlation coefficient analysis of co-clustering of CEPU-1 and LAMP on forebrain neurons

The dual staining patterns from three different areas of the forebrain neuron membrane were selected using LEICA Lite™ software and compared using Image J plugin™ software to calculate Pearson's correlation coefficient. Correlation between CEPU-1 and LAMP (CL) on the surface of the forebrain neurons has a Pearsons' value of 0.48 (yellow histogram). Correlation between T-cadherin with LAMP (TcadL) and CEPU-1 (TcadC) has Pearsons' values of 0.19 and 0.1 respectively (orange histograms). The significantly stronger correlation between CEPU-1 and LAMP compared to that between T-cadherin with LAMP and CEPU-1 suggests only CEPU-1 and LAMP co-localise to areas of the forebrain membrane, supporting the formation of putative IgLON complexes.

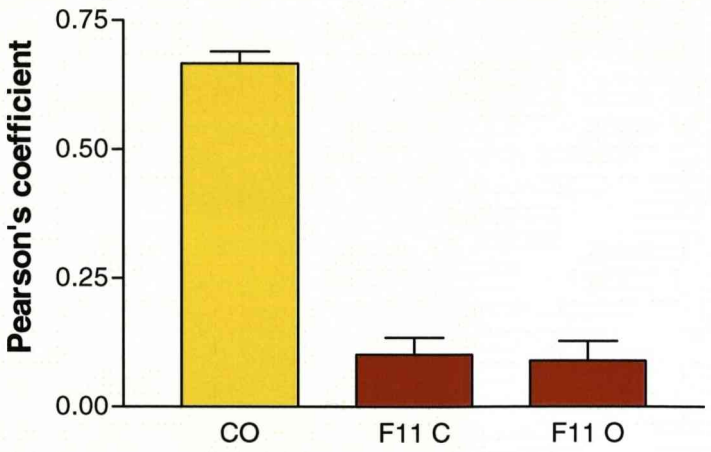

Figure 6.8 B Pearson's correlation coefficient analysis of co-localisation of CO on forebrain neurons

Similarly, CEPU-1 and OBCAM (CO) have a Pearson's value of 0.666 indicating a strong correlation to the same areas of the forebrain membrane (yellow histogram) The correlation between F11 with CEPU-1, (F11 C) and OBCAM, (F11 O) have a much lower Pearson's value 0.102, 0.090 (respective orange histograms) suggesting F11 has little correlation to CEPU-1 or OBCAM. This confirms CEPU-1 and OBCAM specifically co-cluster to an area of the forebrain membrane supporting the formation of putative CO heterodimeric complexes.

DISCUSSION

The first approach to demonstrate the existence of putative cis heterodimeric IgLON complexes was by immuno-purification. CO was PiPLC digested from the surface of CO-CHO cells into solution and OBCAM rabbit serum antibodies, immobilised on nitrocellulose, immuno-purified OBCAM. Subsequent staining of western blots of the immuno-purified proteins revealed both OBCAM and CEPU-1, suggesting CEPU-1 was complexed with OBCAM on the CHO cell surface. On western blots CEPU-1 and OBCAM rat antisera were specific, but as some CEPU-1 was non-specifically immuno-purified by immobilised OBCAM antibodies from the CEPU-1-CHO cell PiPLC supernatant so the experiment was invalidated in terms of conclusively demonstrating the complex.

A similar approach of affinity-purification using a HISx6 tag improved the experiment. OBCAM IgLON was HISx6 tagged and doubly transfected CHO cell lines expressing HISx6 OBCAM alongside LAMP and CEPU-1 were prepared. In these experiments nickel beads captured the HISx6 tagged OBCAM and co-purification of CEPU-1 and LAMP provided evidence for the putative IgLON complexes. The experiment using the cell line expressing LAMP alongside HISx6 OBCAM was more robust in identifying the LO complex than the cell line expressing CEPU-1 identifying CO.

The captured proteins from the doubly transfected CHO cell lines stained at the higher molecular weight of 110 kDa with IgLON antisera on western blots suggested a dimer had been eluted by the beads. LAMP affinity-purified by the HISx6 tag on O^H had possibly remained associated as the LO^H putative complex. The CHO cells used to prepare the supernatants were confluent so the 110 kDa band could have potentially formed from both *cis* and *trans* interactions between the IgLONs on the CHO-cell surface. However, as LAMP has such a weak *trans* homophilic interaction the band more likely arises from a *cis* heterophilic interaction.

The final approach of antibody co-clustering of IgLONs on the surface of forebrain neurons provided additional evidence for the putative *cis* heterodimeric IgLON complex. In these experiments cultured E8 forebrain dissociated neurons were live stained with two different IgLON antisera. The first antiserum clustered IgLON molecules together on the plasma membrane of the neuron and was

visualised as punctuate staining. Staining with a second antiserum co-clustered the two IgLONs to the same location on the membrane. Image J analysis of the overlay of the two IgLON staining patterns confirmed they had co-clustered to the same location. T-cadherin and F11, similar GPI anchored proteins did not associate with IgLONs to the same location and so acted as a negative control for non-specific co-clustering. The specific co-clustering of CEPU-1 with LAMP; CEPU-1 with OBCAM and OBCAM with LAMP suggested they had formed putative *cis* CL CO and LO heterodimeric complexes on the surface of the forebrain neurons.

Chapter Seven

Final Discussion

FINAL DISCUSSION

This thesis provides novel information on the comparative strengths of homophilic and heterophilic *trans* binding interactions between IgLON cell adhesion molecules CEPU-1, OBCAM and LAMP. Evidence is also provided for the formation of *cis* heterodimeric complexes between CEPU-1+LAMP (CL); LAMP+OBCAM (LO); CEPU1+OBCAM (CO) and similar *cis* interactions are proposed between Neurotractin (the fourth member of the family) with LAMP, OBCAM and CEPU-1. These complexes are described as dimeric IgLONs or Diglons. Evidence for IgLONs functioning as Diglons, to inhibit neurite outgrowth from forebrain neurons through Gi/o proteins and possibly the RHO signalling pathway is presented.

Initially, evidence for the putative Diglon *cis* complexes was indirect and came from an assay based on altered *trans* binding affinity of IgLON-FC recombinant proteins to transiently transfected CHO cells. In these assays LO and CL on the surface of CHO cells disrupted the *trans* binding of LAMP-FC. OBCAM and CEPU-1 were proposed to have sequestered LAMP into putative LO and CL *cis* complexes resulting in *trans* LAMP-FC binding sites becoming unavailable. CO-CHO cell line significantly reduced the *trans* affinity for LAMP-FC in an ELISA assay to support a *cis* interaction between CEPU-1 and OBCAM as a putative CO Diglon complex. There is no evidence to support IgLONs forming *cis* heterodimeric interactions with other CAMs outside of the family (Gil et al., 2002) so the unexpected inability of LAMP-FC recombinant protein to interact with forebrain (and other types of IgLON-expressing neurons) is proposed to be due to heterophilic *cis* interactions between IgLONs altering their *trans* binding affinity. Previously the function of IgLONs has been studied as individual members of the family, so considering the formation of these *cis* and possibly *trans* heterodimeric complexes is novel.

Other GPI-anchored IgSF molecules are known to form *cis* and *trans* interactions. For example axonin-1 has 6 Ig and 4 FN type III domains, interacts homophilically and also heterophilically with other NCAMs and extracellular matrix components. Domain-specific monoclonal antibodies studies have proposed a model for axonin-1 having a *cis* interaction between the C-terminal FN-III domains to align the axonin-1 molecules into a two dimensional array. At the N-terminus the end two

Ig domains form a U-shaped arrangement as a compact head and *trans* homophilic interactions then interlaces these compact heads in a zipper-like manner (Kunz et al., 2002).

Additional indirect evidence for Diglon complexes was obtained from functional studies in which initiation of neurite outgrowth was inhibited from a sub-population of E7/8 forebrain neurons cultured on CO and CL-CHO cell lines. When released from the CHO cell surface and used as a substrate CO and CL maintained inhibition of initiation of forebrain neurite outgrowth, suggesting the interaction between the two IgLONs had remained stable even when not attached to the CHO-cell membrane. Similarly, a mixed solution of CEPU-1 and OBCAM released from single IgLON CHO-cell lines also inhibited neurite extension from forebrain neurons. IgLONs may have formed the CO complex in solution, but this assay rose the possibly that IgLONs may act in synergy to inhibit initiation of neurite outgrowth. In previous experiments a mixture of C-FC and O-FC recombinant protein did not inhibit neurite outgrowth suggested IgLONs cannot act in synergy (Michael Lyons unpublished data). In these experiments C and O monomers are in close proximity but as they are fixed by the attached FC they are unlikely to be able to interact. Together these experiments suggest an interaction between IgLONs is required before they can function to inhibit initiation of neurite outgrowth.

The formation of these putative Diglons complexes begins to address the anomaly of the ability of GP55 to inhibit neurite outgrowth, whereas single IgLONs have never satisfactorily demonstrated a definite functional affect. GP55 adult protein is a mixture of IgLONs so potentially could form a range of IgLON/Diglon complexes to inhibit the initiation of neurite outgrowth. These *in vitro* assays of developing neurons encountering dimeric IgLONs may be replicated in *vivo* as areas of co-expression of two members of the IgLON family is found in such areas as the cerebral cortex hippocampus and retina (Struyk et al., 1995; Gil et al., 2002; Miyata et al., 2003b), and maybe related to synaptogenesis (Horton and Levitt, 1988; Zacco et al., 1990; Funatsu et al., 1999; Miyata et al., 2000; Lodge et al., 2000; Miyata et al., 2003c; Chen et al., 2001; Schafer et al., 2005; Yamada et al., 2007).

Affinity-isolation studies went on to provide some physical evidence for the formation of Diglon complexes. In these experiments isolation of a single IgLON from a solution of putative Diglons also co-purified an associated IgLON, but it was not possible to determine if the putative complex had formed by a *cis* or *trans*

interaction on the surface of the CHO cell membrane. However, since monomeric CEPU-se has been demonstrated to have a very weak *trans* interaction with IgLON-CHO cell lines (Lodge et al., 2000) a *trans* interaction between monomers is not as likely. Furthermore, antibody co-clustering experiments strongly supported a *cis* interaction. In these experiments pairs of IgLONs co-localised to the same location on the membrane of forebrain neurons to suggest a definite *cis* interaction.

The data presented suggests that putative Diglon complexes form to potentially play a role in axon guidance by inhibiting initiation of neurite outgrowth by an as yet unknown mechanism. Diglons may become part of at least three possible types of receptor complexes to inhibit neurite outgrowth, illustrated in figure 7.1.

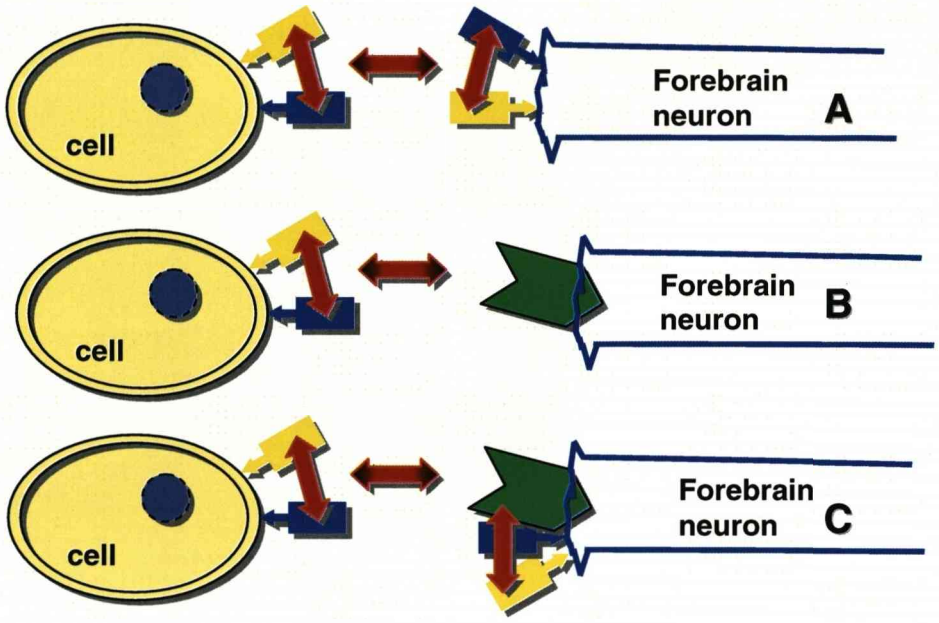

Figure 7.1 Proposed Diglon receptor complexes on the surface of neurons

It is proposed Diglons form by a cis interaction (double headed vertical red arrows) between two IgLONs (yellow and blue boxes) and have a trans interaction to affect neurite outgrowth (double headed horizontal arrows). In part A, a trans interaction is proposed between Diglons expressed on forebrain neurons and extracellular Diglons. For example in this diagram the extracellular Diglons are expressed on an opposing cell. In part B, extracellular Diglons are proposed to function as a ligand activating an unknown transmembrane receptor (green arrow head) expressed on the surface of the forebrain neuron. Finally, part C, proposes IgLONs or Diglons form part of a cis complex with an unknown receptor on the surface of the forebrain neuron, which in turn interacts in trans with extracellular Diglons to induce neurite inhibition.

A *trans* complex possibly forms between Diglons on the surface of the neurons and Diglons in the extracellular environment (figure 7.1A). However, it is difficult to imagine how Diglons could interact directly in *trans in vivo* due to their small size. IgLONs only have three Ig domains, whereas other cell adhesion molecules present on the surface of neurons are much larger, for example Axonin 1, L1, have six Ig domains plus additional FN-III domains, therefore IgLONs may not come into close enough physical contact in *vivo* to be able to interact directly in *trans*. Electron micrographs have measured the gap between pre and postsynaptic axo-dendritic synapses as 25-30 nm. Each Ig domain is estimated as 4.5nm x 3nm x 1.8 nm so IgLONs would only touch at the synapse and are not likely to be large enough to actually span the synapse (Ehinger et al., 1970). There is no evidence so far as to how secreted forms of CEPU-1-se and OBCAM-se function, or if there are additional secreted isoforms of Neurotractin and LAMP. Secreted IgLONs may provide a mechanism to interact as part of a receptor complex to help span the synapse in a similar way to Amalgam. Amalgam being a secreted *Drosophila* protein with three Ig domains that becomes part of a signalling complex, interacting directly with the trans-membrane receptor neurotactin, signalling through the tyrosine kinase Abl to direct axonal growth (Liebl et al., 2003).

GPI anchored proteins have been shown to interact in *trans* with neuronal transmembrane receptors to influence neurite outgrowth, so it is more likely Diglons in the extracellular environment are acting as a ligand for a transmembrane receptor expressed by forebrain neurons (figure 7.1B). Class A Ephrins are an example of GPI anchored molecules that function in this way. They initiate a forward signal through Eph receptors expressed on retinal ganglion cells, to guide axons to their correct location during the development of the retinotopic map (Frisen et al., 1998; Feldheim et al., 2000; Feldheim et al., 2004). Alternately IgLONs or Diglons may interact in *cis* to become part of the receptor complex on the forebrain neuron, before they interact in *trans* with Diglons to inhibit initiation of neurite outgrowth (figure 7.1C). The IgSF molecule L1 forms this type of complex, influencing a *cis* receptor complex through an additional *trans* interaction. L1 forms an association in *cis* with neuropilin on the surface of cortical neurons, which in turn is activated by secreted sema 3 and signals through plexin to inhibit neurite outgrowth (Castellani et al., 2000). This inhibition of neurite outgrowth is reversed by a *trans* interaction of L1 with neuropilin, the specific binding site being located to the first Ig domain of L1 (Castellani, 2002). The

additional *trans* interaction of L1 is thought to function by blocking the co-internalisation of L1 and neuropilin (Castellani et al., 2004).

Members of the IgLON family have previously been investigated as individual molecules but the possibility that IgLONs form *cis* heterodimeric complexes will change the way they are regarded in terms of how they function during neuronal development. Immuno-histochemical and in-situ hybridisation studies have demonstrated several types of cultured neurons express multiple members of the IgLON family, and tissue sections reveal distinct patterns of overlap of IgLON expression to suggest the opportunity for Diglons to form *in-vivo.* For example, LAMP co-localises with CEPU-1 and OBCAM in retinal sections (Lodge et al., 2001) OBCAM co-localises with CEPU-1 and KILON in the hippocampus, as does LAMP and CEPU-1 (Gil et al., 2002; Miyata et al., 2003b; Struyk et al., 1995). These co-localised IgLONs may potentially be functioning as Diglon heterodimeric complexes. The suggestion that IgLONs function as Diglons, does not exclude IgLONs functioning as individual molecules. Single IgLONs are expressed at some locations, for example strong expression of Neurotractin is found on cultured glial cells from chick forebrain, but relatively little expression of other IgLONs is detected. In E18 chick cerebellum frozen sections Neurotractin was the only IgLON detected in the white matter, a region rich in oligodendocytes (Youssef, S., PhD thesis 2006).

IgLONs have no cytoplasmic domain so they are more likely to function as a ligand, requiring either a *cis* or *trans* interaction with a transmembrane neuronal receptor. It is proposed once they become part of a complex they may initiate the signal to inhibit the extension of neurites. PTX reversed neurite initiation of outgrowth from neurons cultured on GP55 substrate to suggest that trimeric Go/i proteins are part of the complex that initiates IgLON signal transduction (Clarke and Moss, 1994; Clarke and Moss, 1997). Similarly, PTX reversed Diglon-induced inhibition of neurite outgrowth from E7/8 forebrain neurons indicated trimeric Go/i proteins may also play a role in Diglon signal transduction. IgLONs are located to specific lipid raft regions of the membrane by their GPI anchor. These rafts regions are areas rich in intracellular signalling intermediates, including trimeric G-proteins, GTPases, Src family of tyrosine receptor kinases, (Tsui-Pierchala et al., 2002; Kamiguchi, 2006a) so IgLONs have the opportunity to interact with a variety of trans-membrane proteins.

Many guidance molecules act through small GTPases, such as the Rho family of proteins. Rho guanine exchange factors (GEFs) and guanine activating protein (GAPs) initiate signals through Rho, Cdc 42 and Rac to the cytoskeleton during axonal guidance (Huber et al., 2003). Inhibition of neurite outgrowth by putative Diglon CO was reversed by a Rho kinase inhibitor to suggest a role for the Rho GTPase signalling pathway linking Diglons to the cytoskeleton. How Diglons initiate a signal through to Rho GTPases is as yet unknown, but the data presented in this thesis for requirement of the presence of a heterodimeric complex for IgLONs to function will help in the search for the receptor and the signalling pathways involved.

The overall proposal is Diglon complexes act in *trans* as extracellular ligands to activate an unknown receptor on the surface of neurons. This receptor may possibly require an additional *cis* interaction with Diglons present on the surface of the neuron. Once activated the receptor possibly initiates a signal through trimeric G proteins and/or the RHO kinase pathway to restrict neurite extension (figure 7.2).

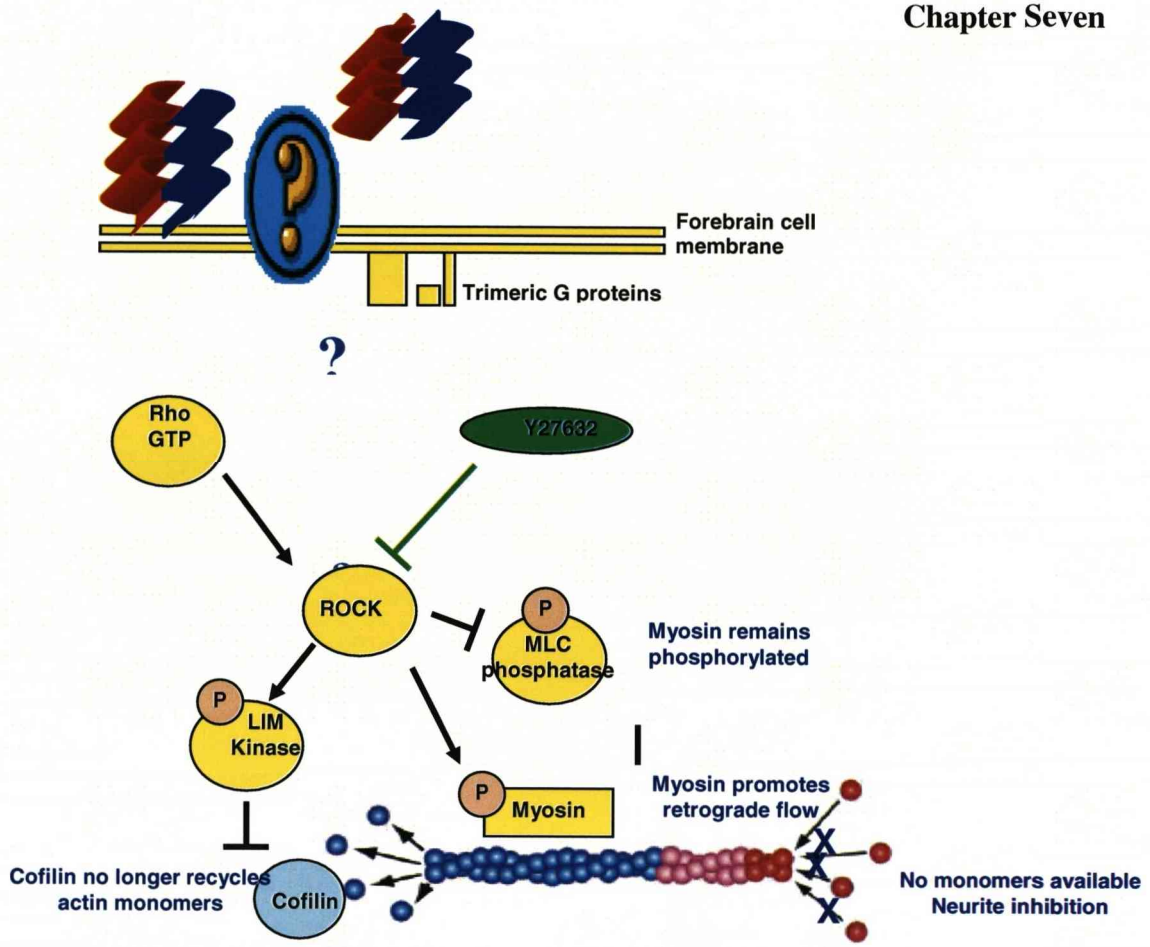

Figure 7.2 Proposed mechanisms for Diglon inhibition of neurite outgrowth

PTX inhibitor studies suggest putative Diglons (red and blue IgLON cartoons) signal via trimeric G proteins (yellow boxes) through an unknown receptor (?). From studies using the ROCK inhibitor Y27632 (green oval) it is proposed Diglon ligand binding initiates the ROCK kinase signalling cascade to inhibit neurite extension. The ROCK signalling cascade influences the cytoskeleton of the extending axon. ROCK phosphorylates (orange circles P) LIM Kinase to prevent it activating the actin severing protein cofilin. Cofilin no longer recycles actin monomers from the minus end of the actin filament (blue circles) to the leading edge, so polymerisation at the growth cone is halted (red circles). Furthermore retrograde flow of monomers away from the leading edge by phosphorylated myosin continues since ROCK also phosphorylates myosin light chain (MLC) phosphatase to keep myosin active, leaving no actin monomers available for actin polymerisation at the growth cone so axonal extension is halted. Figure based on diagrams from Huber 2003 and Dent 2003.

Several other members of the IgSF act as part of receptor complexes, often activated by secreted guidance molecules. Slit plays a leading role in guiding axons across the midline through an interaction with the IgSF receptor molecule Robo (Long et al., 2004). Netrin directs neurite outgrowth during the attraction of spinal cord commissural axons to the floor plate via interactions with IgSF receptors DCC and UNC (Keleman and Dickson, 2001). Netrin interaction with a homodimeric DCC receptor stimulating neurite outgrowth, but if the receptor is altered to a heterophilic *cis* complex between DCC and UNC-5 neurite outgrowth is inhibited (Hong et al., 1999). Possibly the IgLON family are similar in that *cis* heterodimers form part of a signalling complex to inhibit neurite outgrowth.

Once the growth cone reaches its target a series of homophilic and heterophilic interactions between membrane bound cell adhesion proteins maintains initial contact. Members of the IgSF including N-CAM, L1 nectin, SynCAM neurexin and neuroligins, as well as Ephrin/ Eph molecules and the cadherin family of Ca^{2+} dependent proteins are all involved in connecting the incoming axon with the target (Yamada and Nelson, 2007). There is increasing evidence from expression studies that IgLONs maybe linked to the formation of synaptic connections. Early in development IgLON expression is found on axonal tracts and then may switch to dendrites, finally locating to the post synaptic membrane. Expression studies have linked expression of neurotrimin to axonal fasciculation, the formation of excitatory synapses and their stabilisation into adulthood in the rat cerebellum (Chen et al., 2001). Staining alongside specific markers linked OBCAM expression to dendrites of cortical, hippocampal and hypothalamic magnocellular neurons(Miyata et al., 2003a) Co-localisation of Kilon and OBCAM has been demonstrated on the dendrites of magnocellular neurons on post synaptic membranes alongside the synaptic marker protein vesicle associated membrane protein 2 (Miyata et al., 2003b). In addition to expression data manipulation of the levels of OBCAM expression has suggested OBCAM is directly involved in synaptogenesis. In these experiments transfection of cultured hippocampal neurons with an OBCAM mRNA plasmid vector increased OBCAM expression and augmented the number of synaptic connections, whereas suppression of OBCAM with specific antibodies and antisense oligo-deoxyneucleotides impaired the formation of synapses (Yamada et al., 2007). OBCAM continues to influence synapse formation post natally. OBCAM was one of the genes found to be required for the establishment and maintenance of binocular

connections in the cat visual cortex after eye opening (Prasad et al., 2002). There are distinctive patterns of IgLON co-expression linked to synapse formation in other parts of the visual system. For example in the E18 chick retina LAMP and CEPU-1 locate to the outer-plexiform layer whilst LAMP and OBCAM is found in the inner-plexiform, areas rich in synaptic connections (Lodge et al., 2000).

Diglon inhibition of neurite outgrowth was only found in a subpopulation of E7-8 forebrain neurons and no inhibition was observed at the younger age of E6. As IgLON expression alters with development by switching to dendrites it is possible that only those neurons preparing to form synapses may have been inhibited by the extracellular Diglons in these forebrain neurite outgrowth assays. The key question is to find the receptors expressed by this sub-population of neuronal cells and understand how Diglons interact in *cis* and/or in *trans* as part of that receptor complex.

In summary IgLONs have multiple roles during neuronal development which continue on in the adult. Expression begins early in development, where IgLONs are thought to influence cell differentiation and migration; putative Diglon complexes may potentially have a role in axon guidance and synaptogenesis. Expression of IgLONs increases throughout development and is highest post-natally. In the adult, IgLON expression in the brain has been linked to synaptic plasticity, learning and behaviour. Increased LAMP expression in mice has been linked to anxiety and a reluctance to explore (Nelovkov et al., 2003) whereas LAMP deficient mice demonstrated exaggerated behaviour in novel environments (Catania et al., 2008). Outside of the nervous system loss of IgLON expression has been linked to several cancers, suggesting IgLON genes act as tumour suppressors. Loss of OBCAM was demonstrated in ovarian, kidney and brain tumours ((Reed et al., 2007; Sellar et al., 2003) additional loss of LAMP and Kilon being found in some ovarian tumours (Ntougkos et al., 2005). Understanding the interactions of IgLONs and how they function in axon guidance, synaptogenesis, the maintenance of synapses and synapse plasticity may have important clinical applications in spinal injury, neurodegenerative diseases, mental health and tumourogenesis.

References

REFERENCES

Aizawa, H., S. Wakatsuki, A. Ishii, K. Moriyama, Y. Sasaki, K. Ohashi, Y. Sekine-Aizawa, A. Sehara-Fujisawa, K. Mizuno, Y. Goshima, and I. Yahara. 2001. Phosphorylation of cofilin by LIM-kinase is necessary for semaphorin 3A-induced growth cone collapse. Nat Neurosci. 4:367-73.

Aizenman, Y., M.E. Weichsel, Jr., and J. de Vellis. 1986. Changes in insulin and transferrin requirements of pure brain neuronal cultures during embryonic development. Proc Natl Acad Sci U S A. 83:2263-6.

Ango, F., G. di Cristo, H. Higashiyama, V. Bennett, P. Wu, and Z.J. Huang. 2004. Ankyrin-based subcellular gradient of neurofascin, an immunoglobulin family protein, directs GABAergic innervation at purkinje axon initial segment. Cell. 119:257-72.

Baas, P.W. 2002. Neuronal polarity: microtubules strike back. Nat Cell Biol. 4:E194-5.

Baas, P.W., and M.M. Black. 1990. Individual microtubules in the axon consist of domains that differ in both composition and stability. J Cell Biol. 111:495-509.

Barra, H.S., C.A. Arce, and C.E. Argarana. 1988. Posttranslational tyrosination/detyrosination of tubulin. Mol Neurobiol. 2:133-53.

Bear, J.E., T.M. Svitkina, M. Krause, D.A. Schafer, J.J. Loureiro, G.A. Strasser, I.V. Maly, O.Y. Chaga, J.A. Cooper, G.G. Borisy, and F.B. Gertler. 2002. Antagonism between Ena/VASP proteins and actin filament capping regulates fibroblast motility. Cell. 109:509-21.

Biederer, T., Y. Sara, M. Mozhayeva, D. Atasoy, X. Liu, E.T. Kavalali, and T.C. Sudhof. 2002. SynCAM, a synaptic adhesion molecule that drives synapse assembly. Science. 297:1525-31.

Brackenbury, R., B.C. Sorkin, and B.A. Cunningham. 1987. Molecular features of cell adhesion molecules involved in neural development. Res Publ Assoc Res Nerv Ment Dis. 65:155-67.

Brauer, A.U., N.E. Savaskan, M. Plaschke, S. Prehn, O. Ninnemann, and R. Nitsch. 2000. IG-molecule Kilon shows differential expression pattern from LAMP in the developing and adult rat hippocampus. Hippocampus. 10:632-44.

Brose, K., K.S. Bland, K.H. Wang, D. Arnott, W. Henzel, C.S. Goodman, M. Tessier-Lavigne, and T. Kidd. 1999. Slit proteins bind Robo receptors and have an evolutionarily conserved role in repulsive axon guidance. Cell. 96:795-806.

Brown, D.A., and E. London. 2000. Structure and function of sphingolipid- and cholesterol-rich membrane rafts. J Biol Chem. 275:17221-4.

Brummendorf, T., and F.G. Rathjen. 1996. Structure/function relationships of axon-associated adhesion receptors of the immunoglobulin superfamily. Curr Opin Neurobiol. 6:584-93.

Brummendorf, T., F. Spaltmann, and U. Treubert. 1997. Cloning and characterization of a neural cell recognition molecule on axons of the retinotectal system and spinal cord. Eur J Neurosci. 9:1105-16.

Buck, K.B., and J.Q. Zheng. 2002. Growth cone turning induced by direct local modification of microtubule dynamics. J Neurosci. 22:9358-67.

Cajal,R.y.1890. Sur l'origine at les ramifications des fibres nerveuses de la moelle embryonaire. Anat Anz 5:609-613

Castellani, V. 2002. The function of neuropilin/L1 complex. Adv Exp Med Biol. 515:91-102.

Castellani, V., A. Chedotal, M. Schachner, C. Faivre-Sarrailh, and G. Rougon. 2000. Analysis of the L1-deficient mouse phenotype reveals cross-talk between Sema3A and L1 signaling pathways in axonal guidance. Neuron. 27:237-49.

Castellani, V., J. Falk, and G. Rougon. 2004. Semaphorin3A-induced receptor endocytosis during axon guidance responses is mediated by L1 CAM. Mol Cell Neurosci. 26:89-100.

Catania, E.H., A. Pimenta, and P. Levitt. 2008. Genetic deletion of Lsamp causes exaggerated behavioral activation in novel environments. Behav Brain Res. 188:380-90.

Chen, G., X. Wu, and S. Tuncdemir. 2007a. Cell adhesion and synaptogenesis. Sheng Li Xue Bao. 59:697-706.

Chen, H., F. Ye, J. Zhang, W. Lu, Q. Cheng, and X. Xie. 2007b. Loss of OPCML expression and the correlation with CpG island methylation and LOH in ovarian serous carcinoma. Eur J Gynaecol Oncol. 28:464-7.

Chen, S., O. Gil, Y.Q. Ren, G. Zanazzi, J.L. Salzer, and D.E. Hillman. 2001. Neurotrimin expression during cerebellar development suggests roles in axon fasciculation and synaptogenesis. J Neurocytol. 30:927-37.

Chiba, A., and H. Keshishian. 1996. Neuronal pathfinding and recognition: roles of cell adhesion molecules. Dev Biol. 180:424-32.

Chih, B., H. Engelman, and P. Scheiffele. 2005. Control of excitatory and inhibitory synapse formation by neuroligins. Science. 307:1324-8.

Chilton, J.K. 2006. Molecular mechanisms of axon guidance. Dev Biol. 292:13-24.

Chisholm, A., and M. Tessier-Lavigne. 1999. Conservation and divergence of axon guidance mechanisms. Curr Opin Neurobiol. 9:603-15.

Chizhikov, V.V., and K.J. Millen. 2005. Roof plate-dependent patterning of the vertebrate dorsal central nervous system. Dev Biol. 277:287-95.

Clarke, G.A., and D.J. Moss. 1994. Identification of a novel protein from adult chicken brain that inhibits neurite outgrowth. J Cell Sci. 107 (Pt 12):3393-402.

Clarke, G.A., and D.J. Moss. 1997. GP55 inhibits both cell adhesion and growth of neurons, but not non-neuronal cells, via a G-protein-coupled receptor. Eur J Neurosci. 9:334-41.

Clegg, D.O., K.L. Wingerd, S.T. Hikita, and E.C. Tolhurst. 2003. Integrins in the development, function and dysfunction of the nervous system. Front Biosci. 8:d723-50.

Colamarino, S.A., and M. Tessier-Lavigne. 1995. The axonal chemoattractant netrin-1 is also a chemorepellent for trochlear motor axons. Cell. 81:621-9.

Crossin, K.L., and L.A. Krushel. 2000. Cellular signaling by neural cell adhesion molecules of the immunoglobulin superfamily. Dev Dyn. 218:260-79.

Cutforth, T., and C.J. Harrison. 2002. Ephs and ephrins close ranks. Trends Neurosci. 25:332-4.

Dean, C., F.G. Scholl, J. Choih, S. DeMaria, J. Berger, E. Isacoff, and P. Scheiffele. 2003. Neurexin mediates the assembly of presynaptic terminals. Nat Neurosci. 6:708-16.

Dent, E.W., and F.B. Gertler. 2003. Cytoskeletal dynamics and transport in growth cone motility and axon guidance. Neuron. 40:209-27.

Dent, E.W., and K. Kalil. 2001. Axon branching requires interactions between dynamic microtubules and actin filaments. J Neurosci. 21:9757-69.

Dickson, B.J. 2002. Molecular mechanisms of axon guidance. Science. 298:1959-64.

Dickson, B.J., and G.F. Gilestro. 2006. Regulation of commissural axon pathfinding by slit and its Robo receptors. Annu Rev Cell Dev Biol. 22:651-75.

Ditlevsen, D.K., G.K. Povlsen, V. Berezin, and E. Bock. 2008. NCAM-induced intracellular signaling revisited. J Neurosci Res. 86:727-43.

Doherty, P., M.S. Fazeli, and F.S. Walsh. 1995. The neural cell adhesion molecule and synaptic plasticity. J Neurobiol. 26:437-46.

Eagleson, K.L., A.F. Pimenta, M.M. Burns, L.D. Fairfull, P.K. Cornuet, L. Zhang, and P. Levitt. 2003. Distinct domains of the limbic system-associated membrane protein (LAMP) mediate discrete effects on neurite outgrowth. Mol Cell Neurosci. 24:725-40.

Ehinger, B., B. Falck, and B. Sporrong. 1970. Possible axo-axonal synapses between peripheral adrenergic and cholinergic nerve terminals. Z Zellforsch Mikrosk Anat. 107:508-21.

Endo, M., K. Ohashi, Y. Sasaki, Y. Goshima, R. Niwa, T. Uemura, and K. Mizuno. 2003. Control of growth cone motility and morphology by LIM kinase and Slingshot via phosphorylation and dephosphorylation of cofilin. J Neurosci. 23:2527-37.

Ericson, J., J. Muhr, T.M. Jessell, and T. Edlund. 1995. Sonic hedgehog: a common signal for ventral patterning along the rostrocaudal axis of the neural tube. Int J Dev Biol. 39:809-16.

Erskine, L., and E. Herrera. 2007. The retinal ganglion cell axon's journey: insights into molecular mechanisms of axon guidance. Dev Biol. 308:1-14.

Faivre-Sarrailh, C., J.Y. Lena, L. Had, M. Vignes, and U. Lindberg. 1993. Location of profilin at presynaptic sites in the cerebellar cortex; implication for the regulation of the actin-polymerization state during axonal elongation and synaptogenesis. J Neurocytol. 22:1060-72.

Feldheim, D.A., Y.I. Kim, A.D. Bergemann, J. Frisen, M. Barbacid, and J.G. Flanagan. 2000. Genetic analysis of ephrin-A2 and ephrin-A5 shows their requirement in multiple aspects of retinocollicular mapping. Neuron. 25:563-74.

Feldheim, D.A., M. Nakamoto, M. Osterfield, N.W. Gale, T.M. DeChiara, R. Rohatgi, G.D. Yancopoulos, and J.G. Flanagan. 2004. Loss-of-function analysis of EphA receptors in retinotectal mapping. J Neurosci. 24:2542-50.

Frank, M., and R. Kemler. 2002. Protocadherins. Curr Opin Cell Biol. 14:557-62.

Fremion, F., I. Darboux, M. Diano, R. Hipeau-Jacquotte, M.A. Seeger, and M. Piovant. 2000. Amalgam is a ligand for the transmembrane receptor neurotactin and is required for neurotactin-mediated cell adhesion and axon fasciculation in Drosophila. Embo J. 19:4463-72.

Friedman, H.V., T. Bresler, C.C. Garner, and N.E. Ziv. 2000. Assembly of new individual excitatory synapses: time course and temporal order of synaptic molecule recruitment. Neuron. 27:57-69.

Friedrichson, T., and T.V. Kurzchalia. 1998. Microdomains of GPI-anchored proteins in living cells revealed by crosslinking. Nature. 394:802-5.

Frisen, J., P.A. Yates, T. McLaughlin, G.C. Friedman, D.D. O'Leary, and M. Barbacid. 1998. Ephrin-A5 (AL-1/RAGS) is essential for proper retinal axon guidance and topographic mapping in the mammalian visual system. Neuron. 20:235-43.

Funatsu, N., S. Miyata, H. Kumanogoh, M. Shigeta, K. Hamada, Y. Endo, Y. Sokawa, and S. Maekawa. 1999. Characterization of a novel rat brain

glycosylphosphatidylinositol-anchored protein (Kilon), a member of the IgLON cell adhesion molecule family. J Biol Chem. 274:8224-30.

Gauthier, L.R., and S.M. Robbins. 2003. Ephrin signaling: One raft to rule them all? One raft to sort them? One raft to spread their call and in signaling bind them? Life Sci. 74:207-16.

Gerrow, K., and A. El-Husseini. 2006. Cell adhesion molecules at the synapse. Front Biosci. 11:2400-19.

Gil, O.D., G. Zanazzi, A.F. Struyk, and J.L. Salzer. 1998. Neurotrimin mediates bifunctional effects on neurite outgrowth via homophilic and heterophilic interactions. J Neurosci. 18:9312-25.

Gil, O.D., L. Zhang, S. Chen, Y.Q. Ren, A. Pimenta, G. Zanazzi, D. Hillman, P. Levitt, and J.L. Salzer. 2002. Complementary expression and heterophilic interactions between IgLON family members neurotrimin and LAMP. J Neurobiol. 51:190-204.

Goldberg, D.J., M.S. Foley, D. Tang, and P.W. Grabham. 2000. Recruitment of the Arp2/3 complex and mena for the stimulation of actin polymerization in growth cones by nerve growth factor. J Neurosci Res. 60:458-67.

Gordon-Weeks, P.R. 1991. Evidence for microtubule capture by filopodial actin filaments in growth cones. Neuroreport. 2:573-6.

Gordon-Weeks, P.R., and I. Fischer. 2000. MAP1B expression and microtubule stability in growing and regenerating axons. Microsc Res Tech. 48:63-74.

Guirland, C., S. Suzuki, M. Kojima, B. Lu, and J.Q. Zheng. 2004. Lipid rafts mediate chemotropic guidance of nerve growth cones. Neuron. 42:51-62.

Halloran, M.C., and M.A. Wolman. 2006. Repulsion or adhesion: receptors make the call. Curr Opin Cell Biol. 18:533-40.

Hancox, K.A., A.A. Gooley, and P.L. Jeffrey. 1997. AvGp50, a predominantly axonally expressed glycoprotein, is a member of the IgLON's subfamily of cell adhesion molecules (CAMs). Brain Res Mol Brain Res. 44:273-85.

Harder, T., P. Scheiffele, P. Verkade, and K. Simons. 1998. Lipid domain structure of the plasma membrane revealed by patching of membrane components. J Cell Biol. 141:929-42.

Harrison, R.G. 1910. The outgrowth of the nerve fibre as a model of protoplasmic movement. Journal of Experimental Zoology. 9:787.

Herincs, Z., V. Corset, N. Cahuzac, C. Furne, V. Castellani, A.O. Hueber, and P. Mehlen. 2005. DCC association with lipid rafts is required for netrin-1-mediated axon guidance. J Cell Sci. 118:1687-92.

Higgs, H.N., and T.D. Pollard. 2001. Regulation of actin filament network formation through ARP2/3 complex: activation by a diverse array of proteins. Annu Rev Biochem. 70:649-76.

Hong, K., L. Hinck, M. Nishiyama, M.M. Poo, M. Tessier-Lavigne, and E. Stein. 1999. A ligand-gated association between cytoplasmic domains of UNC5 and DCC family receptors converts netrin-induced growth cone attraction to repulsion. Cell. 97:927-41.

Hopf, F.W., J. Waters, S. Mehta, and S.J. Smith. 2002. Stability and plasticity of developing synapses in hippocampal neuronal cultures. J Neurosci. 22:775-81.

Horton, H.L., and P. Levitt. 1988. A unique membrane protein is expressed on early developing limbic system axons and cortical targets. J Neurosci. 8:4653-61.

Howard, M.R., A.P. Lodge, J.E. Reed, C.J. McNamee, and D.J. Moss. 2002. High-level expression of recombinant Fc chimeric proteins in suspension cultures of stably transfected J558L cells. Biotechniques. 32:1282-6, 1288.

Hu, H. 1999. Chemorepulsion of neuronal migration by Slit2 in the developing mammalian forebrain. Neuron. 23:703-11.

Huang, E.J., and L.F. Reichardt. 2001. Neurotrophins: roles in neuronal development and function. Annu Rev Neurosci. 24:677-736.

Huber, A.B., A.L. Kolodkin, D.D. Ginty, and J.F. Cloutier. 2003. Signaling at the growth cone: ligand-receptor complexes and the control of axon growth and guidance. Annu Rev Neurosci. 26:509-63.

Huot, J. 2004. Ephrin signaling in axon guidance. Prog Neuropsychopharmacol Biol Psychiatry. 28:813-8.

Igarashi, M., S.M. Strittmatter, T. Vartanian, and M.C. Fishman. 1993. Mediation by G proteins of signals that cause collapse of growth cones. Science. 259:77-9.

Ishizaki, T., M. Uehata, I. Tamechika, J. Keel, K. Nonomura, M. Maekawa, and S. Narumiya. 2000. Pharmacological properties of Y-27632, a specific inhibitor of rho-associated kinases. Mol Pharmacol. 57:976-83.

Jessell, T.M., and J. Dodd. 1990. Floor plate-derived signals and the control of neural cell pattern in vertebrates. Harvey Lect. 86:87-128.

Juliano, R.L. 2002. Signal transduction by cell adhesion receptors and the cytoskeleton: functions of integrins, cadherins, selectins, and immunoglobulin-superfamily members. Annu Rev Pharmacol Toxicol. 42:283-323.

Jungbluth, S., C. Phelps, and A. Lumsden. 2001. CEPU-1 expression in the early embryonic chick brain. Mech Dev. 101:195-7.

Kalil, K., and E.W. Dent. 2005. Touch and go: guidance cues signal to the growth cone cytoskeleton. Curr Opin Neurobiol. 15:521-6.

Kamiguchi, H. 2006a. [Biophysical mechanisms of neurite growth mediated by the cell adhesion molecule L1]. Tanpakushitsu Kakusan Koso. 51:623-8.

Kamiguchi, H. 2006b. The region-specific activities of lipid rafts during axon growth and guidance. J Neurochem. 98:330-5.

Keleman, K., and B.J. Dickson. 2001. Short- and long-range repulsion by the Drosophila Unc5 netrin receptor. Neuron. 32:605-17.

Keleman, K., S. Rajagopalan, D. Cleppien, D. Teis, K. Paiha, L.A. Huber, G.M. Technau, and B.J. Dickson. 2002. Comm sorts robo to control axon guidance at the Drosophila midline. Cell. 110:415-27.

Keleman, K., C. Ribeiro, and B.J. Dickson. 2005. Comm function in commissural axon guidance: cell-autonomous sorting of Robo in vivo. Nat Neurosci. 8:156-63.

Kennedy, T.E., T. Serafini, J.R. de la Torre, and M. Tessier-Lavigne. 1994. Netrins are diffusible chemotropic factors for commissural axons in the embryonic spinal cord. Cell. 78:425-35.

Kim, D.S., T.H. Rhew, D.J. Moss, and J.Y. Kim. 1999. cDNA cloning of the CEPUS, a secreted type of neural glycoprotein belonging to the immunoglobulin-like opioid binding cell adhesion molecule (OBCAM) subfamily. Mol Cells. 9:270-6.

Kimura, Y., A. Katoh, T. Kaneko, K. Takahama, and H. Tanaka. 2001. Two members of the IgLON family are expressed in a restricted region of the developing chick brain and neural crest. Dev Growth Differ. 43:257-63.

Kiselyov, V.V., G. Skladchikova, A.M. Hinsby, P.H. Jensen, N. Kulahin, V. Soroka, N. Pedersen, V. Tsetlin, F.M. Poulsen, V. Berezin, and E. Bock. 2003. Structural basis for a direct interaction between FGFR1 and NCAM and evidence for a regulatory role of ATP. Structure. 11:691-701.

Kiselyov, V.V., V. Soroka, V. Berezin, and E. Bock. 2005. Structural biology of NCAM homophilic binding and activation of FGFR. J Neurochem. 94:1169-79.

Klein, R. 2001. Excitatory Eph receptors and adhesive ephrin ligands. Curr Opin Cell Biol. 13:196-203.

Knoll, B., and U. Drescher. 2002. Ephrin-As as receptors in topographic projections. Trends Neurosci. 25:145-9.

Kolodkin, A.L., D.V. Levengood, E.G. Rowe, Y.T. Tai, R.J. Giger, and D.D. Ginty. 1997. Neuropilin is a semaphorin III receptor. Cell. 90:753-62.

Kramer, S.G., T. Kidd, J.H. Simpson, and C.S. Goodman. 2001. Switching repulsion to attraction: changing responses to slit during transition in mesoderm migration. Science. 292:737-40.

Kullander, K., and R. Klein. 2002. Mechanisms and functions of Eph and ephrin signalling. Nat Rev Mol Cell Biol. 3:475-86.

Kunz, B., R. Lierheimer, C. Rader, M. Spirig, U. Ziegler, and P. Sonderegger. 2002. Axonin-1/TAG-1 mediates cell-cell adhesion by a cis-assisted trans-interaction. J Biol Chem. 277:4551-7.

LaBonne, C., and M. Bronner-Fraser. 1999. Molecular mechanisms of neural crest formation. Annu Rev Cell Dev Biol. 15:81-112.

Lardi-Studler, B., and J.M. Fritschy. 2007. Matching of pre- and postsynaptic specializations during synaptogenesis. Neuroscientist. 13:115-26.

Lee, K.J., P. Dietrich, and T.M. Jessell. 2000. Genetic ablation reveals that the roof plate is essential for dorsal interneuron specification. Nature. 403:734-40.

Levinson, J.N., N. Chery, K. Huang, T.P. Wong, K. Gerrow, R. Kang, O. Prange, Y.T. Wang, and A. El-Husseini. 2005. Neuroligins mediate excitatory and inhibitory synapse formation: involvement of PSD-95 and neurexin-1beta in neuroligin-induced synaptic specificity. J Biol Chem. 280:17312-9.

Levitt, P. 1984. A monoclonal antibody to limbic system neurons. Science. 223:299-301.

Liebl, E.C., R.G. Rowe, D.J. Forsthoefel, A.L. Stammler, E.R. Schmidt, M. Turski, and M.A. Seeger. 2003. Interactions between the secreted protein Amalgam, its transmembrane receptor Neurotactin and the Abelson tyrosine kinase affect axon pathfinding. Development. 130:3217-26.

Liem, H.H., F. Cardenas, M. Tavassoli, M.B. Poh-Fitzpatrick, and U. Muller-Eberhard. 1979. Quantitative determination of hemoglobin and cytochemical staining for peroxidase using 3,3',5,5'-tetramethylbenzidine dihydrochloride, a safe substitute for benzidine. Anal Biochem. 98:388-93.

Lin, A.C., and C.E. Holt. 2007. Local translation and directional steering in axons. Embo J. 26:3729-36.

Lin, C.H., E.M. Espreafico, M.S. Mooseker, and P. Forscher. 1996. Myosin drives retrograde F-actin flow in neuronal growth cones. Neuron. 16:769-82.

Lodge, A.P., M.R. Howard, C.J. McNamee, and D.J. Moss. 2000. Co-localisation, heterophilic interactions and regulated expression of IgLON family proteins in the chick nervous system. Brain Res Mol Brain Res. 82:84-94.

Lodge, A.P., C.J. McNamee, M.R. Howard, J.E. Reed, and D.J. Moss. 2001. Identification and characterization of CEPU-Se-A secreted isoform of the IgLON family protein, CEPU-1. Mol Cell Neurosci. 17:746-60.

Long, H., C. Sabatier, L. Ma, A. Plump, W. Yuan, D.M. Ornitz, A. Tamada, F. Murakami, C.S. Goodman, and M. Tessier-Lavigne. 2004. Conserved roles for Slit and Robo proteins in midline commissural axon guidance. Neuron. 42:213-23.

Lu, M., W. Witke, D.J. Kwiatkowski, and K.S. Kosik. 1997. Delayed retraction of filopodia in gelsolin null mice. J Cell Biol. 138:1279-87.

Mallavarapu, A., and T. Mitchison. 1999. Regulated actin cytoskeleton assembly at filopodium tips controls their extension and retraction. J Cell Biol. 146:1097-106.

Mann, F., V. Zhukareva, A. Pimenta, P. Levitt, and J. Bolz. 1998. Membrane-associated molecules guide limbic and nonlimbic thalamocortical projections. J Neurosci. 18:9409-19.

Marg, A., P. Sirim, F. Spaltmann, A. Plagge, G. Kauselmann, F. Buck, F.G. Rathjen, and T. Brummendorf. 1999. Neurotractin, a novel neurite outgrowth-promoting Ig-like protein that interacts with CEPU-1 and LAMP. J Cell Biol. 145:865-76.

McNamee, C.J., J.E. Reed, M.R. Howard, A.P. Lodge, and D.J. Moss. 2002. Promotion of neuronal cell adhesion by members of the IgLON family occurs in the absence of either support or modification of neurite outgrowth. J Neurochem. 80:941-8.

Meberg, P.J. 2000. Signal-regulated ADF/cofilin activity and growth cone motility. Mol Neurobiol. 21:97-107.

Meberg, P.J., and J.R. Bamburg. 2000. Increase in neurite outgrowth mediated by overexpression of actin depolymerizing factor. J Neurosci. 20:2459-69.

Mehlen, P. 2003. Neurobiology: a new way to network. Nature. 424:381-2.

Mitchison, T., and M. Kirschner. 1984. Dynamic instability of microtubule growth. Nature. 312:237-42.

Miyata, S., N. Funatsu, W. Matsunaga, T. Kiyohara, Y. Sokawa, and S. Maekawa. 2000. Expression of the IgLON cell adhesion molecules Kilon and OBCAM in hypothalamic magnocellular neurons. J Comp Neurol. 424:74-85.

Miyata, S., N. Matsumoto, and S. Maekawa. 2003a. Polarized targeting of IgLON cell adhesion molecule OBCAM to dendrites in cultured neurons. Brain Res. 979:129-36.

Miyata, S., N. Matsumoto, K. Taguchi, A. Akagi, T. Iino, N. Funatsu, and S. Maekawa. 2003b. Biochemical and ultrastructural analyses of IgLON cell adhesion molecules, Kilon and OBCAM in the rat brain. Neuroscience. 117:645-58.

Miyata, S., K. Taguchi, and S. Maekawa. 2003c. Dendrite-associated opioid-binding cell adhesion molecule localizes at neurosecretory granules in the hypothalamic magnocellular neurons. Neuroscience. 122:169-81.

Mizoguchi, A., H. Nakanishi, K. Kimura, K. Matsubara, K. Ozaki-Kuroda, T. Katata, T. Honda, Y. Kiyohara, K. Heo, M. Higashi, T. Tsutsumi, S. Sonoda, C. Ide, and Y. Takai. 2002. Nectin: an adhesion molecule involved in formation of synapses. J Cell Biol. 156:555-65.

Muller, D., P. Mendez, M. De Roo, P. Klauser, S. Steen, and L. Poglia. 2008. Role of NCAM in Spine Dynamics and Synaptogenesis. Neurochem Res.

Munoz-Sanjuan, I., and A.H. Brivanlou. 2002. Neural induction, the default model and embryonic stem cells. Nat Rev Neurosci. 3:271-80.

Munro, S. 2003. Lipid rafts: elusive or illusive? Cell. 115:377-88.

Murai, K.K., and E.B. Pasquale. 2003. 'Eph'ective signaling: forward, reverse and crosstalk. J Cell Sci. 116:2823-32.

Nakai, Y., and H. Kamiguchi. 2002. Migration of nerve growth cones requires detergent-resistant membranes in a spatially defined and substrate-dependent manner. J Cell Biol. 159:1097-108.

Narumiya, S., T. Ishizaki, and M. Uehata. 2000. Use and properties of ROCK-specific inhibitor Y-27632. Methods Enzymol. 325:273-84.

Neiiendam, J.L., L.B. Kohler, C. Christensen, S. Li, M.V. Pedersen, D.K. Ditlevsen, M.K. Kornum, V.V. Kiselyov, V. Berezin, and E. Bock. 2004. An NCAM-derived FGF-receptor agonist, the FGL-peptide, induces neurite outgrowth and neuronal survival in primary rat neurons. J Neurochem. 91:920-35.

Nelovkov, A., M.A. Philips, S. Koks, and E. Vasar. 2003. Rats with low exploratory activity in the elevated plus-maze have the increased expression of limbic system-associated membrane protein gene in the periaqueductal grey. Neurosci Lett. 352:179-82.

Niethammer, P., M. Delling, V. Sytnyk, A. Dityatev, K. Fukami, and M. Schachner. 2002. Cosignaling of NCAM via lipid rafts and the FGF receptor is required for neuritogenesis. J Cell Biol. 157:521-32.

Noble, M., M. Albrechtsen, C. Moller, J. Lyles, E. Bock, C. Goridis, M. Watanabe, and U. Rutishauser. 1985. Glial cells express N-CAM/D2-CAM-like polypeptides in vitro. Nature. 316:725-8.

Ntougkos, E., R. Rush, D. Scott, T. Frankenberg, H. Gabra, J.F. Smyth, and G.C. Sellar. 2005. The IgLON family in epithelial ovarian cancer: expression profiles and clinicopathologic correlates. Clin Cancer Res. 11:5764-8.

Pimenta, A.F., B.S. Reinoso, and P. Levitt. 1996. Expression of the mRNAs encoding the limbic system-associated membrane protein (LAMP): II. Fetal rat brain. J Comp Neurol. 375:289-302.

Pimenta, A.F., V. Zhukareva, M.F. Barbe, B.S. Reinoso, C. Grimley, W. Henzel, I. Fischer, and P. Levitt. 1995. The limbic system-associated membrane protein is an Ig superfamily member that mediates selective neuronal growth and axon targeting. Neuron. 15:287-97.

Placzek, M., M. Tessier-Lavigne, T. Yamada, T. Jessell, and J. Dodd. 1990. Mesodermal control of neural cell identity: floor plate induction by the notochord. Science. 250:985-8.

Prasad, S.S., L.Z. Kojic, P. Li, D.E. Mitchell, A. Hachisuka, J. Sawada, Q. Gu, and M.S. Cynader. 2002. Gene expression patterns during enhanced periods of visual cortex plasticity. Neuroscience. 111:35-45.

Ranscht, B. 2000. Cadherins: molecular codes for axon guidance and synapse formation. Int J Dev Neurosci. 18:643-51.

Rao, M. 2004. Stem and precursor cells in the nervous system. J Neurotrauma. 21:415-27.

Raper, J.A. 2000. Semaphorins and their receptors in vertebrates and invertebrates. Curr Opin Neurobiol. 10:88-94.

Reed, J., C. McNamee, S. Rackstraw, J. Jenkins, and D. Moss. 2004. Diglons are heterodimeric proteins composed of IgLON subunits, and Diglon-CO inhibits neurite outgrowth from cerebellar granule cells. J Cell Sci. 117:3961-73.

Reed, J.E., J.R. Dunn, D.G. du Plessis, E.J. Shaw, P. Reeves, A.L. Gee, P.C. Warnke, G.C. Sellar, D.J. Moss, and C. Walker. 2007. Expression of cellular adhesion molecule 'OPCML' is down-regulated in gliomas and other brain tumours. Neuropathol Appl Neurobiol. 33:77-85.

Reinoso, B.S., A.F. Pimenta, and P. Levitt. 1996. Expression of the mRNAs encoding the limbic system-associated membrane protein (LAMP): I. Adult rat brain. J Comp Neurol. 375:274-88.

Rohatgi, R., L. Ma, H. Miki, M. Lopez, T. Kirchhausen, T. Takenawa, and M.W. Kirschner. 1999. The interaction between N-WASP and the Arp2/3 complex links Cdc42-dependent signals to actin assembly. Cell. 97:221-31.

Ronn, L.C., V. Berezin, and E. Bock. 2000. The neural cell adhesion molecule in synaptic plasticity and ageing. Int J Dev Neurosci. 18:193-9.

Rothberg, J.M., J.R. Jacobs, C.S. Goodman, and S. Artavanis-Tsakonas. 1990. slit: an extracellular protein necessary for development of midline glia and commissural axon pathways contains both EGF and LRR domains. Genes Dev. 4:2169-87.

Rougon, G., and O. Hobert. 2003. New insights into the diversity and function of neuronal immunoglobulin superfamily molecules. Annu Rev Neurosci. 26:207-38.

Saffell, J.L., E.J. Williams, I.J. Mason, F.S. Walsh, and P. Doherty. 1997. Expression of a dominant negative FGF receptor inhibits axonal growth and FGF receptor phosphorylation stimulated by CAMs. Neuron. 18:231-42.

Sara, Y., T. Biederer, D. Atasoy, A. Chubykin, M.G. Mozhayeva, T.C. Sudhof, and E.T. Kavalali. 2005. Selective capability of SynCAM and neuroligin for functional synapse assembly. J Neurosci. 25:260-70.

Schafer, M., A.U. Brauer, N.E. Savaskan, F.G. Rathjen, and T. Brummendorf. 2005. Neurotractin/kilon promotes neurite outgrowth and is expressed on reactive astrocytes after entorhinal cortex lesion. Mol Cell Neurosci. 29:580-90.

Schofield, P.R., K.C. McFarland, J.S. Hayflick, J.N. Wilcox, T.M. Cho, S. Roy, N.M. Lee, H.H. Loh, and P.H. Seeburg. 1989. Molecular characterization of a new immunoglobulin superfamily protein with potential roles in opioid binding and cell contact. Embo J. 8:489-95.

Seeger, M.A., L. Haffley, and T.C. Kaufman. 1988. Characterization of amalgam: a member of the immunoglobulin superfamily from Drosophila. Cell. 55:589-600.

Sellar, G.C., K.P. Watt, G.J. Rabiasz, E.A. Stronach, L. Li, E.P. Miller, C.E. Massie, J. Miller, B. Contreras-Moreira, D. Scott, I. Brown, A.R. Williams, P.A. Bates, J.F. Smyth, and H. Gabra. 2003. OPCML at 11q25 is epigenetically inactivated and has tumor-suppressor function in epithelial ovarian cancer. Nat Genet. 34:337-43.

Serafini, T. 1997. An old friend in a new home: cadherins at the synapse. Trends Neurosci. 20:322-3.

Serafini, T., S.A. Colamarino, E.D. Leonardo, H. Wang, R. Beddington, W.C. Skarnes, and M. Tessier-Lavigne. 1996. Netrin-1 is required for commissural axon guidance in the developing vertebrate nervous system. Cell. 87:1001-14.

Shapiro, L., and D.R. Colman. 1999. The diversity of cadherins and implications for a synaptic adhesive code in the CNS. Neuron. 23:427-30.

Sharma, P., R. Varma, R.C. Sarasij, Ira, K. Gousset, G. Krishnamoorthy, M. Rao, and S. Mayor. 2004. Nanoscale organization of multiple GPI-anchored proteins in living cell membranes. Cell. 116:577-89.

Simons, K., and E. Ikonen. 1997. Functional rafts in cell membranes. Nature. 387:569-72.

Simons, K., and D. Toomre. 2000. Lipid rafts and signal transduction. Nat Rev Mol Cell Biol. 1:31-9.

Sofroniew, M.V., C.L. Howe, and W.C. Mobley. 2001. Nerve growth factor signaling, neuroprotection, and neural repair. Annu Rev Neurosci. 24:1217-81.

Spaltmann, F., and T. Brummendorf. 1996. CEPU-1, a novel immunoglobulin superfamily molecule, is expressed by developing cerebellar Purkinje cells. J Neurosci. 16:1770-9.

Stein, E., and M. Tessier-Lavigne. 2001. Hierarchical organization of guidance receptors: silencing of netrin attraction by slit through a Robo/DCC receptor complex. Science. 291:1928-38.

Stemple, D.L. 2005. Structure and function of the notochord: an essential organ for chordate development. Development. 132:2503-12.

Struyk, A.F., P.D. Canoll, M.J. Wolfgang, C.L. Rosen, P. D'Eustachio, and J.L. Salzer. 1995. Cloning of neurotrimin defines a new subfamily of differentially expressed neural cell adhesion molecules. J Neurosci. 15:2141-56.

Suter, D.M., and P. Forscher. 2000. Substrate-cytoskeletal coupling as a mechanism for the regulation of growth cone motility and guidance. J Neurobiol. 44:97-113.

Takahashi, T., A. Fournier, F. Nakamura, L.H. Wang, Y. Murakami, R.G. Kalb, H. Fujisawa, and S.M. Strittmatter. 1999. Plexin-neuropilin-1 complexes form functional semaphorin-3A receptors. Cell. 99:59-69.

Takeichi, M. 2007. The cadherin superfamily in neuronal connections and interactions. Nat Rev Neurosci. 8:11-20.

Tamagnone, L., and P.M. Comoglio. 2000. Signalling by semaphorin receptors: cell guidance and beyond. Trends Cell Biol. 10:377-83.

Tamagnone, L., and P.M. Comoglio. 2004. To move or not to move? Semaphorin signalling in cell migration. EMBO Rep. 5:356-61.

Tsui-Pierchala, B.A., M. Encinas, J. Milbrandt, and E.M. Johnson, Jr. 2002. Lipid rafts in neuronal signaling and function. Trends Neurosci. 25:412-7.

van Driel, D., J.M. Provis, and F.A. Billson. 1990. Early differentiation of ganglion, amacrine, bipolar, and Muller cells in the developing fovea of human retina. J Comp Neurol. 291:203-19.

Vogt, A.K., G.J. Brewer, T. Decker, S. Bocker-Meffert, V. Jacobsen, M. Kreiter, W. Knoll, and A. Offenhausser. 2005. Independence of synaptic specificity from neuritic guidance. Neuroscience. 134:783-90.

Wahl, S., H. Barth, T. Ciossek, K. Aktories, and B.K. Mueller. 2000. Ephrin-A5 induces collapse of growth cones by activating Rho and Rho kinase. J Cell Biol. 149:263-70.

Waites, C.L., A.M. Craig, and C.C. Garner. 2005. Mechanisms of vertebrate synaptogenesis. Annu Rev Neurosci. 28:251-74.

Wen, Z., and J.Q. Zheng. 2006. Directional guidance of nerve growth cones. Curr Opin Neurobiol. 16:52-8.

Wilkinson, D.G. 2001. Multiple roles of EPH receptors and ephrins in neural development. Nat Rev Neurosci. 2:155-64.

Wilson, D.J., D.S. Kim, G.A. Clarke, S. Marshall-Clarke, and D.J. Moss. 1996. A family of glycoproteins (GP55), which inhibit neurite outgrowth, are members of the Ig superfamily and are related to OBCAM, neurotrimin, LAMP and CEPU-1. J Cell Sci. 109 (Pt 13):3129-38.

Wilson, L., and M. Maden. 2005. The mechanisms of dorsoventral patterning in the vertebrate neural tube. Dev Biol. 282:1-13.

Yamada, M., T. Hashimoto, N. Hayashi, M. Higuchi, A. Murakami, T. Nakashima, S. Maekawa, and S. Miyata. 2007. Synaptic adhesion molecule OBCAM; synaptogenesis and dynamic internalization. Brain Res. 1165:5-14.

Yamada, S., and W.J. Nelson. 2007. Synapses: sites of cell recognition, adhesion, and functional specification. Annu Rev Biochem. 76:267-94.

Yamagata, M., J.A. Weiner, and J.R. Sanes. 2002. Sidekicks: synaptic adhesion molecules that promote lamina-specific connectivity in the retina. Cell. 110:649-60.

Yazdani, U., and J.R. Terman. 2006. The semaphorins. Genome Biol. 7:211.

Youseff, Sahar. 2006. IgLONs Expression in the developing chick nervous system. PhD thesis Liverpool University.

Zacco, A., V. Cooper, P.D. Chantler, S. Fisher-Hyland, H.L. Horton, and P. Levitt. 1990. Isolation, biochemical characterization and ultrastructural analysis of the limbic system-associated membrane protein (LAMP), a protein expressed by neurons comprising functional neural circuits. J Neurosci. 10:73-90.

Zhou, F.Q., C.M. Waterman-Storer, and C.S. Cohan. 2002. Focal loss of actin bundles causes microtubule redistribution and growth cone turning. J Cell Biol. 157:839-49.

Zhukareva, V., and P. Levitt. 1995. The limbic system-associated membrane protein (LAMP) selectively mediates interactions with specific central neuron populations. Development. 121:1161-72.

Zou, Y. 2004. Wnt signaling in axon guidance. Trends Neurosci. 27:528-32.

Appendix

Diglons are heterodimeric proteins composed of IgLON subunits, and Diglon-CO inhibits neurite outgrowth from cerebellar granule cells

James Reed[1], Christine McNamee[1], Stephen Rackstraw[2], John Jenkins[2] and Diana Moss[1,*]

[1]Department of Human Anatomy and Cell Biology, Liverpool University, Sherrington Buildings, Ashton Street, Liverpool, L69 3GE, UK
[2]Department of Medicine, Liverpool University, Sherrington Buildings, Ashton Street, Liverpool, L69 3GE, UK
*Author for correspondence (e-mail: d.moss@liv.ac.uk)

Accepted 7 April 2004
Journal of Cell Science 117, 3961-3973 Published by The Company of Biologists 2004
doi:10.1242/jcs.01261

Summary

IgLONs are a family of four cell adhesion molecules belonging to the Ig superfamily that are thought to play a role in cell-cell recognition and growth-cone migration. One member of the family, opioid-binding cell-adhesion molecule (OBCAM), might act as a tumour suppressor. Previous work has shown that limbic-system-associated protein (LAMP), CEPU-1/Neurotrimin and OBCAM interact homophilically and heterophilically within the family. Here, we show that, based on their relative affinities, CEPU-1 might be both a homo- and a heterophilic cell adhesion molecule, whereas LAMP and OBCAM act only as heterophilic cell adhesion molecules. A binding assay using recombinant IgLONs fused to human Fc showed that IgLONs are organized in the plane of the membrane as heterodimers, and we propose that IgLONs function predominantly as subunits of heterodimeric proteins (Diglons). Thus, the four IgLONs can form six Diglons. Furthermore, although singly transfected cell lines have little effect on neurite outgrowth, CHO cell lines expressing both CEPU-1 and OBCAM (Diglon-CO) inhibit neurite outgrowth from cerebellar granule cells.

Key words: Cell adhesion, Ig superfamily, Neurite outgrowth, Tumour suppressor gene, GPI anchor, Membrane protein complex

Introduction

Cell adhesion molecules (CAMs) of the Ig superfamily are involved in many cellular processes during development, including regulation of cell proliferation, differentiation and migration (Brummendorf and Lemmon, 2001). Within the nervous system, various members of the Ig superfamily play defined roles in axon growth and guidance, and cell-cell recognition during synapse formation. Many CAMs associate laterally and function in cell surface molecular complexes. For example, L1 can associate with neuropilin-1 to form the Sema3A receptor (Castellani et al., 2000; Castellani et al., 2002), as well as interacting with, and signalling via, the fibroblast growth factor receptor (Walsh and Doherty, 1997). Glycosylphosphatidyl inositol (GPI)-anchored glycoproteins cluster in lipid rafts (Friedrichson and Kurzchalia, 1998; Varma and Mayor, 1998), encouraging their lateral association (Harris and Siu, 2002), and many or all will interact in cis with a transmembrane glycoprotein (Malhotra et al., 1998; Tansey et al., 2000).

IgLONs are a family of four CAMs belonging to the Ig superfamily. Limbic-system-associated protein (LAMP) was the first member to be identified, followed by opioid-binding CAM (OBCAM), Neurotrimin (NTM)/CEPU-1 and Kilon/Neurotractin (Funatsu et al., 1999; Levitt, 1984; Marg et al., 1999; Schofield et al., 1989; Spaltmann and Brummendorf, 1996; Struyk et al., 1995). Each member has been variously characterized in terms of molecular structure, molecular binding interactions, expression and ability to modify neurite outgrowth and cell adhesion. Typically, all four IgLONs consist of three Ig domains and are anchored in the plasma membrane via a GPI anchor. The GPI anchor sequesters them to the detergent-insoluble, cholesterol-rich lipid rafts, and the ability of IgLONs to signal to the interior of the cell will be influenced by this location and their requirement for a transmembrane receptor (Simons and Toomre, 2000). LAMP and CEPU-1 also exist as α and β isoforms, where the β isoform has an additional 11 or 12 amino acids between the third Ig domain and the GPI anchor; the function of this extra peptide is unknown (Brummendorf et al., 1997; Spaltmann and Brummendorf, 1996). The chick orthologue of Kilon can also be found as a two-Ig-domain form (Marg et al., 1999) and, furthermore, there is a secreted isoform of CEPU-1, CEPU-Se, that is missing the GPI anchor entirely (Lodge et al., 2001).

Early experiments indicated that LAMP and NTM/CEPU-1 were homophilic CAMs and, more recently, it has been shown that all IgLONs interact heterophilically within the family (Gil et al., 2002; Lodge et al., 2000; Marg et al., 1999; Zhukareva and Levitt, 1995). Expression of the different members has been examined in the developing nervous system of chick embryos and embryonic and postnatal rats. In general, two or more IgLONs are often expressed within a specific tissue at any particular time, and this is clearly observed in the chick retina, where expression of LAMP, OBCAM and NTM/CEPU-1 has been examined. LAMP and CEPU-1 are found in the outer plexiform layer, whereas LAMP and OBCAM are found in the inner plexiform layer (Lodge et al., 2000). Recently, it has been shown that IgLONs are expressed outside the nervous system,

and one member of the family, OBCAM, might act as a tumour suppressor in ovarian epithelial cancer (Sellar et al., 2003).

The ability of individual members of the IgLON family to modulate neurite outgrowth has been investigated by several groups. In some cases, little or no response has been observed and, in others, moderate enhancement or inhibition has been seen (Gil et al., 1998; Hancox et al., 1997; Lodge et al., 2001; Mann et al., 1998; Marg et al., 1999; McNamee et al., 2002). Interestingly, the most striking results were obtained with GP55, a glycoprotein isolated from adult brain that contains a mixture of all members of the IgLON family (Clarke and Moss, 1994). In this case, complete inhibition of neurite outgrowth from dorsal root ganglion (DRG) and forebrain neurons was seen, and this inhibition was reversed by pertussis toxin, suggesting the involvement of a G-protein-coupled receptor (Clarke and Moss, 1997; Wilson et al., 1996). Nevertheless, experiments with isolated members of the family failed to exert any similar activity (McNamee et al., 2002). One puzzling result obtained from this study was the inability of sympathetic neurons to adhere to LAMP and OBCAM, despite expressing LAMP, CEPU-1 and OBCAM (McNamee et al., 2002). This suggested an incomplete understanding of the molecular interactions of the IgLON family.

In this paper, we have analysed the homo- and heterophilic interactions of three members of the IgLON family. Heterophilic interactions for LAMP and OBCAM have higher affinity than homophilic interactions in trans, and all three IgLONs are shown to interact in cis, suggesting that they act predominantly as subunits of heterodimeric proteins. Furthermore, one dimeric IgLON (Diglon-CO) inhibits neurite outgrowth, reminiscent of the activity of GP55, whereas the IgLON subunits alone have no effect.

Materials and Methods

Materials

Antisera recognizing chicken LAMP, OBCAM and CEPU-1 were described previously (Lodge et al., 2000). α1LAMP-Fc, α2OBCAM-Fc and α2βCEPU-1-Fc (GenBank accession numbers for the respective IgLON sequences are Q98919, Q98892 and Q90773) were prepared either from stably transfected J558L mouse myeloma cells as described previously (Howard et al., 2002) or from calcium-phosphate-mediated transient transfection of HEK 293 human embryonic kidney cells, using methods described elsewhere (Chen and Okayama, 1988). CHO cell lines stably expressing cell surface α1LAMP, α2OBCAM, α2βCEPU-1 and α2CEPU-1 were prepared and cultured as described previously (Lodge et al., 2001).

Immunofluorescence microscopy

CHO cells were live stained with IgLON-Fc or IgLON-specific antisera, essentially as described previously (Lodge et al., 2000). Cells grown on coverslips were incubated at room temperature for 20 minutes in blocking buffer [0.12 M sodium phosphate buffer (pH 7.4), 1% bovine serum albumin (BSA)] containing antisera (1:100) or IgLON-Fc (25 μg ml^{-1}) and binding was detected by incubation with Texas-Red-conjugated anti-human IgG or goat anti-rat IgG (1:100; both from Jackson ImmunoResearch). Average fluorescence intensity of staining was measured using Metamorph (Universal Imaging Corporation), and values were normalized to background and statistics compiled using Excel (Microsoft).

Construction of GFP-tagged IgLON constructs

The plasmid vectors pSlax and pIRES EGFP were gifts from J. Gilthorpe (King's College, London, UK). pOIG and pLIG, plasmid vectors expressing either chicken α1OBCAM (GenBank accession number AF292934) or α1LAMP under the control of a β-actin promoter and enhanced green fluorescent protein (EGFP) downstream of an internal ribosome entry site (IRES) sequence were based on the modified pIRES GFP vector. Polymerase chain reaction (PCR) using the primer pairs: 5′-TGGCTGTCGACCATGGGGGTC-3′ and 5′-ATCAAAAGTCGAGGAGGAGGCG-3′ generated full-length α1OBCAM immediately preceded by an *Nco*I site. Following cloning of the 1046 bp product into pCR®2.1-TOPO (Invitrogen), the α1OBCAM open reading frame was ligated into the shuttle vector pSlax at *Bam*HI and *Nco*I, then subcloned into pIRES GFP at *Cla*I and *Not*I to produce pOIG. Full-length α1LAMP was amplified by PCR using the primer pairs: 5′-AAGCTTGCCATGGTAGCGAGG-GC-3′ and 5′-TCTAGATTAACACTTGCTGAGTAGGC-3′, and the 1032 bp product was cloned into pCR®II-TOPO (Invitrogen). The α1LAMP open reading frame was subcloned directly into pIRES GFP at *Eco*RI and analysed for the correct orientation by restriction enzyme mapping to produce pLIG.

Transient transfection of singly transfected CHO cells

Wild-type or stably transfected IgLON-CHO cells were seeded at 1.5×10^4 cells per well in a 24-well plate, grown overnight and transfected with pLIG or pOIG using FuGENE 6 (Roche) at a 1:3 (weight:volume) ratio according to the manufacturer's instructions. Cells were incubated in the complex for 48 hours and analysed by immunofluorescence microscopy.

Preparation of CEPU-1/OBCAM-expressing CHO cells

α2CEPU-1 was cloned into the plasmid vector pBudCE4.1 (Invitrogen), downstream of the EF-1α promoter at the *Xho*I and *Kpn*I sites to generate pBud(α2C). α2OBCAM was cloned into pBud(α2C), downstream of the CMV promoter at the *Hin*dIII and *Xba*I sites, to produce pBud(α2C-α2O). Wild-type CHO cells were transfected with pBud(α2C-α2O) using FuGENE 6 at a 1:3 (weight:volume) ratio and selected in 400 μg ml^{-1} Zeocin™ (Invitrogen). Colonies were assessed by immunofluorescence microscopy with anti-CEPU-1 and anti-OBCAM antibodies and isolated by two rounds of dilution subcloning. Expression of CEPU-1 and OBCAM was confirmed by dot blots and western blots. Cells were extracted in 20 mM Tris-HCl pH 7.6, 2 mM EGTA, 1% NP-40 and Complete™ (Roche) at 37°C for 15 minutes and centrifuged at 50,000 ***g*** at room temperature for 15 minutes. For dot blots, 2 μl of supernatant was spotted on nitrocellulose and then processed as for a western blot (Lodge et al., 2000).

Neuronal cell culture and adhesion and outgrowth assays

Cerebellar granule cells (CGCs) were prepared from embryonic-day 15 (E15) chick cerebellum, essentially as described (Cambray-Deakin, 1995). Briefly, cerebella were shredded with forceps, incubated with 0.25% trypsin (GIBCO) and the cerebellar pieces were triturated in Hanks' balanced salt solution (HBSS) containing 3 mg ml^{-1} BSA, 0.25% glucose, 1.4 mg ml^{-1} $MgSO_4$, 330 ng ml^{-1} DNase I (Sigma-Aldrich) and 4 mg ml^{-1} soybean trypsin inhibitor (Sigma-Aldrich). Cells were overlaid on a gradient of 4% BSA in HBSS, centrifuged at 180 ***g*** for 5 minutes and plated in CGC culture medium [Dulbecco's modified Eagle's medium containing 5% foetal calf serum (FCS) (HyClone), 2 mM GlutaMAX™-I (GIBCO), 25 mM KCl, 0.9% glucose, 0.1 mg ml^{-1} penicillin, 100 U ml^{-1} streptomycin and 2.5% whole chick embryo extract, prepared as described (Howard and Bronner-Fraser, 1985)]. Neuronal adhesion assays were performed as described previously (McNamee et al., 2002), using 9×10^5 CGC per well. Experiments were carried out in duplicate (4 hours) or triplicate (18 hours), counting blind five randomly chosen

microscope fields (1 mm^2) per coverslip. For neuronal outgrowth assays, wild-type or stably transfected IgLON-CHO cell lines were seeded onto coverslips in a 24-well plate at 2.5×10^5 cells per well and grown to confluence. CGCs at a cell density of 1×10^5 cells per well were plated onto CHO cell monolayers and, after 28-31 hours at 37°C in a 5% CO_2 atmosphere, cells were stained with anti-chicken GAP-43 at 1:500 (Allsopp and Moss, 1989), followed by Texas-Red-conjugated anti-rabbit IgG (1:25; Jackson ImmunoResearch). Triplicate experiments, comprising three coverslips per CHO cell type, were carried out, and the proportion of neurite outgrowth was determined, counting blind at least 100 neurons per coverslip. Neurite lengths from 50 fields per experiment were measured using Metamorph, excluding any neurites less than 10 μm in length, and statistics were compiled and analysed with Excel and SPSS using one-way analysis of variance (ANOVA).

Reverse-transcription PCR

Total RNA was isolated from E16 chick embryo cerebellum using TRIzol® (GIBCO) and cDNA was made using SuperScript™II (Invitrogen) according to the manufacturer's instructions. IgLON transcripts were amplified using the following primer pairs: LAMP, 5′-GGTACAGGGATGACACCAGGAT-3′ and 5′-TGGCATTTGTG-ACTCCCAGCTTGT-3′, 153 bp product; OBCAM, 5′-GTCGGAG-AAGGACTATGGCAACT-3′ and 5′-CACTCCCTTATCAAAAGTC-GAGGA-3′, 190 bp product; CEPU-1, 5′-GACGACAAGCGGCTG-GCTGAA-3′ and 5′-CTTTCTGCTGTGGTGGTCGTGCC-3′, 331 bp product; CEPU-Se, 5′-GACGACAAGCGGCTGGCTGAA-3′ and 5′-CCACTGCACGTCTTGCACAGTG-3′, 242 bp product; and glyceraldehyde-3-phosphate dehydrogenase (GAPDH), 5′-TCCAAG-TGGTGGCCATCAATGATC-3′ and 5′-TTCTGGGCAGCACCTCT-GTCATC-3′, 532 bp product.

Preparation and flow cytometry of IgLON-coated polystyrene beads

Carboxylated fluorescent microparticles (Polysciences) were covalently coupled to 400 μg ml^{-1} protein G (Calbiochem) using the carbodiimide method (Polysciences data sheet 238C) and blocked with 5% ovalbumin at room temperature for 30 minutes with end-to-end mixing. 2.5 μg IgLON-Fc or Ox40-HuIg Fc control protein (gift from S. Marshall-Clarke, Liverpool University, Liverpool, UK) were added to a 20% suspension of microparticles in borate buffer and gently agitated at room temperature for 15 minutes. After sonication to obtain single particles, microparticles were allowed to aggregate for 15 minutes, diluted in FACSFlow™ (Becton Dickinson) and analysed on a FACSVantage™ SE (Becton Dickinson) equipped with a laser configured to 488 nm ultraviolet light (Coherent Enterprise) and a model 127 He/Ne laser tuned to 633 nm (Spectra-Physics). Forward scatter, side scatter, FL1 (Yellow Green beads) and FL4 (Brilliant Blue beads) parameter data were collected. 10,000 events per sample were analysed using CellQuest™ Pro 4.0 (Becton Dickinson). Statistics were analysed with SPSS using one-way ANOVA.

Cell-based ELISA

Wild-type or stably transfected IgLON CHO cell lines were seeded into a 96-well plate at 3×10^4 cells per well and grown for 18 hours at 37°C. Cells were incubated at room temperature for 1 hour in fresh culture medium containing 0 μg ml^{-1}, 0.1 μg ml^{-1}, 1 μg ml^{-1} or 10 μg ml^{-1} chimaeric IgLON-Fc, washed three times in PBS and fixed in 4% paraformaldehyde, 120 mM sucrose for 10 minutes. IgLON-Fc binding was detected by incubation with horseradish-peroxidase-coupled anti-human Fc (1:5000; DAKO) at room temperature for 1 hour. After 30 minutes in the presence of 3,3′,5,5′-tetramethylbenzidine substrate (Sigma-Aldrich), colour development was stopped with 1 M H_2SO_4 and the absorbance read at 450 nm.

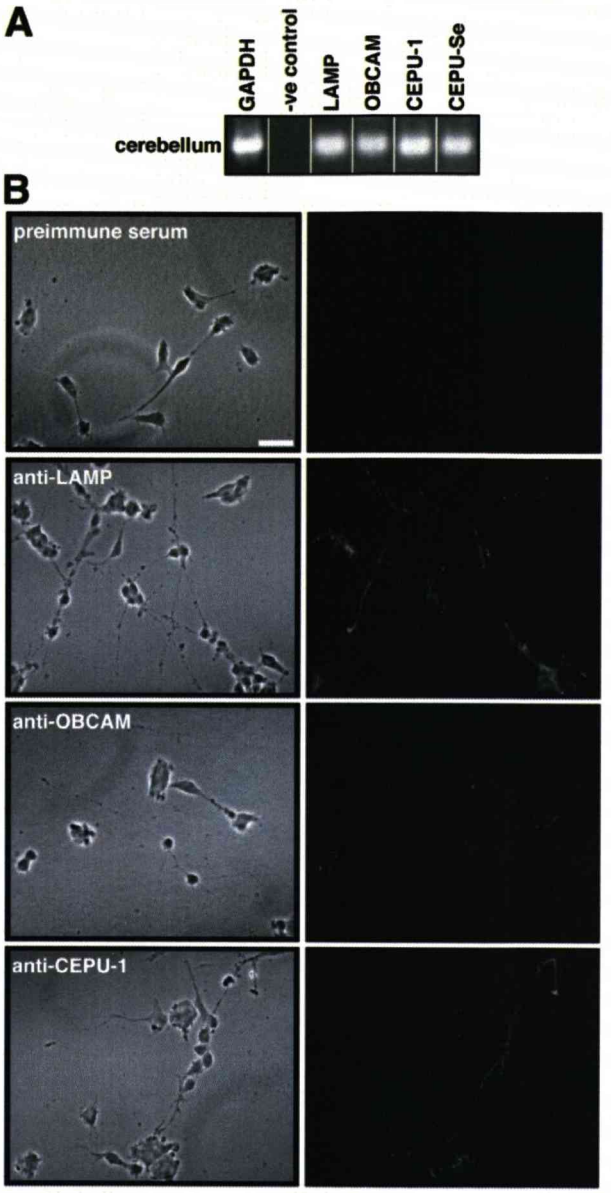

Fig. 1. CGC express LAMP, OBCAM and CEPU-1 on their surface. (A) RT-PCR was carried out on cDNA prepared from E15 cerebellum. Primers were designed to amplify a central region of LAMP and OBCAM occurring in all known isoforms, or to detect CEPU-1 and CEPU-Se, specifically. All three members of the family and both GPI-anchored and secreted forms of CEPU-1 are expressed. (B) Immunofluorescence microscopy of live-stained CGC revealed that LAMP, OBCAM and CEPU-1 are expressed on the cell surface. In all cases, specific punctate staining could be observed. Bar, 25 μm.

Results

LAMP-Fc does not bind to CGCs that express LAMP, OBCAM and CEPU-1

We have shown previously that sympathetic neurons, which express LAMP, OBCAM and CEPU-1, bind only to CEPU-1-Fc in cell adhesion assays (Lodge et al., 2000; McNamee et al.,

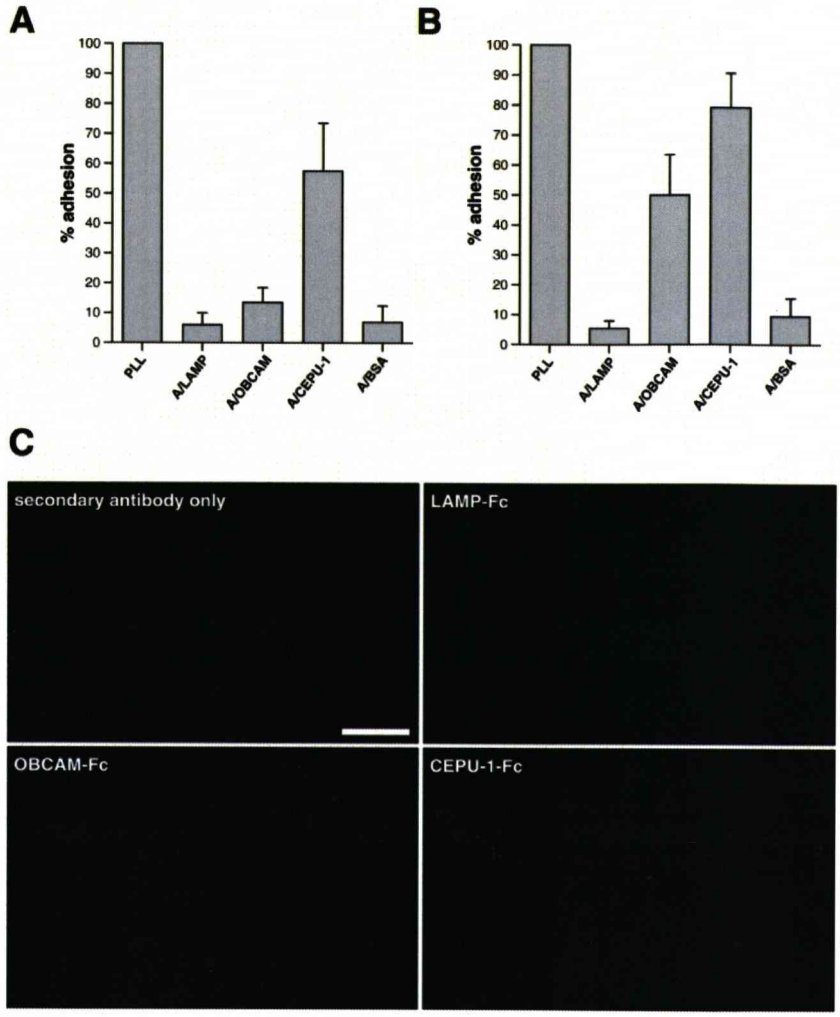

Fig. 2. Recombinant IgLON-Fc proteins show differential interactions with CGCs. CGCs adhere preferentially to CEPU-1-Fc and fail to adhere to LAMP-Fc. Dissociated CGCs were incubated on coverslips sequentially coated with protein A and recombinant IgLON-Fc for (A) 4 hours (n=2) or (B) 18 hours (n=3), and adhering cells were counted. After 4 hours, the number of cells adhering to CEPU-1-Fc was approximately 60% of that adhering to poly-L-lysine and was significantly above background (P<0.0001), whereas adhesion to LAMP and OBCAM was similar to background. After 18 hours, adhesion to CEPU-1-Fc had increased to 80% of the poly-L-lysine control and adhesion to OBCAM-Fc was now 50% of the poly-L-lysine control and significantly above background (P<0.0001). Adhesion to LAMP-Fc remained similar to background. (C) Live staining of CGC with IgLON-Fc revealed a punctate stain with both CEPU-1-Fc and OBCAM-Fc, but LAMP-Fc staining was similar to the secondary antibody alone. In keeping with the adhesion results shown above, the CEPU-1-Fc staining was more intense than that observed with OBCAM-Fc. Bar, 25 μm.

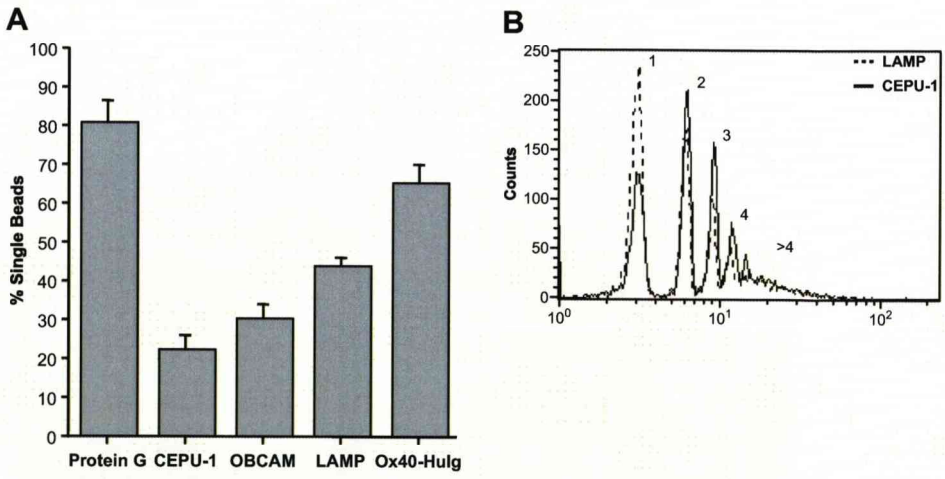

Fig. 3. IgLON homodimers have different binding affinities. Fluorescent beads coupled to protein G coated with recombinant LAMP-Fc, OBCAM-Fc or CEPU-1-Fc were allowed to aggregate for 15 minutes and analysed by flow cytometry. (A) CEPU-1-Fc-coated beads showed the best aggregation, with only 22% of beads remaining single, compared with 30% for OBCAM-Fc and 45% for LAMP-Fc. An unrelated lymphocyte protein Ox40-HuIg Fc gave 68%, and protein-G-coupled beads gave 80% (n=4). CEPU-1 and OBCAM were significantly different from LAMP (P<0.004 and P<0.04, respectively). (B) CEPU-1-Fc-coated beads formed larger aggregates than LAMP-Fc-coated beads. The number of single CEPU-1-Fc beads was small compared with single LAMP beads, and the number of CEPU-1 aggregates with three or more beads was much larger.

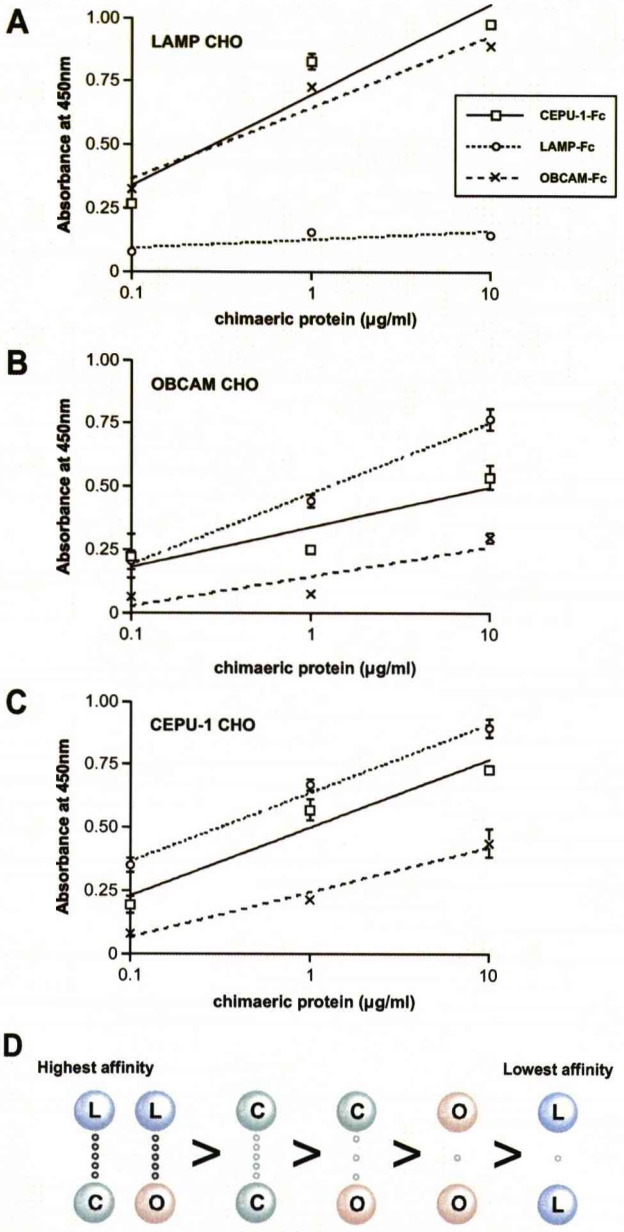

Fig. 4. LAMP binds with highest affinity to OBCAM and CEPU-1. CHO cell lines were grown in 96-well plates and incubated with varying concentrations of chimaeric proteins. (A) For LAMP-CHO, strong binding was observed with OBCAM-Fc and CEPU-1-Fc, both of which displayed almost identical absorbance for each concentration tested. However, with LAMP-Fc, the absorbance remained at background levels, even at 10 μg ml^{-1}. (B) For OBCAM-CHO, highest absorbance values were observed with LAMP-Fc at 10 μg ml^{-1} (~0.75), as predicted by the previous result. The next highest was CEPU-1-Fc at 10 μg ml^{-1} (~0.35) and the lowest was OBCAM-Fc at 10 μg ml^{-1} (~0.2). (C) For CEPU-CHO, highest absorbance was observed with LAMP-Fc at 10 μg ml^{-1} (~0.8), followed by CEPU-1-Fc at 10 μg ml^{-1} (~0.7) and the lowest was OBCAM-Fc at 10 μg ml^{-1} (~0.35), as expected. Error bars lie within the symbol for some points. (D) Taking together the relative affinities of the homophilic interactions from Fig. 3 and the comparative affinity of the homo- and heterophilic interactions, we propose this hierarchy for the relative affinity of IgLON interactions in trans.

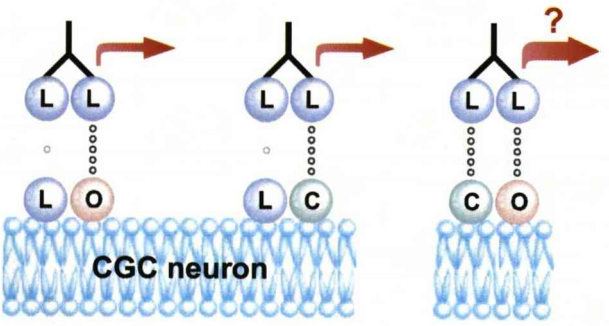

Fig. 5. Do IgLONs form heterodimers in cis? We propose that IgLONs preferentially form heterodimers on the surface of neurons. The homodimeric IgLON-Fc proteins might not bind to the heterodimers because dimerization induces a conformational change that interferes with binding, because of steric hindrance or because the affinity of one head to one of the heterodimeric subunits is too low to stabilize the complex.

2002). This result had no obvious explanation. To confirm and extend this finding, we tested whether CGC also show a similar discrepancy in their interactions with members of the IgLON family. CGCs express LAMP, OBCAM and CEPU-1 as shown by reverse-transcription PCR (RT-PCR), and immunofluorescence staining revealed that all three are located on their surface (Fig. 1). Nevertheless, cell adhesion assays showed that CGCs bound well to CEPU-1-Fc and only weakly to LAMP-Fc at both 4 hours and 18 hours (Fig. 2A,B). The initial adhesion to OBCAM-Fc at 4 hours was relatively low, but this improved with time and approached the activity of CEPU-1-Fc after 18 hours (Fig. 2B). To investigate whether the relative affinity of protein-protein interactions between the different IgLON molecules varied, the ability of the chimaeric proteins to bind to the surface of CGCs was tested. Although weaker than binding with antibody, both CEPU-1-Fc and OBCAM-Fc binding was observed, but LAMP-Fc binding to the surface of CGC was not detectable (Fig. 2C). This latter experiment strongly suggested that the difference in cell adhesion is primarily due to variations in protein binding rather than indirect effects.

Differential affinity of homophilic interactions

The unexpected interactions between the recombinant chimaeric proteins and neurons suggested an incomplete understanding of the molecular complexes formed by this family, and prompted a comparison of the relative affinity of the homophilic interactions of LAMP, OBCAM and CEPU-1. Recombinant IgLONs attach to protein-G-coupled fluorescent polystyrene beads by their Fc tail, leaving both IgLON heads available for binding. Aggregation experiments showed that CEPU-1-Fc interacted with higher affinity, because fewer single beads were observed (Fig. 3). LAMP-Fc had the lowest affinity for itself as judged by the larger number of single beads (Fig. 3A) and smaller size of the aggregated beads (Fig. 3B),

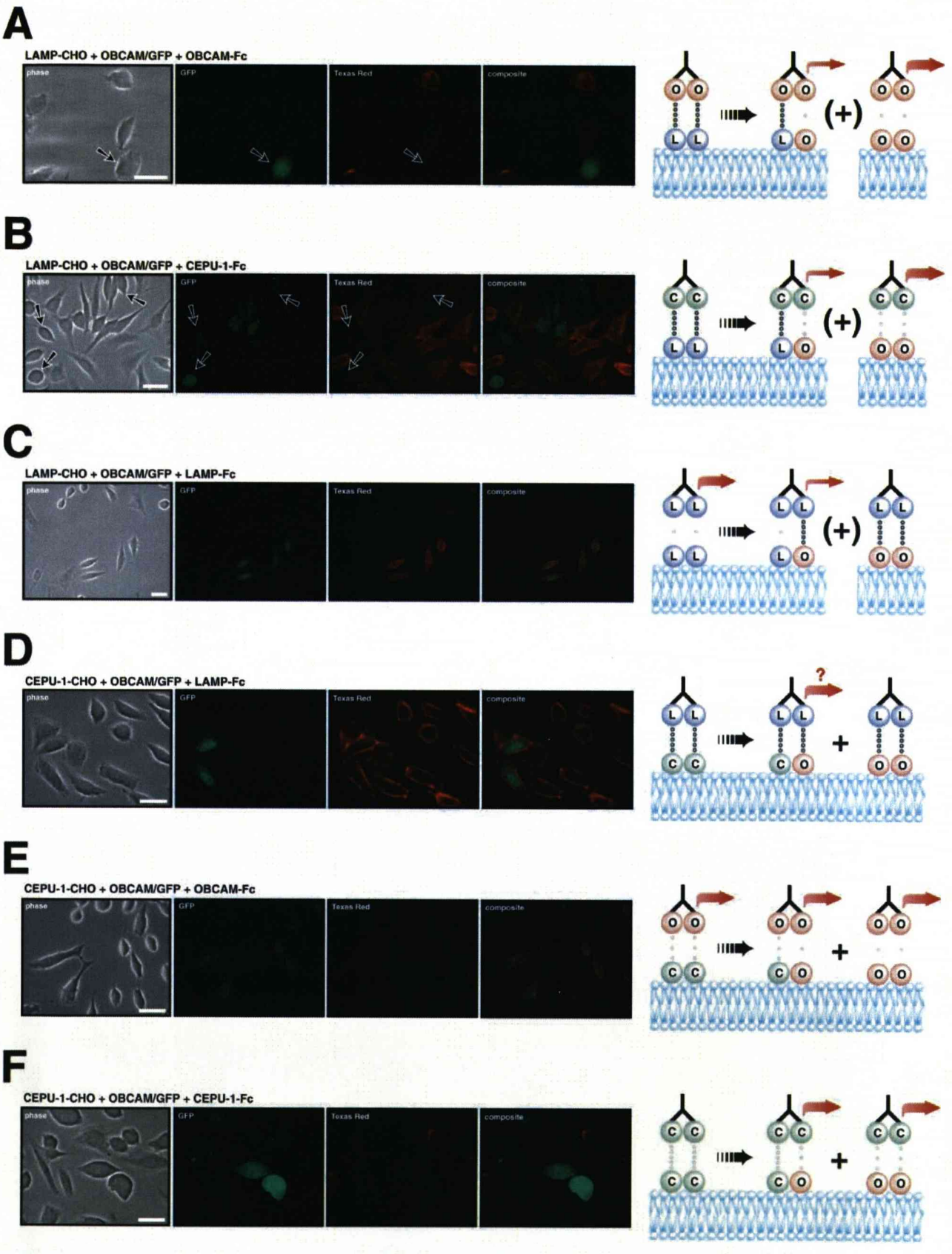
A
LAMP-CHO + OBCAM/GFP + OBCAM-Fc
phase
GFP
Texas Red
composite
(+)
B
LAMP-CHO + OBCAM/GFP + CEPU-1-Fc
phase
GFP
Texas Red
composite
(+)
C
LAMP-CHO + OBCAM/GFP + LAMP-Fc
phase
GFP
Texas Red
composite
(+)
D
CEPU-1-CHO + OBCAM/GFP + LAMP-Fc
phase
GFP
Texas Red
composite
?
+
E
CEPU-1-CHO + OBCAM/GFP + OBCAM-Fc
phase
GFP
Texas Red
composite
+
F
CEPU-1-CHO + OBCAM/GFP + CEPU-1-Fc
phase
GFP
Texas Red
composite
+

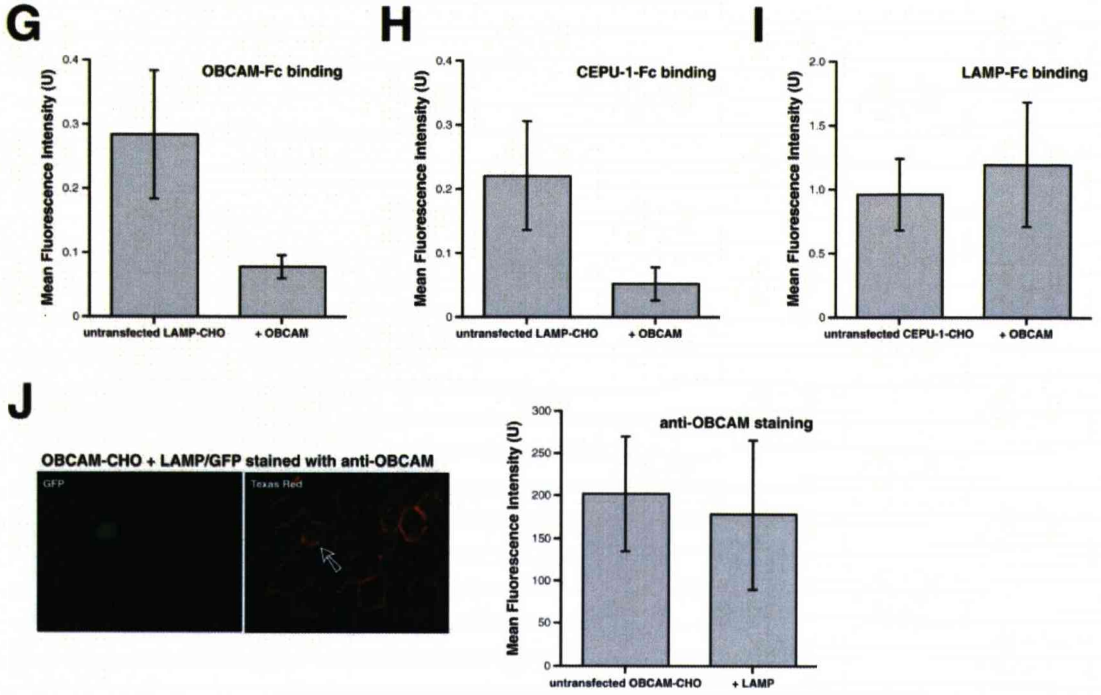

Fig. 6. Heterodimeric proteins form on the surface of CHO cells expressing both LAMP and OBCAM. CHO cells stably expressing LAMP or CEPU-1 were transiently transfected with pOIG. Cells were stained with LAMP-Fc, OBCAM-Fc or CEPU-1-Fc. (A) LAMP-CHO cells bound OBCAM-Fc with high affinity but, when OBCAM was expressed, staining was specifically reduced (arrow). Non-transiently transfected cells have either LAMP monomers or dimers on their cell surface but, after expression of OBCAM, LAMP is sequestered by OBCAM in heterodimers. OBCAM:LAMP heterodimers no longer stabilize OBCAM-Fc binding. If OBCAM expression exceeds LAMP expression then OBCAM monomers or dimers will also be available, but these will similarly fail to stabilize OBCAM-Fc binding. (B) LAMP-CHO cells bound CEPU-1-Fc with high affinity but, when OBCAM was expressed, staining was specifically reduced (arrow). CEPU-1-Fc binds well to cells expressing only LAMP, but binding is destabilized by the introduction of OBCAM and the subsequent incorporation of LAMP into LAMP:OBCAM dimers. (C) LAMP-CHO cells bound LAMP-Fc very weakly, but expression of OBCAM increased LAMP-Fc binding owing to greater retention of LAMP-Fc by the LAMP:OBCAM dimers (compared with LAMP homodimers) and perhaps the presence of free OBCAM, which would bind LAMP-Fc with relatively high affinity. Introduction of OBCAM into CEPU-1-CHO cells resulted in little change in fluorescence intensity. (D) LAMP-Fc bound with similar (high) affinity to CEPU-1-CHO and to the OBCAM:OBCAM dimers that might form. However, it is unclear from this experiment whether CEPU-1:OBCAM dimers also form and whether LAMP-Fc can interact with them. Intense fluorescence staining of all cells was observed. (E) OBCAM-Fc and (F) CEPU-1-Fc stained CEPU-1-CHO cells less intensely than LAMP-Fc but, again, OBCAM expression did not change the intensity of fluorescence staining. It is important that, in these last three experiments, transient transfection of OBCAM cDNA was insufficient on its own to change the ability of the chimaeric proteins to bind. For all cases, expression of EGFP alone did not alter IgLON binding. Bar, 25 μm. The fluorescence intensity of untransfected and pOIG-transfected LAMP-CHO cells was quantified. Transfection of OBCAM significantly reduced the binding of (G) OBCAM-Fc or (H) CEPU-1-Fc as judged by the reduction in fluorescence intensity. (I) The fluorescence intensity of untransfected and pOIG-transfected CEPU-1-CHO cells was quantified. Transfection of OBCAM did not significantly alter the binding of LAMP-Fc as judged by fluorescence intensity. (J) The expression of OBCAM on pLIG-transfected CHO cells was unchanged as judged by immunofluorescence staining with antisera to OBCAM.

whereas OBCAM-Fc gave intermediate values. These results mirrored the ability of the chimaeric proteins to bind to the surface of CGCs and sympathetic neurons. Nevertheless, they do not provide an adequate explanation for why LAMP-Fc does not bind to the surface of neurons, because both CEPU-1 and OBCAM are expressed and should be available to bind LAMP-Fc. This prompted us to examine the heterophilic interactions of members of the IgLON family.

Some heterophilic interactions predominate over homophilic interactions (in trans)

To quantify the relative affinity of the homo- and heterophilic interactions, we used a cell-based ELISA assay (Fig. 4). These experiments demonstrated that LAMP bound with highest affinity to OBCAM and CEPU-1 (Fig. 4B,C). By contrast, the OBCAM/CEPU-1 heterophilic complexes were less stable than the heterophilic complexes involving LAMP (Fig. 4B,C). The homophilic interactions of both OBCAM and LAMP were weak (Fig. 4A,B), whereas CEPU-1/CEPU-1 homophilic interactions had relatively high affinity (Fig. 4C), confirming the results obtained from the bead aggregation experiments. It is unclear why CEPU-1/CEPU-1 interactions should have higher affinity than other homophilic interactions, but the recombinant CEPU-1 used in these experiments includes the β exon (whereas the LAMP used was the α isoform), so βCEPU-1 might have a role as a homophilic CAM as well as a heterophilic CAM. It remains to be seen whether this is due to

the β exon or whether CEPU-1 is different in this respect from LAMP and OBCAM. Taken together, these experiments revealed a hierarchy for the homo- and heterophilic interactions as shown in Fig. 4D.

IgLONs form dimers in the plane of the membrane

Nevertheless, this hierarchy of binding does not explain the original observation that LAMP-Fc binds weakly or not at all to CGCs and sympathetic and DRG neurons (McNamee et al., 2002). Even though LAMP-Fc does not bind well to itself, it is clear that LAMP-Fc should bind well to CEPU-1 and OBCAM, which are both present on the surface of CGC. To explain our observations, we need to consider the possible interactions between IgLONs in the plane of the membrane. It has been shown previously that NTM/CEPU-1 will form homodimers in the plane of the membrane (Struyk et al., 1995). We have also observed the formation of homodimers and homotetramers for LAMP and OBCAM, as well as CEPU-1, when cells are confluent (data not shown). We suggest that the tetramers are formed from two pairs of homodimers that have formed in cis, and that these dimers then interact in trans. Thus, in response to external stimuli, all three IgLONs form homodimers and tetramers. When two or more IgLONs are expressed, is it possible that heterophilic dimers might form in cis? And, if so, does this explain why LAMP-Fc does not bind to the neuronal cell surface (Fig. 5)?

Do IgLONs form heterodimers in cis?

This question was investigated by transiently transfecting OBCAM or LAMP into CHO cell lines already expressing one IgLON. The dimeric recombinant proteins were used to detect the presence of monomers that are available to form homodimers (Fig. 6). In the first series of experiments, OBCAM was transiently transfected into LAMP-CHO cells. LAMP monomers and dimers bind OBCAM-Fc with high affinity, whereas OBCAM monomers and dimers bind OBCAM-Fc with low affinity. Crucially, we propose that OBCAM:LAMP heterodimers will also fail to bind OBCAM-Fc owing to their lower affinity for one head, steric hindrance or conformational changes. Thus, OBCAM-Fc can be used to determine whether LAMP monomers or dimers remain available after expression of OBCAM, or whether they are irreversibly sequestered into LAMP:OBCAM dimers. When OBCAM was transiently transfected into LAMP-CHO cells, OBCAM-Fc binding was substantially reduced, a result that can only be accounted for by the irreversible sequestration of LAMP into LAMP:OBCAM dimers (Fig. 6A,G). LAMP expression on the surface of the cells was unchanged by the expression of OBCAM, as judged by immunofluorescence staining with LAMP antisera (data not shown). Likewise, the binding of CEPU-1-Fc was reduced by the introduction of OBCAM (Fig. 6B,H). Again, the formation of LAMP:OBCAM dimers in cis results in the destabilization of the tetrameric complex formed with CEPU-1-Fc, owing to failure of the homodimeric protein to bind to the heterodimer. By contrast, LAMP-Fc binding increased when OBCAM was co-expressed (Fig. 6C), probably owing to overexpression of OBCAM compared with the LAMP already present on the cell surface.

When OBCAM was expressed in CEPU-1-CHO cells, no substantial change in the binding of LAMP-Fc, CEPU-1-Fc or OBCAM-Fc was observed. Because the affinity of all three chimaeric proteins is similar for both CEPU-1 and OBCAM, this experiment does not demonstrate clearly whether CEPU-1:OBCAM dimers form. However, the increase in overall IgLON concentration owing to the transient expression of OBCAM does not cause a detectable change (Fig. 6D-F,I), supporting our hypothesis that the differences in fluorescence intensity seen with other combinations are caused by the formation of heterodimers and not by changes in the overall level of IgLON expression. The expression of a second IgLON and GFP does not appreciably affect the expression of the first, as shown by staining OBCAM-CHO cells, transiently expressing LAMP and GFP, with OBCAM antisera (Fig. 6J).

To confirm the formation of LAMP:OBCAM dimers and test for the formation of LAMP:CEPU-1 dimers, we repeated these experiments but transiently transfected LAMP into OBCAM-CHO and CEPU-1-CHO cells. Similar results to those observed in Fig. 6 were obtained (Fig. 7). The expression of LAMP in OBCAM-CHO cells destabilized LAMP-Fc binding, again suggesting that LAMP dimerizes with OBCAM in cis (Fig. 7A). Similarly, expression of LAMP in CEPU-1-CHO cells destabilized LAMP-Fc binding, providing evidence for the formation of LAMP:CEPU-1 dimers in cis (Fig. 7B). In both cases, LAMP expression enhanced binding of OBCAM-Fc and CEPU-1-Fc probably because of overexpression of LAMP compared with CEPU-1 or OBCAM (Fig. 7C,D). In conclusion, these experiments provide evidence for the formation of LAMP:OBCAM and LAMP:CEPU-1 heterodimers in cis, suggesting that each IgLON protein is a subunit of a heterodimeric glycoprotein formed from two GPI-anchored polypeptide chains.

It cannot be determined from these experiments whether CEPU-1:OBCAM dimers in cis are also formed. Therefore, we prepared CHO cell lines stably expressing both αCEPU-1 and OBCAM (CO-CHO). CO-CHO cells expressed both OBCAM and CEPU-1, as shown by immunofluorescence and dot blots (data not shown). We tested the ability of these cells to modify neurite outgrowth from CGCs compared with the CHO cells expressing αCEPU-1, βCEPU-1 or OBCAM alone. Outgrowth on wild-type or LAMP-, OBCAM- and αCEPU-1- or βCEPU-1- expressing CHO cells varied between 28.6% and 34.6%, and the differences were not statistically significant. Outgrowth on the CO-CHO cells was 17.4%, a reduction of 45% from the average of the αCEPU-1-CHO and OBCAM-CHO values, respectively (Fig. 8A). Thus, co-expression of CEPU-1 and OBCAM on CHO cells resulted in activity not seen with either alone. We propose that CEPU-1:OBCAM dimers are the functional molecule, and their ability to inhibit neurite outgrowth is reminiscent of the activity originally observed with the mixture of IgLONs (GP55) (Clarke and Moss, 1994; Wilson et al., 1996).

Although initiation of neurite outgrowth is blocked in some CGCs, approximately 17% do still extend neurites. To test whether neurite extension is affected by CEPU-1:OBCAM dimers in these neurons, we compared the lengths of the neurites grown on wild-type, CEPU-1-CHO, OBCAM-CHO and CO-CHO cells. CEPU-1-CHO and CO-CHO cells showed a small reduction in neurite length compared with the wild type, and neurites on OBCAM-CHO cells were slightly longer (Fig. 8B). Nevertheless, these differences are small and the

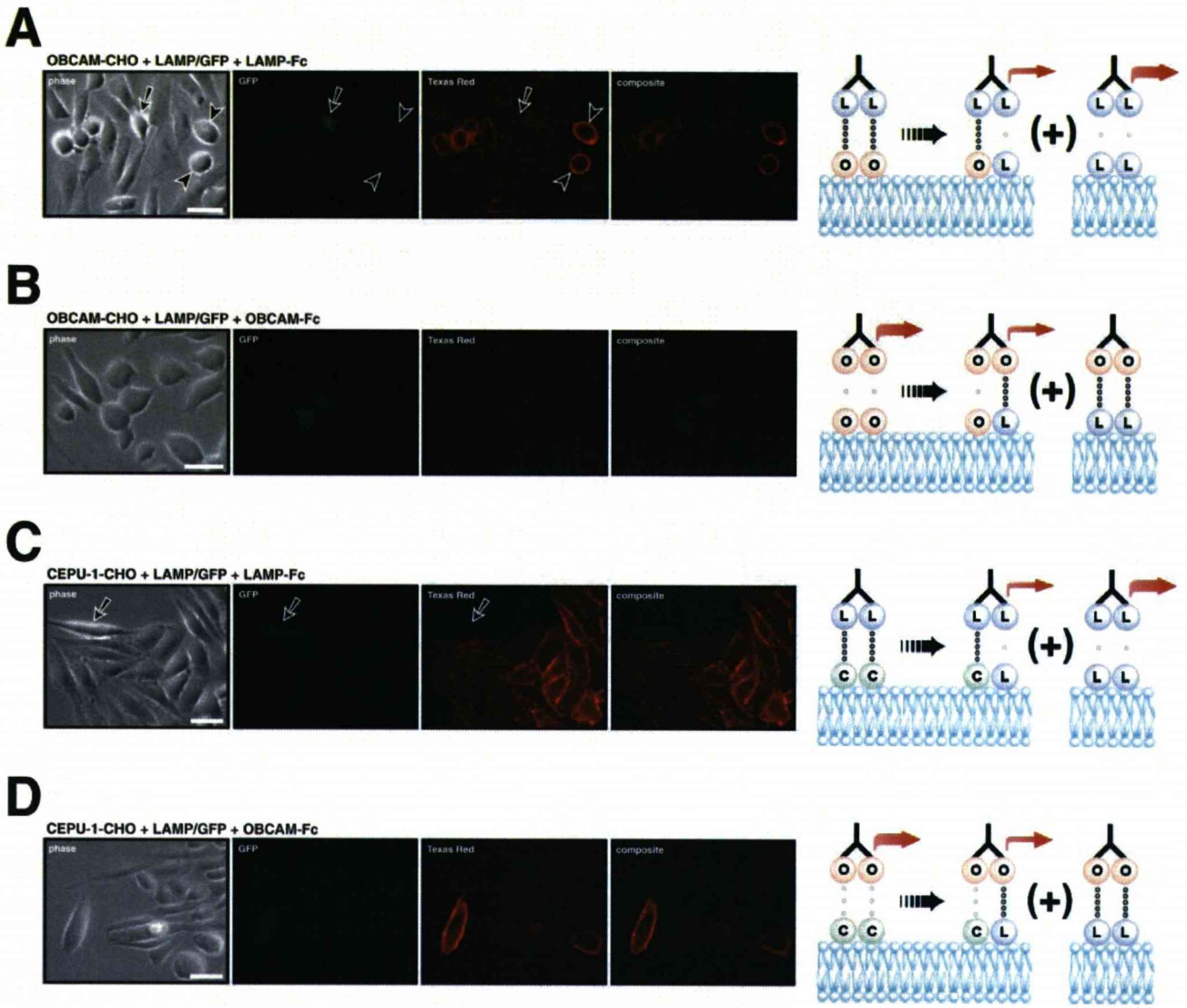

Fig. 7. Heterodimeric proteins form on the surface of CHO cells expressing LAMP and either OBCAM or CEPU-1. (A) Expression of LAMP in OBCAM-CHO cells destabilized the surface binding of LAMP-Fc. The arrowed cell, identified by GFP fluorescence, showed essentially no staining for LAMP-Fc despite its rounded, phase-bright morphology. Notice cells indicated with arrowheads that were also phase bright and stained intensely with LAMP-Fc. Expression of LAMP on the cell surface results in sequestration of free OBCAM into LAMP:OBCAM dimers, leaving no detectable OBCAM monomers or homodimers. (B) Expression of LAMP in OBCAM-CHO cells produced a small increase in fluorescence intensity when stained with OBCAM-Fc, possibly owing to increased affinity for LAMP:OBCAM dimers or overexpression of LAMP. Similar results were observed for CEPU-1-Fc (data not shown). (C) Expression of LAMP in CEPU-1-CHO cells also resulted in loss of LAMP-Fc binding (arrow). This is explained by the formation of LAMP:CEPU-1 dimers in cis, which destabilizes the binding of LAMP-Fc. (D) OBCAM-Fc binding increased as a result of LAMP expression, again because of the greater affinity of OBCAM-Fc for the heterodimer and/or the overexpression of LAMP. Similar results were observed for CEPU-1-Fc (data not shown). Bar, 25 μm.

most striking activity of the CEPU-1:OBCAM dimer is the inhibition of neurite outgrowth from a subpopulation of CGCs.

Based on affinity, LAMP dimers should interact with CEPU-1:OBCAM dimers. Surprisingly, LAMP-Fc did not bind to the CO-CHO cells in the cell-based ELISA any better than to the LAMP-CHO cells, and binding was significantly worse than to the CEPU-1-CHO or OBCAM-CHO cells (Fig. 8C). This provides further evidence that CEPU-1 and OBCAM exist principally as heterodimers on the surface of the CHO cells and suggests that, upon dimerization, one or both subunits either have their binding site for LAMP obscured or adopt a different conformation. In conclusion, CEPU-1:OBCAM dimers might also exist on the surface of CGC, but LAMP-Fc binding is not stabilized.

Discussion

We started with the observation that recombinant LAMP-Fc

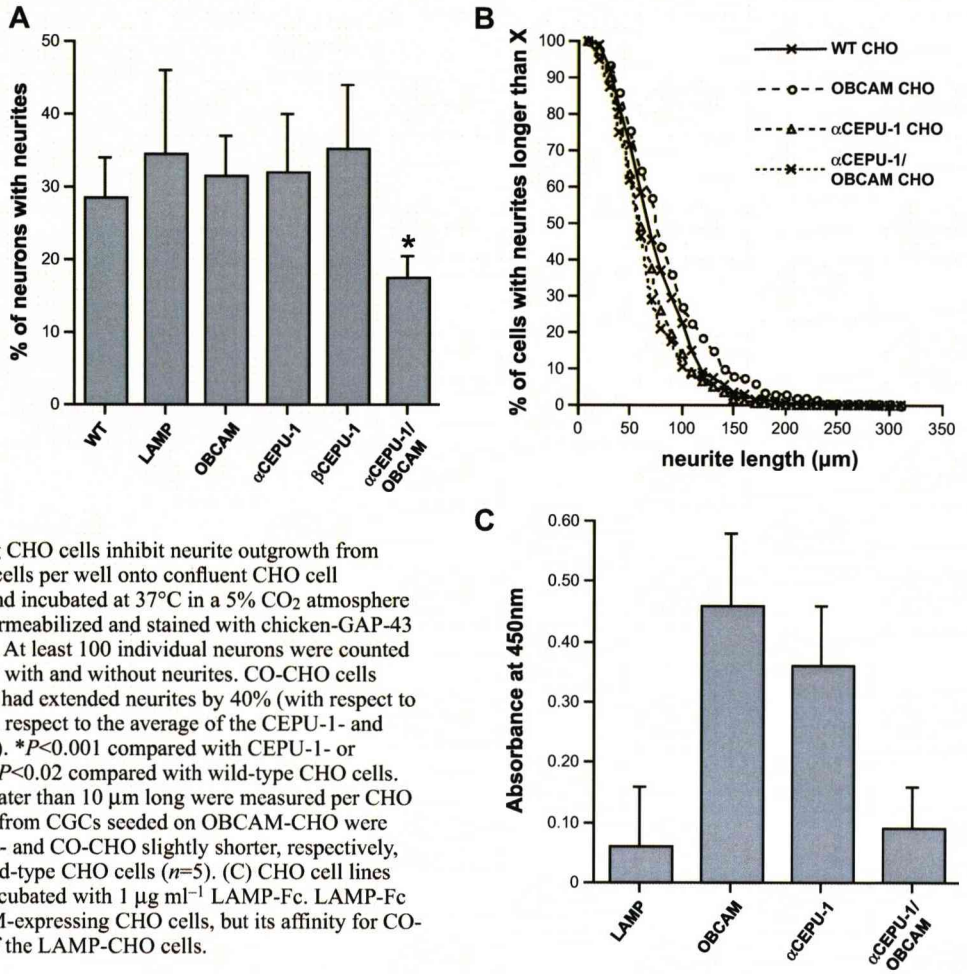

Fig. 8. CEPU-1/OBCAM-expressing CHO cells inhibit neurite outgrowth from CGCs. CGCs were seeded at 1×10^5 cells per well onto confluent CHO cell monolayers growing on coverslips and incubated at 37°C in a 5% CO_2 atmosphere for 28-31 hours. Cells were fixed, permeabilized and stained with chicken-GAP-43 antibody to identify the neurons. (A) At least 100 individual neurons were counted per coverslip, comparing the number with and without neurites. CO-CHO cells inhibited the number of neurons that had extended neurites by 40% (with respect to wild-type CHO cells) and 45% (with respect to the average of the CEPU-1- and OBCAM-expressing cell lines) (n=5). *P<0.001 compared with CEPU-1- or OBCAM-expressing CHO cells and P<0.02 compared with wild-type CHO cells. (B) At least 220 random neurites greater than 10 μm long were measured per CHO cell line using Metamorph. Neurites from CGCs seeded on OBCAM-CHO were slightly longer and those on CEPU-1- and CO-CHO slightly shorter, respectively, than those from CGCs seeded on wild-type CHO cells (n=5). (C) CHO cell lines were grown in a 96-well plate and incubated with 1 μg ml^{-1} LAMP-Fc. LAMP-Fc bound well to CEPU-1- and OBCAM-expressing CHO cells, but its affinity for CO-CHO cells was comparable to that of the LAMP-CHO cells.

does not bind to the surface of neurons. This was contrary to predictions based on previous studies that showed homo- and heterophilic binding of almost all members of the family. This prompted careful analysis of the relative affinities of both homo- and heterophilic IgLON interactions in trans and allowed us to generate a hierarchy in which LAMP/CEPU-1 and LAMP/OBCAM interactions have the highest affinity. Heterophilic interactions between CEPU-1 and OBCAM have lower affinity, falling between those observed for the homophilic interactions CEPU-1/CEPU-1 and OBCAM/OBCAM. LAMP/LAMP shows the lowest affinity of any combination tested. These experiments used αLAMP and βCEPU-1, and it remains to be determined whether the inclusion of the β exon modifies either homo- or heterophilic interactions for LAMP or CEPU-1. It is interesting that initial studies of chick Kilon (Neurotractin) described heterophilic interactions between Kilon and CEPU-1, whereas Kilon/LAMP interactions were considerably weaker and no evidence for homophilic interactions of Kilon was presented (Marg et al., 1999). In addition, recent chemical cross-linking experiments on rat cerebral cortex provide evidence for Kilon-OBCAM heterophilic complexes (Miyata et al., 2003). Thus, homophilic interactions of OBCAM, LAMP and Kilon appear to be relatively unimportant compared with their heterophilic interactions, and only CEPU-1 (Neurotrimin) might act as a homophilic CAM.

The key conclusion of this paper is that IgLONs form and function as heterophilic dimers in the plane of the membrane. We propose that each IgLON protein is predominantly a subunit of a heterodimeric adhesion molecule (Fig. 9). For simplicity, we have termed the heterodimeric proteins 'Diglons' (dimeric IgLONs) and the different potential combinations are shown. We used the homodimeric recombinant proteins to assay the formation of some heterodimers [i.e. LAMP:OBCAM (Diglon-LO) and LAMP:CEPU-1 (Diglon-LC)] in the plane of the membrane. When LAMP is introduced into the OBCAM-CHO cells (by transient transfection), OBCAM:LAMP dimers form and LAMP-Fc binding is no longer stabilized. These results suggest there is little free OBCAM available to form homodimers and that LAMP:OBCAM dimers are sufficiently stable to prevent LAMP-Fc from sequestering the OBCAM. The conclusion is that heterodimers form in the absence of external stimuli such as cell-cell interactions and despite the addition of chimaeric proteins that would otherwise stimulate the formation of homodimers. Furthermore, LAMP-Fc is unable to form a stable complex by cross-linking OBCAM from two different LAMP:OBCAM dimers. Similar

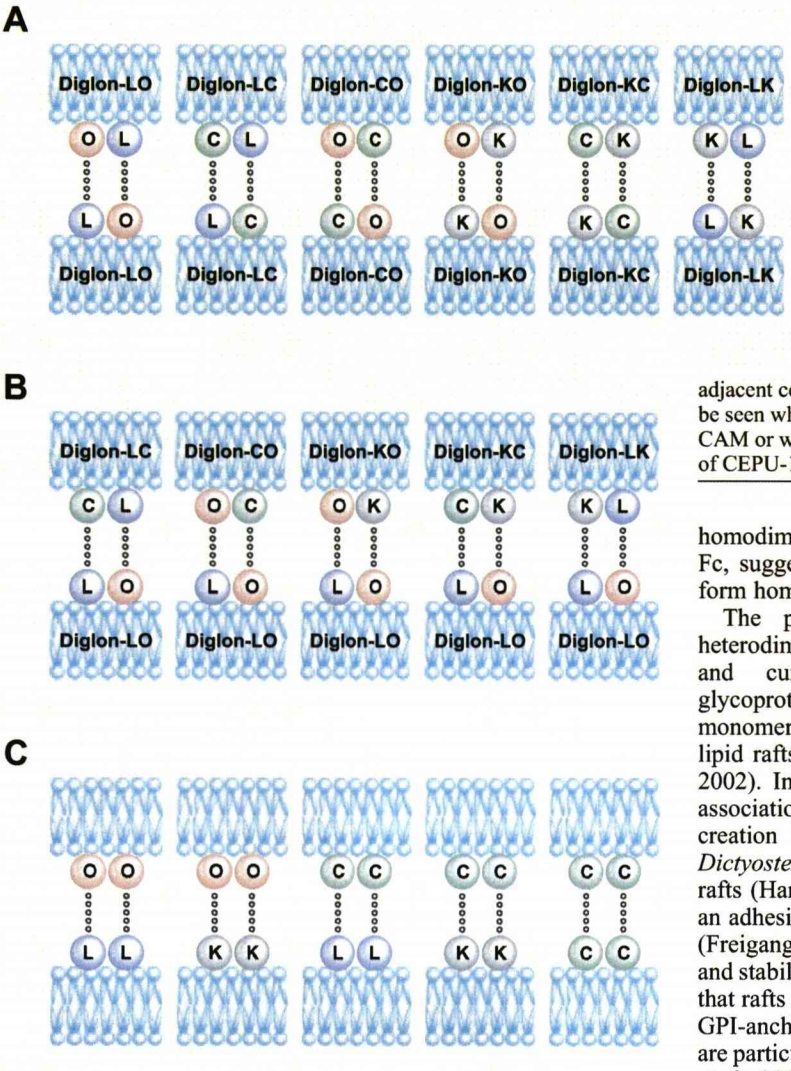

Fig. 9. Proposed IgLON and Diglon CAMs. We have shown that LAMP associates in cis with either OBCAM or CEPU-1, and that CEPU-1 and OBCAM also associate in cis; we also propose that the same combinations might be possible for Kilon. (A) The proposed dimeric IgLONs (Diglons). (B) Diglon-LO might, in principle, bind to one or more of the other Diglons. (C) It is unclear whether IgLONs will also function as independent CAMs; this will be the case if cells express only one member of the family or unequal amounts of two or more IgLONs. Based on the results presented here, the most likely combinations are shown. LAMP and OBCAM are unlikely to function as homophilic CAMs, but a cell expressing only LAMP will adhere effectively to an adjacent cell expressing only OBCAM or CEPU-1. It remains to be seen whether CEPU-1 is unique in acting as a homophilic CAM or whether this is an activity restricted to the minor isoforms of CEPU-1 (and LAMP) that have a β exon.

experiments revealed the formation of LAMP:CEPU-1 dimers. It was not possible to determine whether CEPU-1:OBCAM dimers form using this approach, but a cell line expressing both IgLONs inhibited neurite outgrowth from CGC, an activity not seen with either molecule alone. Previous experiments in which DRG neurons were grown on a mixture of LAMP-, OBCAM- and CEPU-1-Fc proteins combined with laminin also showed no inhibitory activity (McNamee et al., 2002). This suggests that simply mixing CEPU-1 and OBCAM together, without the option of forming dimers, is insufficient to generate activity. Furthermore, LAMP-Fc failed to bind to the CO-CHO cells, a result best explained by the formation of a heterodimer. We have not tested the ability of Kilon to form heterodimers in cis but, based on the information about its trans interactions, we suggest that Kilon will also form heterodimers with CEPU-1, LAMP and OBCAM. We can now explain why LAMP and OBCAM-Fc do not bind detectably to the surface of neurons. LAMP-Fc will not bind to Diglon-LO, -LC or -CO, presumably because of steric hindrance or conformational changes. We propose that LAMP-Fc will not bind to Diglon-KO, -KC and -LK for similar reasons. Thus, the only homodimeric protein that does bind to neurons is CEPU-1-Fc, suggesting that CEPU-1 might be the only IgLON to form homodimers.

The proposal that GPI-anchored proteins form a heterodimeric membrane protein is novel. Previous work and current theories suggest that GPI-anchored glycoproteins are introduced into the plasma membrane as monomers, possibly in lipid shells, which then cluster in lipid rafts (Anderson and Jacobson, 2002; Harris and Siu, 2002). In some cases, this clustering can result in lateral associations, leading to dimer formation and the subsequent creation of higher-order oligomeric complexes. The *Dictyostelium* adhesion molecule gp80 oligomerizes in lipid rafts (Harris et al., 2001), and axonin-1 is thought to form an adhesion lattice by homophilic cis and trans interactions (Freigang et al., 2000; Kunz et al., 2002). The typical size and stability of lipid rafts is contentious, but recent proposals that rafts are less than 5 nm in size and contain three to four GPI-anchored proteins of more than one molecular species are particularly interesting and fit well with our data (Sharma et al., 2004). Axonin-1/TAG-1 also forms interactions in cis with the transmembrane glycoproteins NgCAM (Kunz et al., 1998) and L1 (Malhotra et al., 1998), and this is a common theme, because it provides a mechanism for GPI-anchored glycoproteins to signal intracellularly (Castellani et al., 2002; Malhotra et al., 1998; Olive et al., 1995; Tansey et al., 2000). In these cases, it is not clear whether the binding partner is selected on the cell surface depending on the partners expressed and/or in response to external stimuli. Our evidence raises the possibility that IgLONs might form into heterodimeric proteins in vesicles before arrival at the cell surface, and the option to form homodimers is unavailable.

In early experiments, GP55 inhibited the initiation of neurite outgrowth from 100% of DRG neurons. GP55 consisted of a mixture of all the IgLONs in adult chick brain, so it is likely that all the Diglons were present. Here, we have tested the activity of Diglon-CO and shown that it blocks initiation of neurite outgrowth from a subpopulation of CGCs. Other Diglons might act on different subpopulations, and it will be interesting to assay the relative expression of each IgLON subunit in individual CGCs. The neurites that do grow on Diglon-CO-expressing cells are slightly shorter than neurites

on wild-type and OBCAM-CHO cells, but the lengths are similar to those on CEPU-1-CHO cells alone. Thus, the blocking of neurite outgrowth initiation is the most prominent activity of Diglon-CO. However, it remains to be seen whether established growth cones from neurons that do respond to Diglon-CO will also be inhibited. The molecular identity of the receptor on CGC is not known, although a Diglon rather than an IgLON is the most likely candidate. The results described in this paper will substantially change the way in which the activities of the IgLON family are investigated. Cell lines expressing two or more members of the family and heterodimeric recombinant proteins will be required to characterize the involvement of IgLONs in initiation and guidance of axons, cell-cell recognition and control of cell division.

It is now crucial to investigate the complement of IgLONs expressed on the surface of individual cells in order to determine which Diglons are present and, where more than two IgLON subunits are expressed, which combinations are preferred. Is the expression of the different gene products coordinated or can LAMP-OBCAM heterodimers exist alongside excess OBCAM? In Fig. 9, we suggest that the four IgLONs might form six Diglons, each of which might interact with itself or one or more of the other five Diglons. In addition, if some cells do express a single IgLON, each member of the family has a choice of two (or, in the case of CEPU-1, three) other IgLONs that it might interact with. The putative transmembrane receptor that Diglons or IgLONs interact with in cis has not yet been identified but, depending on whether there is a single receptor or several related receptors, the IgLONs and Diglons might mediate a considerable range of cellular responses.

The experiments described here are particularly timely, because recent reports that IgLONs are expressed beyond the nervous system and that OBCAM might act as a tumour suppressor gene (Sellar et al., 2003) will increase the potential roles of IgLON family proteins beyond the development and function of the nervous system to include development of other tissues and organs, and oncogenesis.

We thank R. Read for technical support, D. Fernig for valuable discussions, P. Murray for critical reading of the manuscript and J. Gilthorpe for providing pSlax and pIRES EGFP plasmids. This work was supported by a Wellcome Trust grant 058129 to D.J.M.

References

Allsopp, T. E. and Moss, D. J. (1989). A developmentally regulated chicken neuronal protein associated with the cortical cytoskeleton. *J. Neurosci.* **9**, 13-24.

Anderson, R. G. and Jacobson, K. (2002). A role for lipid shells in targeting proteins to caveolae, rafts, and other lipid domains. *Science* **296**, 1821-1825.

Brummendorf, T. and Lemmon, V. (2001). Immunoglobulin superfamily receptors: cis-interactions, intracellular adapters and alternative splicing regulate adhesion. *Curr. Opin. Cell Biol.* **13**, 611-618.

Brummendorf, T., Spaltmann, F. and Treubert, U. (1997). Cloning and characterization of a neural cell recognition molecule on axons of the retinotectal system and spinal cord. *Eur. J. Neurosci.* **9**, 1105-1116.

Cambray-Deakin, M. A. (1995). Cerebellar granule cells: *Neural Cell Culture* (ed. J. Cohen and G. P. Wilkin). Oxford, UK: Oxford University Press.

Castellani, V., Chedotal, A., Schachner, M., Faivre-Sarrailh, C. and Rougon, G. (2000). Analysis of the L1-deficient mouse phenotype reveals cross-talk between Sema3A and L1 signaling pathways in axonal guidance. *Neuron* **27**, 237-249.

Castellani, V., de Angelis, E., Kenwrick, S. and Rougon, G. (2002). Cis and trans interactions of L1 with neuropilin-1 control axonal responses to semaphorin 3A. *EMBO J.* **21**, 6348-6357.

Chen, C. A. and Okayama, H. (1988). Calcium phosphate-mediated gene transfer: a highly efficient transfection system for stably transforming cells with plasmid DNA. *BioTechniques* **6**, 632-638.

Clarke, G. A. and Moss, D. J. (1994). Identification of a novel protein from adult chicken brain that inhibits neurite outgrowth. *J. Cell Sci.* **107**, 3393-3402.

Clarke, G. A. and Moss, D. J. (1997). GP55 inhibits both cell adhesion and growth of neurons, but not non-neuronal cells via a G-protein-coupled receptor. *Eur. J. Neurosci.* **9**, 334-341.

Freigang, J., Proba, K., Leder, L., Diederichs, K., Sonderegger, P. and Welte, W. (2000). The crystal structure of the ligand binding module of axonin-1/TAG-1 suggests a zipper mechanism for neural cell adhesion. *Cell* **101**, 425-433.

Friedrichson, T. and Kurzchalia, T. V. (1998). Microdomains of GPI-anchored proteins in living cells revealed by crosslinking. *Nature* **394**, 802-805.

Funatsu, N., Miyata, S., Kumanogoh, H., Shigeta, M., Hamada, K., Endo, Y., Sokawa, Y. and Maekawa, S. (1999). Characterization of a novel rat brain glycosylphosphatidylinositol-anchored protein (Kilon), a member of the IgLON cell adhesion molecule family. *J. Biol. Chem.* **274**, 8224-8230.

Gil, O. D., Zanazzi, G., Struyk, A. F. and Salzer, J. L. (1998). Neurotrimin mediates bifunctional effects on neurite outgrowth via homophilic and heterophilic interactions. *J. Neurosci.* **18**, 9312-9325.

Gil, O. D., Zhang, L., Chen, S., Ren, Y. Q., Pimenta, A., Zanazzi, G., Hillman, D., Levitt, P. and Salzer, J. L. (2002). Complementary expression and heterophilic interactions between IgLON family members neurotrimin and LAMP. *J. Neurobiol.* **51**, 190-204.

Hancox, K. A., Gooley, A. A. and Jeffrey, P. L. (1997). AvGp50, a predominantly axonally expressed glycoprotein, is a member of the IgLON's subfamily of cell adhesion molecules (CAMs). *Mol. Brain Res.* **44**, 273-285.

Harris, T. J., Ravandi, A. and Siu, C. H. (2001). Assembly of glycoprotein-80 adhesion complexes in *Dictyostelium*. Receptor compartmentalization and oligomerization in membrane rafts. *J. Biol. Chem.* **276**, 48764-48774.

Harris, T. J. and Siu, C. H. (2002). Reciprocal raft-receptor interactions and the assembly of adhesion complexes. *BioEssays* **24**, 996-1003.

Howard, M. J. and Bronner-Fraser, M. (1985). The influence of neural tube-derived factors on differentiation of neural crest cells in vitro. I. Histochemical study on the appearance of adrenergic cells. *J. Neurosci.* **5**, 3302-3309.

Howard, M. R., Lodge, A. P., Reed, J. E., McNamee, C. J. and Moss, D. J. (2002). High-level expression of recombinant Fc chimeric proteins in suspension cultures of stably transfected J558L cells. *BioTechniques* **32**, 1282-1288.

Kunz, S., Spirig, M., Ginsburg, C., Buchstaller, A., Berger, P., Lanz, R., Rader, C., Vogt, L., Kunz, B. and Sonderegger, P. (1998). Neurite fasciculation mediated by complexes of axonin-1 and Ng cell adhesion molecule. *J. Cell Biol.* **143**, 1673-1690.

Kunz, B., Lierheimer, R., Rader, C., Spirig, M., Ziegler, U. and Sonderegger, P. (2002). Axonin-1/TAG-1 mediates cell-cell adhesion by a cis-assisted trans-interaction. *J. Biol. Chem.* **277**, 4551-4557.

Levitt, P. (1984). A monoclonal antibody to limbic system neurons. *Science* **223**, 299-301.

Lodge, A. P., Howard, M. R., McNamee, C. J. and Moss, D. J. (2000). Co-localisation, heterophilic interactions and regulated expression of IgLON family proteins in the chick nervous system. *Brain Res. Mol. Brain Res.* **82**, 84-94.

Lodge, A. P., McNamee, C. J., Howard, M. R., Reed, J. E. and Moss, D. J. (2001). Identification and characterization of CEPU-Se, a secreted isoform of the IgLON family protein, CEPU-1. *Mol. Cell. Neurosci.* **17**, 746-760.

Malhotra, J. D., Tsiotra, P., Karagogeos, D. and Hortsch, M. (1998). Cis-activation of L1-mediated ankyrin recruitment by TAG-1 homophilic cell adhesion. *J. Biol. Chem.* **273**, 33354-33359.

Mann, F., Zhukareva, V., Pimenta, A., Levitt, P. and Bolz, J. (1998). Membrane-associated molecules guide limbic and nonlimbic thalamocortical projections. *J. Neurosci.* **18**, 9409-9419.

Marg, A., Sirim, P., Spaltmann, F., Plagge, A., Kauselmann, G., Buck, F., Rathjen, F. G. and Brummendorf, T. (1999). Neurotractin, a novel neurite outgrowth-promoting Ig-like protein that interacts with CEPU-1 and LAMP. *J. Cell Biol.* **145**, 865-876.

McNamee, C. J., Reed, J. E., Howard, M. R., Lodge, A. P. and Moss, D. J. (2002). Promotion of neuronal cell adhesion by members of the IgLON family occurs in the absence of either support or modification of neurite outgrowth. *J. Neurochem.* **80**, 941-948.

Miyata, S., Matsumoto, N., Taguchi, K., Akagi, A., Iino, T., Funatsu, N. and Maekawa, S. (2003). Biochemical and ultrastructural analyses of IgLON cell adhesion molecules, Kilon and OBCAM in the rat brain. *Neuroscience* **117**, 645-658.

Olive, S., Dubois, C., Schachner, M. and Rougon, G. (1995). The F3 neuronal glycosylphosphatidylinositol-linked molecule is localized to glycolipid-enriched membrane subdomains and interacts with L1 and Fyn kinase in cerebellum. *J. Neurochem.* **65**, 2307-2317.

Schofield, P. R., McFarland, K. C., Hayflick, J. S., Wilcox, J. N., Cho, T. M., Roy, S., Lee, N. M., Loh, H. H. and Seeburg, P. H. (1989). Molecular characterization of a new immunoglobulin superfamily protein with potential roles in opioid binding and cell contact. *EMBO J.* **8**, 489-495.

Sellar, G. C., Watt, K. P., Rabiasz, B. K., Stronach, E. A., Li, L., Miller, E. P., Massie, C., Williams, A. R., Bates, P. A., Contreras-Moreira, B. et al. (2003). The IgLON family member OPCML (OBCAM) at 11q25 is epigenetically inactivated and demonstrates tumour suppressor function in epithelial ovarian cancer. *Nat. Genet.* **34**, 337-343.

Sharma, P., Varma, R., Sarasij, R. C., Ira, Gousset, K., Krishnamoorthy, G., Rao, M. and Mayor, S. (2004). Nanoscale organization of multiple GPI-anchored proteins in living cell membranes. *Cell* **116**, 577-589.

Simons, K. and Toomre, D. (2000). Lipid rafts and signal transduction. *Nat. Rev. Mol. Cell. Biol.* **1**, 31-39.

Spaltmann, F. and Brummendorf, T. (1996). CEPU-1, a novel immunoglobulin superfamily molecule, is expressed by developing cerebellar Purkinje cells. *J. Neurosci.* **16**, 1770-1779.

Struyk, A. F., Canoll, P. D., Wolfgang, M. J., Rosen, C. L., Deustachio, P. and Salzer, J. L. (1995). Cloning of neurotrimin defines a new subfamily of differentially expressed neural cell-adhesion molecules. *J. Neurosci.* **15**, 2141-2156.

Tansey, M. G., Baloh, R. H., Milbrandt, J. and Johnson, E. M., Jr (2000). GFRalpha-mediated localization of RET to lipid rafts is required for effective downstream signaling, differentiation, and neuronal survival. *Neuron* **25**, 611-623.

Varma, R. and Mayor, S. (1998). GPI-anchored proteins are organized in submicron domains at the cell surface. *Nature* **394**, 798-801.

Walsh, F. S. and Doherty, P. (1997). Neural cell adhesion molecules of the immunoglobulin superfamily: role in axon growth and guidance. *Annu. Rev. Cell Dev. Biol.* **13**, 425-456.

Wilson, D. J. A., Kim, D. S., Clarke, G. A., Marshall Clarke, S. and Moss, D. J. (1996). A family of glycoproteins (GP55), which inhibit neurite outgrowth, are members of the Ig superfamily and are related to OBCAM, neurotrimin, LAMP and CEPU-1. *J. Cell Sci.* **109**, 3129-3138.

Zhukareva, V. and Levitt, P. (1995). The limbic system-associated membrane-protein (LAMP) selectively mediates interactions with specific central neuron populations. *Development* **121**, 1161-1172.